Technische Universität Dresden, Faculty of Environmental Sciences

SWIMMING POOL WATER TREATMENT WITH CONVENTIONAL AND ALTERNATIVE WATER TREATMENT TECHNOLOGIES

A thesis submitted to attain the degree of

DOKTORINGENIEUR (Dr.-Ing.)

presented by

Bertram Skibinski

Dipl.-Ing., Technische Universität Dresden

born on Jan, 05th 1984 in Marienberg

Reviewers:

Prof. Dr. rer. nat. Eckhard Worch, Technische Universität Dresden

Prof. Dr.-Ing. Wolfgang Uhl, Norwegian Institute for Water research

Prof. Dr.-Ing. Martin Jekel, Technische Universität Berlin

Day of oral defence: 22.02.2017 (Dresden)

“Science is not finished until it is communicated”
SIR MARK WALPORT

Table of contents

1 General introduction

Swimming is a popular year-round activity widely enjoyed for leisure, recreation and exercise by more than 250 - 300 million people in Germany per year [1, 2]. Comparable numbers of annual visitors have been reported for the United States (368 million people) [3]. A survey conducted in Germany in 2001 revealed that swimming is ranked on the second place of the most popular recreational activities placed only behind cycling [4]. These findings correlate with reported data from the United Kingdom [5] and the US [6]. The high level of acceptance of swimming among the population results in a high number of public and private pool facilities. The total number of public pools in Germany has been estimated in the year 2012 with 7.499 (excluding natural pools, counting combined indoor-outdoor pools twice) [7]. Comparable pool counts have been reported for Germany in the year 2002 [8, 9]. Including private pool facilities, the highest number of in-ground and above-ground pools in Europe has been reported for France (1.466.000), Spain (1.200.000) and Germany (862.000) [10].

A major drawback resulting from the simultaneous use of swimming pools by many people is the fact that serious diseases can be easily spread [11]. These waterborne infections are often associated with pathogens embracing viruses, bacteria and protozoa [11-21]. Previous studies showed that a high number of living cells and pathogens are introduced into pool water by shedding from the human skin [22, 23] or by fecal release [13, 14, 22, 24].

To assure the hygienic safety in pool systems, requirements for the quality of pool water have been set down in standards and regulations such as the German Protection Against Infection Act (IfSG Infektionsschutzgesetz) [25]. On the basis of the IfSG, the German swimming pool standard DIN 19643 sets specific microbiological and chemical quality parameters for swimming pools [26].

To guaranty the hygienic safety for bathers, swimming pools have a re-circulating water system that allows removing microorganisms and unwanted chemical substances from the water body by water treatment (Figure 1.1). The different treatment concepts, as they are allowed to be used in public pools in Germany are defined in DIN 19643 as well [26]. Therein, water treatment by filtration with upstream flocculation is described to be the first barrier against microorganisms followed by disinfection, which is the second barrier [26]. Chemicals used as disinfectant must be capable of inactivating microorganisms by 99.99% within 30 seconds (i.e. the indicator microorganism *Pseudomonas aeruginosa*). Only chlorine-based chemicals are permitted to be used for disinfection in Germany. Besides chlorine gas (Cl_2), salts

of hypochlorite are most commonly used in large pools [3]. Chlorine disproportionates in water forming chloride and hypochlorite ions (OCl^-). Salts of hypochlorite hydrolyze in aqueous solutions forming hypochlorite ions as well. At neutral pH, as it is usual for pool water, the hypochlorite ion protonates forming the highly reactive hypochlorous acid (HOCl) [27, 28]. The sum of Cl_2, HOCl and OCl^- is denoted as free chlorine while HOCl comprises the highest disinfection efficiency among the different species. Free chlorine and in particular HOCl does not only inactivate microorganisms at the dosing point but comprises a depot effect and assures hygienic safety in the basin itself. Due to this reason, a constant concentration of free chlorine has to be established in the pool basin and free chlorine concentrations are subject to continuous surveillance [26].

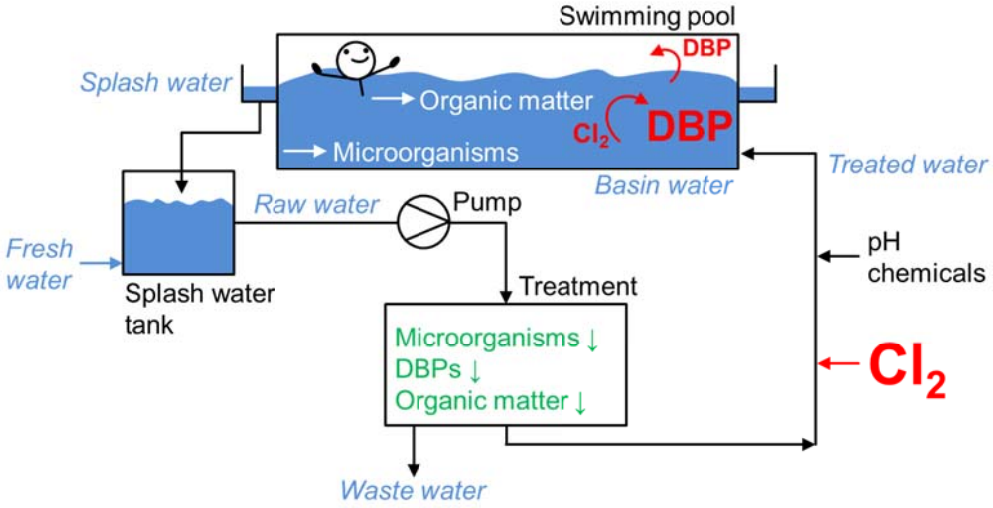

Figure 1.1: Simplified scheme of a swimming pool system with re-circulated water flow, treatment section and the pollutants removed by water treatment and DBP formation from chlorine reactions.

Besides its beneficial effect as disinfectant, HOCl is known to react with dissolved and particulate organic matter present in swimming pool water forming a variety of potentially harmful disinfection by-products (DBPs) [3, 29-34]. Organic matter present in pool water is known to primarily originate from the bather and from fresh water [35]. Given that some of the formed DBPs are volatile [30], bathers can not only take them up by dermal absorption or orally but also by inhalation over the respiratory pathway [1, 36]. Due to the limited air exchange in indoor swimming pools, special concerns raised in the past decades with regard to volatile DBPs, which are associated with adverse health effects such as irritation of the respiratory tract, eyes or skin [37-39] or developing asthma [40-43]. Moreover, epidemiologic studies showed that some of the DBPs are suspected human carcinogens or being considered to be mutagenic [33, 44-46].

Thus, to guarantee optimal conditions for bathers, pool water treatment has to assure an efficient disinfection (i.e. low pathogenic risk) whilst having a minimal DBP formation. Zwiener et al. (2007) defined the following basic requirements for a suitable pool water treatment [3]:

(i) removal of pathogens and particles,
(ii) removal of dissolved organic matter and DBPs and
(iii) sufficient disinfection with the lowest possible DBP formation.

Recent research particularly emphasizes the importance of removing organic matter [24, 47, 48] and DBPs [49, 50] in the treatment train to lower concentration levels of DBPs in pool water. However, conventional pool water treatment (i.e. flocculation-sand filtration-chlorination) is suggested to insufficiently remove both, dissolved organic contaminants and DBPs [51, 52]. This leads to their accumulation in the swimming pool water cycle and increasing DBP concentrations over the operation time [53]. To prevent accumulation of substances, fresh water is often added to the pool water cycle for the purpose of dilution, which in turn increases the water and energy demand for operating a swimming pool system.

To overcome the process of accumulation of DBPs and precursor substances in pool water while lowering the need for fresh water, alternative water treatment technologies have been introduced over the last decade [54]. Some of the most promising technologies which could accompany or partially replace conventional water treatment such as membrane filtration or oxidation processes [54, 55] have recently been integrated in the revised German pool standard DIN 19643 [56]. However, a detailed evaluation of their removal efficiencies for DBPs and DBP precursors under typical swimming pool operation is, in large parts, still subject to future research.

2 Thesis outline

This thesis is intended to provide profound knowledge about the potential of various novel and conventional combinations of water treatment technologies to reduce hazardous impurities present in pool water. The pool water quality is primarily assessed by means of the emerging class of hazardous low molecular weight disinfection by-products (DBPs) and their organic or inorganic precursors. A special focus of this thesis will be on the removal of inorganic chloramines in granular activated carbon filters. Inorganic chloramines are of particular interest since they are often used as an indicator parameter in the surveillance of DBPs in pool water. Further, they are known precursors for the formation of highly carcinogenic DBPs (e.g. N-nitrosodimethylamine (NDMA)).

It is therefore the aim of the research presented in this thesis to provide insights and clarifications with regard to the following questions:

(i) To which extend do novel and conventional water treatment technologies contribute to the mitigation of DBPs and DBP precursors in swimming pool water?
(ii) Which mechanisms and processes determine the removal of inorganic chloramines in granular activated carbon filtration?
(iii) To which extend does granular activated carbon filtration contribute to the mitigation of inorganic chloramines and NDMA in pool water?

Background information, results and conclusions of this thesis are given in **Chapters 3 to 7**.

Chapter 3 provides a brief overview on the complex system of a modern swimming pool system and the chlorine chemistry within it. The current state of knowledge will be introduced in a causal order starting with an overview of sources for particulate and dissolved organic compounds in pool water followed by an explanation of reactions between the organic material and chlorine that lead to the formation of hazardous DBPs. Finally, the current state of art with regard to DBP mitigation by pool water treatment will be introduced.

Chapter 4 provides a comprehensive assessment of the efficiency of different water treatment combinations towards the mitigation of dissolved organic precursors and DBPs in swimming pool water. A swimming pool model was engineered in the frame of this thesis to determine removal efficiencies for organic substances and DBPs under fully controlled and reproducible conditions.

Chapter 5 and **Chapter 6** provide information on the removal of inorganic chloramines by granular activated carbon treatment. In **Chapter 5,** mechanisms are described that limit the overall reactivity for chloramine removal in a granular activated carbon filters. Further, the process of decreasing carbon reactivity for chloramine removal is investigated in detail. **Chapter 6** gives information on the importance of surface chemical carbon properties with regard to the type of product formed when chloramines are transformed in a GAC filter. Simulations with a numerical model of a swimming pool system have been conducted to highlight the importance of the type of carbon used in a granular activated carbon filter operated in a swimming pool system. Depending on the type of carbon used, the concentration of carcinogenic NDMA, which is formed via reactions including chloramines, are calculated and compared.

Chapter 7 contains the final conclusions about the use of conventional and novel processes for water treatment with regard to the mitigation of organic and inorganic precursors and DBPs in swimming pool water.

3 Background

3.1 Loading of swimming pool water with particulate and dissolved substances

3.1.1 Pollutants and sources

Two of the main sources of unwanted impurities found in swimming pool systems are the bathers entering the pool [22, 24] and filling water which is used for the purpose of dilution (typically taken from drinking water mains) [35, 57]. In the case of outdoor swimming pools, additional particulate and dissolved pollutants can be introduced from surrounding green areas [58].

Particulate matter introduced into pool water includes microorganisms (virus, bacteria and protozoa), anthropogenic particles (e.g. skin or hair cells) [24], ingredients of personal-care products such as sun screening-agents [59] and particles present in the filling water. Organic particles present in swimming pool water react with chlorine and thus, contribute to the formation of harmful disinfection by-products (DBPs) [34]. As the disinfection effectivity of chlorine is lowered for microorganisms that are attached to the surface of particles [60], the concentration of the sum of organic and inorganic particles is subject to pool water regulations (e.g. in means of the turbidity).

Further, swimming pool water is loaded with dissolved substances originating from human body fluids [22, 24, 53], personal-care products [59] and filling water (i.e. drinking water) [35]. Loading of chlorinated pools with organic matter (OM) from all of these sources has previously been associated with increasing DBP concentrations. However, the potential to form certain DBPs has been found to be different for dissolved organic matter (DOM) from filling water compared to DOM from human body excretions [35]. This effect is mainly caused by differences in functionality [61, 62] and molecular size [35, 63] of the respective DOM.

3.1.2 Loading of pool water with particulate substances

3.1.2.1 Particulate substances from bathers

The average total particle release of bathers (organic and inorganic) has been estimated recently with $1.46 \cdot 10^9$ particles per bather (30 min pool visit, size range of 2 - 50 µm) [22]. The quantitative particle release among individual subjects varied by a factor of ~65 ($0.97 \cdot 10^9$ - $63 \cdot 10^9$ particles per bather in the first 30 s) and strongly depended on individual characteristics of the bathers [24]. Since particles are primarily attached to the human skin and hair, the particle release rate drops after an

initial time of recreational activity until the release becomes negligible [22]. Previous studies particularly highlighted the importance of organic particles from hair and skin for the formation of DBPs in swimming pool systems [34, 59]. Kim et al. (2002) observed an elevating concentration of total organic carbon (TOC) when adding anthropogenic particles into pool water. When chlorinating the pool water, DBP concentrations increased with increasing amount of organic particles added [59]. DBP precursors in human hair are most likely amino acids (cysteine, serine and glutamic acid) [34] while corneocyte cells, lipids (ceramides, free fatty acids and cholesterol), urea (8 µg cm^{-2}) and amino acids [64] are DBPs precursors present in the external skin layer of humans (stratum corneum) that is exposed to chlorinated pool water.

Another emerging class of particles originating from bathers that has recently been associated with constrains regarding the pool water quality are sunscreen lotions [65]. Sunscreen lotions contain particulate UV filter substances that reduce the transmissivity of UV irradiation by reflection or absorption of light [66]. These filters could be of inorganic nature such as TiO_2 [67] and ZnO [68] but also organic nature such as ethylcellulose, PLGA (poly(lactic-co-glycolic acid)) or Tinosorb M (methylene-bis-benzotriazolyl tetramethylbutylphenol) [69], which are used in lotions in concentrations of up to 10% by weight [70]. Until now, no study is known that quantitatively evaluated the release of organic particles from these products under conditions that are typical for real pool environments. Further, bathers release fecally-derived and non-fecally-derived microorganisms that have previously been associated with various waterborne outbreaks in swimming pools (virus, bacteria and protozoa) [21]. The amount of microorganisms (expressed as colony forming units (CFU)) released per bather ranges between 10^8 - 10^9 CFU [71]. Table 3.1 summarizes the most relevant microorganisms released by bathers.

Table 3.1: Microorganisms associated with waterborne outbreaks in recreational systems released by bathers (as given by [21]).

	Virus	**Bacteria**	**Protozoa**
Fecally-derived	Adenovirus, Enterovirus, Hepatitis A, Norovirus	E.coli, Shigella spp.	Cryptosporidium, Giardia
Non-fecally-derived	Adenovirus, Molluscipoxvirus, Papillomavirus	Legionella spp., Leptospira spp., Mycobacterium spp., Pseudomonas spp., Staphylococcus	Maegleria flowleri, Acanthamoeba spp., Plasmodium spp.

Table 3.2 presents the quantitative data reported for anthropogenic load of pool water by viruses, bacteria and protozoa. Noticeable is the lack of data with regards to

the anthropogenic loading with viruses. Values given in in Table 3.2 are representative for average swimmers without obvious diseases. The release of microbiological contaminants of infected people (e.g. cryptosporidiosis) is higher by several orders of magnitude compared to average conditions [72].

Table 3.2: Quantities of microorganisms released by bathers (partially taken from [100]).

	Release per bather	**Comments**	**Ref.**
Viruses			
Enteric viruses	$1.6 \cdot 10^4$	30 min shower	[73, 74]
	$1.4 \cdot 10^7 – 3.0 \cdot 10^{13}$	Theoretically derived from literature data	[74]
Bacteria			
Coliform bacteria	$3.78 \cdot 10^7$	10 - 15 min shower, 25 subjects	[73]
	$1.1 \cdot 10^6 \pm 5.13 \cdot 10^7$	10 - 30 min, pool experiment	[75]
	$1.4 \cdot 10^{5\ up}$, $1.5 \cdot 10^{5\ sp}$	15 min of exposure, immersed bodies in 550 L water, 6 subjects^{up}, 20 subjects^{sp}	[76]
Fecal coliform bacteria	$2.27 \cdot 10^6$	10 - 15 min shower, 25 subjects	[73]
	$1.2 \cdot 10^5$	15 min in bathtub, 8 subjects	[77]
E.coli	$\sim 1 \cdot 10^{3\ ID}$ - $2 \cdot 10^{4\ OD}$	60 s shower, 25 subjects^{ID}, 8 subjects^{OD}	[24]
	$6.6 \cdot 10^{4\ up}$, $2.1 \cdot 10^{5\ sp}$	15 min of exposure, immersed bodies in 550 L water, 6 subjects^{up}, 20 subjects^{sp}	[76]
Enterococci	$5.5 \cdot 10^5$	15 min of exposure, immersed bodies in 4,700 L water, 10 subjects	[23]
	$\sim 3 \cdot 10^{3\ ID}$, $2 \cdot 10^{4\ OD}$	60 s shower, 25 subjects^{ID},8 subjects^{OD}	[24]
	$6.6 \cdot 10^4$	15 min of exposure	[77]
Staphylo-coccus aureus	$6.1 \cdot 10^6$	15 min of exposure, immersed bodies in 4,700 L water, 10 subjects	[23]
	$\sim 1 \cdot 10^{6\ ID}$, $1 \cdot 10^{7\ OD}$	60 s shower experiment, 25 subjects^{ID}, 8 subjects^{OD}	[24]
	$7.5 \cdot 10^6$	15 min of exposure	[77]
Streptococci	$6.6 \cdot 10^{5\ up}$, $1.6 \cdot 10^{5\ sp}$	15 min of exposure, immersed bodies in 550 L water, 6 subjects^{up}, 20 subjects^{sp}	[76]
Protozoa			
Protozoa	$1.4 \cdot 10^4$ - $3.0 \cdot 10^7$	Theoretically derived from literature data	[74]

^{up} … Unshowered subjects
^{sp} … Showered subjects
^{ID} … Indoor pool
^{OD} … Outdoor pool

3.1.2.2 Particulate substances from filling water

Since most pool facilities in Germany use drinking water as filling water, no pre-treatment is typically used before feeding it into the pool system. Thus, the quality of filling water is basically equal to the bulk water quality in the distribution network. Particle concentrations in drinking water are determined by various local and system specific factors of the drinking water main such as the characteristics of the offtake location, local hydraulic conditions in the distribution network, the type of piping material used, the type of raw water used and the type of drinking water treatment employed [78, 79]. Given the complexity of influencing factors, the ranges of reported properties of suspended particles in European drinking waters are very wide (see Table 3.3). Due to the required level of microbial safety of drinking water [11], loading of pool water with pathogens from filling water could be neglected.

Table 3.3: Selection of characteristics reported for suspended particles taken from drinking water mains across Europe.

Parameter	**Value**	**Ref.**
Volume concentration	714 – 28,097 μm^3 mL^{-1} (size 1 µm - 31 µm)	[78, 80]
Total suspended solids	<13 – 71 μg L^{-1}	[80]
Particle size	~1 – 120 µm	[78, 81, 82]
Particle number	50-120 mL^{-1} (>1 µm)	[80]
Particle density	1,000 – 1,300 kg m^{-3}	[81]
Organic content	~30 – 70 % (by weight)	[83]
Elemental composition	[a]	[80, 82]
Total cell count	10^4 - 10^5 cells mL^{-1}	[82, 84, 85]

[a] … Differences in the elemental composition are given elsewhere [80, 82] but have not been presented here due to the complexity of this matter

3.1.3 Loading of pool water with dissolved substances

3.1.3.1 Dissolved substances from bathers

Loading of pool water with dissolved organic matter (DOM) from bathers has been found to depend on water parameters (e.g. temperature), personal characteristics of the bathers and the level of exercise [22, 24, 86]. Sweat (0.08 - 1.62 L h^{-1} [22, 87-92]) and urine (30 – 70 mL per bather [93, 94]) are the main sources of anthropogenic release of DOM. The total anthropogenic loading with DOM is reported to range between 0.5 - 1.4 g_{DOC} per bather [95]. A breakdown of the chemical components of sweat and urine has been previously reported in great detail by

Consolazio at al. (1963) and Putnam (1971) [86, 96]. Up to 158 different chemical constituents are present in urine samples while 58 were found in sweat samples (including inorganic salts and organic compounds) [86, 96]. It revealed that urea (0.56 - 2.46 g per bather [31, 97]), creatinine (2 – 85 mg per bather [98]), ammonium salts (30 – 60 mg per bather [57]), amino acids (15 – 50 mg per bather [57]) and other organic acids represent the main organic components of human sweat and urine [86, 93, 96, 99]. Recent studies conducted by Keuten et al. (2012, 2014) showed that the anthropogenic release of organic matter could be subdivided into (i) initial, (ii) continual and (iii) incidental release (see Table 3.4) [22, 24].

Table 3.4: Stages of anthropogenic pollutants release. Taken from [22]. (Conditions: 30 min duration, without pre-swim shower, individual energy consumption of 60 – 70% of the maximum value)[a].

	TOC in mg per bather	**TN[c] in mg per bather**
Initial (first 60 s)	217	57
Continual (up to 30 min)	250	77.3
Incidental [b]	192	70
Total	659	204

[a] … Please note that different anthropogenic releases have been reported in previous studies by the same group of authors [100].

[b] … Based on a 30 mL urine release per bather

[c] … Total nitrogen (TN)

Additional dissolved components could be released from bathers by sunscreen lotions applied previous to bathing activities. Ingredients of these lotions remain on the surface of human skin and permeate only in small amounts in the upper skin layers [101]. Consequently, these substances are washed from the human skin while bathing. Data about the anthropogenic release of ingredients of sunscreen lotions and personal care products into pools is very rare. Previous studies suggest that up to 100% of soluble components and 25% – 50% of lipophilic components present in sunscreen lotions could be released into pool water [65]. Assuming each bather applying in the mean 13 g of sunscreen lotion [102], concentrations of released sunscreen-compounds in pool water could be in the range of µg or even mg per liter [102]. Glauner (2007) showed that the sum of the concentrations of 4 sun screening agents (octyl methoxycinnamate, octocrylene, phenylbenzimidazole sulfonic acid and enzacamen) in a paddling pool was up to 59.1 µg L^{-1} [102]. The formation of DBPs by chlorination of these agents is still widely unknown.

Several authors showed that the concentration of dissolved organic carbon (DOC) in swimming pool water significantly correlates with the number of swimmers attending

the pool. DOC concentrations of pools are substantially higher compared to the concentration of DOC found in the corresponding filling water [35, 103]. These findings particularly highlight the importance of anthropogenic DOM release for the overall quality of swimming pool water.

3.1.3.2 Dissolved substances from filling water

DOM found in filling water (i.e. drinking water) is a mixture of dissolved substances with aromatic, aliphatic, phenolic and quinonic structures and a specific distribution of molecular weights and functionalities. The overall concentration of dissolved organic carbon (DOC) and dissolved organic nitrogen (DON) in drinking waters from Europe, Australia and the US have been found to vary between 0.5 - 6.7 mg_{DOC} L^{-1} and 0.1 - 0.5 mg_{DON} L^{-1}, respectively [35, 103, 104]. Previous studies showed that fractionation of DOM into broad chemical classes of different molecular size is an appropriate first step to further examine its structure [63, 105-107]. The following 6 major sub-fractions of DOM have been identified for natural waters based on their molecular size: biopolymers (BP), humic substances (HS), building blocks (BB), low molecular-weight acids (LMW acids), low molecular-weight neutrals (LMW neutrals) and hydrophobic organic carbon (HOC) [63]. HS, namely humic acids (HA) and fulvic acids (FA), are the prevailing DOM fraction found in finished drinking waters [108]. Previous results indicate that aromatic higher molecular weight HS are preferably removed during different drinking water treatment processes [109, 110]. Thus, hydrophilic, less aromatic humic substances remain in the finished drinking water that is used as filling water in swimming pools. Functional groups of humic acids include carboxylic acid groups (-COOH), phenolic and alcoholic hydroxy groups (-OH) as well as aldehyde (-CHO) and methoxy groups (-O-CH_3) [111]. Since HS are known to significantly contribute to the formation of harmful DBPs [56], filling water has to be pre-treated in case it contains high concentrations of HS.

3.1.4 Surrogates

As shown in Section 3.1.1 – 3.1.3, the composition and amount of particulate and dissolved substances introduced into swimming pool water by bathers and filling water are subject to substantial variations. The fact that comparative studies in the field of swimming pool water treatment have to be performed under reproducible conditions [53] rises the need to control the rate of input of pollutants [53]. Previous studies propose to use surrogates (substitutes) that mimic physicochemical or environmental attributes of the item of interest. Surrogates are available in large amounts and constant quality and thus, permit experiments to be performed under fully controlled conditions [112-114]. Surrogates could be either recipes of chemicals,

organisms or particles [112] and have to be selected according to the specific need of the research question. Three main attribute classes have been identified for choosing surrogates used for water treatment processes (see Figure 3.1) [112].

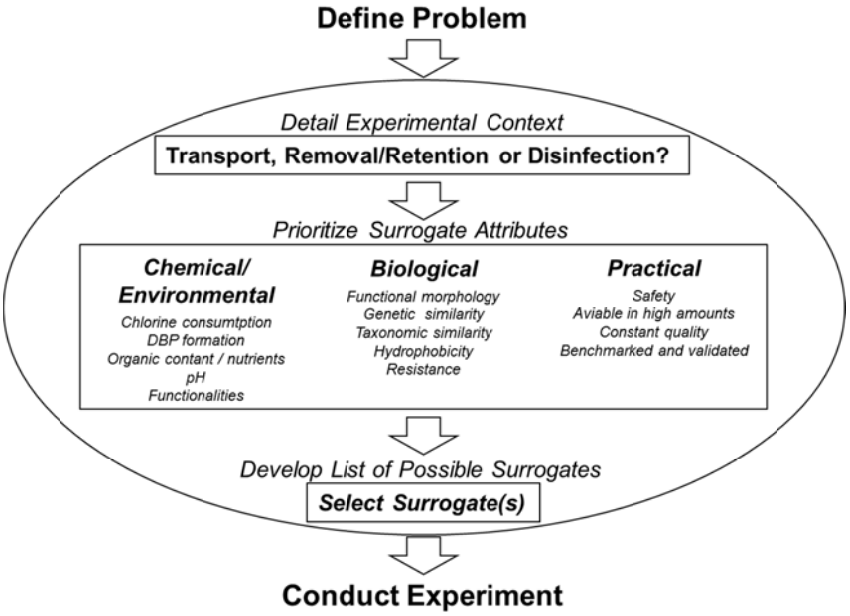

Figure 3.1: Conceptual decision framework for selecting water relevant surrogates.

Until now, only a limited amount of analogues has been proposed in the field of swimming pool water treatment and closely related research fields. Table 3.5 lists a selection of these analogues with special regard to the dissolved organic matter introduced by filling water and the bathers.

Table 3.5: Selection of analogues for dissolved organic matter from pool water[a].

Pollutant	Analogue	Comment	Ref.
DOM from filling water	Suwanee river HA and FA	Derived from river water; High structural similarities compared to natural humic substances; Expensive	[115, 116]
	Sigma Aldrich HA	Derived from soil samples; Widely used as a surrogate for water treatment processes; Important structural difference compared to natural humic substances; Only limited usability as surrogate for water treatment; Little financial efforts	[116-119]
	Own isolates of HA and FA from local water sources	Good structural similarities with natural humic substances; Seasonal variations in chemical composition; High effort for isolation and pre-concentration; Liquid samples undergo major changes in molecular size and structure by time	[120, 121]

Continuation of Table 3.5

Pollutant	Analogue	Comment	Ref.
DOM from bathers	Artificial mixtures representing sweat and urine (Body fluid analogues)	Three different BFA compositions are known from the literature containing: albumin, aspartic acid, citric acid, histidine, creatinine, glucuronic acid, glycine, glutamic acid, hippuric acid, histidine, lactic acid, lysine, urea, uric acid; Some important nitrogen containing precursors are not included (e.g. α-amino acids)	[47, 53, 122]

3.2 Chemistry of chlorine under special consideration of pool water conditions

3.2.1 Chlorine speciation and decay

In order to assure a sufficient disinfection capacity of swimming pool water, the concentration of free chlorine (Cl_2, HOCl, OCl^-) has to be kept in a range from 0.3 - 0.6 mg L^{-1} (as Cl_2) in German swimming pools [26]. Comparable free chlorine levels are recommended for Swiss pool water [123] while higher concentrations of free chlorine are recommended in the US, UK and Australia [3] but should in no case exceed 3 - 4 mg L^{-1} (as Cl_2) in public swimming pools (as required by WHO and ANSI guidelines [21, 124]). According to DIN 19643, chlorine could be added to pool water in liquid form (sodium hypochlorite), solid form (calcium hypochlorite) or as molecular chlorine (Cl_2) in the form of chlorine gas or from electrolysis (of e.g. hydrochloric acid) [26]. Chlorine (Cl_2) disproportionates in water forming hypochlorous acid (HOCl) according to the following reaction:

$$Cl_2 + H_2O \underset{k_{-1}}{\overset{k_1}{\leftrightarrows}} HOCl + Cl^- + H^+, \quad K_{Cl_2} = 5.1 \cdot 10^{-4}\ mol^2\ L^{-2}\ (25°C)\ [125] \qquad (3.1)$$

HOCl is a weak acid and dissociates in aqueous solution forming hypochlorite ions (OCl^-):

$$HOCl \leftrightarrows OCl^- + H^+, \quad K_{a,HOCl} = 2.9 \cdot 10^{-8}\ mol\ L^{-1}\ (25°C)\ [126] \qquad (3.2)$$

Previous studies suggest that also other chlorine intermediates (Cl_3^-, Cl_2O, H_2OCl^+) can be formed in environmental processes (Equation (3.3) - (3.5)) [27]. However, concentrations of these chlorine species are low, which is why they are recognized only very little in water treatment processes [27].

$$2\ HOCl \leftrightarrows Cl_2O + H_2O,\ K_{Cl_2O} = 8.74 \cdot 10^{-3}\ L\ mol^{-1}\ (25°C)\ [127] \quad (3.3)$$

$$Cl_2 + Cl^- \leftrightarrows Cl_3^-,\ K_{Cl_3^-} = 0.18\ L\ mol^{-1}\ (25°C)\ [128] \quad (3.4)$$

$$HOCl + H^+ \leftrightarrows H_2OCl^+,\ K_{H_2OCl^+} = \sim 10^{-26}\ L\ mol^{-1}\ (25°C)\ [129] \quad (3.5)$$

Figure 3.2 (A,B) illustrates the speciation of different aqueous chlorine species (Cl_2, HOCl, OCl^-, Cl_3^-, Cl_2O, H_2OCl^+) in dependence of the pH under typical pool water conditions. Given that the pH of pool water has to be maintained between pH 6.5 - 7.2 in German pools [26], almost all Cl_2 is disproportionated and HOCl becomes the prevailing chlorine species [27, 56].

Among the various chlorine species, HOCl comprises the highest oxidation potential [28]. Conclusively, HOCl has a much higher reactivity with organic material compared to OCl^- [28]. Given that the concentration of Cl_2 in pool water is typically very low in the desired pH range, its possible importance is often discounted.

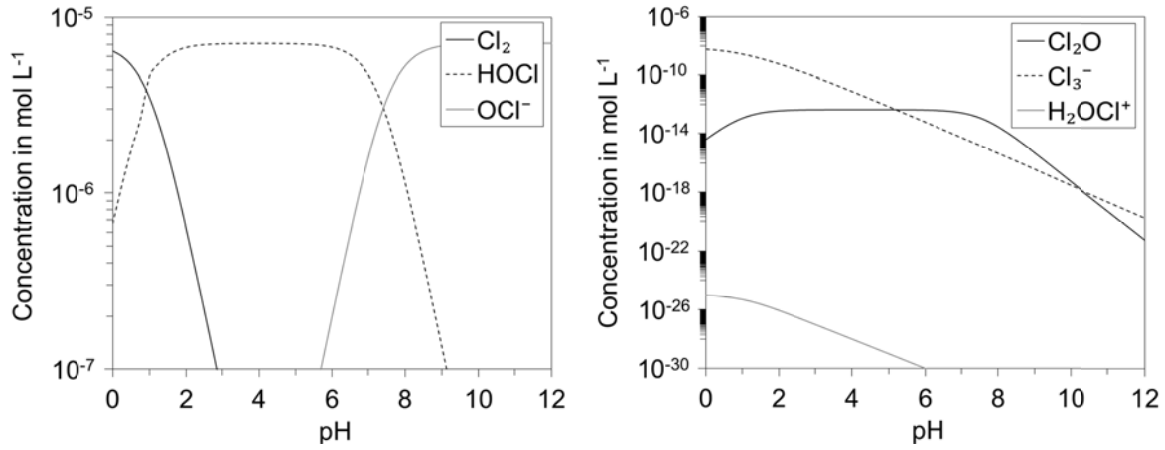

Figure 3.2: Distribution of chlorine species versus pH according to Equations (3.1) - (3.5) (adapted from [27]) (Conditions: chlorine concentration = $7.1 \cdot 10^{-6}$ mol L^{-1} (0.5 mg L^{-1} (as Cl_2)), chloride concentration = $5 \cdot 10^{-3}$ mol, T = 25°C).

3.2.2 Disinfection potential

Typical hydraulic retention times in swimming pool basins (i.e. the water recirculation turnover time) vary between 3 – 5 h depending on the recommendations respected for pool design (e.g. German norm DIN 19643, Swiss norm SIA 385/9, WHO guidelines or others [21, 26, 123, 139]). Due to these long retention times, chlorine, which has a certain depot effect, is used as a residual disinfectant to prevent bacterial growth in the basin and thus, ensure hygienic safety for bathers. Disinfection of pool water by ozonation or UV irradiation is only meant to amend chlorine disinfection by inactivating those bacteria that are resistant to chlorine (e.g.

Crypotosporidia) [140]. Inactivation of relevant microorganisms by primary or secondary disinfectants proceeds stepwise in the flowing order: (i) formation of covalent N-Cl bonds on the surface of microbes (chlorine cover on bacterial surfaces), (ii) penetration of chlorine species into the cell, which is the step limiting the overall killing rate, and (iii) destruction of vitally important cell components [141-143]. The widely accepted simplified Chick-Watson model expresses disinfection kinetics of microorganisms (Equation (3.6)) [144, 145].

$$\ln\left(\frac{N_t}{N_0}\right) = k_{CW} \cdot c \cdot t \qquad (3.6)$$

Here, t is the contact time, N_t and N_0 are the concentrations of the microorganism at time t and at time 0, k_{CW} is the first-order rate constant for inactivation and c is the concentration of disinfectant. At a given inactivation ratio $N_t\ N_0^{-1}$, the product c·t represents the disinfection dose needed. Table 3.6 lists c·t values for primary and secondary disinfectants for microorganisms that have been found in pool water.

Table 3.6: Concentration-time values (c·t) in mg min L^{-1} for 99 % inactivation of microorganisms by primary and secondary disinfectants [146].

Microorganism	**Free chlorine (pH 6 – 7)**	**Chloramine (pH 8 – 9)**	**Chlorine dioxide (pH 6 - 7)**	**Ozone (pH 6 – 7)**
E. coli	0.034 – 0.05	95 - 180	0.4 – 0.75	0.02
Poliovirus 1	1.1 – 2.5	768 - 3740	0.2 – 6.7	0.1 – 0.2
Rotavirus	0.01 – 0.05	3806 - 6476	0.2 – 2.1	0.006 – 0.06
Giardia lamblia cysts	47 - >150	2200[a]	26[a]	0.5 – 0.6
Cryptosporidium parvum	7200[b]	7200[c]	78[c]	5 – 10[b]

[a] … Values for 99% inactivation at pH 6 - 9
[b] … 99% inactivation at pH 7 and 25°C
[c] … 90% inactivation at pH 7 and 25°C

It is widely accepted that HOCl exhibits a bactericidal power which is approximately 100 times higher compared to NH_2Cl [147] or OCl^- [130]. Since OCl^- comprises a much lower disinfection potential compared to HOCl, the disinfection potential of chlorine in swimming pool water decreases significantly with increasing pH.

In public swimming pools in Germany, the concentration of inorganic chloramines (quantified as combined chlorine) could be as high as 0.2 mg L^{-1} (as Cl_2) (limited by the threshold given in DIN 19643) [26]. However, the bactericidal effect of inorganic chloramines is considered to be negligible compared to the primary disinfection with free chlorine. This assumption is supported by the fact that a proportion of combined

chlorine unintentionally refers to inorganic but also organic chloramines [149, 150], which have no or poor germicidal efficiency [148].

3.3 Disinfection by-products in swimming pool water

3.3.1 Formation and occurrence of disinfection by-products in swimming pool water

Primary and secondary disinfectants react with organic and inorganic precursors introduced into swimming pool water (see Section 3.1) forming a variety of hazardous disinfection by-products (DBPs). Additional to DBPs formed by chlorination alone, DBPs could be formed by dual water treatment with chlorine and other processes such as UV irradiation or ozonation. The variety of organic precursors, disinfectants used and secondary effects of combined water treatment lead to a huge diversity of DBPs found in swimming pool water. More than 100 DBPs have been identified previously in swimming pools [33], with trihalomethanes (THM), haloacetic acids (HAA), chloramines (CA) and haloacetonitriles (HANs) being the most studied examples [3, 30]. Table 3.7 summarizes the most important DBPs found in swimming pool water in dependence on the disinfectant or treatment method causing their formation.

The halogenated compounds that are subject to regular surveillance in pools, cumulatively account for ~50 % - ~92 % of the adsorbable organic halogens (AOX) present in chlorinated water samples [102, 151]. The AOX sums up organic halogens that adsorb onto activated carbon and is used as a measure for the sum of less volatile DBPs found in swimming pool water. Thus, a significant proportion of halogenated substances in swimming pools is not subject to continuous water quality monitoring [102].

Table 3.7: Selection of DBPs formed in swimming pool water depending on the type of disinfectant or treatment method employed[a].

Type of disinfection used	DBPs formed			Ref.
	Carbon-containing	Nitrogen-containing	Other	
Chlorine	Trihalomethanes, haloacetic acids, haloketones, haloaldehydes, halobenzoquinones, chloral hydrate, halophenols	Haloacetonitriles, chloropicrin, cyanogen chloride, chloramines	Chlorate	[29, 30, 33, 35, 59, 61, 152-156]
Chloramines	Haloacetaldehydes	Nitrosamines, chloramines, cyanogen chloride		[62, 157-160]
Ozone[b]	Haloaldehydes, carboxylic acids, bromoform, haloketones	Nitrosamines	Bromate	[55, 57, 137, 160, 161]
UV irradiation[b, c]	Trihalomethanes, halopropanones	Haloacetonitriles, cyanogen chloride, chloramines, nitrosamines, dichloromethylamine	Chlorate	[49, 55, 154, 159, 162-164]

[a] … Modified version of the table given by [165]

[b] … In combination with chlorination or chloramination

[c] … Formation of DBPs has been found to strongly depend on the emission spectra of the UV lamp and the UV dose applied

DBPs could be classified in carbon-containing (C-DBPs) and those that also or solely contain nitrogen (N-DBPs). Major representatives of C-DBPs found in pool water are trihalomathanes (THMs) and haloacetic acids (HAAs) [33]. At chlorine concentrations that are typical for pool water, the sum of HAAs primarily consists of dichloroacetic acid and trichloroacetic acids [166] while chloroform is usually the predominant THM [33]. At high bromide concentrations (e.g. when using high saline waters), bromoform becomes the predominant THM species [33]. Typical concentrations of HAAs in pool water in Germany are slightly lower compared to those of THMs [21, 166] (see Table 3.8). The opposite has been shown in swimming pools located in the US, where higher free chlorine concentrations are applied compared to German swimming pools [167].

N-DBPs are formed by the reaction of chlorine with nitrogen-containing organic substances that are primarily introduced into pool water by the bathers (see Section 3.1.3) [29, 33, 153]. Although N-DBPs (e.g. haloacetonitriles (HANs)) are known to be more toxic compared to carbon-based DBPs [168], their concentration levels are still not implemented in pool water standardisations in Europe or the US.

Recent studies particularly focused on the formation and occurrence of trichloramine (NCl_3), a volatile DBP formed by chlorination of urea and ammonium which are two of the main nitrogen-containing precursors introduced into pool water by the bathers (see Section 3.1.3.1). Trichloramine (TCA) is of particular interest since it causes adverse health effects such as irritations of the skin, eyes and respiratory tract [169] and is suggested to foster development of asthma [40]. Table 3.8 lists concentration ranges of a selection of relevant DBPs present in swimming pools in Germany and Switzerland (e.g. at moderate free chlorine concentrations ranging from 0.2 to 0.7 mgL^{-1} (as Cl_2) [26, 123]). Depending on the type of DBP, typical concentrations in pool water range between ng L^{-1} to mg L^{-1}.

Table 3.8: Concentration ranges for a selection of relevant DBPs in swimming pools with concentrations of free chlorine of 0.2 to 0.7 mgL^{-1} (as Cl_2).

DBP / DBP class	**Concentration**	**Ref.**
AOX	161 – 353 µg L^{-1} (as Cl)	[46, 55]
Combined chlorine[a]	~0.05 – ~0.8 mg L^{-1} (as Cl_2)	[39, 97, 170]
Trichloramine[b]	~0.01 – ~0.07 mg L^{-1} (as Cl_2)	[50, 170]
Total trihalomethanes (TTHM)	0 – 83 µg L^{-1} (as $CHCl_3$)	[46, 54, 55, 151]
Total halogenated acetic acids (HAA)	0 – 716 µg L^{-1}	[151]
Total haloacetonitriles (HAN)	2.8 – 22 µg L^{-1}	[151]
Tirchloronitromethane (Clorpicrin)	n.q. – 2.4 µg L^{-1}	[151]
N-nitrosodimethylamine (NDMA)	n.q. – 46 ng L^{-1}	[171]
Dichloroacetonitrile	n.q. – 12.9 µg L^{-1}	[172]

n.q. … Not quantifiable
[a] … Determined by the DPD method (see [173])
[b] … Determined by the MIMS-method

Besides the structure and amount of organic precursors present in pool water, the pH value, the concentration and type of disinfectant, the temperature and ion strength of pool water affect the concentration and composition of DBPs [59, 174, 175]. Decreasing the pH for instance enhances the formation of HANs [34] but lowers the formation of THMs in pool water [176, 177]. Controversy results are reported about the effect of pH change on the concentration of HAAs. While some studies reported increasing HAA concentration with decreasing pH [178], the exact opposite has been found in other studies [34]. Recent studies by Afifi and Blatchley (2015) indicated that seasonal variations in the concentrations of various DBPs occurring in a high school indoor swimming facility in the US could be as high as two orders of magnitude [179]. Given the manifold of influencing factors, concentrations of DBPs in swimming pool

water have to be taken on a regular basis to gain a comprehensive overview of typical concentration ranges.

Some of the water borne DBPs found in swimming pools are volatile and thus, partition between the water and gas phase. Concentrations of volatile DBPs in the air space above a swimming pool basin strongly correlate with the characteristics of the air-water surface (e.g. number of swimmers and attractions) [61, 180], the ventilation system and the Henry's law constant (K_{iH}) of the DBP of interest [36].

The Heny's law constant equals the ratio of the vapour pressure of a DBP p_i (in bar) and its aqueous concentration $c_{a,i}$ (in mol L^{-1}) (see Equation (3.7)).

$$K_{iH} = \frac{p_i}{c_{a,i}} \tag{3.7}$$

Concentrations of volatile DBPs in swimming pool air have been reported for chloroform (Henry constant 3.9 L bar mol^{-1} (25 °C)) and trichloramine (Henry constant 10.1 L bar mol^{-1} (25 °C)) as follows: 1.7 - 1630 mg m^{-3} (Chloroform) [179-181] and 0.05 - 18.8 mg m^{-3} (Trichloramine) [97, 153, 179]. In German pools with moderate free chlorine levels, the most comprehensive screening respecting air samples taken in 92 indoor pools revealed that 90% of trichloramine concentrations were below 0.37 mg m^{-3} [182].

3.3.2 Main formation pathways of selected DBPs in swimming pool water

3.3.2.1 Trihalomethanes (THM)

Previous studies showed that primarily phenolic structures, ketones and carboxylic structures react with HOCl to form THMs [27, 183, 184]. Humic acids, which are some of the dominating components of filling water DOM [63], are suggested to have a very high THM yield when being chlorinated compared to anthropogenic substances brought into swimming pool water by the bathers [35]. This finding has been recently confirmed by Hua et al. (2016), who determined the specific formation potential ($\mu mol_{THM}\ mg_C^{-1}$) of trichloromethane (TCM) from chlorination of humic acids and BFA substances (Table 3.9) [185]. Among the substances found in human body fluids (see Table 3.5) citric acid comprises the highest formation potential for THMs and HAAs [35].

Table 3.9: Apparent second order rate constants (k_{app}) and formation potential for the formation of trichloromethane by the reaction of humic acids and BFA substances with free chlorine after 168 h of reaction (TCM_{FP}) (pH = 7.2 and T = 28±1 °C) [185].

DBP precursors	**k_{app} in L mol^{-1} h^{-1}**	**TCM_{FP} in µmol mg$_C^{-1}$**
Uric acid	$7.22 \cdot 10^{-5}$	0.02
Urea	$1.79 \cdot 10^{-4}$	0.03
L-Histidine	$7.69 \cdot 10^{-5}$	0.23
Creatinine	$6.91 \cdot 10^{-5}$	0.03
Ammonium	no contribution	
Hippuric acid	$4.83 \cdot 10^{-5}$	0.02
Citric acid	$5.12 \cdot 10^{-5}$	11.7
Humic acid	$1.36 \cdot 10^{-4}$	0.82

Chlorination studies with aromatic model compounds for humic acids (e.g. resorcinol) revealed that chlorine initially reacts with aromatic compounds by stepwise electrophilic substitution (see Figure 3.3) [184], which has also been shown for phenol like structures [27]. With ongoing substitution, the charge density of the aromatic ring increases which leads to a faster substitution reaction [186]. Hydrolysis and an oxidative bond cleavage at the chlorinated aromatic ring structure leads to an opening of the ring under the formation of ketones. Chloroform is finally formed by a rate limiting base catalyzed hydrolysis of the chlorinated ketone structure (see Figure 3.3) [165, 184].

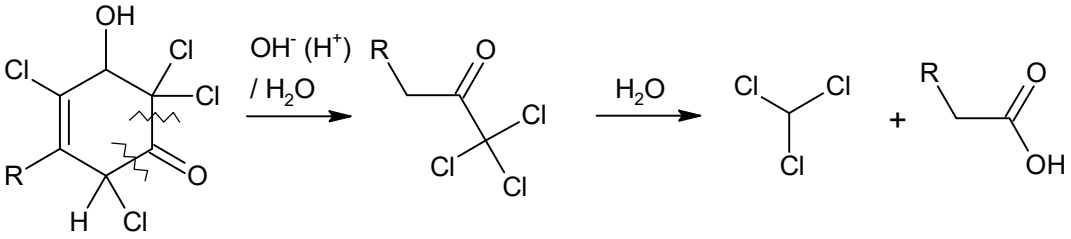

Figure 3.3: Pathway for the formation of chloroform ($CHCl_3$) from chlorination of the humic acids model compound resorcinol (according to [165, 184]).

Among the substances used to simulate the mixture of body fluids excreted into pool water by the bathers (see Table 3.5), citric acid and urea have been found to be the main precursors for trichloromethane production (see Table 3.9 and [187]). Larson and Rockwell (1978) propose that chlorination of citric acid is initiated by a rate limiting oxidative decarbonisation of the carboxyl group leading to the formation of

β-ketoglutaric acid [188]. Formation of trichloromethane from 3-ketoglutaric acid is assumed to proceed via chlorine-substitution of the carboxyl groups followed by base catalyzed hydrolysis of the formed trichloromethyl ketone (see Figure 3.4) [188].

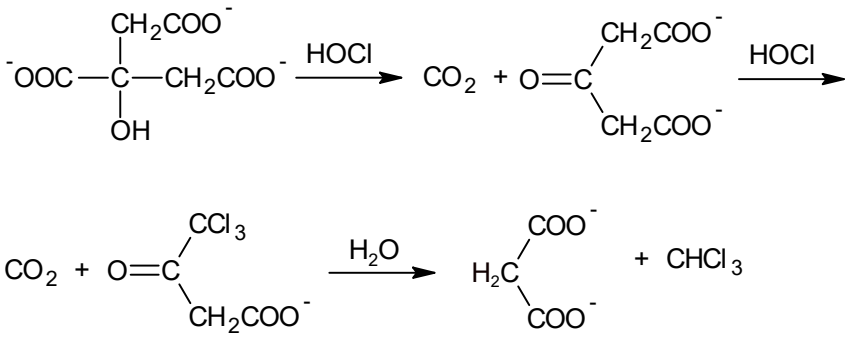

Figure 3.4: Pathway for the formation of trichloromethane ($CHCl_3$) from chlorination of citric acid (taken from [188]).

3.3.2.2 Inorganic chloramines and N-nitrosodimethylamine (NDMA)

Chlorine is considered to be a primary disinfectant in swimming pool water. However, its reaction with nitrogenous precursors in swimming pool water (e.g. ammonium [135], urea [136] or secondary amines [136]) is initially induced by the formation of inorganic chloramines (mono-, di- and trichloramine) and organic chloramines [27, 137]. The primary reactions for chloramination are represented by Equation (3.8) – (3.10) [135]. Since inorganic chloramines have a certain oxidative activity, they are denoted as secondary disinfectants.

$$NH_3 + HOCl \xrightarrow{k_1} NH_2Cl + H_2O, \quad k_1 = 4.2 \cdot 10^6 \text{ mol s}^{-1} \text{ (25°C, pH ~7)} \tag{3.8}$$

$$NH_2Cl + HOCl \xrightarrow{k_2} NHCl_2 + H_2O, \quad k_2 = 3.5 \cdot 10^2 \text{ mol s}^{-1} \text{ (25°C, pH ~7)} \tag{3.9}$$

$$NHCl_2 + HOCl \xrightarrow{k_3} NCl_3 + H_2O, \quad k_3 = 2.1 \text{ mol s}^{-1} \text{ (25°C, pH ~7)} \tag{3.10}$$

The distribution of the active chlorine species and inorganic chloramines in aqueous solutions at equilibrium has been found to be a function of the solution pH and the initial ratio of chlorine to nitrogen (Cl:N) (see Figure 3.5) [135]. A more comprehensive scheme of the chlormaination reactions has been proposed previously by Jafvert and Valentine (1992) (see Table 8.2) [135]. At conditions typical for swimming pool water, monochloramine (NH_2Cl) is the predominant inorganic chloramine species [30].

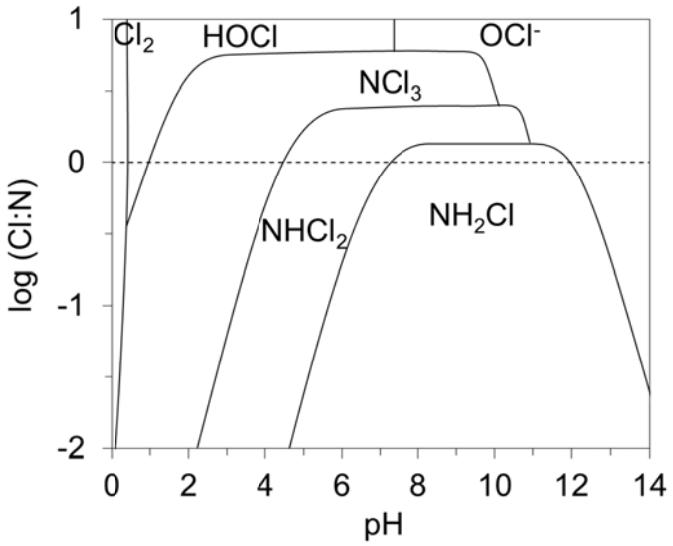

Figure 3.5: Illustration of the theoretical predominant species of chlorine and inorganic chloramines as a function of pH and log(Cl:N) (adapted from [138]). (Conditions: chlorine concentration = $7.1 \cdot 10^{-6}$ mol L^{-1} (0.5 mg L^{-1} (as Cl_2)), chloride concentration = $5 \cdot 10^{-3}$ mol, T = 25°C).

The reaction of urea with molecular chlorine (Cl_2), which is present in only small concentrations in pool water (see Figure 3.2), initially induces chlorination of the amide nitrogen in urea. Further chlorination by hypochlorous acid (HOCl) leads to the formation of trichloramine (NCl_3) (see Figure 3.6). Considering this, many previous authors suggest urea to be the predominant precursor for trichloramine formation under swimming pool water conditions [61, 136, 170, 192]. It is important here to note that the enzymatic transformation of urea to ammonia via urease has been reported to be negligible under swimming pool water conditions [193]. Further, the reaction of HOCl with α-amino acids (e.g. l-histidine) and creatinine has been found to induce trichloramine formation as well [29, 61].

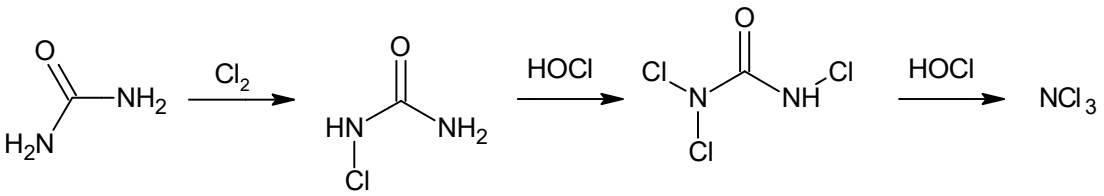

Figure 3.6: Pathway for the formation of trichloramine (NCl_3) from chlorination of urea [136].

Mono- and dichloramine have been proposed previously to be main educts for the formation of highly cancerogenic N-nitrosodimethylamine (NDMA). Two main formation pathways for NDMA have been reported previously between mono- or dichloramine and dimethylamine (DMA), a substance that is ingested in our food, is formed by normal human intestinal flora and is synthesized endogenously by mammals [194]. The slow reaction between monochloramine and DMA is initially

induced by the formation of unsymmetrical dimethylhydrazine (UDMH). In a second step, NH_2Cl oxidizes UDMH to form NDMA (<3% yields) (Figure 3.7) [195, 196].

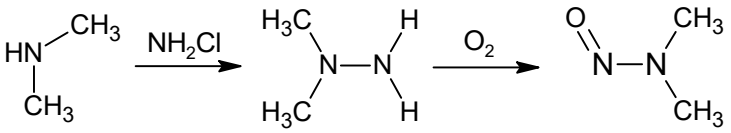

Figure 3.7: Pathway for the formation of NDMA from the reaction of monochloramine with DMA.

A faster pathway for NDMA formation has been proposed by Schreiber and Mitch (2006) by the reaction of dichloramine with DMA. Initially, chlorinated UDMH is assumed to be formed, followed by the oxidation of chlorinated UDMH to NDMA by the incorporation of dissolved oxygen (Figure 3.8) [157]. Under typical swimming pool water conditions, the majority of NDMA formation is assumed to take place via the dichloramine pathway [157].

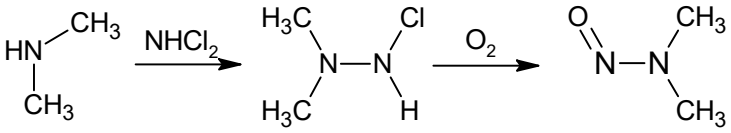

Figure 3.8: Formation pathway of NDMA from the reaction of dichloramine and DMA.

3.3.2.3 Halogenated acetic acids (HAA)

A general approach to describe the formation pathway of HAAs by the reaction of chlorine with organic matter has been proposed by Hua and Reckhow (2008) (see Figure 3.9). It has been suggested that the initial chlorine substitution shown in Figure 3.9 is the rate limiting step for the overall reaction [27].

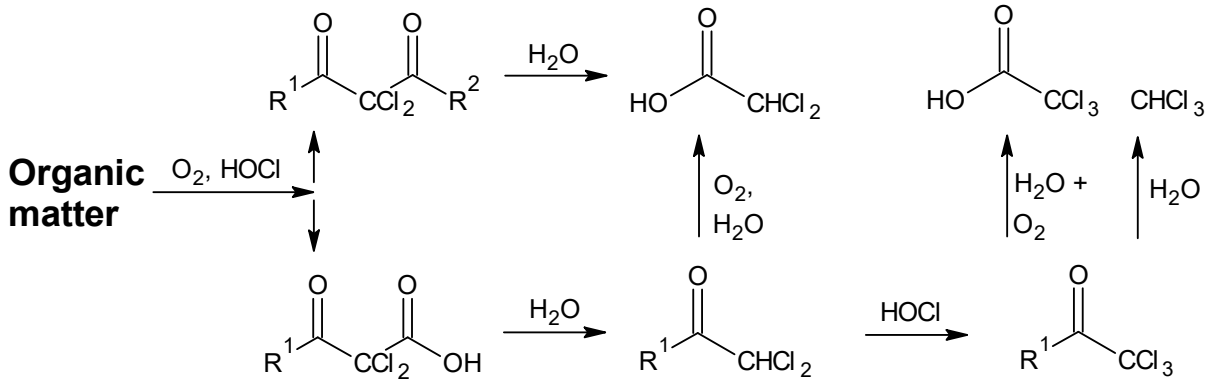

Figure 3.9: Simplified pathway for the formation of HAAs and THMs from the reaction of chlorine/chloramines with organic matter (according to [197]).

Previous studies by Kanan and Karanfil (2011) showed that chlorination of almost all BFA substances and humic acids leads to the formation of HAA. Amongst these substances, chlorination of citric acid and humic acids comprised the highest formation potential for HAAs [35]. Previous chlorination studies revealed that more THMs than HAAs are formed from organic matter present in filling water (e.g. humic acids), while more HAAs than THMs are formed from organic matter released by bathers (e.g. body fluid analogues (BFA)) [35, 59].

3.3.2.4 Haloacetonitriles (HAN) and other nitrogen containing DBPs

Haloacetonitriles (e.g. dichloroacetonitrile) and other nitrogen containing DBPs (e.g. cyanogen chloride and trichloronitromethane) are primarily formed via the reaction of amines and amino acids (e.g. l-histidine, glycine) with free chlorine. Trichloronitromethane is suggested to be solely formed from the reaction of amino acids with free chlorine [29, 30]. At an ratio of Cl:N > 1, the reaction of HOCl with amino acids leads to the formation of nitriles. In a second chlorination step, chlorinated nitriles such as cyanogen chloride (CNCl) and chloroacetonitriles are formed. A comprehensive reaction scheme on the formation of nitriles and other nitrogen compounds from the chlorination of amides and amino acids has been proposed by Schmalz (2012) [183].

3.3.3 Exposure path ways, adverse health effects and toxicity of disinfection by-products

Knowledge about exposure pathway of DBPs in swimming pools is of particular interest to properly access their toxicity and health effects on bathers. The published data on swimming pool exposure in the literature includes information on only a few single DBPs [198] found in pool water which likely comprises up to >600 DBPs [45]. The few exposure assessments reported primarily focused on THMs, HAAs and trichloramine. In swimming pool systems, exposure via the dermal, inhalation and ingestion route appears to be important while the main exposure route depends on individual characteristics of the DBP of interest (see Figure 3.10) [199].

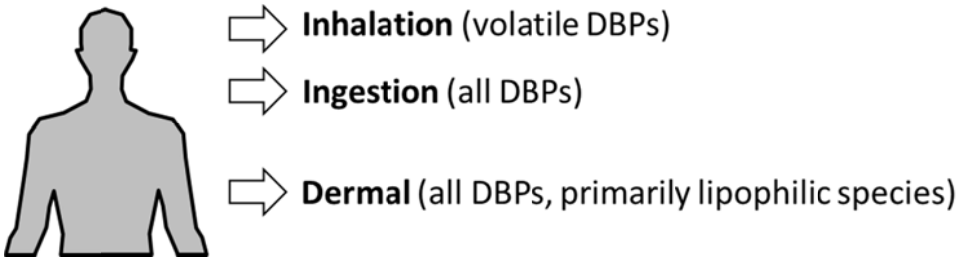

Figure 3.10: Exposure routes of DBPs in swimming pool systems.

By correlating the chloroform concentration in human blood, urine and alveolar air with that found in pool water and pool air, Erdinger et al. (2004) and Caro and Gallego (2008) showed that inhalation is more relevant for the uptake of volatile DBPs compared to the dermal route. Approximately 24 – 30 % of chloroform body burden results from dermal uptake while the remaining body burden is assigned to inhalation [1, 200, 201]. Further, exposure of THMs has been found to be less toxic via ingestion than via dermal absorption and inhalation. This effect is caused by enzymatic detoxification reactions in the liver that degrade DBPs [202]. Although a comprehensive exposure assessment for trichloramine (four times as volatile as chloroform) is still subject to investigation, the majority of existing analytical and epidemiological studies focus on trichloramine exposure via inhalation [61, 97, 203]. Since HAAs are non-volatile on the one hand and hydrophilic (e.g. with little skin permeability) on the other hand, ingestion has been found to be the major exposure route (94% of the total bod burden), followed by inhalation (via aerosols [204]) and the dermal route [205]. Given the complexity of hazardous DBPs in swimming pools, the beneficial effects of swimming with regard to recreation and sport must be confronted with the potential health risks associated with being exposed to these DBPs [198]. Epidemiological studies revealed correlations between attending chlorinated swimming pools (e.g. being exposed to different DBPs) and the following adverse effects on human health: (i) eye, skin and respiratory tract irritations (inorganic chloramines (primarily trichloramine)) [169], (ii) development of asthma (trichloramine) [42], (iii) bladder cancer (THMs) [44, 206] and (iv) adverse reproductive outcomes (controversial results for different DBPs) [207]. The toxicity of hazardous substances such as DBPs is typically characterized by their cytotoxicity and genotoxicity. The cytotoxicity describes the biological compatibility of a single substance by determining physiological effects of cells resulting from exposure. The genotoxicity is determined as a measure for the DNA damage caused by the substance. Table 3.10 lists DBPs found in swimming pool water according to their cytotoxicity and genotoxicity.

Table 3.10: Selection of DBPs found in pool water ranked according to their cyto- and genotoxicity (decreasing order) [168, 183].

Cytotoxicity	Genotoxicity
Dibromoacetonitrile, =Iodoacetonitrile	Iodoacetic acid
Bromonitromethane	Dibromoacetonitrile
Bromoacetic acid	Halogenated nitromethanes
Dichloroacetonitrile	Bromochloroacetonitrile
MX (3-chloro-4-(dichloromethyl)-5-hydroxy-2(5H)furanone)	Chloroacetonitrile
Chloronitromethane	Chloronitromethane
Tribromoacetic acid	Bromoacetic acid
Iodoacetic acid	Iodoacetonitrile
Dibromonitromethane	Chloroacetic acid
Bromochloroacetonitrile	Trichloroacetonitrile
Bromodichloronitromethane	Tribromoacetic acid
Chloroacetonitrile	Dibromonitromethane
Dichloronitromethane, =Trichloronitromethane	Bromoacetonitrile
Dichloroacetic acid	MX (3-chloro-4-(dichloromethyl)-5-hydroxy-2(5H)furanone)
Bromoacetonitrile	=Dichloronitromethane
Dibromochloronitromethane, =Tribromonitromethane	Dibromoacetic acid
Bromochloronitromethane	Dichloroacetonitrile
Trichloroacetonitrile	
Dibromoacetic acid	
Chloroacetic acid	
Trichloroacetic acid	

3.4 Swimming pool operation and requirements for pool water quality

A swimming pool system basically consists of a closed water cycle between the basin and the water treatment section. A simplified flow scheme of a common swimming pool system, which is in-line with the German pool standard DIN 19643, is presented in Figure 1.1. Swimming pool water taken from the basin (overflow water and splash water) is led into a splash water tank by gravitation. The splash water tank functions as a compensation and storage tank. To prevent accumulation of hazardous substances and microorganisms in the pool water cycle (e.g. due to an ineffective treatment section [53]), a proportion of 30 L per bather of fresh water is led into the splash water tank for the purpose of dilution. As fresh water has to have almost drinking water quality, it is typically taken from water mains [208]. The raw water taken from the splash water tank is actively fed by a pump into the treatment section. Finally, the treated water is fed back into the basin [26].

The hydraulic residence time of a swimming pool basin and thus, the total turnover water flow is not directly given by the German DIN regulation. Instead, the turnover water flow Q (in L h^{-1}) is calculated depending on the type of pool (e.g. swimming

pool, diving pool), the pools size and the treatment scheme employed (see Equation (3.11)) [26].

$$Q = \frac{N_b}{k_t} = \frac{A_p \cdot n_b}{a_b \cdot k_t} \quad (3.11)$$

Here, N_b is the maximum allowed attendance rate of bathers entering the pool (in h^{-1}) and k_t (in m^{-3}) is a specific loading factor that depends on the treatment concept employed and equals the maximum amount of bathers permitted to enter the pool per cubic meter of treated pool water (e.g. 0.5 m^{-3} for combinations of processes with fixed-bed filters and precoat filters). In Equation (3.6), N_b is calculated as the product of $A_p \cdot n_b \cdot a_b^{-1}$ where A_p (in m^2) is the total surface area of the respective pool basin, n_b (in h^{-1}) is the frequency factor for bathers entering the pool (typically taken as 1) and a_b is the specific surface area that is assigned to a bather during his activities in the pool (e.g. 4.5 m^2 per bather for swimming pools or 2.7 m^2 per bather for non-swimmer pools). Table 3.11 shows the typical residence times of different pool types calculated according to the German DIN 19643.

Table 3.11: Selection of dimensions and residence times of different types of swimming pools according to DIN 19643 [26]. A conventional water treatment comprising a loading factor (k_t) of 0.5 m^{-3} was considered for all pool types.

Pool type	**A_p in m^2 (Volume in m^3)**	**a_b in m^2**	**n_b in h^{-1}**	**Q in m^3 h^{-1}**	**Residence time in h**
Swimmer pool	750 (1575)	4.5	1	333	4.7
Non-swimmer pool	511 (409)	2.7	1	379	1.1
Hot water pool	511 (613)	4	2	511	1.2

Since water used for initial filling of pool basins has to have drinking water quality [26], pool water initially contains only a few mg L^{-1} of dissolved organic carbon (DOC) and thus, is not favorable for microbial growth [165]. However, with increasing attendance of bathers, the concentration of organics increases until a steady state is reached due to the dilution of pool water with fresh water (typically after ~150 - 600 h of operation [51]). As contact times in swimming pools are very long (see Table 3.11), pool water becomes a potential environment which favors the growth of microorganisms that are introduced by bathers (see Table 3.2) which in turn causes serious health issues [21]. These include infections of skin, eyes, middle ear and the alimentary tract [209, 210]. Thus, to assure hygienically safe pool water, the German pool water norm (DIN 19643) requires (i) disinfection, (ii) treatment of pool water as well as (iii) the continuous surveillance of microbiological, chemical and physical water quality parameters (see Table 3.12).

Microbiological water quality parameters

Due to the huge variety of microbiological contaminants found in pool water (Table 3.1), only the concentration of a selection of indicator organisms is measured on a regular basis in pools in Germany (including E. coli, Coliform bacteria, Pseudomonas aeruginosa and Legionella pneumophila (see Table 3.12)). Interestingly, no European norm implemented Cryptosporidium oocysts or Giardia lamblia cysts for regular monitoring in swimming pools [211], although they have been found to be highly chlorine resistant (see c·t values in Table 3.6). Further, the concentration of viruses which have been associated with serious infections in swimming pools as well (e.g. Adenovirus, Enterovirus or Norovirus [21]) is not subject to regular surveillance in any European country at the moment.

Chemical and physical water quality parameters

In Germany, only disinfectants based on chlorine got permission to be used in swimming pool water treatment. The minimum and maximum concentrations of free chlorine (as Cl_2) permitted in the basin are given in Table 3.12. The reason for higher chlorine concentrations in other countries such as the US primarily results from the indicator organism used to access the demand of disinfectant need for hygienically safe pool water. In Germany for instance, the concentration of the chlorine sensitive bacteria Pseudomonas aeruginosa has to be lowered by 4 log values within 30 seconds of contact time with the chlorinated pool water [26]. Due to the fact that HOCl (pK_a = 7.54) comprises the highest oxidation potential among the various chlorine species, the pH of pool water has to be maintained between pH 6.5 – 7.2 [26] in German pools (see Table 3.12).

Organic as well as inorganic impurities may react with free chlorine, lowering the concentration of disinfectant present in pool water. To provide a sufficient level of free chlorine in pool water, the concentration of substances potentially being able to be oxidized by free chlorine is limited in German pools by means of the oxidative capacity. The oxidative capacity of pool water is measured as the consumption of potassium permanganate ($KMnO_4$)) [212]. Manganese is present in its highest oxidation state in the permanganate anion (MnO_4^-) and thus, acts as a strong oxidant in redox reactions. MnO_4^- comprises almost the same standard redox-potential (+1.51 V) compared to HOCl (+1.49 V) [28] and thus, is a suitable indicator to assess only those substances that comprise a certain reactivity towards free chlorine. Some countries use the total organic carbon concentration (TOC) instead of the oxidative capacity to access the quality of pool water (e.g. in Switzerland [123]).

The concentration of disinfection by-products (DBPs) is routinely monitored in the pool basin by means of the not well defined sum parameter “combined chlorine” and

total trihalomethanes (TTHM). Combined chlorine, which represents the sum of all inorganic chloramines (mono-, di- and trichloramine), is considered to be an general indicator parameter for DBPs and thus, is monitored continuously on site by online acquisition [183].

Table 3.12: Limits for a selection of water quality parameters regulated in German pool water [26]. Values are given for a standard swimming pool with conventional water treatment using aluminum based coagulants (i.e. k_t = 0.5).

Parameter	**Treated water**		**Pool water**		**Unit**
	min	**max**	**min**	**max**	
Microbiological water quality parameters					
Heterotrophic plate count	-	20	-	100	CFU[a] mL^{-1}
Escherichia coli	-	0	-	0	CFU 100 mL^{-1}
Pseudomonas aeruginosa	-	0	-	0	CFU 100 mL^{-1}
Legionella spp.	-	-[b]	-	-[b]	CFU 100 mL^{-1}
Chemical and Physical water quality parameters					
Free chlorine	0.3		0.3	0.6	mg L^{-1} (as Cl_2)
pH value	6.5	7.2	6.5	7.2	-
Turbidity	-	0.2	-	0.5	FNU[c]
Specific absorption coefficient at 436 nm	-	0.4	-	0.5	m^{-1}
Acid capacity to pH 4.3	-	-	0.7	-	mmol L^{-1}
$KMnO_4$ consumption (O_2 consumption)	-	2 (0.5)	-	3 (0.75)	mg L^{-1}
Nitrate	-	-	-	20	mg L^{-1} (above the nitrate concentration of filling water)
pH value	-	6.5	7.2	6.5	-
Combined chlorine	-	0.2	-	0.2	mg L^{-1} (as Cl_2)
Trihalomethanes	-	-	-	0.02	mg L^{-1} (as chloroform)
Bromate	-	-	-	2.0	mg L^{-1}
∑ Chlorite + chlorate	-	-	-	30.0	mg L^{-1}

[a] … Colony-forming units (CFU)
[b] … Measures to be taken in case that Legionella have been detected are described in DIN 19643
[c] … Formazine nephelometric units (FNU)

3.5 Water treatment and DBP mitigation strategies in swimming pool systems

3.5.1 General aspects

Besides treatment of swimming pool water by technological processes, the following strategies that contribute to the reduction of DBPs, DBP precursors and microorganisms in swimming pool water have been reported previously:

(i) Pre-swim showering of bathers to reduce both chemical and microbiological pollutants introduced into swimming pool water [24, 97].
(ii) Dilution of pool water by addition of fresh water [213].
(iii) Mitigation of DBP formation by pH and temperature adjustment [177].

Whilst the current state of knowledge regarding the treatment efficiency of conventional and novel pool water treatment technologies will be presented in more detail in the following Chapters, the strategies mentioned above (i, ii and iii) are not further discussed in this thesis since they were out to the overall scope.

Combinations of water treatment processes permitted to be used in public swimming pools in Germany are defined in the standard DIN 19643. In the years 1997 and 2000, four treatment methods have been defined:

(i) Adsorption - flocculation - filtration - chlorination
(ii) Flocculation - filtration - ozone treatment - fixed-bed adsorption - chlorination
(iii) Flocculation - ozone treatment - multilayer filtration - chlorination
(iv) Flocculation - filtration - fixed-bed adsorption - chlorination

These combinations are typically referred to as “conventional” water treatment concepts. In the year 2012, the DIN 19643 was reworked and processes based on ultrafiltration and UV irradiation (medium pressure mercury lamps) were added. The way of how different processes could be combined has been left more open compared to previous versions of the DIN 19643 [214]. The following permitted treatment combinations are described in DIN 19643 (2012):

DIN 19643-2 (Process combinations including fixed-bed and precoat filtration) [56]:

(i) Flocculation - filtration - chlorination
(ii) Flocculation - multi-layer filtration with activated carbon - chlorination
(iii) Adsorption at powdered activated carbon - flocculation - filtration - chlorination
(iv) Flocculation - filtration - adsorption at granular activated carbon - chlorination
(v) Flocculation - filtration - UV irradiation (medium pressure Hg-lamp) - chlorination
(vi) Flocculation - multi-layer filtration with activated carbon - UV irradiation (medium pressure Hg-lamp) - chlorination
(vii) Adsorption at powdered activated carbon - precoat filtration - chlorination

DIN 19643-3 (Process combinations including ozone treatment) [215]:

(i) Flocculation - filtration - ozone treatment - fixed-bed adsorption - chlorination
(ii) Flocculation - ozone treatment - multi-layer filtration (with adsorbent) - chlorination

DIN 19643-4 (Process combinations including ultrafiltration) [208]:

Process combinations with ultrafiltration (UF) include all combinations mentioned in DIN 19643-2 but instead of a single- or multi-layer filter, an ultrafiltration membrane is used.

3.5.2 Removal of DBPs and DBP precursors with conventional and novel water treatment technologies

3.5.2.1 Coagulation-flocculation and sand filtration

The coagulation-flocculation process facilitates the agglomeration of suspended, colloidal particles and, to a certain extent, dissolved substances, which enhances their removal in the downstream sand filter. Only salts of aluminium or iron are allowed to be used as coagulants in pool water treatment in Germany [26].

Until now, relatively little is known about the capability of common sand filters to remove microorganisms, DBPs and dissolved organic matter from pool water. Removal rates obtained from slow sand filters (0.05 – 0.3 m h^{-1} [216]) operated for

drinking water treatment are hardly transferable to the pool water setting, where rapid sand filters are operated at very high filter velocities of 25 - 30 m h^{-1} [26, 72]. Transferability of results obtained by using rapid filters for drinking water treatment to the pool water setting are difficult as well since the mean molecular weight of organic matter found in pool water is smaller compared to that of drinking waters or raw waters due to (i) the introduction of low molecular weight substances by the bathers [114] and (ii) the oxidative bond cleavage in organic molecules initiated by free chlorine present in pool water (see Section 3.3.2). These low molecular weight substances are hardly removable by the flocculation sand filtration process [217], especially under the low coagulants doses applied in pool water treatment. A survey from the year 2006 which included 36 German swimming pools revealed that approximately 50 % of the surveyed pool facilities used doses of 0.001 – 0.002 g (as Al) of alumn-based coagulants per m^3 of pool water [218]. This range even falls below the minimum level of coagulant doses required by the DIN 19643 (>0.05 g m^{-3} (as Al)) [56]. Typical DOC removal values for sand filters operated in pool water settings are reported to be as low as 10 % [102]. Conclusively, conventional water treatment (flocculation-sand filtration) was rated to insufficiently remove pool water contaminants, especially under heavy bather load [52].

Further, sand filters have been found to be incapable to significantly reduce the concentration of AOX and low molecular weight DBPs in pool water. Instead, it has even been found that long backflush cycles of sand filters (several days) lead to long contact times of particulate matter accumulated in the filter bed with free chlorine. Under certain operation condition, the accumulation of organic material in the filter and subsequent reaction with free chlorine leads to the formation of DBPs across the filter bed [219]. Given the poor efficiency of deep bed filters for the removal of dissolved substances, the flocculation sand filtration process is primarily applied in pool water treatment with the aim to remove particulate and colloidal matter form the aqueous phase. Previous research has shown that Cryptosporidium oocysts (size of 4.9 µm [220]) or equally sized polystyrene spheres (1 – 7 µm) are removed by 0.4 – 2.0 log units in rapid sand filters operated under pool water conditions with addition of coagulants [221, 222]. Removal values are much lower for conventional deep bed filters operated without the addition of coagulants (<0.3 log units [222]).

3.5.2.2 Membrane filtration

In recent years, pool water treatment concepts based on ultrafiltration (UF) became promising alternatives to conventional water treatment processes based on sand filters [219, 223, 224]. Given its small pore size of <100 nm, UF membranes are

physical barriers with high removal efficiencies for relevant human pathogens as small as viruses [225]. A breakthrough of microorganisms as it might occur for sand filters is unlikely as long as membrane integrity is ensured [226]. UF membrane treatment is often used in combination with PAC as adsorptive coating material [227-229]. However, comparative studies by Glauner (2007) revealed that both, UF alone as well as UF with PAC coating were not capable to significantly remove DOC from swimming pool water [102, 230]. Further, UF alone was not capable to remove volatile DBPs due to their low molecular weight, which is typically smaller compared to the molecular weight cut-off of the UF membrane [55]. UF in combination with PAC has a certain advantage compared to sand and GAC filtration with regard to the consumption of free chlorine. While up to 82 % of free chlorine remains in the water body when using UF in combination with a PAC coating, no free chlorine was present when sand filtration with subsequent GAC filtration was used for water treatment [102]. Previous studies showed that operational costs of UF processes for swimming pool water treatment are approximately higher by a factor of 2 compared to conventional processes based on sand filters [224].

To reduce operational costs of membrane processes, microfiltration (MF) membranes featuring higher permeabilities compared to UF could be used. However, MF membranes comprise larger pore sizes compared to UF membranes. It is still subject to future research to elucidate removal efficiencies of MF membranes under typical pool water conditions and compare the results to UF membranes as well as conventional sand filters.

Previous studies showed that MF and UF membranes have a limited ability to remove dissolved organic impurities [55, 231]. Nanofiltration (NF) membranes instead comprise a lower molecular weight cut-off compared to UF membranes and thus, are capable to remove a considerable proportion of dissolved organic matter from pool water(~40 - 60 %). Removal values were approximately three times as high compared to UF [55]. Both UF and NF membranes predominantly remove compounds with high molecular weight (e.g. humic substances) [230] while only NF membranes were capable to remove a significant proportion of low molecular weight, non-volatile compounds. These compounds have been found to compromise a high genotoxicity compared to other molecular size fractions of organic matter found in pool water [46]. Despite its low molecular weight cut-off, NF alone was also not capable to significantly remove low molecular weight DBPs such as THMs [54]. Despite its superior removal of dissolved organic components from pool water, operation of NF membranes in pool water treatment is not considered to be a feasible process due to economic reasons (e.g. high energy consumption) [232].

3.5.2.3 Oxidation by free chlorine and ozone

Free chlorine is the most common disinfectant used in swimming pools. Due to its high oxidation potential (see Section 3.2.2), free chlorine reactions with organic matter present in pool water partially lead to the complete removal of organic-C compounds by mineralization or volatilization [53]. Further, ammonia and inorganic chloramines could be fully oxidized under the formation of more innocuous products (nitrogen, nitrous oxide and nitrate) at a stoichiometric excess of chlorine over nitrogen. This process is referred to as “breakpoint” chlorination [28]. However, previous research implies that some organic-N and organic-C compounds present in pool water (e.g. urea, creatinine and amino acids) are not fully mineralized even under breakpoint conditions thus, forming hazardous DBPs [29, 233-235].

Besides using chlorine alone, combined treatment by chlorine and ozone is used in pool water treatment. Ozone is a strong oxidizing agent and directly reacts with the treatment targets (e.g. DOC) in a specific oxidation reaction (see Equation (3.12)). Previous studies showed that ozone reacts only slowly with organic N-compounds, organic C-compounds and ammonia [236, 237]. The reaction of ozone with chlorinated C-compounds is even slower. Since ozone competes with chlorine for the same sites in organic molecules to be oxidized, the chlorine reactivity towards DOC present in pool water decreases and thus, the formation of DBPs decreases [55, 238-240].

$$DOC + O_3 \rightarrow DOC_{\text{selectively oxidized}} \quad (3.12)$$

$$H_2O + O_3 \rightarrow O_2 + 2\ OH\bullet \quad (3.13)$$
(catalyzed by OH^-, slow at low pH [242])

$$DOC + OH\bullet \rightarrow DOC_{\text{radical oxidized}} \quad (3.14)$$

Due to the low reactivity of ozone with organic matter, it partly decompose to secondary oxidants such as hydroxyl radicals (OH•, Equation (3.13) [242]), which in turn oxidize a range of dissolved pollutants in a non-specific and fast oxidation reaction (Equation (3.14)). The reaction of organic matter with hydroxyl radicals increases the DBPs formation potential during chlorination [55, 164]. The reactivity of ozone towards DBPs is only slow while the reactivity of the secondary oxidant OH• is much higher. For instance the reaction rate constant of monochloramine with ozone is very slow ($k = 2.6 \cdot 10^1$ L mol^{-1} s^{-1} [236]) while it is $2.8 \cdot 10^9$ L mol^{-1} s^{-1} for the reaction of OH• with DBPs [241]. It has to be noted here that the formation of hydroxyl radicals is a complex process and Equations 3.13 and 3.14 represent only a very simplified reaction scheme.

Previous research that elaborated on the use of ozone in swimming pool water treatment prior to chlorination revealed that ozone treatment alone only slightly removed organic carbon (by mineralization) [55] while it increased the THM formation potential. However, the THM formation potential decreased with subsequent ozone treatments (e.g. with increasing turnover times) [242]. Further, ozone treatment has been found to significantly decrease the formation potential of AOX in pool water and the concentration of inorganic chloramines [55, 243]. According to the German pool standard DIN 19643, all or a part of the recirculated pool water is ozonated at contact times >3 min [215]. To prevent ozone escaping to the air above the swimming pool and to prevent the formation of chlorate in the swimming pool [244], ozone residues have to be fully degraded in a granular activated carbon filter (GAC filter), which has to be implemented downstream to the ozonation. Interestingly, only a small proportion of the ozone dosage reacts with organic matter while the major proportion of ozone is destroyed in the GAC filter [237].

3.5.2.4 Activated carbon treatment

Activated carbons are widely used in water treatment processes. All conventional pool water treatment combinations permitted in Germany (Section 3.5.1) include either powdered activated carbon (PAC) or granular activated carbon (GAC) treatment [245].

While fixed-bed filters comprising GAC are typically placed behind a filtration step (see Section 3.5.1), PAC is typically dosed inline, prior to the filtration step and prior to dosing of the coagulants [228].

Until now, only little is known about the removal performance of PAC or GAC treatment with regard to the removal of DBPs or organic precursor substances from the oxidative environment of swimming pool water. The majority of data reported on the performance of PAC or GAC has been generated in the field of drinking water production [246]. Given the different nature of organic matter found in pool water and the complexity of swimming pool facilities (bather load, water circulation, elevated temperature, presence of chlorine) the transfer of results of activated carbon performances found in the field of drinking water treatment to pool water settings is only hardly possible [54].

The main advantage of using an adsorptive precoat PAC layer instead of a GAC filter is the fact that loaded PAC is removed from the system with each backflushing cycle of the corresponding sand filter or membrane while the GAC filter is typically operated for 1 - 2 years before exchanging the carbon grains. Thus, impurities that

are adsorbed on the PAC surface immediately leave the pool water system without being available for further reactions with free chlorine. However, waste management for PACs taken from pool water processes is typically difficult due to the high AOX content of of used PAC from pool water treatment [228].

Activated carbons adsorb a multiplicity of organic substances mainly by π-π interactions (in the case of aromatic adsorbates), weak intermolecular interactions (e.g. van der Waals forces) or, with minor relevance, by electrostatic interactions between the carbon surface and the organic molecules [246, 247]. The overall process of adsorption depends on both, the adsorption capacity of the adsorbent and the time required to reach the state of adsorption equilibrium (adsorption kinetics) [246].

Data reported about the adsorption capacity of activated carbons for low molecular weight substances introduced by the bathers (i.e. body fluid analogues, see Section 3.1.3.1) is very scarce. The little data reported regards mainly the adsorption capacity of activated carbons for ammonia, which has been reported to be poor due to the nonpolar surface chemistry of activated carbons [248, 249]. Previous studies revealed that the surface chemistry of activated carbons is one of the major factors influencing the adsorption mechanism of organic molecules from dilute aqueous solutions [250-252]. It revealed for instance that carbons with a high polarity (typically expressed as the sum of the N and O content) have been shown to comprise a low adsorption capacity and vice versa [253]. Further, the surface charge has been shown to influence the overall adsorption capacity. Previous studies showed that starting from neutral conditions, decreasing the pH value for a certain degree lowers the proportion of negative charges on the carbons surface and in organic matter leading to a more neutral surface charge at the sheer plane (i.e. the zeta-potential). It has been shown for some organic water impurities that this change in the surface charge increases the overall adsorption capacity of activated carbons [247]. However, the pool water pH is regulated in Germany to pH 6.5 – 7.2, giving only little potential for optimization in this regard. Physical properties of the carbon such as the internal pore surface and the pore size distribution have been rated to be important for the adsorption process as well. In particular, the proportion of pores with a width of 1.3 – 1.8 times the kinetic diameter of the targeted adsorbate control the overall adsorption capacity of activated carbons [254]. For most organic contaminants found in pool water (see Table 3.5), this relevant pore size falls in the size range of secondary micropores (0.8 – 2 nm) and mesopores [255, 256]. Previous studies revealed that complex organic matter such as humic acids that are introduced via filling water (see Section 3.1.3.2) may block the micropore region of activated

carbons [257]. Consequently, the adsorption capacity for organic pollutants with low molecular weight introduced by bathers may decrease more dramatically for microporous carbons than in adsorbents with larger pores [257]. The effective molecular size of the adsorbate has also been shown to be a crucial factor for the adsorption capacity of carbons. Activated carbon adsorption is suggested to be more effective for low molecular weight substances (BFA substances) compared to high molecular humic substances (humic acids) [258]. The adsorption capacity of activated carbons for humic substances has been shown to drop rapidly with ongoing filtration time due to constraints resulting from pore blockage [258].

Trihalomethanes (THMs) and haloacetic acids (HAA), two of the major DBP classes found in pool water, are usually removed from the aqueous phase by adsorption via activated carbon treatment [245]. The breakthrough capacity of a GAC filter containing a bituminous coal carbon (Filtrasorb F-400, Chemviron Carbon) operated under drinking water conditions were 2.83 g kg_{GAC}^{-1} (TTHM, as $CHCl_3$) and 4.37 g kg_{GAC}^{-1} (HAA5) [259]. The better adsorbability of HAAs compared to THMs has been shown in PAC applications in the field of drinking water treatment as well [260]. However, no data exists for the breakthrough behaviour of DBPs in GAC filters or precoat PAC layers operated under oxidative swimming pool conditions. Some studies performed under pool water conditions even indicate that THMs could be produced across carbon filters operated under pool water conditions [245, 261]. This effect is caused by chlorine reactions with the adsorbed or desorbed organic matter [261] and depends on the empty bed contact time applied.

In most cases, the time dependent course of the adsorption process (i.e. the adsorption kinetics) in dilute aqueous solutions is limited by the mass transfer from the bulk phase to the adsorption sites within the carbon particles (e.g. intraparticle diffusion (i.e. pore diffusion and/or surface diffusion) and film diffusion). These mass transfer resistances determine the time required to reach the state of equilibrium [246]. Figure 3.11 presents a simplified scheme of the overall process of adsorption and (if applicable) surface reaction in carbon particles [262].

For fixed-bed adsorbers (i.e. GAC filter or precoat layers of PAC on top of a sand filter or a membrane), film diffusion affects the time depended adsorption behavior to some extent and should be considered when describing the overall adsorption process [227]. However, PAC is dosed into the piping system of a pool water treatment train before it is rejected by the subsequent filtration step. The time PAC is suspended inline the piping system before it is rejected typically is 30 – 40 s. Due to the favoring hydrodynamic conditions at high flow velocities in piping systems, film diffusion can be neglected there [246]. Adsorption kinetics of the rejected PAC are

assumed to primarily depend on diffusional processes and thus, the grain size of the respective activated carbon [229].

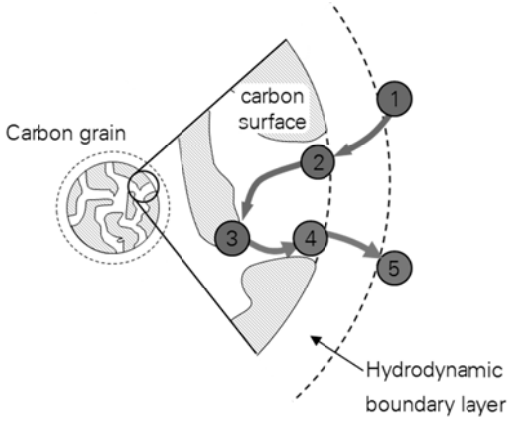

Figure 3.11: Steps of a heterogeneous reaction. (1) Film diffusion, (2) Intraparticle diffusion, (3) Adsorption, intrinsic chemical reaction and desorption, (4) Intraparticle diffusion and (5) Film diffusion.

It has been shown that free chlorine [263, 264] as well as inorganic chloramines [265, 266] are chemically reduced by surface reactions on activated carbons.

The process of degradation of free chlorine across an activated carbon filter in pool water treatment causes two major drawbacks: (i) free chlorine needs to be continuously dosed into the water stream behind the carbon filter to constantly assure the required free chlorine level in the basin and (ii) the lower, chlorine free, regions of activated carbon filters become microbiologically contaminated (e.g. with *Legionella pneumophila* [267] or *Pseudomonas aeruginosa* [245]). The latter affects the quality of the basin water with regard to the microbiological quality parameters given by German regulations (see Table 3.12). Further, microbial colonization blocks the pore system of GACs which might cause a low removal of organic matter across the bed depth [261]. However, it has been found that HAAs could be biologically degraded on the surface of biologically active filters leading to a significant HAA removal across a GAC filter of up to 60% depending on the empty bed contact time applied [261].

The progress of degradation of inorganic chloramines in activated carbon filters has been described previously, whereby studies primarily focused on the impact of operational parameters on the overall reactivity (i.e. the impact of: DOM present in the water body [254, 266], carbon type [254] and type of chloramine species [265, 266]). However, no study is known that particularly aimed at identifying processes that (i) limit the overall reaction rate of a GAC filter for chloramine removal

and (ii) affect the overall stoichiometry of the chloramine reaction. The stoichiometry of the chloramine-GAC reactions is of particular interest for pool water treatment because monochloramine, the predominant inorganic chloramine present in pool water [30], is only partly degraded to N_2 [266], which will not react any further with other substances present in pool water. The predominant proportion of monochloramine is transformed to NH_4^+, which will remain in the pool water cycle and reacts with chlorine in the pool basin forming inorganic chloramines again [268]. Detailed chemical equations are presented later in this thesis (see Section 5.1 and 6.2.5.2). It is still subject to investigation to point out the importance of the type of transformation product formed in GAC filters on the overall water quality of pool water, especially with regard to the surveillance parameter “combined chlorine” (see Table 3.12).

3.5.2.5 UV irradiation

In the last decades, UV irradiation has been increasingly used in pool water treatment to reduce the concentration of DBPs [48], DBP precursors [49] and to inactivate chlorine resistant bacteria such as *Cryptosporidium* species [269]. Although low pressure (LP) [162, 163] and medium pressure (MP) [48] mercury lamps have been applied for pool water treatment previously, only medium pressure UV lamps are permitted to be used in public swimming pools in Germany [56]. In other countries such as France, both, UV(LP) and UV(MP) lamps are permitted to be used for pool water treatment [270]. UV(LP) and UV(MP) mercury lamps differ with regard to the emission spectra and the electric outputs. While LP mercury lamps deliver primarily monochromatic UV irradiation at a characteristic wavelength of 253.7 nm and electrical powers of 75 to 300 Watts, MP lamps, whose power varies from 600 to 4000 Watts, are characterized by polychromatic output spectra [271].

Mineralization via direct photolysis of organic matter by UV(LP) irradiation has been reported to be negligible [272, 273]. However, UV(LP) irradiation is capable to induce significant structural changes in high molecular weight substances which leads to an apparent increase in lower molecular weight substances in the effluent of the UV reactor [274]. With regard to natural organic matter, larger molecules have higher molar absorptivities, absorb more photons and hence, photolysis proceeds faster compared to smaller molecules [275]. UV(MP) irradiation has been found to be capable to mineralize organic matter to a certain degree and thus, is capable to reduce the concentration of organic DBP precursors in pool water [49].

Combined UV/chlorine treatment in swimming pool systems has been found to degrade free chlorine (see Equation (3.15) - (3.17)), which leads to a higher overall

consumption of free chlorine in the pool system. HOCl and OCl^- have been shown to absorb photons in the UV-B and UV-C wavelength range, which leads to the decay of chlorine species in swimming pool water [130]. Previous studies showed that photolysis of HOCl and OCl^- induces the formation of reactive intermediates such as Cl•, OH•, OCl• and $O^{\bullet-}$ (Equation (3.15) - (3.17)) [132, 133]. HOCl has been shown to be a significant scavenger for the formed free radicals [134]. These secondary reactions between HOCl and the reactive intermediates as well as other chain termination reactions have been found to lead to additional depletion of residual free chlorine (Equation (3.17) - (3.21)). Final end products of the photolytical HOCl destruction are HCl, O_2 and $HClO_3$. To minimize the UV induced depletion of free chlorine in pool systems, chlorine dosing should always been placed downstream to a UV lamp [276].

$$HOCl + h\nu \rightarrow OH\bullet + Cl\bullet \quad (3.15)$$

$$OCl^- + h\nu \rightarrow O^{\bullet-} + Cl\bullet \quad (3.16)$$

$$HOCl + OH\bullet \rightarrow H_2O + OCl\bullet \quad (3.17)$$

$$HOCl + Cl\bullet \rightarrow HCl + OCl\bullet \quad (3.18)$$

$$Cl\bullet + OCl\bullet + H_2O \rightarrow 2\ HOCl \quad (3.19)$$

$$2\ OCl\bullet + H_2O \rightarrow HCl + HClO_3 \quad (3.20)$$

$$O^{\bullet-} + H_2O \rightarrow OH\bullet + OH^- \quad (3.21)$$

Further, combined UV/chlorine treatment of swimming pool water leads to the formation of highly reactive intermediates (e.g., $Cl^{\bullet}$, $OH^{\bullet}$, singlet oxygen ($^1O_2$) and $NH_2^{\bullet}$ [133, 134, 277]). Secondary reactions of organic matter with these intermediates, which are preferably formed by MP(UV) irradiation [49, 278], could lead to an additional mineralization of DOC present in pool water.

The impact of UV irradiation on the formation of DBPs, particularly THMs, has been intensively studied previously. Given that low molecular weight molecules are highly reactive with chlorine, UV induced structural changes of organic material towards low molecular weight substances initially increase the formation potential for THMs [279]. Only a sufficient removal of DOC by UV induced mineralization led to a mitigation of THMs [272]. Further, combined UV(MP)/chlorine treatment leads to the progressive transformation of bromoform ($CHBr_3$) into chloroform ($CHCl_3$) and dichlorobromomethane ($CHBrCl_2$). Since bromine–carbon bonds have a band

absorption in the spectral range of UV(MP) lamps and the energy needed to break bromine–carbon bonds is lower compared to the energy needed to break chlorine-carbon bonds, bromine atoms in bromoform are progressively substituted by chlorine atoms with ongoing UV treatment [49]. The effect of UV irradiation was most pronounced with regard to the reduction of THMs. However, experiments with sequential exposure to UV (either UV(LP) or UV (MP)) and free chlorine revealed an increase in the concentration of haloacetic acids (HAAs), cyanogen chloride (CNCl) [276] and inorganic chloramines [277]. Li and Blatchley (2009) found that UV induced degradation of inorganic chloramines leads to the formation of unwanted products such as nitrate, nitrite and nitrous oxide [277] and possibly ammonia [277, 280]. Other authors suggest that UV irradiation could be complemented by an downstream biological activated carbon treatment, where formed nitrite could be removed [281].

4 Comparing the impact of different water treatment processes on the concentration of DBPs and DBP precursors in swimming pool water.

Abstract

To mitigate microbial activity in swimming pools and to assure hygienic safety for bathers, swimming pools have a re-circulating water system ensuring continuous water treatment and disinfection by chlorination. A major drawback associated with the use of chlorine as disinfectant is its potential to react with organic matter (OM) present in pool water to form harmful disinfection by-products (DBP). Different combinations of conventional and novel treatment processes could be applied to lower the concentration of DBPs and OM in pool water. In this Chapter, the treatment performance of various treatment combinations was compared using a pilot scale swimming pool model that was operated under reproducible and fully controlled conditions. The quality of the pool water was determined by means of volatile DBPs and the concentration and composition of dissolved organic carbon (DOC). The relative removal of DOC across the considered treatment trains ranged between 0.1±2.9 % to 7.70±4.5 % while conventional water treatment (coagulation, sand filtration combined with granular activated carbon (GAC) filtration) revealed to be most effective. Microbial processes in the deeper, chlorine-free regions of the GAC filter have been found to play an important role in removing organic substances. Almost all treatment combinations were capable to remove trihalomethanes to some degree and trichloramine and dichloroacetronitrile almost completely. However, the results demonstrate that effective removal of DBPs across the treatment train does not necessarily result in low DBP concentrations in the basin of a pool. This raises the importance of the DBP formation potential of the organic precursors, which has been shown to strongly depend on the treatment concept applied. Irrespective of the filtration technique employed, treatment combinations employing UV irradiation as second treatment step revealed higher concentrations of volatile DBPs in the pool compared to treatment combinations employing GAC filtration as second treatment step.

4.1 Introduction

By their nature, people dispose microorganisms and organic substances into swimming pool water while bathing [22, 24]. To avoid microbiological pollution and to protect bathers from infections, pool water is disinfected using free chlorine [26]. By the reaction of organic substances with free chlorine, a wide range of harmful disinfection by-products (DBP) are formed. These halogenated reaction products are characterized as eye and skin irritating, carcinogenic or as triggers of respiratory problems [32, 41].

Many previous studies dealt with the occurrence and formation of DBPs in swimming pool water [31, 35]. More than 100 DBPs have been identified in swimming pools [33], with trihalomethanes (THM), halogenated acetic acids (HAA), chloramines (CA) and haloacetonitriles being the most studied examples [3, 30]. The amount and type of DBPs in swimming pool water depend primarily on the precursor load from the bathers, the composition of fresh water added to the pool and the type and dose of the disinfectant used [35]. To assure an efficient disinfection (i.e. low pathogenic risk) whilst having a minimal concentration of DBPs in the pool, swimming pool water is continuously circulated in a closed loop over a treatment train with the aim to reduce the concentration of organic substances and DBPs. The treatment train consists of different consecutive treatment steps.

Besides conventional water treatment processes such as coagulation sand filtration or granular activated carbon (GAC) filtration, treatment combinations including novel technologies such as ultrafiltration (UF) or UV irradiation are increasingly used for pool water treatment [3, 55]. However, only a few studies determined the impact of UF and UV irradiation on the water quality in pools [3, 49, 162, 231, 282-284]. The few results reported are hardly comparable because the loading with organic substances varied among the different test pools. In order to compare the efficiency of different pool water treatment technologies, pilot studies have to be carried out under fully controlled conditions (i.e. controlling of the load with organic matter, operation conditions and fresh water quality).

Solely Judd et al. (2000) and Goeres et al. (2004) established a swimming pool system in compliance with the before mentioned provisions [53, 122]. Goeres et al. focused their work on biofilm formation and did not further evaluate the removal efficiencies of different treatment processes. Judd et al. compared different swimming pool water treatment technologies using a pilot scale swimming pool model. However, the authors stated that the number of treatment combination compared was not enough to get a full picture of the various treatment combinations

typically used in swimming pools. Moreover, the assessment of the water quality was limited to a small selection of DBPs [285], not respecting other relevant nitrogenous DBPs such as trichloramine, dichloroacetonitrile or trichloronitromethane.

Concluding from the current state of knowledge, the aim of this Chapter is to compare the impact of different novel and conventional water treatment combinations on the concentration of DBPs and organic precursors in the basin. The results should help to assess the treatment efficiency of a high number of treatment combinations commonly applied in swimming pool water treatment on a reproducible basis.

4.2 Materials and Methods

4.2.1 The swimming pool model

4.2.1.1 Components

A pilot scale swimming pool model (Figure 4.1) that allows comparability to real indoor swimming pools by considering a high number of important system parameters and their interactions was established to compare different combinations of treatment processes. The model consists of a basin (1.6 x 0.8 x 2.1 m, L x W x D) with air space, a stirred (~200 rpm), double walled and temperature controlled splash water tank and a modular water treatment train. A pump P1 (CRNE1-7, Grundfos) takes water from the splash water tank and feeds it at a volume flow rate of 0.57 $m^3\ h^{-1}$ over the treatment train back into the basin by 48 evenly distributed nozzles at the bottom. The circulated water volume was calculated based on the water surface of the basin (A_p = 1.28 m^2) according to Equation (3.11) using a specific surface area a_b of 4.5 m^2 per bather, a frequency factor n_b of 1 and a loading factor k_t of 0.5 m^{-3}. The modular treatment train of the swimming pool model consists of conventional and novel treatment processes which are described in detail in Section 4.2.1.3. Two ventilators (V1 and V2) feed air into the air space above the basin. Air entered the air space by a perforated flow channel which was placed on the side walls right above the water level. The ratio between recirculated air (V1) and fresh air (V2) was controlled by two orifice plates to maintain an absolute humidity of 11 - 14 g kg_{air}^{-1} in 1.5 m above the water level. The air was heated by two in-line heating coils. Dimensions and flow rates of the pool model were chosen according to the German swimming pool standard DIN 19643 [26] and are described in the following Sections.

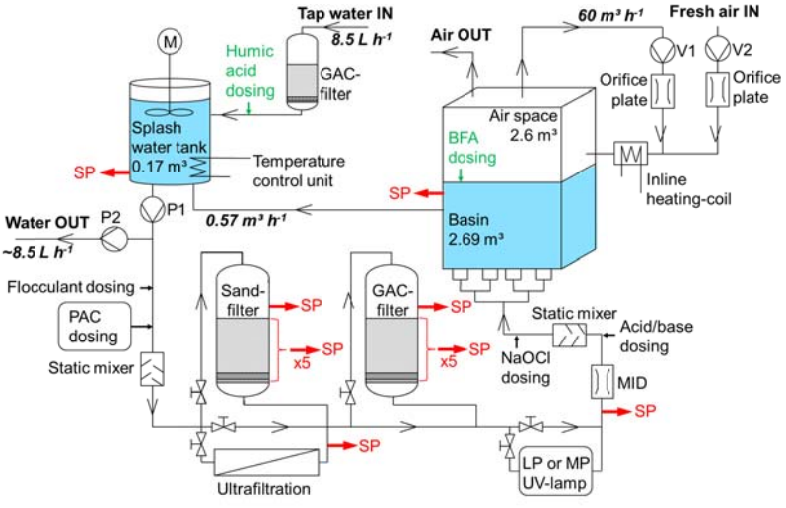

Figure 4.1: Flow scheme of the swimming pool model. Red arrows indicate sampling ports (SP denotes sampling ports).

4.2.1.2 Dosing of fresh water and bather load

In total 8.5 L h^{-1} of fresh water were fed in to the splash water tank for the purpose of dilution. This amount was calculated according to DIN 19843 using the maximum permitted bather loading of the pool model (~0.28 bather h^{-1}) and a fresh water flow rate of 30 L per bather [26]. To maintain a constant water volume in the system, the same amount of pool water was taken from the system by a peristaltic pump P2 (503S, Watson Marlow). Previous studies showed that the concentration and composition of DOC in tap water depend on the raw water source used for drinking water production (i.e. ground water or surface water) [35, 59] and seasonal changes [286]. To ensure fully controlled conditions, the local tap water used in this study was pre-treated by GAC filtration leading to a DOC of <0.1 mg L^{-1}. The low DOC-concentration of less than 0.1 mg L^{-1} was attributed to adsorption and biodegradation. After GAC filtration, a synthetic humic acids (HA) solution was added to the fresh water stream to reach a DOC concentration of 1 mg L^{-1} before it was dosed into the splash water tank. The dosed HA solution was prepared by dilution of a humic acids sodium salt (Sigma Aldrich) in deionized water and subsequently removing the colloidal and particular HA proportion by ultrafiltration (MWCO = 100 kDa). Tremendous amounts of HA were needed for operating the swimming pool model. Due to financial constraints, Sigma Aldrich HA has been used in this study instead of expensive natural humic substances extracted from aqueous solution (e.g. humic acids standard from the International Humic Substances Society). The input of soluble organic matter by the bather was simulated by dosing a body fluid analogue (BFA) [53] into the pool at 4 evenly distributed dosing points in 1.2 m water depth (~0.025 L h^{-1}). The BFA stock solution was prepared by dilution of the solid chemicals (all purchased from VWR, Germany) in deionized water. Table 4.1 summarizes the composition and dosing rate of the BFA substances. Dosing of all chemical was performed using peristaltic pumps (dulco flex DF4a, Prominent).

Table 4.1: Composition of the BFA stock solution and dosing rates applied in the swimming pool model.

BFA-substance	Molecular weight in Da	Concentration in the BFA mixture[a] in $g_{subst}\ L^{-1}$	Dosing rate in the pool model[b] in $mg_{subst}\ h^{-1}$ ($mg_{TN}\ h^{-1}$)
Ammonia chloride	53.49	1.21	30 (8.0)
Urea	60.06	8.95	224 (105.8)
Creatinine	113.11	1.11	27 (10.3)
Uric acid	168.11	0.30	7.4 (2.5)
Citric acid	192.12	0.39	9.7 (0)
L-histidine	155.15	0.74	18 (5.0)
Hippuric acid	179.18	1.06	26 (2.0)

[a] … As given by [53]

[b] … The dosing rate was calculated based on the amount of total nitrogen (TN) known to be introduced by bathers (~470 mg_{TN} per bather). This amount includes initial bathing load (80 mg_{TN} per bather), continual bathing load (120 mg_{TN} per bather) and accidental bathing load (270 mg_{TN} per bather) [100]. It was assumed that ~0.28 bather entered the pool model per hour.

4.2.1.3 Pool water treatment combinations

Table 4.2 presents the treatment combinations tested in the swimming pool model (Figure 4.1). The operation conditions of each single treatment process were chosen according to the German swimming pool standard DIN 19643 or according to recommendations of the module suppliers. Table 8.1 in the supporting information (SI) give further information about the design of each single treatment step and summarizes its operation conditions.

Table 4.2: Treatment combinations used for the pilot scale experiments.

Experiment No. (Exp.)	Treatment combination			
1	Flocculation	Sand filtration	GAC filtration	Chlorination
2	Flocculation	Sand filtration	UV irradiation (LP)[a]	Chlorination
3	Flocculation	Sand filtration	UV irradiation (MP)[a]	Chlorination
4	Flocculation	Ultrafiltration	UV irradiation (LP)[a]	Chlorination
5	Flocculation	Ultrafiltration	UV irradiation (MP)[a]	Chlorination
6	Flocculation	Adsorption at PAC[b]	Ultrafiltration	Chlorination
7	Flocculation	Adsorption at PAC[b]	Sand filtration	Chlorination

[a] … Low pressure (LP), medium pressure (MP)

[b] … Powdered activated carbon (PAC)

4.2.1.4 Operation of the swimming pool model

For each treatment combination, an individual experiment was performed according to the following procedure: (i) filling the basin and the treatment train with DOC-free tap water, (ii) starting water circulation (experimental run time t = 0) and (iii) starting continued dosing of BFA, HA, fresh water, chlorine, pH chemicals and coagulant for 24 h per day until DOC concentrations reached stationary conditions. The continuous loading with BFA and HA for 24 h was chosen to simulate the worst case scenario for a swimming pool system. All water and air flow rates of the swimming pool model are presented in Figure 4.1. Other standard operation parameters such as the concentration of free chlorine (c_{Cl2}), the pH value (pH), the temperature of pool water in the basin (T_{basin} measured in 0.12 m below the water level) and the air temperature in the hut (T_{air} measured in 1.5 m above the water level) were maintained on a constant level during all experiments by feedback control.

4.2.1.5 Sampling procedures

As presented in Figure 4.1, sampling ports for aqueous samples were placed before and after each pool water treatment step, in the basin (placed in 0.12 m below the water level) and over the bed depth of the GAC filter and Sand filter (placed in 0 m, 0.2 m, 0.4 m, 0.6 m, 0.8 m and 1.0 m across the bed depth). Automatic sampling was performed across the treatment train by consecutively opening magnetic valves at the sampling ports according to a pre-defined regime. After opening a sampling port, a water stream was fed at ~20 L h^{-1} to a standard electrode system, an online analyzer for dissolved organic carbon and a continuously operating membrane inline mass spectrometer for automatic analysis of volatile disinfection by-products.

Manual samples were taken at the sampling ports to analyze the composition of organic water constituents by size exclusion chromatography. Additionally, a continuous sampling stream was taken from the basin to a standard electrode system for online analysis and feedback control of relevant process parameters.

4.2.1.6 Simulation of the reference state

For the purpose of comparison, the concentration of organic matter in the swimming pool model was simulated under absence of water treatment (i.e. neglecting the removal of organic substances across the treatment-train and transformation of organic substances by the reaction with chlorine). In the following, this state was denoted as reference state. For simulation of the reference state, a simplified numerical model of the pilot scale system was established using the simulation

environment AQUASIM [131]. The numerical model is described in detail in Section 8.1.2 of the supporting information (SI). In order to transform simulated concentrations of single BFA substances from the AQUASIM model to the fractions of organic matter defined by Huber et al. (2011a) [63], a simple data processing procedure was developed (see Section 8.1.6 (SI)).

4.2.2 Analytical methods

4.2.2.1 Online measurement of relevant process parameters

Standard process parameters (free chlorine, combined chlorine, pH and T_{basin}) were analyzed by a standard electrode system (Meinsberg, Germany). The electrode system was calibrated at least twice a week. Calibration of free and combined chlorine electrodes was performed by the DPD colorimetric method [173]. A Unicam UV2-200 UV/VIS spectrophotometer equipped with a 5 cm quartz cuvette was used for DPD absorbance measurements.

Organic carbon was measured semi-continuously as non-purgeable organic carbon (NPOC) by the catalytic combustion method using a TOC-VCSH analyzer (Shidmadzu, Germany). The mean value and confidence intervals were determined by three repeated measurements. Correlation of NPOC and DOC showed that all organic carbon in the swimming pool model was present as dissolved matter (Figure 8.4 (SI)). Thus, NPOC was denoted as DOC in the following.

4.2.2.2 Characterization of dissolved organic matter composition

The characterization of DOC was performed using liquid size exclusion chromatography with DOC, dissolved organic nitrogen (DON) and UV detection (254 nm) (LC-OCD-OND-UVD, Model 8, DOC Labor, Germany) as described by Huber et al. (2011a) [63]. The method allows breaking down DOC and DON into fractions according to their apparent molecular weight (i.e. biopolymers, humic substances (HS), building blocks (BB), low molecular weight acids (LMW-acids) and low molecular weight neutrals (LMW-neutrals)). Following previous recommendations, the fraction of LMW-acids was calculated without correction accounting for the fraction of low molecular weight humic acids [287].

Using the ultraviolet absorbance of the sample at a wavelength of 254 nm (SAC_{254nm}), the specific UV absorbance of the sample (SUVA) was calculated by forming the ratio of SAC_{254nm} and DOC. The repeatability standard deviation of the LC-OCD method was determined for the relative proportion of each fraction as

follows: biopolymers (0.66 %), humic substances (4.9 %), building blocks (3.1 %), low molecular weight acids (2.2 %), neutrals (5.5 %) and SUVA (0.18 L mg^{-1} m^{-1}).

To allocate single BFA substances to one of the molecular weight fractions, standards of each component of the BFA substance (2.5 mg L^{-1} (as DOC)) and the humic acids (1 mg L^{-1} (as DOC)) were prepared in ultrapure water and analyzed with LC-OCD-OND-UVD. Corresponding chromatograms and descriptions are presented in Figure 8.5 (SI).

Quantification of urea and ammonium was performed using a modified version of the LC-OCD method proposed by Huber et al. (2011b) [288]. A detailed description of the method is given in Section 8.1.5 of the SI.

4.2.2.3 Analysis of volatile disinfection by products

Eleven volatile DBPs were measured by on-line membrane-introduction mass spectrometry as described previously [30]. A MIMS 2000 from Microlab (Aarhus, Denmark) with a Prisma QME 220 mass spectrometer (Pfeiffer Vacuum, Germany) with electron ionization (at 60 eV) was used for analysis. The sample flow rate was ~10 mL min^{-1} and the temperature of the membrane inlet was fixed at 40 °C. For analysis, non-reinforced silicon membranes with a thickness of either 0.125 mm or 0.25 mm were used (PERTHESE® LP 500-3 or NP 500-1, Perouse Plastie, France). The selected ion monitoring mode of the mass spectrometer was used for quantification of the DBPs. Signal intensities of the following m/z values and respective fragments were used to quantify the volatile DBPs in purified water samples: trichloramine (88, $N^{37}Cl_2•^+$), trichloromethane (83, $CH^{35}Cl_2•^+$), tribromomethane (173, $CH^{79}Br^{81}Br•^+$), dibromochloromethane (208, $CH^{79}Br_2{}^{37}Cl•^+$, $CH^{79}Br^{81}Br^{35}Cl•^+$), dichlorobromomethane (29, $CH^{81}Br^{35}Cl•^+$, $CH^{79}Br^{37}Cl•^+$), trichloronitromethane (chloropicrin) (117, $C^{35}Cl_3•^+$) and dichloroacetonitrile (76, $CH^{37}ClN•^+$). Further information on MIMS calibration and analysis is given in Section 8.1.7 (SI).

4.2.2.4 Bacterial cell count

Total cell concentrations in water samples from the swimming pool model were analyzed by quantitative flow cytometry (Accuri C6, BD Bioscience) together with fluorescence staining of microbial cells with the nucleic acid stain SYBRsGreen I (1:100 dilution in DMSO) according to the method described by Hammes et al. (2008) [84]. Staining was performed prior to FCM analysis in the dark for at least 13 min at 38 °C. SYBR Green I and propidium iodide (6 µM) were used in

combination according to Hammes et al. (2012) to differentiate between living and dead cells [289].

4.2.2.5 Concentration of bromide ions

The concentration of bromide ions was determined in the BFA stock solution, the humic acids, the NaOCl stock solution and the filling water according to DIN 10304-1 using liquid ion chromatography [290].

4.2.3 Water samples from a real swimming pool under heavy bather load

In order to access the transferability of results gained from this study, the composition of organic matter in the swimming pool model was compared to that of a heavily loaded real swimming pool. The real pool water sample was taken in 30 cm below the water level at the middle of the short side of a local swimming pool.

4.2.4 Statistical analysis

Unless otherwise mentioned, indicated errors represent the 95 %-confidence interval. To determine if any of the measured fractions of organic matter found in the pool water samples could function as an indicator for DBP formation, correlation coefficients between the concentrations of the volatile DBPs and that of the fractions of organic matter were calculated according to Spearman's rank method. Spearman's rank correlation coefficients define the relationship between the two parameters assuming a monotonic function without assuming their probability distribution.

Student's t-tests were used for hypothesis testing a on the basis of a difference between concentrations of organic substances or DBPs among the different treatment concepts. The null hypothesis, which stated that no differences were observed, was rejected for a probability of $p < 0.05$.

4.3 Results and Discussion

4.3.1 Process operation until stationary conditions were reached

The time dependent DOC concentrations in the swimming pool model for the tested water treatment concepts (Exp. 1 – 7 and reference state) are shown in Figure 4.2. The concentrations of BFA substances used to calculate the DOC concentration in the reference state are presented in Section 8.1.6 of the SI. It revealed that the DOC concentration increased steadily by time for all treatment concepts, until a maximum was reached after ~24.9 – 27 d. This duration equals approximately twice the hydraulic retention time in the model pool (~14.2 d). Here it is important to note that Exp. 7 (PAC-Sand) was started immediately after the previous experiment was stopped. Consequently, the DOC concentration did not start from zero and the time needed to reach stationary conditions was much shorter than in Exp. 1 – 6. The standard process parameters pH, T_{basin} and the concentration of free chlorine (c_{Cl2}) did not significantly vary over the run time of all experiments. The corresponding mean values of the process parameters determined for Exp. 1 to Exp. 7 were as follows: c_{Cl2} = 0.54 ± 0.13 mg L^{-1} (as Cl_2), pH = 7.08 ± 0.14, T_{basin} = 28.0 ± 0.4 °C and T_{air} = 27.2 ± 2.2 °C (errors represent the standard derivation). The assurance of continuous and reproducible process parameters is of crucial importance because formation and decay rates of DBPs as well as the amount and type of DBP formed is known to strongly depend on these parameters [174, 175].

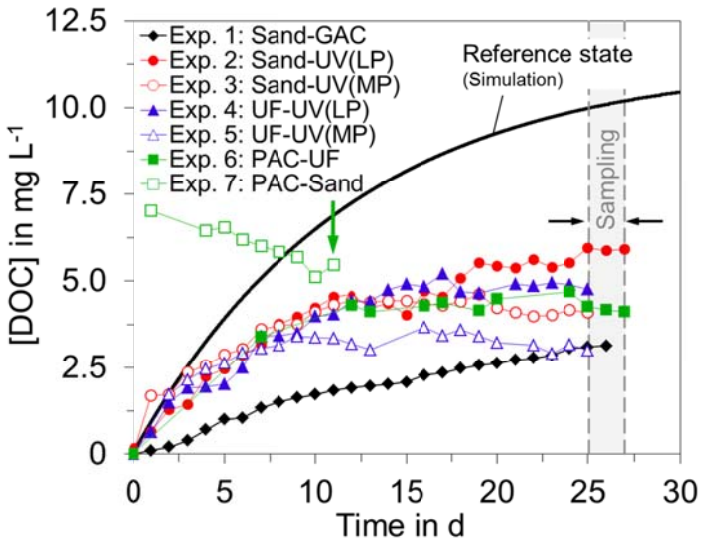

Figure 4.2: Time dependent DOC concentration in the basin (0.12 m below water level) of Exp. 1 - 7 and the simulated reference state. Broken vertical lines (grey) represent the period when samples were taken to determine water quality under stationary conditions. The arrow indicates the time when samples were taken in Exp. 7. The DOC concentrations were smoothed by plotting average values (averaged over 24 h).

4.3.2 Impact of pool water treatment on the concentration of dissolved organic matter

4.3.2.1 Dissolved organic matter in the basin under stationary conditions

The stationary concentration of DOC, the composition of DOC as well as the specific UV absorbance at 254 nm (SUVA) in the basin of the swimming pool model for all considered treatment combinations as measured by the LC-OCD method are presented in Table 4.3.

Total dissolved organic matter

The mean DOC concentration (measured as NPOC) in the basin of Exp. 1 - 7 ranged between 2.99±0.09 mg L^{-1} (UF-UV(MP)) and 5.94±0.11 mg L^{-1} (Sand-UV(LP)) while the DOC concentration of the reference state was 10 mg L^{-1}. As compared to the swimming pool model, only slightly lower DOC concentrations have been reported previously for real pool water samples (1.2 to ~4.2 mg L^{-1} [3, 46, 55, 291]). The concentration of DOC in the real pool water sample taken from the high loaded swimming pool (see Section 4.2.3) was 2.01 mg L^{-1}. The small discrepancy in DOC content between the pool model and real pool water samples can be explained by the difference in pool attendance, which is typically 10 - 13 h per day in real pools [31] and was simulated for 24 h per day in the swimming pool model. The following comparisons between the different treatment concepts employed in this study are noteworthy:

(i) The amount of DOC found in the basin was significantly higher for combinations with sand filtration compared to those with ultrafiltration (UF) (comparing Exp. 2 with Exp. 4, Exp. 3 with Exp. 5 and Exp. 6 with Exp. 7).
(ii) The amount of DOC found in the basin was significantly higher for combinations with UV(LP) than with UV(MP) (comparing Exp. 2 with Exp. 3 and Exp. 4 with Exp. 5).
(iii) Using powdered activated carbon (PAC) as a coating layer on sand filters instead of a GAC filter revealed higher DOC concentrations in the pool. (comparing Exp. 1 with Exp. 7).

Due to the low molecular weight of the BFA substances (Table 4.1), differences in the removal performance between sand filter and UF (MWCO 100 kDa) by physical sieving can be neglected. It is suggested that the observed differences can partly be explained by the different coagulants used (polyaluminium chloride (PACl) for sand filtration, prehydrolized aluminium chlorohydrate (pACH) for UF). PACl and pACH are

known to perform differently in pre-coagulation filtration hybrid processes due to their features of chemical speciation [292].

When comparing treatment combinations with the same filtration step but different UV treatment (i.e. UV(LP) vs UV(MP)), differences in stationary DOC concentrations in the pool were very high. The higher level of DOC found for UV(LP) irradiation compared to UV(MP) irradiation could be explained by direct photolysis of organic molecules by UV(MP) irradiation [49]. Mineralization by photolysis via UV(LP) irradiation is suggested to be negligible [273]. It is also likely that secondary reactions of the organic matter with highly reactive intermediates (e.g., $Cl^{\bullet}$, $OH^{\bullet}$, singlet oxygen ($^1O_2$) and $NH_2^{\bullet}$ [133, 134, 277]), which are formed by combined UV/chlorine treatment in swimming pools, could lead to a partially mineralization of DOC present in pool water. The fact that these highly reactive species are preferably formed by UV(MP) irradiation [49, 278] supports the different DOC levels found in the swimming pool model.

The weak effect of PAC dosing compared to GAC filtration could be explained by the low amounts of PAC typically used in pool treatment that are not capable to remove large amounts of organic precursors.

Dissolved organic matter composition

In Exp. 1 – 7, LMW-neutrals were the prevailing fraction of organic matter with a proportion ranging from 80.8 - 91.5 % ($[DOC]_{fraction}$ $[DOC]_{total}^{-1}$). The remaining DOC in Exp. 1 to 7 was bound in building blocks (3.9 – 8.9 %), LMW-acids (1.4 – 6.7 %) and humic substances (1.4 – 4.8 %).

Stationary concentrations of humic substances in Exp. 1 to 7 were lower by 65 to 87 % compared to the reference state. These findings indicate that water treatment and DOC mineralization by chlorine were effective in removing high and medium molecular weight HA introduced via filling water.

Stationary concentrations of the LMW-neutral fraction contain 79.2 - 96.6 % of urea ($[DOC]_{urea}$ $[DOC]_{neutrals}^{-1}$). With regard to LMW-neutrals, concentrations were lower by 41 to 74 % in Exp. 1 to 7 compared to the reference state. Treatment combinations that make use of ultrafiltration revealed generally lower stationary concentrations of LMW-neutrals compared to those with sand filtration (comparing Exp. 2 with Exp. 4, Exp. 3 with Exp. 5 and Exp. 6 with Exp. 7). This fact is of particular interest because the non-volatile low molecular weight

fraction of halogenated organic matter found in pool water (<200 g mol^{-1}) is associated with the highest genotoxicity [46].

The stationary DOC concentration of LMW-acids in the reference state was almost zero (0.02 mg L^{-1}) while 0.05 - 0.38 mg L^{-1} were found in Exp. 1 – 7. Conclusively, LMW-acids must have been formed over the course of Exp. 1 – 7 by oxidation of BFA substances and humic acids [136, 233]. Treatment concepts with UV irradiation (LP or MP) as second treatment step had higher concentrations of LMW-acids compared to those with activated carbon treatment as second treatment step (comparing Exp. 2 – 5 with Exp. 1, 6 and 7). These findings indicate that either UV and chlorine co-exposure lead to high concentrations of low molecular weight organic matter, which is in accordance with previous findings [162, 293], or the adsorptive removal of formed LMW humic acids substances (quantified together with monoprotic acids in the LMW-acids fraction (see Section 4.2.2.2)) must have been high for activated carbon treatment (PAC or GAC). The concentration of LMW-acids was the lowest for water treatment with sand filtration and subsequent GAC filtration (Exp. 1) (0.05 mg L^{-1}).

Stationary concentrations of ammonium were on a negligible level in all experiments (<10 µg L^{-1} (as N)), which could be explained by the high rate constant known for the reaction of ammonium with chlorine ($1.5 \cdot 10^{10}$ mol h^{-1} (at pH 7) [135]). With regard to SUVA, a measure for the aromaticity and grade of saturation of organic substances [294], treatment combinations with UV irradiation (LP or MP) led to lower values (0.41 – 1.08 L mg^{-1} m^{-1}) than without UV irradiation (0.83 - 3.20 mg $L^{-1}m^{-1}$). This effect could be explained by an enhanced opening of the ring structure of some of the BFA substances observed during chlorine/UV co-exposure [98, 154]. Another explanation for the low SUVA values observed when UV irradiation is employed could be the fact that UV irradiation is capable to break N-Cl bonds [277]. Since N-Cl bonds comprise a certain absorption at a wavelength of 254 nm, this bond breakage could cause a decrease in the SAC_{254nm} and SUVA.

Table 4.3: Mean values of DOC, SUVA and fractions of organic matter in the basin of the swimming pool model at stationary conditions for different treatment concepts. Values in brackets represent the relative proportion of each DOC fraction in relation to the total DOC measured with the LC-OCD method (i.e. $[DOC]_{fraction}$ $[DOC]_{total}^{-1}$).

Parameter	Unit	Reference state[a]	Sand-GAC	Sand-UV(LP)	Sand-UV(MP)	UF-UV(LP)	UF-UV(MP)	PAC-UF	PAC-Sand
			Exp. 1	Exp. 2	Exp. 3	Exp. 4	Exp. 5	Exp. 6	Exp. 7
DOC[b]	mg L^{-1} (as C)	9.99	3.11±0.01	5.94±0.11	4.49±0.23	4.98±0.03	2.99±0.09	4.06±0.16	5.90±0.06
DOC_{total}[c]	mg L^{-1} (as C)	9.99	3.53	5.65	4.64	4.85	2.82	4.48	5.93
$DOC_{Biopolymers}$	mg L^{-1} (as C)	0.00 (0.0)	0.02 (0.5)	0.00 (0.1)	0.00 (0.1)	0.00 (0.1)	0.00 (0.0)	0.01 (0.1)	0.00 (0.1)
DOC_{Humics}	mg L^{-1} (as C)	0.60 (6.0)	0.10 (2.7)	0.08 (1.4)	0.19 (4.1)	0.14 (2.8)	0.13 (4.5)	0.21 (4.8)	0.17 (2.8)
$DOC_{Building\ Blocks}$	mg L^{-1} (as C)	0.49 (4.9)	0.14 (3.9)	0.33 (5.8)	0.41 (8.9)	0.35 (7.3)	0.21 (7.4)	0.22 (5.0)	0.28 (4.6)
$DOC_{LMW\text{-}acids + LMW\ HS}$	mg L^{-1} (as C)	0.02 (0.2)	0.05 (1.4)	0.38 (6.7)	0.28 (6.1)	0.28 (5.9)	0.18 (6.3)	0.09 (2.1)	0.25 (4.3)
$DOC_{LMW\text{-}neutrals\ (incl.\ urea)}$	mg L^{-1} (as C)	8.88 (88.9)	3.23 (91.5)	4.86 (86.0)	3.75 (80.8)	4.07 (84.0)	2.30 (81.8)	3.94 (88.0)	5.23 (88.2)
Urea	mg L^{-1} (as C)	4.75 (47.5)	3.07 (87.0)	4.20 (74.4)	3.44 (74.1)	2.79 (57.5)	2.07 (73.5)	2.65 (59.1)	4.67 (78.8)
Ammonia[d]	µg L^{-1} (as N)	0.85	n.d.	n.a.	7.6	2.2	1.0	n.a.	n.d.
$SAC_{254\ nm}$	m^{-1}		4.94	4.02	5.18	2.22	2.65	4.84	5.14
SUVA	L mg^{-1} m^{-1}		1.59	0.68	1.15	0.45	0.89	1.19	0.87

[a] … LC-OCD chromatogram of the reference state is presented in Figure 8.8 (SI)
[b] … As measured by the thermal combustion method as NPOC, Errors represent the standard deviation
[c] … Calculated as the sum of all DOC fraction (measured by LC-OCD)
[d] … n.a. = sample not analysed, n.d. = sample analyzed but compound was none detected

4.3.2.2 Comparing the organic matter composition of real swimming pool water with that of the swimming pool model

Figure 4.3 presents LC-OCD chromatograms of OM present in water samples taken from Exp. 1 – 7 with that of heavily loaded real swimming pool water. For better comparability, all chromatograms were normalized to a DOC concentration of 1 mg L^{-1}. The relative DOC composition of all samples is summarized in Table 4.3. Both, the heavily loaded full-scale swimming pool water and water samples taken from the pool model had low concentrations of HS, a significant proportion of BB and LMW-acids, and a dominating proportion of LMW-neutrals. The dominating peak at a retention time of ~74 min indicates the presence of urea in all samples. Some minor differences were found in the LC-OCD chromatograms at detection times around 50 min and 60 to 65 min (LMW-neutrals). These differences could not be explained in detail but were related to the limited diversity of substances of the BFA, which did not fully represent the huge complexity of substances in the pool water sample [96].

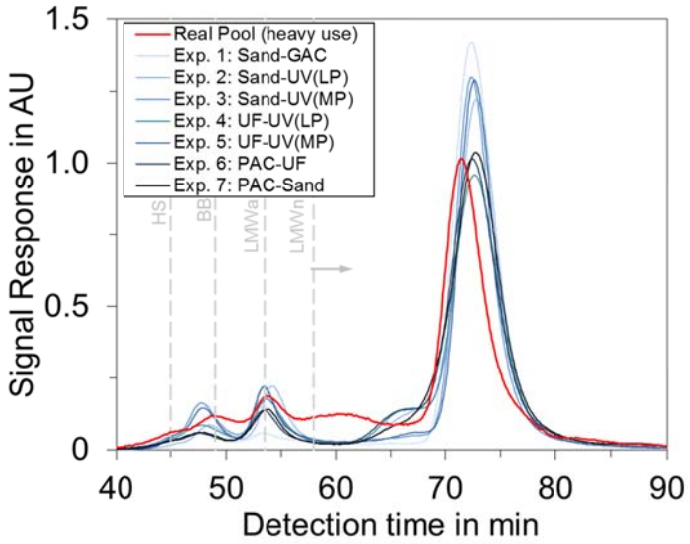

Figure 4.3: Comparison of LC-OCD chromatograms of water samples from Exp. 1 – 7 and real swimming pool water. Chromatograms have been measured using the LC-OCD method with the normal eluent (see Figure 8.5 A (SI))

4.3.2.3 Removal of dissolved organic matter across the treatment train

Figure 8.9 (SI) presents the concentration of DOC across the treatment train of Exp. 1 - 7. This data was used to calculate the relative amount of DOC removed over the entire treatment train ($[DOC]_{removed}$ $[DOC]_{basin}^{-1}$) drawn against the stationary concentrations of DOC in the basin of Exp. 1 to 7 shown in Figure 4.4. The amount of DOC removed across the treatment trains ranged between 0.01 to 0.23 mg L^{-1} (equals 0.1±2.9 % to 7.70±4.5 %) depending on the treatment combination used.

The high level of the 95%-confidence interval determined for the DOC removal across the entire treatment train shown in Figure 4.4 is caused by the uncertainty of the DOC concentrations measured in the in- and outflow of the treatment train, which were relatively high compared to the little amount of DOC removed. The DOC removal values in Exp. 1 to 7 were in good agreement with previous data reported for pool water treatment combinations with UF (~11 % [231], ~9 % [102], 18 % [55]) or sand filtration (~10 % [102]). From the data shown in Figure 4.4, it becomes obvious that even a low removal of DOC across the treatment train results in a significant reduction in the stationary DOC concentration in the basin. The difference in DOC concentration between the simulated reference state and Exp. 1 to 7 shown in Figure 4.4 could be explained by the fact that no chlorine reactions were respected for the former (see Section 4.2.1.6). Following these findings, the assumption of Judd and Black (2000, 2003), stating that DOC removal observed in pool water systems is significantly obtained via DOC oxidation by chlorine (mineralization and volatilization) [51, 53], has to be complemented by the fact that an additional and relevant mitigation of the DOC in the basin could be achieved by effective DOC removal across the treatment train.

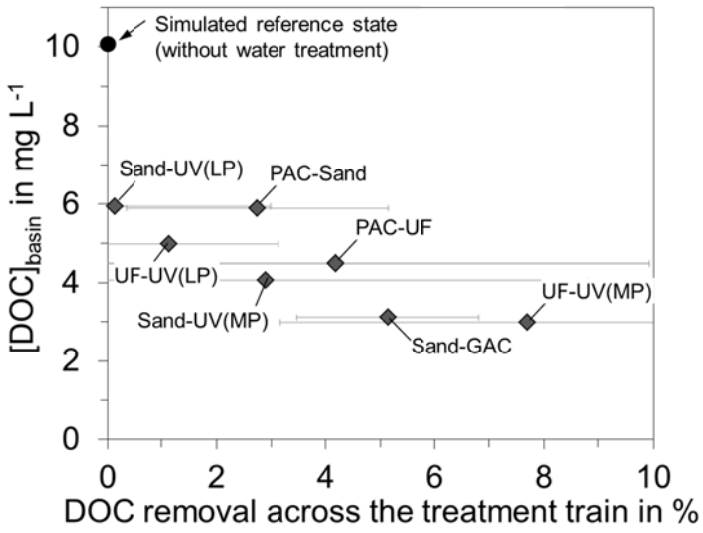

Figure 4.4: Relation between DOC removal across the treatment train of different treatment combinations ($[DOC]_{treated}$ $[DOC]_{basin}^{-1}$) and the mean DOC concentration in the basin when stationary conditions were reached.

Additionally, Figure 8.9 (SI) presents the composition of DOC as well as the specific UV absorbance (SUVA) across the treatment train of Exp. 1 – 7 when stationary conditions were reached. Due to the limited resolution of the LC-OCD method, differences in the concentration of organic matter fractions between in- and outflow of single treatment steps were often not significant. One of the exceptions was Exp. 1 (Sand-GAC) where a significant removal of building blocks (~62 %),

LMW-acids (~68 %) and an increase in SUVA (from 1.39 L mg^{-1} m^{-1} to 2.23 L mg^{-1} m^{-1}) was determined across the bed depth of the GAC filter. The high DOC removal is most likely caused by microbial degradation in the deeper regions of the GAC filter (>20 cm bed depth). As shown in Figure 4.2, the entire amount of free chlorine is removed in the uppermost region of the GAC filter (0 – 20 cm). The chlorine reduction is caused by the reaction at the carbon surface [295]. Consequently, the deeper regions of the GAC filter bed became microbiological contaminated resulting in an increasing amount of living cells measured in water samples taken at bed depth below 20 cm (see Figure 4.5).

While the DOC concentration decreases, the SAC_{254nm} increased across the bed depth in the lower regions of the GAC filter (see Figure 8.9 (SI)). Contrary results have been reported in previous biofiltration studies, where SAC_{254nm} and DOC decreased simultaneously while the SUVA (ratio of SAC_{254nm} to DOC) increased slightly [296]. The increase of SAC_{254nm} observed in this study could be caused by microbiological induced degradation of complex organic material (e.g. humic substances) to short chained products which comprise a higher UV absorbance at 254 nm.

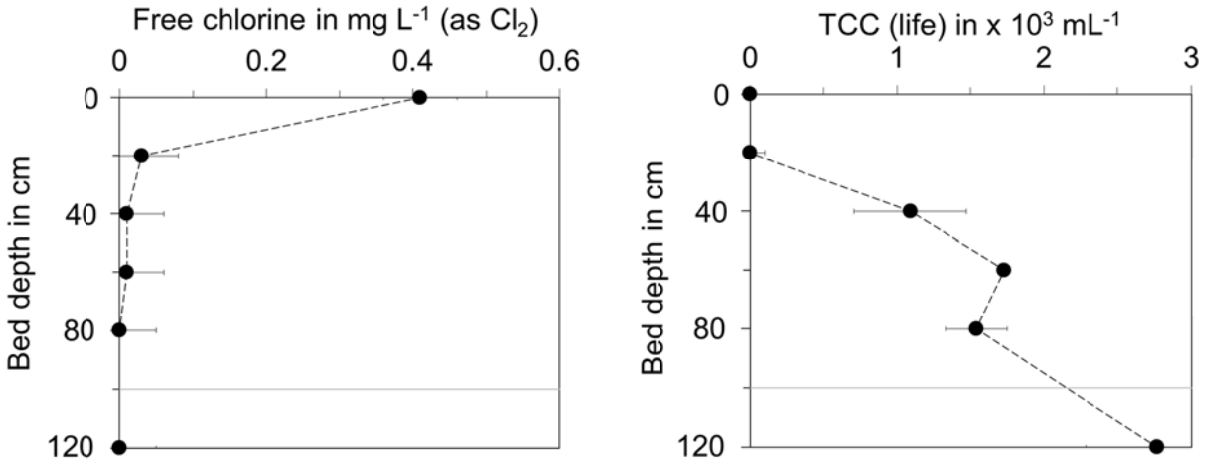

Figure 4.5: Profiles of stationary concentrations of free chlorine and total cell count (TCC) across the bed depth of the GAC filter (Exp. 1). Solid grey lines represent the boundary between the filter layer of GAC and the supporting layer of coarse quartz grains.

4.3.3 Impact of pool water treatment on the concentration of volatile disinfection by-products

4.3.3.1 Volatile disinfection by-products in the basin under stationary conditions

Figure 8.10 (SI) illustrates stationary concentrations of free chlorine, combined chlorine and volatile DBPs in the basin of the swimming pool model for different treatment concepts employed (Exp. 1 to 7).

Combined chlorine

The stationary concentration of combined chlorine, which is a measure for the sum of inorganic as well as some organic chloramines [150], remained below the threshold of 0.2 mg L^{-1} (as Cl_2) (given by DIN 19643 [26]) for the treatment combinations Sand-GAC, Sand-UV(LP) and Sand-UV(MP). The threshold was slightly exceeded for treatment combinations of Sand-UV(MP) and UF-UV(LP) and significantly exceeded for both treatment combinations with precoat filtration employing PAC.

Trichloramine

Stationary trichloramine concentrations in the swimming pool model varied for Exp. 1 to Exp. 7 only by a factor of ~2 (0.11 to 0.24 mg L^{-1} (as Cl_2)), which is lower than for the other volatile DBPs (see below). The low variability in stationary trichloramine concentrations indicates that water treatment has just minor influences on trichloramine levels. These findings give evidence that removing trichloramine in the treatment train does not compensate for the fast trichloramine formation occurring in the swimming pool basin and thus, is not a feasible mitigation strategy [61, 170]. Previous studies by Soltermann et al. (2014) showed that equal concentrations of free chlorine in real pools (of 0.5 mg L^{-1} (as Cl_2)) led to lower trichloramine concentrations (~0.03 mg L^{-1} (as Cl_2) [170]) compared to those determined in the swimming pool model (0.11 to 0.24 mg L^{-1} (as Cl_2) in Exp. 1 - 7). The observed discrepancy could be explained by (i) a different residence time in the basin, which was 4.73 h in this study but as low as ~1 h in the study of Soltermann et al. (2014), (ii) the water level in the swimming pool model, which was not agitated and led to low partition of trichloramine to the air phase (Henry coefficient of 10 bar L mol^{-1} (25 °C) [297]) and (iii) the high concentrations of inorganic chloramines (i.e. combined chlorine) measured in this study, which could serve as a source for additional trichloramine formation. The latter might partly be explained by chlorination of monochloramine, which increased trichloramine formation in the basin [135]. The unusual high stationary concentrations of

trichloramine in Exp. 6 and 7 correlated well with the high concentration of combined chlorine.

Trihalomethanes, Dichloroacetonitrile and Chloropicrin

Contrary to trichloramine, the stationary concentrations of other volatile DBPs varied in Exp. 1 to Exp. 7 by a factor of >10 (TTHM: 11.0 – 48.2 µg L^{-1} (as $CHCl_3$), dichloroacetonitrile: 4.2 – 62.6 µg L^{-1}, chloropicrine: 0.2 (LOD) - 1.2 µg L^{-1}) (see Figure 4.6). In a survey of 11 real pool systems, Weaver et al. (2009) found similar variations for volatile DBPs [30]. The concentration of total THMs (TTHM) was higher for treatment combinations with UV irradiation (Exp. 2 - 5) than without (Exp. 1, 6, 7). The additional formation of TTHMs in the case of UV irradiation could be explained by additional UV-induced formation of free chlorine from combined chlorine or by a UV-induced increase of the reactivity of organic matter towards free chlorine [49]. Brominated THMs are of special interest since they are known to have higher genotoxicity than chloroform [33]. The presence of brominated THMs in the swimming pool model can be explained by bromide ions, which were found in the sodium hypochlorite stock solution dosed into the pool (3.2 mg L^{-1} of Br^- ions at a free chlorine concentration of 12 g L^{-1} (as Cl_2)). The molar contribution of brominated THMs with regard to TTHMs ranged among the different treatment concepts between 0 – 45 %. Mainly dibromochloromethane and dichlorobromomethane were found, while levels of tribromomethane were scarcely below the detection limit (except for Exp. 5, where it was 0.8±0.1 µg L^{-1}). The contribution of brominated THMs between treatment concepts with UV irradiation (17.8±18.5 %, Exp. 2 - 5) and those without (1.7±2.1 %, Exp. 1, 6, 7) were likely different ($p < 0.33$) (errors represent standard deviation). These findings contradict previous data, where it has been shown that the energy needed to break bromine–carbon by UV(MP) is lower compared to break other chlorinated species. This fact resulted in an accumulation of $CHCl_3$ and intermediate brominated compounds ($CHBrCl_2$) in pool water [49, 162]. This discrepancy could be explained by the fact that the formation of brominated THMs in the basin of the swimming pool model was higher compared to the photolytic decomposition of brominated THMs in the UV reactor.

The concentration of dichloroacetonitrile was significantly higher for treatment combinations with UV irradiation (Exp. 2 - 5) than without UV irradiation (Exp. 1, 6, 7). These findings are in accordance with previous data of Weng et al. (2012), who found that UV irradiation at 254 nm promotes formation of dichloroacetonitrile from chlorination of BFA substances (e.g. L-histidine) [163]. Concentrations of chloropicrin were mostly below the detection limit and thus, were not discussed any further.

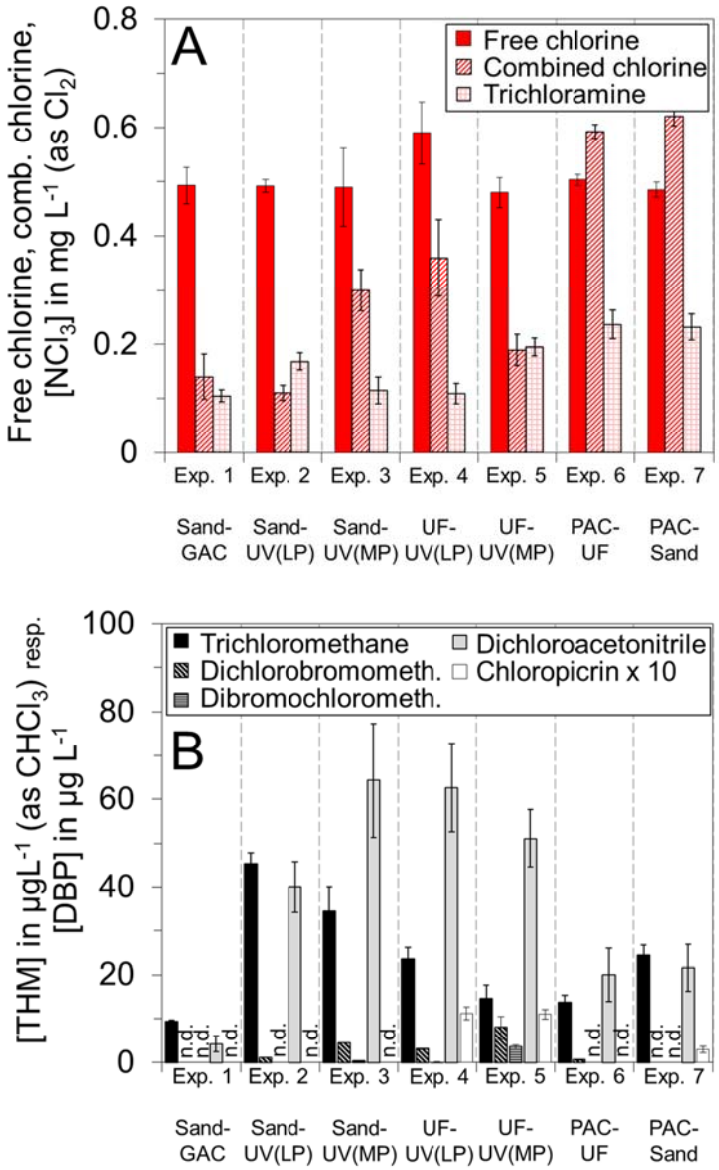

Figure 4.6: Stationary concentrations of free chlorine, combined chlorine, trichloramine (A) and chloroform, dichlorobromomethane, dibromochloromethane, dichoroacetonitril, chloropicrin (B) in the basin of the swimming pool model for different treatment combinations. Concentrations of chloropicrin are multiplied by a factor of 10.

Correlation analysis

Results of the pairwise correlation analysis between stationary concentrations of individual DBPs and different fractions of organic matter are presented in Table 4.4. The concentration of TTHMs had a positive, statistically significant correlation with the organic fraction of building blocks ($p < 0.01$) which could be explained by the high THM formation potential of the citric acid [35] that is primarily assigned to the fraction of building blocks (see Section 8.1.4 (SI)). A highly significant correlation ($p < 0.003$) has been found between the stationary concentration of TTHMs and the fraction of

LMW-acids. It is very likely that in water samples taken from the swimming pool model, the LMW-acids fraction contains mainly LMW humic acids rather than monoprotic acids. This conclusion was drawn since the SAC_{254} of the LMW-acid fraction was very high (results not shown) and chlorinated analogues of monoprotic acids (e.g. acetic acids) were found to eluate at the detection time of LMW-neutrals (Figure 8.6 (SI)). Previous studies agree that humic substances are a major source for THM formation [35, 298]. No evident relationship was found in this study between the stationary concentrations of trichloramine and urea ($p = 0.88$), which agrees with recent results of Soltermann et al. (2014) [170]. Although aromatic nitrogeneous BFA substances, that were mainly assigned to the fraction of LMW-neutrals, are known to serve as precursors for halonitromethanes (e.g. dichloroacetonitrile and chloropicrin [29]), no significant correlation revealed between these substances in this study.

Table 4.4: Correlation analysis of stationary concentrations of DBPs and different fractions of organic matter in the basin of the swimming pool model (Exp. 1 - 7). The table shows Spearman's correlation coefficients and the corresponding p-values in brackets. Correlation analysis for chloropicrin was not conducted because its concentrations were mainly below the limit of detection (see Figure 4.6).

DBP	**DOC**	**Fraction of organic matter**				
		Humic acids (HA)	**Building Blocks (BB)**	**LMW-acids (LMWa)**	**LMW neutals (LMWn)**	**Urea**
Combined chlorine	0.11 (0.82)	0.82 (0.02)	0.07 (0.88)	-0.14 (0.76)	0.39 (0.38)	0.04 (0.94)
Trichlor-amine	0.07 (0.88)	0.50 (0.25)	-0.18 (0.70)	-0.11 (0.82)	0.29 (0.53)	-0.07 (0.88)
TTHMs	0.57 (0.18)	-0.21 (0.64)	0.86 (0.01)	0.93 (0.003)	0.29 (0.53)	0.29 (0.53)
Dichloro-acetonitrile	0.18 (0.70)	0.14 (0.76)	0.89 (0.02)	0.68 (0.09)	-0.04 (0.94)	-0.04 (0.94)

4.3.3.2 Removal of volatile DBPs across the water treatment train

Concentrations of free chlorine, combined chlorine and volatile DBPs measured at different positions across the treatment trains of Exp. 1 – 7 when stationary conditions were reached in the pool model are presented in Figure 8.10 (SI). This data was used to calculate removal values for free chlorine, combined chlorine and volatile DBPs for each single treatment step presented in Figure 4.7 (calculated as $\Delta c\ c_{in}^{-1}$).

The results in Figure 4.7 indicate that the loss of volatile DBPs in the stirred splash water tank of the swimming pool model caused by evaporation ranged between 5.4±4.7 - 15.5±6.3 %.

Sand filtration and UF showed only little effect on the concentrations of the considered volatile DBPs (0.21±11.1 - 10.2±7.3 % removal). No formation of DBPs across the bed depth of the sand filter, as it has been described previously for THMs [219], was observed in this study. Combined chlorine was partly formed across the ultrafiltration module. The selective retention of organic material (e.g. humic acids) on the membrane surface and its subsequent reaction with free chlorine could cause the formation of combined chlorine across the membrane [282]. This is in accordance with the strong correlation that revealed between the concentrations of humic acids and the concentration of combined chlorine in the basin of the swimming pool model determined when stationary conditions were reached (see Table 4.4).

The precoat layer of PAC formed by upstream PAC dosing to UF or sand filtration removed a significant amount of free chlorine, combined chlorine and trichloramine. Differences in the removal efficiencies between free chlorine (~100 %) and combined chlorine (28.2±7.4 % (PAC-Sand) and 38.6±12.6 % (PAC-UF)) could be explained by the different reaction rates reported for the surface reaction of free chlorine and chloramines with carbonaceous materials [266, 295]. However, as being compared to treatment combinations with UV (Exp. 2 – 5), treatment combinations with PAC (Exp. 6 and 7) revealed higher concentrations of combined chlorine in the basin (see Figure 4.6). The removal of dichloroacetonitrile and TTHM by sand filtration or UF did not significantly increase by additional upstream PAC addition.

UV(LP) irradiation at the doses applied in this study (Table 8.1 (SI)) reduced less volatile DBPs and combined chlorine than UV(MP) irradiation. These findings agree with previous results, where it has been shown that concentration levels of THMs could not be reduced by UV(LP) treatment [299], while a minor mitigation of THMs in pool water has been observed for UV(MP) treatment [49]. Although quantum yields for trichloramine photolysis in purified water were found to be similar for UV(LP) and UV(MP) irradiation [50], trichloramine removal was significantly higher in this study for UV(MP) irradiation (91±13 %) as compared to that of UV(LP) irradiation (56 ± 34 %). It is assumed that the relatively high trichloramine removal by UV(MP) irradiation could be explained by additional degradation caused by secondary reactions between trichloramine and free radicals (e.g. $OH^{\bullet}$) [50, 277] which are assumed to be preferably formed by UV(MP) irradiation of chlorinated pool water [49, 278]. Further, UV(MP) could preferably break N-Cl bonds in organic

substances, which in turn is known to make the products again accessible for a reaction with trichloramine [50].

GAC filtration showed the highest removal with regard to volatile DBPs. Almost the entire amount of trichloramine, combined chlorine and chloropicrin was removed by GAC filtration. However, the removal of TTHMs across the bed depth of the GAC filter was very low at ~14 %. Previous studies showed typical breakthrough behaviours for the concentration of THMs in the effluent of GAC filters, which indicates that primarily adsorptive processes control their removal [300, 301]. The GAC filter of the swimming pool model (t_{EBCT} = 1.87 min) has been operated for ~26 days before determining the THM removal. This time is within the reported range of operation times where typically a breakthrough of THMs occurred in other GAC filters operated under drinking water conditions (t_{EBCT} = 5 min) [302]. This fact could to some extend explain the low TTHM removal observed. Results of Kim and Kang (2008) suggest that the removal of THMs in the deeper regions of the GAC filter (Figure 4.5) could have been caused by microbiological processes as well [260].

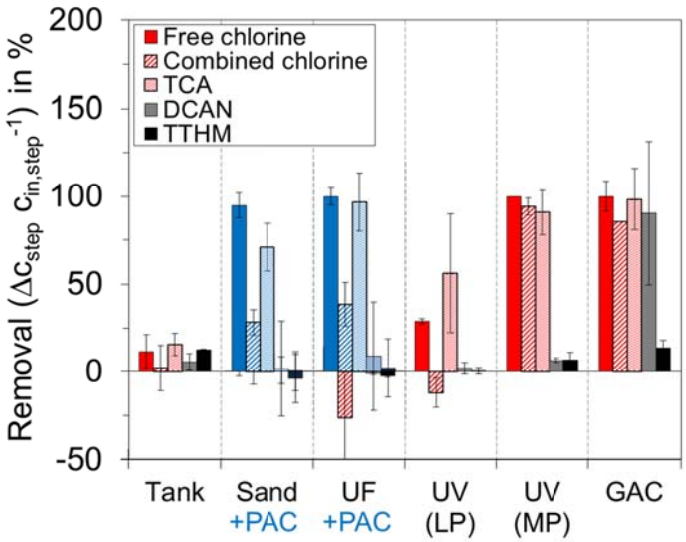

Figure 4.7: Mean removal values of free chlorine, combined chlorine and volatile DBPs across single treatment steps of the swimming pool model measured when stationary conditions were reached. Blue columns for sand and UF treatment represent the removal value in case upstream PAC addition is employed (Exp. 6 and 7). Error bars represent the standard deviation.

4.4 Summary and conclusions

In this study, a pilot scale swimming pool model that facilitates comparison of a variety of different pool water treatment combinations under fully controlled and reproducible process operation and simulated bather loading is presented. The

considered treatment combinations were compared by the removal efficiencies regarding DOC and relevant volatile DBPs. The water quality was only accessed when stationary conditions were reached, which was after 25 – 27 d of fully controlled process operation.

In general, the DOC composition found under stationary conditions was comparable to that found in a highly loaded real pool water sample. However, it must be envisaged that the nature of DOC, and thus, the variety of DBPs formed by chlorination in the pool model are specific to the synthetic loading applied and only partially represent conditions found in real pools.

The relative removal of dissolved organic carbon (DOC) ranged from 0.1±2.9 % to 7.70±4.5 % per cycle depending on the treatment concept employed. Measurements showed a discernible and general trend towards lower stationary DOC concentrations in the pool with increasing DOC removal across the treatment train. In general, stationary DOC concentrations were the lowest for sand filtration with subsequent GAC filtration. The high removal efficiency was primarily related to microbial process in the deeper, chlorine free regions of the GAC filter. Using powdered activated carbon (PAC) as a coating layer on sand filters or ultrafiltration membranes instead of a GAC filter did not reveal equal removal efficiencies for DOC. This effect could be explained by the low amounts of PAC typically used in pool water treatment. Only UV irradiation in combination with UF revealed stationary concentrations of organic matter similar to those found with GAC filtration.

Several treatment combinations were capable to remove THMs to some degree and trichloramine and dichloroacetronitrile almost completely. However, the results demonstrate that the effective removal of DBPs across the treatment train does not necessarily result in low DBP concentrations in the basin. These findings raise the importance of the DBP formation potential and kinetics of the organic matter which has been shown to strongly depend on the treatment concept applied. In the particular case of trichloramine, only weak correlations with the concentration of urea were measured. Our results confirm that the removal of trichloramine across the treatment train is not a feasible mitigation strategy since it cannot compensate for the fast formation of trichloramine in the basin. Our results support the important role of the level of free chlorine for the concentration of trichloramine in pool water as found previously by Soltermann et al. (2015) [165].

Interestingly, the concentration of volatile DBPs was higher for treatment concepts with UV compared to those without UV. This effect could be explained either by additional UV-induced formation of free chlorine from combined chlorine or by an

UV-induced structural change of organic matter which resulted in a higher reactivity with chlorine.

5 Removal of inorganic chloramines with GAC filters: Impact of diffusional mass transport on the overall reactivity

Abstract

In this Chapter, mechanisms that dominate the overall reactivity of granular activated carbon filters for monochloramine removal under swimming pool water conditions are elucidated. The impact of parameters known to influence diffusional mass transport (filter velocity, grain size, water temperature and pore size distribution) on the overall reactivity was studied in fixed-bed experiments.

Over a wide range of commonly used grain sizes (0.3 - 1.9 mm), both, the Thiele modulus of the reaction (42 - 3) and the corresponding effectiveness factor (0.02 – 0.3) indicate that diffusion of monochloramine in the pore system dominates the overall reaction of the GAC-filer. The activation energy for monochloramine removal at different carbons ranged from 20.4 to 29.8 kJ mol^{-1}. Previous studies suggest that this range of activation energies is typical for a strong diffusional control of the reaction. The proportion of large mesopores (>10 nm) in the pore system has a significant impact on the carbon reactivity towards monochloramine. This effect can be explained by the effective diffusion coefficient of monochloramine in the pore system, which was found to be higher for those carbons with a high proportion of large mesopores. Moreover, it has been found that pores <1.3 nm might be barely accessible for the monochloramine conversion reaction. Thus, carbons with a significant proportion of pores larger than this critical pore size should be preferably used for monochloramine removal. Film diffusion was found to have no influence on the overall reactivity of a GAC filter, in particular at high filter velocities as they are typically applied for swimming pool water treatment (>30 m h^{-1}).

5.1 Introduction

Chlorine-based disinfection of swimming pool water is commonly used to ensure the hygienic safety of bathers. A major drawback associated with the use of hypochlorous acid (HOCl) as an disinfectant is its potential to react with inorganic and organic matter present in pool water forming halogenated disinfection by-products (DBPs) [3, 27, 135, 137]. The dominating nitrogen precursors for DBP formation introduced by bathers into the pool are urea ($CO(NH_2)_2$) and ammonia (NH_3) [86, 96, 192]. The reaction of urea [31, 136] and ammonia [189-191] with HOCl is initially induced by the formation of inorganic chloramines (mono-, di- and trichloramine). Chloramines are known to be skin and eye irritating and are suspected to cause respiratory problems [38], including asthma [41, 42, 303, 304]. Consequently, the sum of all inorganic chloramines, which is denoted as combined chlorine, is strictly regulated to a concentration of <0.2 mg L^{-1} (as Cl_2) in German swimming pools [56]. Among the variety of inorganic chloramines, monochloramine (MCA) is the most dominant species in pool water with concentrations up to 1.88 mg L^{-1} (as Cl_2) [30]. Moreover, monochloramine is of particular interest because it was found to be an educt for the formation of cancerogenic N-nitrosodimethylamine (NDMA) [195, 196], which was also found in chlorinated pools [158]. To mitigate the risks for the bathers and to guaranty process operation in conformity with the provisions related to the water quality in swimming pools [56], the concentration of monochloramine in pool water must be controlled. Previous studies have shown that granular activated carbons (GAC) could serve as a reducing agent for monochloramine. Although activated carbons are widely known as effective adsorbents [246, 305], the reduction of monochloramine primarily proceeds via a chemical surface reaction [260, 306-308]. Thus, it is not surprising that the filter capacity for monochloramine removal was higher than expected when only adsorption is considered [265]. Over the course of the reaction, the reactivity of GACs decreased before stationary conditions were reached [266]. As a result of this, activated carbon filters operated under swimming pool water conditions need to be regenerated or replaced every 1 to 2 years. However, the exact mechanism of the initial decrease of reactivity has not been fully understood until now. Bauer and Snoeyink (1973) proposed a two-step process, where monochloramine initially oxidizes free active carbon sites (C*) in a very fast reaction forming surface oxides (C*O) while the monochloramine (MCA) is reduced to ammonium (NH_4^+) (Equation (5.1)). As enough surface oxides were formed, the authors assume that monochloramine undergoes a second, slower reaction, where the surface oxides are reduced back to free active sites while MCA is oxidised to N_2 (Equation (5.2)) [265]. It is assumed that this process causes the decreasing carbon reactivity over time.

$$NH_2Cl + H_2O + C^* \rightarrow NH_4^+ + Cl^- + C^*O \quad (5.1)$$

$$2\ NH_2Cl + C^*O + 2\ H_2O \rightarrow N_2 + 2\ H_3O^+ + 2\ Cl^- + C^* \quad (5.2)$$

However, a more recent study indicates that the ratio of formed transformation products (i.e. NH_4^+ and N_2) did not change over the course of the reaction [309]. These findings contradict the above mentioned mechanism of Bauer and Snoeyink because the ratio of reaction products does not simply derive from a simple addition of Equation 5.1 and 5.2 but depends, as described above, on the time dependent increase of the concentration of surface oxides (C*O). Further, previous studies reasoned that the overall reactivity is dominated by pore diffusion rather than by the chemical surface reactions [254, 310]. Mass transport in the pore system of GACs is known to be influenced by various parameters such as the grain size, water temperature [262], the presence of surface oxides [311] and the pore size distribution of GACs [312]. A comprehensive analysis of the influence of these factors on the overall monochloramine reduction process at GACs is still subject to investigation.

To theoretically describe the monochloramine removal process with GAC filters, the semi-empirical MCAT model was established by Kim (1977) [313] and was recently complemented by Fairey et al. (2007) with respect to the impact of DOM present in the feed water on the overall reactivity of a GAC filter [309]. However, the semi-empirical MCAT model estimates carbon reactivity only after stationary conditions are reached [310] using basic GAC properties such as the porosity and tortuostity of the GACs. This makes the model inapplicable to further elucidate pore diffusional limitations of the monochloramine-GAC reaction.

Considering the current state of knowledge, the process of decreasing reactivity of GACs at the beginning of the monochloramine reaction as well as the impact of pore diffusional limitations on the overall reactivity of a GAC filter are still not fully understood. Conclusively, the aim of this Chapter was to determine the impact of diffusional mass transport on the overall reactivity of a GAC filter for a wide range of operation conditions such as grain size, pore size distribution and water temperature. In-depth knowledge of the processes limiting monochloramine removal by GAC filters should give further indications for future research aimed at refining physical GAC properties for enhanced monochloramine removal.

5.2 Materials and Methods

5.2.1 Determination of the carbon reactivity

5.2.1.1 Kinetic approach

The observable reaction rate constant of a GAC filter for monochloramine removal is given by Equation (5.3) assuming the overall reaction following first-order kinetics [314, 315]:

$$k_{eff} = \frac{1}{t_{EBCT}} \cdot \ln\left(\frac{c_{bed,in}}{c_{bed,out}}\right) \tag{5.3}$$

Here $c_{bed,in}$ and $c_{bed,out}$ are the monochloramine in- and out-flow concentrations and t_{EBCT} represents the empty bed contact time (EBCT) defined with V_{bed}/Q_{bed} or z_{bed}/v_{bed}. V_{bed} and Q_{bed} define the bed volume and the flow rate of the filter column, respectively. The bed depth of the filter column is represented by z_{bed} and v_{bed} represents the flow velocity. Previous studies showed that the reactivity of GACs for monochloramine conversion decreases gradually over the time. However, the time the carbon reactivity decreases is far lower compared to the EBCT in GAC filters, which justifies the use of the pseudo first-order kinetic approach presented in Equation (5.3) [266].

In order to compare the effective reaction rate constant k_{eff} with the theoretical mass transfer coefficient of monochloramine through the laminar film layer k_f (see Equation (5.10)), the former was normalized by the specific outer surface a_o (in $m^2\ m^{-3}$) of the filter bed ($k_{eff,a}$).

The temperature dependence of k_{eff} is given by the Arrhenius Equation:

$$k_{eff}(T) = k_0 \cdot e^{-\frac{E_A}{R_0 T}} \tag{5.4}$$

Here, k_0 and E_A are the frequency factor and the activation energy respectively, R_0 is the universal gas constant and T is the temperature. E_A is derived from the slope of the linear least-squares best fit of the correlation between $\ln(k_{eff})$ and T^{-1} (Arrhenius plots).

5.2.1.2 Experimental determination of the effective reaction rate constant

Process parameters needed to calculate k_{eff} under fully controlled conditions were measured using the laboratory-scale fixed-bed column shown in Figure 5.1. The filter

column was continuously fed at a constant flow rate (Q_{bed}) with a monochloramine solution from a rapidly stirred (~250 rpm) double walled glass tank with feedback controlled pH and temperature (Biostat B, B. Braun, Germany). The concentration of monochloramine in the tank, and thus the inflow concentration $c_{bed,\,in}$ was measured by an amperometric chlorine sensor and was held on a constant level.

The water that passes the filter column was circulated in a closed loop between the tank and the filter column. This operation system allows reaction products to accumulate in the system, which increased the analytical resolution for detection of the NH_4^+ yield of the monochloramine-GAC reaction (results are shown later in this thesis in Section 6.3.1).

Since monochloramine is degraded in the GAC filter, a cooled monochloramine stock solution (4 to 6 °C) was continuously dosed into the tank by a feedback controlled peristaltic micro pump P2 to maintain a constant $c_{bed,in}$. The corresponding dosing rate (Q_{st}) is given by Equation (5.5):

$$Q_{st}=\frac{\left(\frac{\Delta m}{\Delta t}\right)_{st}}{\rho_{st}(T)} \tag{5.5}$$

Here, $\rho_{st}(T)$ is the temperature dependent density of the stock solution and $\Delta m/\Delta t$ is the recorded, time dependent mass loss of the stock solution as determined in time intervals of 0.5 – 1 h. A constant water volume in the FBR system V_{sys} was guaranteed by withdrawing water from the tank by the feedback controlled peristaltic pump P3. The monochloramine outlet concentration of the GAC filter $c_{bed,out}$ was calculated by solving the mass balance around the tank of the FBR system (Equation (5.6)):

$$Q_{bed}\cdot c_{bed,out}-Q_{bed}\cdot c_{bed,in}+Q_{st}\cdot c_{st}-Q_{st}\cdot c_{bed,in}+R_{sys}=V_{sys}\cdot\left(\frac{dc}{dt}\right) \tag{5.6}$$

Here R_{sys} is the time dependent loss of monochloramine in the system without GAC filter and c_{st} is the concentration of the monochloramine stock solution. Blank experiments showed that monochloramine auto-degradation in the FBR system was negligible. Respecting that:

$$R_{sys}=0 \tag{5.7}$$

and assuming the system to operate under stationary conditions, the capacity term in Equation (5.8) gives:

$$V_{sys}\left(\frac{dc}{dt}\right)=0 \tag{5.8}$$

Considering Equation (5.7) and (5.8), $c_{bed,out}$ was calculated by simplification of Equation (5.6) as follows:

$$c_{bed,out}=\frac{\left(\frac{\Delta m}{\Delta t}\right)_{st}}{\rho_{st}\cdot Q_{bed}}\cdot\left(c_{bed,in}-c_{st}\right)+c_{bed,in} \tag{5.9}$$

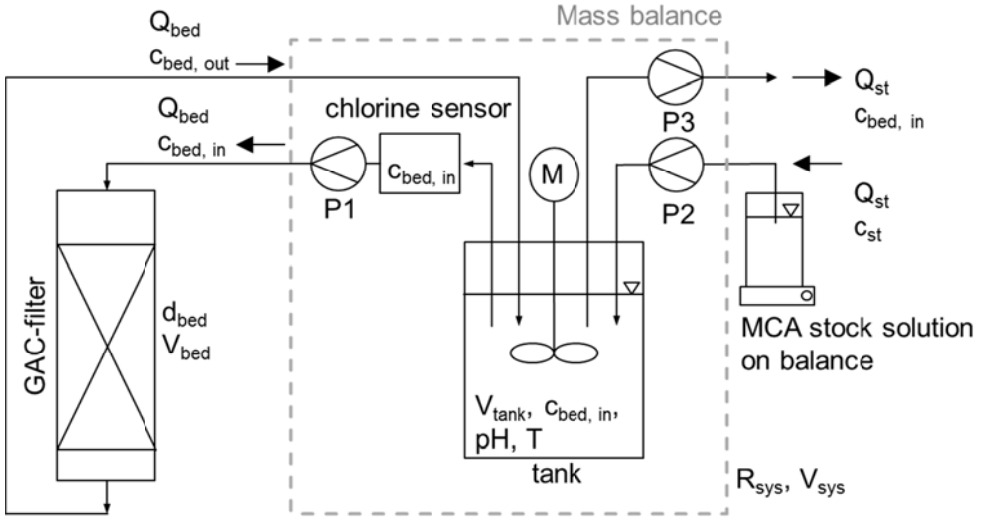

Figure 5.1: Scheme of the laboratory-scale FBR system and relevant mass flows. Dashed grey line represents the mass balance around the tank.

5.2.2 Granular activated carbons and solutions

Four commercially available granular activated carbons (GACs) were used in this study, namely Hydraffin 30 N from Donau Carbon GmbH (30 N), Silcarbon K-835 from Silcarbon Aktivkohle GmbH (K835), Centaur from Chemviron Carbon GmbH (Centaur) and a new type of polymer-based spherically shaped activated carbon (PBASC) Type 100058 from Blücher GmbH (100058).

The carbons, as provided by the manufacturers, were denoted as fresh unfractionated carbons. Grain size fractions of the 30N, K835 and Centaur with mean grain diameters of 0.30 mm (0.25 - 0.355 mm), 0.57 mm (0.50 - 0.63 mm) and 1.90 mm (1.80 - 2.00 mm) were prepared by sieving the fresh unfractionated carbons using a sieve tower (AS 200, Retsch, Germany) and, if necessary, previously grounding the fresh unfractionated carbons using a ball mill. The 100058 carbon was solely used at the original monomodal grain size (d_p) provided by the manufacturer (0.55 mm). Before use, the fresh GACs were treated by the following preparation routine: (i) Soaking in ultrapure water for ~24 h, (ii) Evacuating the soaked carbon

using a vacuum chamber until no air bubbles arise and (iii) Washing and decantation of the carbon using ultrapure water until the supernatant is particle free.

Monochloramine stock solutions as used in the FBR experiments were prepared as described previously by drop-wise addition of a OCl^- solution (pH 10) in a rapidly stirred NH_4Cl or $(NH_4)_2SO_4$ solution (pH 10) at final molar chlorine (as Cl_2) to ammonia ratio of 1.00:1.03 [316].

5.2.3 Fixed-bed experiments

5.2.3.1 General remarks

FBR experiments were conducted to determine k_{eff} either at the beginning of the monochloramine-GAC reaction or after a certain time of operation, when stationary conditions were reached.

The reactivity at the beginning of the reaction was determined after ~0.1 mmol g_{GAC}^{-1} of monochloramine were converted in the GAC filter column. For these experiments, the fresh carbons were used as they were provided by the manufacturer.

To determine the reactivity under stationary conditions, the fixed-bed experiments were divided in two consecutive steps: (i) Altering the carbons on a reproducible basis at $c_{bed,in}$ = 4.5 mg L^{-1} (as Cl_2), T = 30°C and Q_{bed} = 40 L h^{-1} (equals a filter velocity of v_{bed} = 44.1 m h^{-1}) until no change in k_{eff} was observed and stationary conditions were reached and, (ii) Determination of k_{eff} under various operation conditions (e.g. different $c_{bed,in}$, T or v_{bed}). Carbons operating under stationary conditions were denoted as aged carbons. All experiments were performed at a constant pH of 7, as it is recommended for swimming pool water [56]. For pH-adjustment either 0.3 mol L^{-1} phosphoric acid (H_3PO_4) or 0.1 mol L^{-1} sodium hydroxide (NaOH) were used. Moreover, the conductivity of the monochloramine solution at the beginning of the experiments in the tank was set to ~400 µS cm^{-1} by dosing a 1 mol L^{-1} NaCl solution. A detailed description of the FBR experiments is provided in the following Sections. Table 5.1 summarizes the process conditions of all experiments described in the following sections.

5.2.3.2 Verification of the kinetic first-order approach

To experimentally verify the kinetic first-order approach used in this study (see Equation (5.3)), the reactivity of the aged unfractionated K835 carbon was

determined for various monochloramine inflow concentrations. The level of reproducibility for determination of k_{eff} was tested by conducting a set of four repeated experiments.

5.2.3.3 Impact of external mass transport on the overall reactivity

To exclusively access the impact of pore diffusional mass transport on the overall reactivity of the GAC filter, the cross influence by extra-particle mass transport (film diffusion) has to be excluded [262]. To check for the absence of film diffusion, k_{eff} was determined for different flow velocities (v_{bed}) for filter beds of the fresh and aged unfractionated K835 carbon. Following previous recommendations, v_{bed} and the catalyst volume (V_{bed}) were varied simultaneously so that the EBCT in the filter column was constantly set to 2.88 s.

To further elucidate the impact of film diffusion on the overall reactivity, the theoretical mass transfer coefficient of monochloramine through the laminar film layer (k_f) was calculated (Equation (5.10)) [246] and compared to the experimentally derived specific reaction rate constant $k_{eff,a}$.

$$k_f = \frac{Sh \cdot D_{bulk,MCA}}{d_{hy}} \tag{5.10}$$

Here Sh is the Sherwood number, which was calculated according to the empirical approaches of Williamson et al. (1975) (Equation (5.11)) [318] and Genielinski (1963) (Equation (5.12)) {Gnielinski, 1978 #2612}, $D_{bulk,MCA}$ is the bulk diffusion coefficient of monochloramine in water, which was calculated using the Wilke-Chang correlation with $2.03 \cdot 10^{-5}$ cm^2 s^{-1} (at 30°C) [319] and d_{hy} is the representative hydraulic grain size of a carbon with a certain grain size distribution. The calculation of d_{hy} is explained later in Section 5.2.4.2.

$$\begin{aligned} Sh &= 2.4 \cdot \varepsilon_s \cdot Re^{0.34} \cdot Sc^{0.42} \quad && (0.08 > Re < 1 \\ Sh &= 0.442 \cdot \varepsilon_s \cdot Re^{0.69} \cdot Sc^{0.42} \quad && (125 > Re < 50000) \end{aligned} \tag{5.11}$$

$$Sh = (1+1.5 \cdot (1-\varepsilon_s)) \cdot Sh_E \tag{5.12}$$

In Equation (5.12), Sh_E is the Sherwood number in the transient region between laminar and turbulent interfacial flow through the filter bed and ε_s is the interstitial porosity of the filter bed.

Sh_E was calculated as follows [246]:

$$Sh_E = 2 + \sqrt{\left(Sh_{lam}^{\ 2} + Sh_{turb}^{\ 2}\right)} \quad (5.13)$$

with

$$Sh_{lam} = 0.664 \cdot Re^{\frac{1}{2}} \cdot Sc^{\frac{1}{3}} \quad (5.14)$$

and

$$Sh_{turb} = \frac{0.037 \cdot Re^{0.8} \cdot Sc}{1 + 2.443 \cdot Re^{-0.1} \cdot \left(Sc^{\frac{2}{3}} - 1\right)} \quad (5.15).$$

In Equations (5.11), (5.14) and (5.15), Re is the Reynolds number and Sc is the Schmidt number.

5.2.3.4 Impact of internal mass transport on the overall reactivity

Impact of grain size

To check for the importance of grain size on the overall reactivity, k_{eff} was determined for different grain size fractions of the aged 30N carbon. To further elucidate the impact of grain size, the Thiele modulus Φ was calculated according to Equation (5.16) [315]. The Thiele modulus is a dimensionless constant representing the ratio of the overall reaction rate versus the diffusion rate of the reactant in the pore system.

$$\Phi = L \cdot \sqrt{\left(\frac{k_{eff}}{\eta \cdot D_{E,MCA}}\right)} \quad (5.16)$$

Here, L is the diffusion path length within the adsorbent, which becomes $d_p/6$ assuming a spherical shape of the GAC grains [315]. In Equation (5.16), $D_{E,MCA}$ is the effective diffusion coefficient of monochloramine in the pore system and η is the effectiveness factor. The effective diffusion coefficient $D_{E,MCA}$ was estimated based on the pore size distribution of the individual GACs using the random intersecting pore model [320, 321] and assuming surface diffusion of monochloramine in the pore system of the GACs to be negligible [309]:

$$D_{E,MCA} = \frac{1}{\tau} \cdot \frac{\sum_{j=d_{MCA}}^{\infty} D_{bulk,\,MCA} \cdot \left(1 - \frac{d_{MCA}}{d_{p,j}}\right)^4 \cdot V_{p,j}}{\sum_{j=d_{MCA}}^{\infty} V_{p,j}} \qquad (5.17)$$

Here, τ is the tortuosity factor of the GACs, d_{pj} and $V_{p,j}$ are the diameter and the incremental pore volume of a pore in the size fraction j as derived from the pore size distribution of the 30N carbon and d_{MCA} is the minimal pore diameter of the carbon that is still accessible for a monochloramine molecule. The effectiveness factor η is defined as the ratio of the actual reaction rate versus the theoretical reaction rate without diffusional limitations [262]. For a first-order reaction taking place at a spherical grain, η could be determined as follows [322]:

$$\eta = \frac{1}{\Phi} \cdot \left(\frac{1}{\tanh 3\Phi} - \frac{1}{3\Phi}\right) \qquad (5.18)$$

Simultaneous solution of Equations (5.16) and (5.18) gives the corresponding values for η and Φ.

Impact of water temperature

The temperature dependence of monochloramine conversion in the GAC filter was determined by means of the activation energy E_A (see Equation (5.4)) of the reaction for both, the fresh and the aged unfractionated carbons 30N, K835 and Centaur. In order to calculate E_A, k_{eff} was experimentally determined in FBR experiments in wide range of temperatures typically found in in- and out-door swimming pools. Other process parameters except the temperature were kept constant.

Impact of pore size distribution

In this set of experiments, k_{eff} was determined for the aged 30N, K835, Centaur and 100058 carbons. To overcome the disruptive influence of GAC grain size on k_{eff} and to allow comparison between the carbons, only filter beds of equal grain size fractions were used (0.05 mm (100058) and 0.57 mm (30N, K835, Centaur)).

5.2.3.5 Process at the initial phase of the reaction

To describe the process of decreasing reactivity of the heterogeneous monochloramine-GAC reaction, conversion-time curves were determined in FBR experiments for all GACs until stationary conditions in reactivity were reached. The general shape of the conversion-time curves can give evidence supporting

whether one of the two widely recognized reaction models applies (Progressive-Conversion Model (PCM) [315] or Shrinking-Core Model (SCM) [323]).

Table 5.1: Operation conditions of the FBR experiments.

Type of study	Section	Used type of carbon	Variable parameters	Constant parameters
Verification of the kinetic first-order approach	5.3.2	K835 *(unfractionated)*	$c_{bed,\,in}$ = 0.5 - 9 mg L^{-1} (as Cl_2)	v_{bed} = 44.1 m h^{-1} T = 30 °C V_{bed} = 32 mL t_{EBCT} = 2.88 s
Extra-particle mass transfer	5.3.3	K835, 30N *(unfractionated)*	v_{bed} = 8.3 - 132.2 m h^{-1} (V_{bed} = 6 - 96 mL)	T = 30 °C $c_{bed,\,in}$ = 4.5 mg L^{-1} (as Cl_2) t_{EBCT} = 2.88 s
Impact of grain size	5.3.4	30N *(size fractions and unfractionated)*	d_{grain} = 0.30 - 1.9 mm	v_{bed} = 44.1 m h^{-1} T = 30 °C $c_{bed,\,in}$ = 4.5 mg L^{-1} (as Cl_2) V_{bed} = 32 mL t_{EBCT} = 2.88 s
Temperature dependence	5.3.5	30N, K835, Centaur *(unfractionated)*	T = 12 - 45 °C	v_{bed} = 44.1 m h^{-1} $c_{bed,\,in}$ = 4.5 mg L^{-1} (as Cl_2) V_{bed} = 32 mL t_{EBCT} = 2.88 s
Process at the initial phase of the reaction and impact of pore size distribution	5.3.6, 5.3.7	30N, K835, Centaur and 100058 *(0.57 mm size fraction)*	-	v_{bed} = 44.1 m h^{-1} T = 30 °C $c_{bed,\,in}$ = 4.5 mg L^{-1} (as Cl_2) V_{bed} = 32 mL t_{EBCT} = 2.88 s

5.2.4 Analytical methods

5.2.4.1 Quantification of monochloramine and HOCl

Monochloramine concentrations in the tank (Figure 5.1) were measured using a membrane-covered amperometric 2-electrode total chlorine sensor (CTE-1 DMT, Prominent, Germany) which was calibrated on a daily basis using the photometric DPD method [173].

The concentration of the HOCl solution used to prepare the monochloramine stock solution was spectrophotometrically standardized at pH 10 as OCl^- ion using a molar absorption coefficient at 294 nm (ε_{294}) of 348 mol^{-1} cm^{-1} [324].

The monochloramine stock solution was spectrophotometrically standardized at least twice a day according to the method of Schreiber and Mitch, accounting for the overlapping absorbance peaks of monochloramine and dichloramine ($NHCl_2$) at 245 nm and 295 nm ($\varepsilon_{NH2Cl,\ 245\ nm}$ = 445 mol^{-1} cm^{-1}, $\varepsilon_{NHCl2,\ 245\ nm}$ = 208 mol^{-1} cm^{-1}, $\varepsilon_{NH2Cl,\ 295\ nm}$ = 14 mol^{-1}, $\varepsilon_{NHCl2,\ 295\ nm}$ = 267 mol^{-1} cm^{-1}) [325]. Spectroscopic measurements at 360 nm confirmed the absence of trichloramine εNCl_3) in the monochloramine stock solution ($\varepsilon_{NCl3,\ 360\ nm}$ = 126 mol^{-1} cm^{-1}) [326, 327]. The yield for transformation of NH_4^+-N to MCA-N was found to be in a range of 95 % - 100 %. Both, spectroscopic and DPD measurements, were performed using a Unicam UV2-200 UV/VIS spectrophotometer.

5.2.4.2 Physical carbon characterisation

The specific outer surface area a_o of the carbon bed was calculated based on the grain size distribution of the unfractionated carbons as follows:

$$a_0 = \frac{A_{bed}}{V_{bed}} = 6 \cdot \frac{\rho_{bed}}{\rho_{grain}} \cdot \sum_i \frac{q_i}{d_{grain,i}} \cdot \frac{1}{\psi} \tag{5.19}$$

Here ρ_{bed} and ρ_{grain} are the bulk density (dry) and the density of the carbon grains (dry), q_i is the mass fraction of the corresponding mean grain size $d_{grain,i}$ as derived from the grain size distribution and ψ is the dimensionless correction factor, introduced in order to respect the derivation in shape of the carbon grains from a spherical form (ψ = 0,75 for GACs [328]). Grain size distributions of all carbons were analysed according to a common German standard using a sieve tower (AS 200, Retsch, Germany) [329]. The representative hydraulic grain size d_{hy} of the unfractionated carbons was calculated as follows [330]:

$$d_{hy} = \frac{1}{\sum \left(\frac{q_i}{d_{grain,i}} \right)} \tag{5.20}$$

The internal surface area, pore volume and the pore size distribution (PSD) of the fresh unfractionated carbons were determined from nitrogen adsorption/desorption isotherms in a relative pressure range (p/p_0) of 10^{-6} to 1 at 77 K using an Autosorb-1C automated gas-sorption apparatus (Quantachrome, Germany). The internal surface area a_{BET} of the carbons was determined using the BET equations [331]. The surface area and pore size distribution (PSD) of the carbons

were determined using the quenched solid density functional theory (QSDFT) assuming graphite material with pores of slit-like shape [332]. The validity of this assumption is discussed in Section 5.3.2.

The total pore volume was calculated from the nitrogen sorption data at p/p_0 of ~0.98 while the micropore volume was determined using the Dubinin-Radushkevich Equation at p/p_0 of 10^{-6} - 10^{-1}. For calculations, the ASiQWin Software (Version 3.0, Quantacrome Instruments) was used.

The sum of meso- (2 – 50 nm) and macropore (> 50 nm) volume was calculated by subtracting the micropore (< 2 nm) volume from the total pore volume. N_2 adsorption-desorption isotherm were further used to estimate the tortuosity of the carbons using the CSTM-model as described Salmas at al. (2001) [333].

The proportion of macropores (> 50 nm) was determined by mercury intrusion porosimetry using a Porosimeter 2000 apparatus (Carlo Erba Instruments, Milan, Italy). The intrusion experiments were performed in a pressure range of 0.4 MPa to 200 MPa.

To further elucidate the morphology of the 100058 carbon, images were taken from a cross-section of a single carbon grain with a High Resolution Scanning Electron Microscope (HRSEM, FEI Nova NanoSEM, 5 kV). HRSEM-images were taken at 4 different positions across the grains radius. In total 6 close-up HRSEM images of each position across the diameter were taken. The pore size distribution of the 100058 carbon across the grains diameter was analysed by image processing of the close-up HRSEM-images as described previously by Skibinski et al. (2016) [334]. Due to the limited resolution of the HRSEM-images, only pores >10 nm could be analysed.

5.3 Results and Discussion

5.3.1 Physical characterization of the carbons

The physical characteristics of the carbons used in this study are summarized in Table 5.2. Figure 5.2(A) presents N_2 adsorption-desorption isotherms which were type I according to the Brunauer-Deming-Deming-Teller (BDDT) classification for all carbons considered. The significant step of N_2-adsorption in the low pressure region indicates the presence of plentiful micropores [335]. The percentage of micropores with regard to the total pore volume was in the following order: 30N (79 %) < 100058 (82 %) < Centaur (87 %) < K835 (94 %). The relative proportion of mesopores was the highest for the 100058 (18 %) and the Centaur carbon (17 %).

The hysteresis of nitrogen physisorption (difference between adsorption and desorption isotherms) for the 30N and K835 carbon was almost zero. Following the principles of the model of Salmas et al. (2001) (CSTM-model), these findings indicate the tortuosity of the carbons to be near to 1.0 (1.26 for K835 and 1.27 for 30N) [333]. According to the CSTM-model, the tortuosity of the Centaur carbon was calculated with 2.05. Due to its inhomogeneous pore size distribution (Figure 5.3), the tortuosity of the 100058 carbon could not be calculated with the CSTM-model. The fact that adsorption and desorption isotherms branch in parallel to each other and almost horizontally is associated with the presence of narrow pores of slit-like shape, which are commonly found for activated carbons [336]. Mercury intrusion porosimetry measurements showed that the proportion of macropores (macropore volume related to the total pore volume) was very low and ranged between 1.6 - 3.6 %.

Figure 5.2(B) shows the pore size distribution (PSD) of the fresh unfractionated carbons as calculated using the quenched solid density functional theory (QSDFT). In the micropore region (<2 nm), the Centaur, K835 and 100058 carbon had PSD peaks at the smallest detectable pore size of 0.6 nm and at ~1.1 nm. Both, Centaur and K835 had a PSD peak at 1.1 nm while the 30N carbon had peaks at 0.72 nm and 1.5 nm. The characteristic pore size distribution of the Centaur carbon is in agreement with data reported previously [337]. Both, the Centaur and the 100058 carbon comprised a significant proportion of large mesopores >7 nm (0.015 $cm^3\ g^{-1}$ (Centaur) and 0.013 $cm^3\ g^{-1}$ (100058)).

Table 5.2: Physical characterization of the fresh unfractionated carbons 30N, K835, Centaur and 100058.

Carbon type	Hydraulic diameter d_{hy}, in mm	Outer surface a_o in $m^2\ m^{-3}$ [a]	Inner surface a_{BET} in $m^2\ g^{-1}$ [a]	Specific pore volume in $cm^3\ g^{-1}$ (%)				
				Total	Micropores	Mesopores (total)	Mesopores >7 nm[b]	Macro-pores
30N	1.18	5444	1105	0.522	0.411 (79)	0.092 (18)	0.003 (0.6)	0.019 (4)
K835	1.39	4480	1073	0.446	0.419 (94)	0.020 (5)	0.001 (0.2)	0.007 (2)
Centaur	1.00	5532	895	0.408	0.353 (87)	0.046 (11)	0.015 (3.7)	0.009 (2)
100058	0.55	17418	1291	0.605	0.496 (82)	0.102 (17)	0.013 (2.1)	0.007 (1)

[a] … All pores of the activated carbons were potentially accessible for the monochloramine conversion reaction (differences in BET surfaces between granular carbons and their powdered counterparts were <5%).

[b] … As derived from the QSDFT calculation.

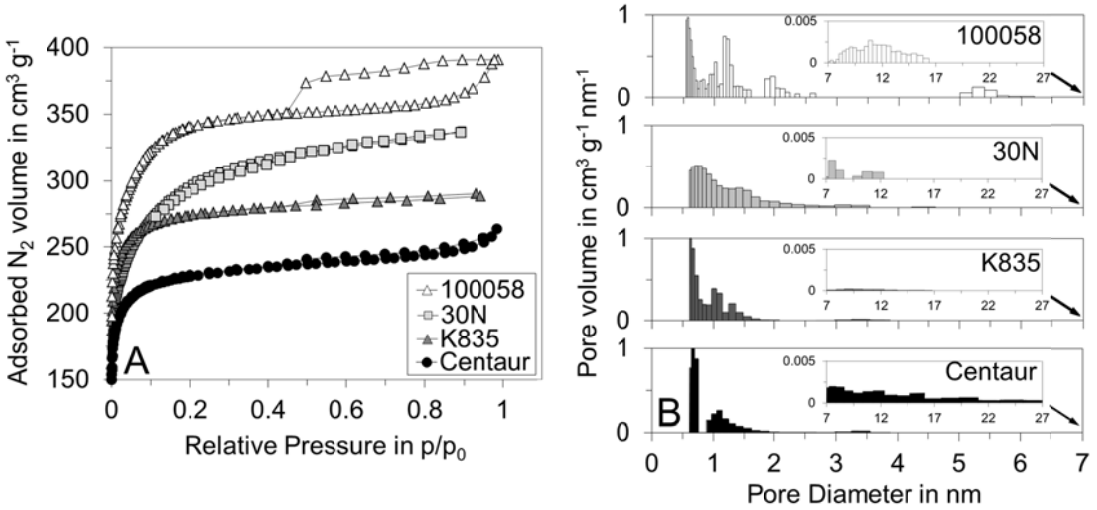

Figure 5.2: N_2 adsorption and desorption isotherms at 77 K (A) and pore size distribution of the unfractionated fresh carbons (B) (inset represents the distribution of large mesopores > 7 nm).

Examples of close-up HRSEM images of the 100058 GAC taken at different positions across the radius of a cross-section are presented in Figure 5.3. It revealed that the obvious textural change across the diameter of the grain (Figure 5.3(A)) is accompanied by a change in the pore size distribution (Figure 5.3(B-D)).

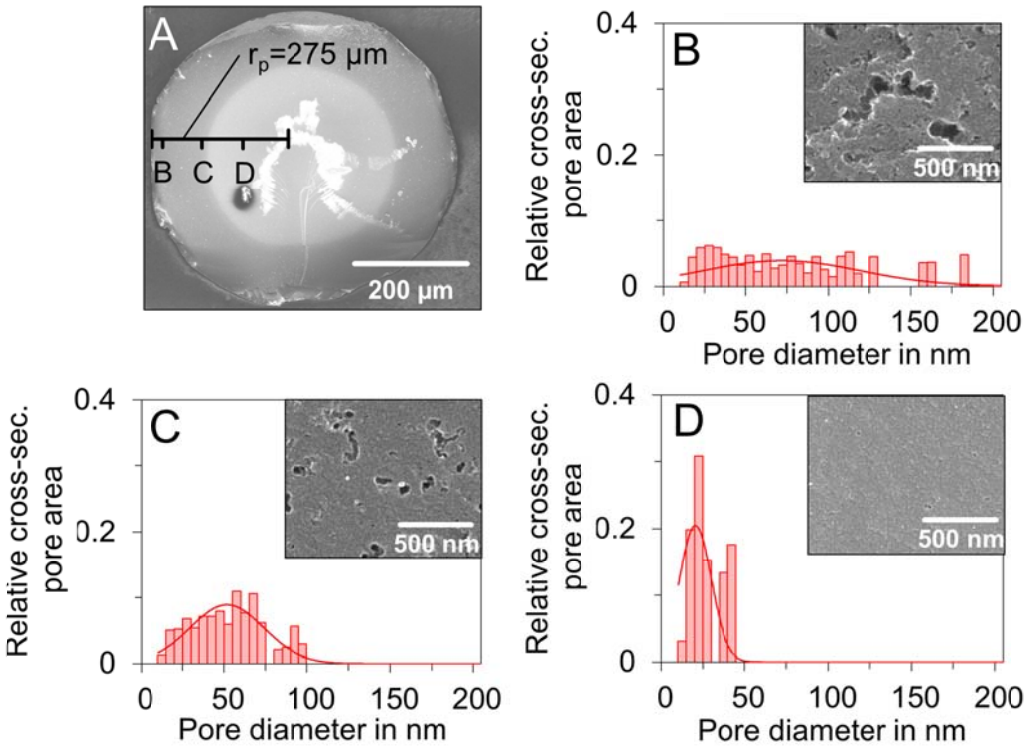

Figure 5.3: HRSEM image of a cross-section of the 100058 carbon at a zoom of 150 (A) and at different positions across the diameter with the corresponding relative cross-sectional pore area distribution at a zoom of 200,000 (B-D). Solid lines in (B-D) represent the log-normal distribution.

From the relative pore size distribution it becomes obvious that plenty of mesopores are present at the outer region of the grain, while their relative proportion decreases towards the centre of the grain. Near of the centre of a grain (position D), no macropores were present and mesopores revealed in a mean diameter of ~25 nm.

5.3.2 Verification of the kinetic first-order approach

Figure 5.4 exemplarily shows time plots of k_{eff}, $c_{bed,in}$ and $c_{bed,out}$ of one of the four repeated verification experiments. The initial drop in carbon reactivity that occurred before stationary conditions were reached (Figure 5.4(A)) was very pronounced (67 %) while the time needed to reach stationary conditions was ~90 h. The operating time to reach stationary conditions was much shorter compared to the time reported by Fairey et al. (2007) (1250 - 3000 h) [309], although comparable monochloramine inflow concentrations were used in both studies. This discrepancy was attributed to the significant differences in EBCT of the filter column (30 s in Fairey's work and 2.8 s in this work) and thus, the difference in the time needed to oxidize the complete filter column.

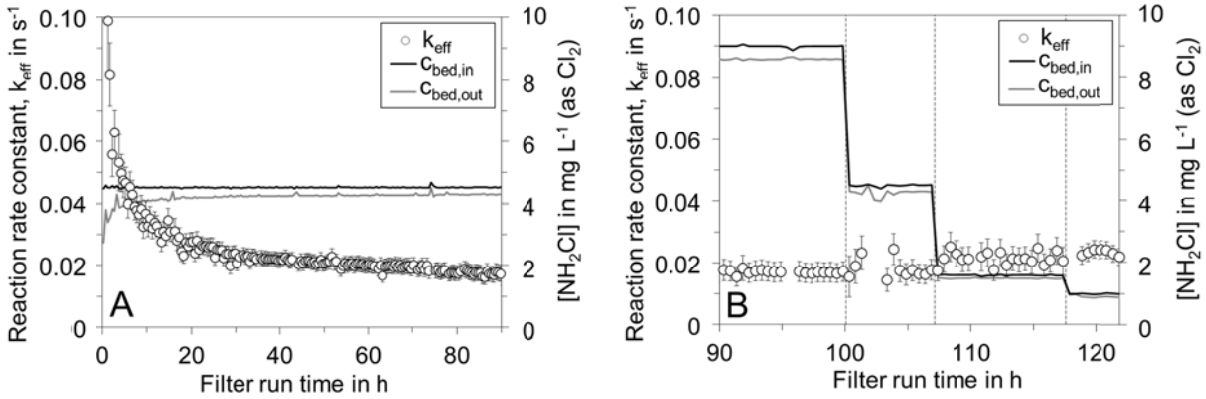

Figure 5.4: Reaction rate constant k_{eff} for monochloramine removal at the K835 carbon as well as in- and outflow concentrations of monochloramine over the filter run time of one of the four repeated verification experiments. Two consecutive experimental steps were conducted: altering the carbon at $c_{bed,in}$ of 4.5 mg L^{-1} (as Cl_2) until stationary conditions were reached (A) and operation of the FBR system at different monochloramine inflow concentrations after stationary conditions were reached (9.0, 4.5, 1.6 and 0.9 mg L^{-1} (as Cl_2)) (B). Error bars represent the standard error of k_{eff} as determined by Gaussian error reproduction.

Figure 5.5 shows the linear least-squares regression analysis between k_{eff} and $c_{bed,in}$. The slope of the linear regression was almost zero ($0.4 \cdot 10^{-3} \pm 0.21 \cdot 10^{-3}$ L mg^{-1} s^{-1}), which indicates that the observed reaction rate constant was independent of the inflow concentration. These findings suggest the validity of the first-order approach

used in Equation (5.3). This was also true for monochloramine concentrations that are as low as they are typically found in swimming pool water (e.g. 0 - 1.8 mg L^{-1} as Cl_2, [30]). The repeatability standard deviation of k_{eff} for the aged carbon K835 determined by four identical repeated validation experiments was ±0.006 s^{-1} (~±4%), which indicates a high reproducibility and exactness of the experimental method used.

To check for heterogeneity of the reaction, the Maitlis' test was conducted [338]. Therefore, the loss of monochloramine in the tank of the FBR system was measured in the middle of an experiment while bypassing the GAC filter column. Results confirmed that no monochloramine was degraded and thus, no reactive agents leached from the GAC.

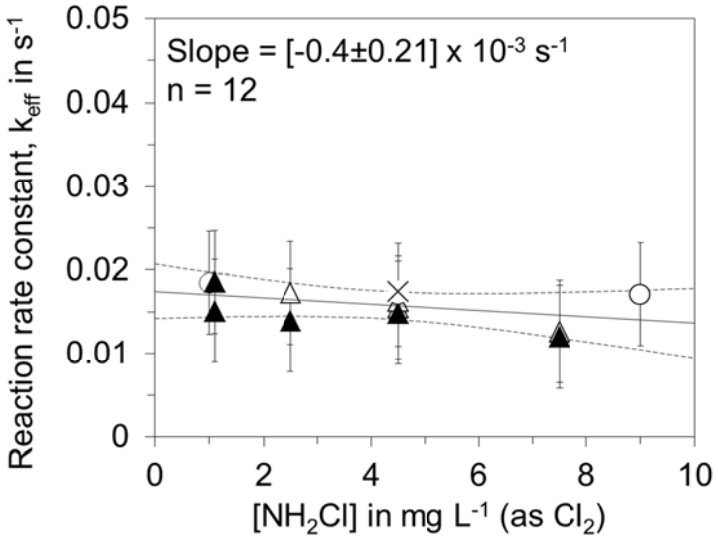

Figure 5.5: Effect of monochloramine inflow concentration on the effective reaction rate constant for monochloramine conversion at the aged unfractionated K835 carbon. Each set of symbols represents an individually repeated experiment. Solid lines represent linear least-squares best fit and dashed lines represent the 95 % confidence band of the fitted regression. Indicated errors represent the repeatability standard deviation.

5.3.3 Exclusion of extra-particle mass transfer limitations

Figure 5.6 shows the dependence of the experimentally determined specific reaction rate constant $k_{eff,a}$ (in m s^{-1}) and the theoretical mass transfer coefficient of monochloramine in the laminar film layer k_f (in m s^{-1}) from the filter velocity v_{bed} for the fresh and aged unfractionated carbon K835. No significant change in $k_{eff,a}$ revealed over the entire range of considered filter velocities for the fresh and aged carbon ($p<0.001$). In dependence of the approximation of the Sherwood number used for calculation of k_f (Schlünder and Gnielinski) [339], the level of $k_{eff,a}$ was

10-times lower compared to k_f. Equal findings were found for the fresh 30N carbon (results not shown). These results indicate that external mass transport is not limiting the overall reactivity for monochloramine removal in GAC filters. The low level of $k_{eff,a}$ is assumed to be caused by diffusional resistances in the pore system. It could be concluded from these results that limitations by mass transfer through the laminar film layer could be neglected over a wide range filter velocities for both, fresh and aged carbons. Although several authors assumed that the negligible impact of film diffusion on the removal of dichloramine at GACs could be transferred to the removal of monochloramine [309, 340, 341], results reported in this study represent the first experimental verification of this assumption.

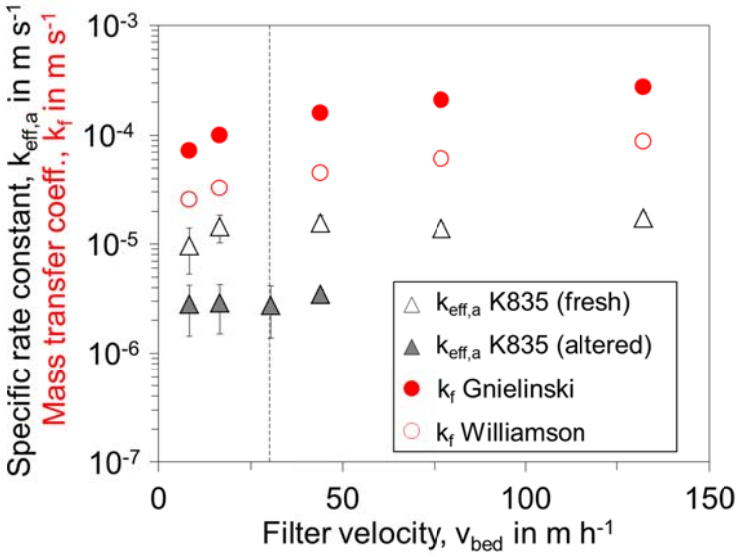

Figure 5.6: Impact of filter velocity on the experimentally determined specific reactivity $k_{eff,a}$ for monochloramine conversion and the theoretical mass transfer coefficient k_f of the unfractionated K835 carbon. Error bars represent the 95 % confidence interval. Mass transfer coefficients k_f were calculated using a mean grain diameter $d_{hy,K835}$ of 1.39 mm. The dashed vertical line represents the recommended filter velocity for GAC filters in swimming pool water treatment in Germany (≤ 30 m h^{-1}) [56].

5.3.4 Impact of grain size

Figure 5.7(A) presents the observed first-order reaction rate constant k_{eff} for monochloramine removal of different grain size fractions of the 30N carbon over the filter run time until stationary conditions were reached. The overall reactivity increased with decreasing grain size almost linear (Figure 5.7(B)). These results are in agreement with previous studies which, however were obtained before stationary conditions were reached [310].

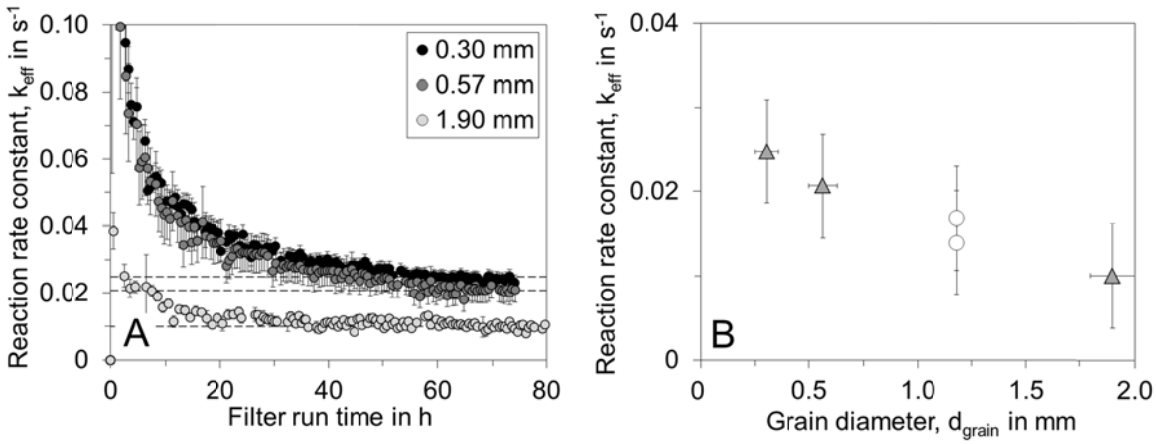

Figure 5.7: Reaction rate constant k_{eff} over the filter runtime for different grain size fractions of the 30N carbon (A) and corresponding relationship between the grain size and k_{eff} (B). Dashed vertical lines in (A) represent the level of carbon reactivity under stationary conditions. Open circle symbols in (B) represent k_{eff} for the unfractionated 30N carbon using $d_{hy,30N}$ = 1.18 mm as representative grain size. Error bars in (A) represent the standard error of k_{eff} as determined by Gaussian error reproduction and in (B) the 95% confidence intervals.

It revealed that the stationary effective surface related reaction rate constants $k_{eff,a}$ of the grain size fractions of the 30N carbon decreased with decreasing grain size ($2.82 \cdot 10^{-6}$ m s^{-1} (1.9 mm), $2.56 \cdot 10^{-6}$ m s^{-1} (1.18 mm), $1.73 \cdot 10^{-6}$ m s^{-1} (0.57 mm), $1.11 \cdot 10^{-6}$ m s^{-1} (0.30 mm)). The outer surfaces a_o used to determine $k_{eff,a}$ of the grain size fractions of the 30N carbon were calculated according to Equation (5.19) as follows: 3550 m^2 m^{-3} (1.9 mm), 7495 m^2 m^{-3} (0.9 mm), 11940 m^2 m^{-3} (0.57 mm) and 22300 m^2 m^{-3} (0.30 mm). These findings indicate that the increasing reactivity observed for smaller grain size fractions under stationary condition is not exclusively caused by the higher outer surface of the filter bed a_o. Instead, diffusional resistances in the pore system are assumed to be low for small grain size fractions, which might explain the high overall reactivity (i.e. shorter diffusion paths).

To access the influence of pore diffusion on the overall reactivity, the Thiele modulus Φ and the effectiveness factor η of the reaction, as they occurred under stationary conditions, were calculated (see Figure 5.8). The Thiele modulus of the grain size fractions 1.9 mm, 1.18 mm (unfractionated GAC) and 0.57 mm were > 4, which confirmed that pore diffusion strongly controls the overall reaction. The Φ value of the smallest grain size fraction (0.30 mm) was 3, which is related to the transient region with moderate pore diffusional influence [315, 342]. Scaramelli (1977) found a Thiele modulus of 0.51 for a GAC with a grain size of ~0.5 mm [266]. The Thiele modulus of the 0.57 mm fraction of the 30N carbon observed in this study was higher by a factor of ~15. This indicates that the importance of pore diffusion on the overall reactivity found in this study was higher compared to previous studies of Scaramelli (1977).

This discrepancy could partly be explained by the fact that $D_{E,MCA}$ of the 30N carbon ($9.43 \cdot 10^{-7}$ $cm^2\ s^{-1}$) used to calculate Φ in this study was lower by a factor of ~4 compared to the value of Scaramelli (1977), who estimated $D_{E,MCA}$ with $5.484 \cdot 10^{-6}$ $cm^2\ s^{-1}$ based only on the GACs porosity and roughly estimated tortuosity [266]. Determination of $D_{E,MCA}$ for the 30N carbon is presented in Section 5.3.7 below.

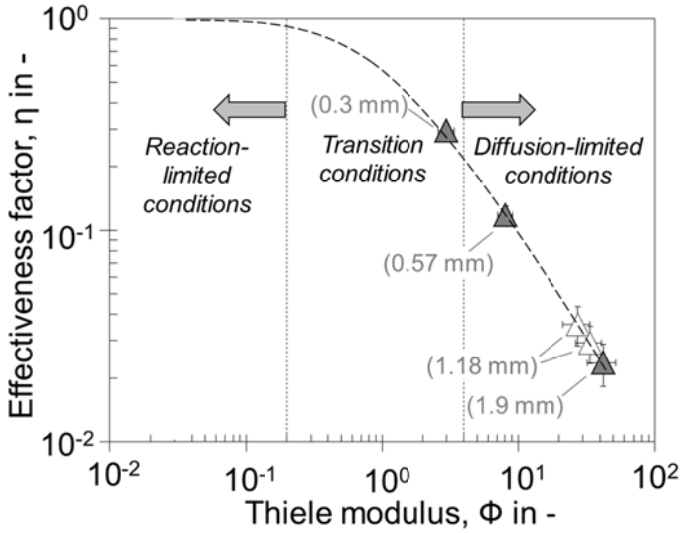

Figure 5.8: Relationship between Thiele modulus Φ and effectiveness factor η of the monochloramine-GAC reaction at stationary conditions for different grain size fractions of the 30N carbon. The effective reaction rate constants (Figure 5.7(B)), as obtained under stationary conditions, were used to calculate Φ and η. Open circle symbols represent k_{eff} for the unfractionated 30N carbon using $d_{hy,30N}$ = 1.18 mm as representative grain size. The dashed black line is for orientation only and represents the expected relationship between Φ and η as discussed elsewhere [262]. Errors represent the 95% confidence intervals.

5.3.5 Impact of water temperature

Figure 5.9 presents Arrhenius plots for monochloramine removal in filter beds of the 30N, K835 and Centaur carbon in a temperature range of 12 - 45 °C. The overall reactivity linearly increases with increasing temperature. The linear correlation coefficients of the Arrhenius plots were r^2 = 0.96 - 0.99, which gives evidence that the model provides an adequate fit to the experimental data. The activation energies E_A of the fresh and aged carbons derived from the Arrhenius plots ranged between 20.4 and 29.8 kJ mol^{-1}. Previous studies have shown that low E_A values (<42 kJ mol^{-1}) usually indicate diffusion-controlled processes, while higher E_A values indicate chemical reaction control [343]. Differences in E_A between the fresh and the aged carbons were not significant ($p<0.001$) indicating that the increasing amount of oxygen groups formed on the carbon surface after treating GACs with

monochloramine had no influence on the overall reactivity. Activation energies found for monochloramine removal at GAC filters in this study were significantly lower compared to previously reported values for the removal of dichloramine (35.6 kJ mol^{-1} at pH 10 [344]) and free chlorine (43.9 kJ mol^{-1} at pH 7.6 [263]). The lower E_A values are in agreement with the higher reactivity of GACs for the removal of dichloramine and free chlorine as compared with monochloramine. As shown previously in this study, the impact of pore diffusion increases with increasing grain size of the used GACs. This increase in diffusional resistance should affect the temperature dependence of the overall reaction as well [315]. However, the difference in the experimentally determined E_A for the size fractions of the 30N carbon (1.18 mm and 0.57 mm) were not significant ($p<0.001$). This discrepancy could be explained by the limited resolution of the method used to determine k_{eff}, which in turn is used to calculate E_A.

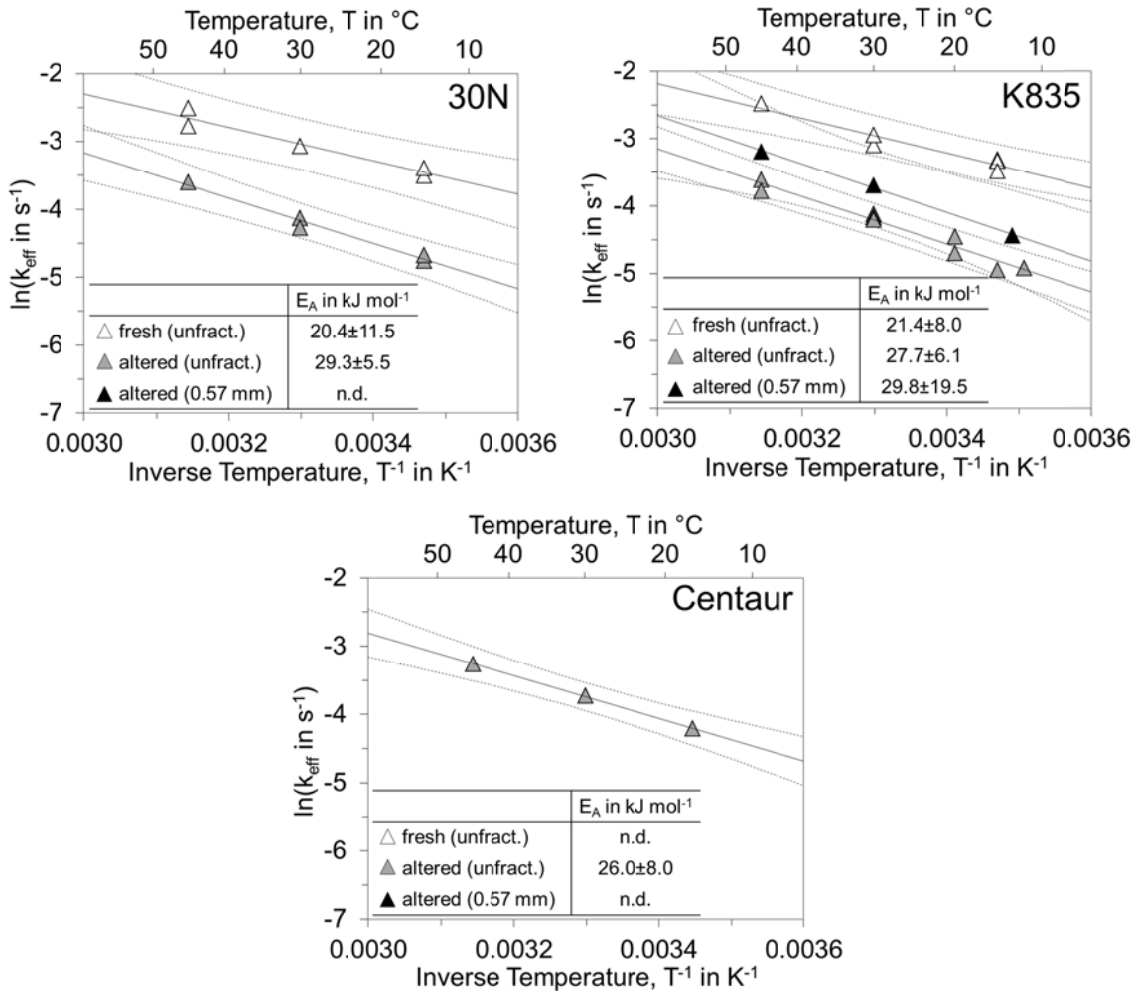

Figure 5.9: Impact of water temperature on the effective reaction rate constant for monochloramine conversion at the carbons 30N, K835 and Centaur. Solid lines represent linear least-squares best fit and dashed lines represent the 95% confidence band of the fitted regression. Errors for E_A represent the standard error of the slope of the linear regression (n.d. = not determined).

5.3.6 Progress of the reaction until stationary conditions were reached

Figure 5.10(A) shows the conversion-time curves of monochloramine in the GAC filter for the 0.57 mm grain size fractions of the 30N, K835, Centaur and 100058 carbon. It is apparent that the conversion-time plot of monochloramine removal for the conventional GACs (30N, K835, Centaur), which comprise a homogeneously distributed and strongly microporous pore size distribution, is hyperbolic while that of the 100058 carbon, with a structured pore size distribution (Figure 5.3), is sigmoid (S-shaped). The conversion-time behaviour of the GACs could be described by the Shrinking-Core Model (SCM) [323]. The SCM describes a reaction, which starts first at the outer surface of the GAC grains, while the reaction front then moves toward the centre of the grains with ongoing reaction time, leaving behind converted material [315]. The difference in conversion-time behaviour between the microporous GACs and the 100058 carbon could be explained by the unusual pore size distribution of the latter as follows:

(i) Due to the high proportion of mesopores near to the external surface of the grains of the 100058 carbon (Figure 5.3(B)), the effective diffusion coefficient of monochloramine ($D_{E,MCA}$) in this area is assumed to be high and the overall reaction becomes controlled by the intrinsic chemical reaction at the beginning.

(ii) The observed decrease in mean pore size towards the centre of the grains of the GAC 100058 is assumed to lead to an increase of the accessible pore area reached by the reaction front when moving towards the centre. As a result, the reactivity of the 100058 carbon increased during the first ~20 min of the reaction.

(iii) With on-going reaction time, the reaction front moves further towards the grains centre and diffusion paths of monochloramine molecules increase until a shift in the reaction controlling mechanism from chemical control to diffusional control occurs. This shift results in a decrease in reactivity, which in turn leads to a sigmoid conversion time curve [345], as it was found for the 100058 carbon.

(iv) Since k_{eff} did not decrease until zero when stationary conditions were reached, the reacted sites of the GAC grains in the filter column must be still reactive to some degree. This effect could be explained by oxygen groups formed according to Equation (5.1) that evolve continuously from the surface as CO or CO_2, thus providing new free active sites [295].

In contrast to the 100058 carbon, the pore structure of the conventional GACs (30N, K835, Centaur) is assumed to be microporous throughout the entire particle.

Thus, the overall process becomes controlled by diffusion right from the start of the reaction, leading to hyperbolic conversion-time curves [345].

5.3.7 Impact of pore size distribution

Figure 5.10(B) presents the effective reaction rate constants k_{eff} for monochloramine removal over the reaction time for GAC filters containing the carbons 30N, K835, Centaur and 100058 (0.57 mm grain size fractions). When stationary conditions were reached, k_{eff} values revealed in the following order: 0.036 s^{-1} (Centaur) > 0.025 s^{-1} (K835) > 0.017 s^{-1} (30N) > 0.016 s^{-1} (100058).

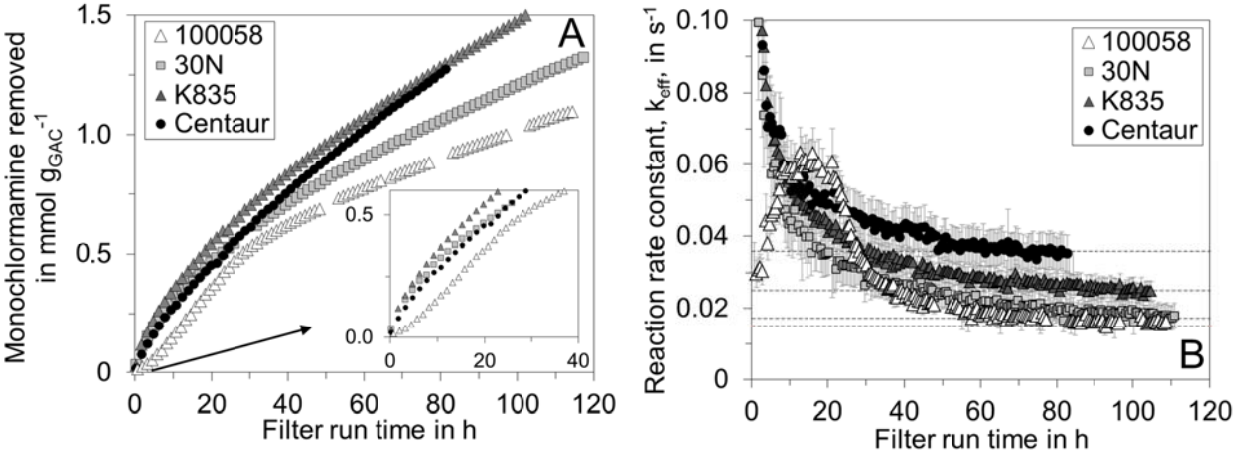

Figure 5.10: Removed monochloramine (A) and reaction rate constant k_{eff} for monochloramine removal (B) over the filter run time for the GACs 100058, 30N, K835 and Centaur. All carbons had the same grain size of ~0.55 mm (0.57 mm for the 100058 carbon). Dashed vertical lines in (B) represent the carbon reactivity when stationary conditions were reached. Error bars in (B) represent the standard error of k_{eff} as determined by Gaussian error reproduction.

Given the strong pore diffusional control of the overall reaction, k_{eff} values for the given set of equally sized GACs are assumed to be primarily affected by the effective diffusion coefficient of monochloramine in the pore system ($D_{E,MCA}$), which in turn is a function of the pore size distribution (Equation (5.17)). Conclusively, the carbon that exhibits the highest $D_{E,MCA}$ should have the highest k_{eff} and vice versa.

Using the effective molecular diameter of monochloramine (~0.5 nm, calculated using the RasMol visualisation tool [346]) as d_{MCA} in Equation (5.17) to calculate $D_{E,MCA}$ for the different carbons gives the following order of $D_{E,MCA}$ values: $2.28 \cdot 10^{-6}$ cm^2 s^{-1} (30N) > $1.42 \cdot 10^{-6}$ cm^2 s^{-1} (K835) > $1.26 \cdot 10^{-6}$ $cm^2 s^{-1}$ (Centaur). Obviously, this order does not correlate well with the one found for k_{eff} shown in Figure 5.10.

By calculating $D_{E,MCA}$ using different values for d_{MCA} > 0.5 nm, it has been found that $D_{E,MCA}$ and k_{eff} correlated well when d_{MCA} was chosen to be equal or larger as ~1.3 nm. Careful interpretation of these results leads to the conclusion that pores <~1.3 nm in width, which is twice the molecular diameter of a monochloramine molecule, might be barely accessible for monochloramine. This clogging could be explained by constrictions at the pore mouth caused by water molecules that adsorb onto oxygen-containing functional groups present at the carbon surface by hydrogen bonding [347-349]. These findings correlate well with the findings of Fairey et al. (2006), who assumed that certain pores might be barely accessible for monochloramine molecules due to diffusional limitations [254].

The significantly higher $D_{E,MCA}$ found for the Centaur carbon for d_{MCA} >~1.3 nm compared to the 30N and K835 carbon mainly results from the large amount of mesopores (>7 nm), which the other carbons did not comprise. It should be noted here that calculation of $D_{E,MCA}$ for the 100058 carbon according to Equation (5.17) is not eligible due to the structured pore size distribution of the carbon grains [320].

5.4 Summary and conclusions

The present work reports kinetic studies for monochloramine removal in GAC filters equipped with commercially available carbons. The investigations intended to: (i) determine the impact of operational filter parameters that are known to limit diffusional mass transport of monochloramine (filter velocity, grain size, water temperature and pore size distribution) and (ii) describe the process that is responsible for the drop of reactivity during the initial phase of the reaction. A kinetic first-order approach, which was used to describe the overall reactivity of GAC filters, was verified in this study in bench-scale fixed-bed reactor experiments.

Both, the activation energies (20.4 - 29.8 kJ mol^{-1}) and the Thiele Modulus (3.0 – 42.1) of the monochloramine-GAC reaction indicate that the overall reaction is strongly controlled by diffusional mass transport in the pore system of the considered GACs. Film diffusion of monochloramine has no impact on the overall reactivity even under high load filtration, as it is usually applied in swimming pool water treatment (filter velocity >30 m h^{-1}).

The use of smaller grain size fractions resulted in an increase of the overall reactivity of the GAC filter. However, it should be noted here that using smaller GAC grain sizes for enhanced monochloramine removal in full-scale applications would give a high pressure loss in fixed-bed GAC filters [340]. Unpublished data indicates that, by comparing the largest (1.9 mm) with the smallest grain size fraction (0.3 mm) of the

30N carbon, the difference in the monochloramine removal was only 15% while the pressure loss strongly increased by factor of ~27.

The pore size distribution of the carbons has been found to have a significant influence on the reaction rate constant of the overall process of monochloramine removal in GAC filters. Concluding from the results of this study, it is assumed that pores <~1.3 nm were not accessible for the monochloramine-GAC reaction while the amount of large mesopores is suggested to be very important for a high overall reactivity of the GAC filter for monochloramine removal.

From the shape of the conversion-time curves of the reaction it was concluded that the drop in reactivity of the GACs observed at the initial phase of the monochloramine-GAC reaction could be explained by increasing pore diffusional resistance that occurred with increasing reaction time. The increasing diffusional control could be explained by the fact that the reaction front starts at the grains outer surface and then moves towards the centre of the GAC grains.

6 Impact of chemical carbon properties on monochloramine removal with GAC filters and its relevance for swimming pool water quality.

Abstract

In this Chapter, yields of NH_4^+ and N_2 for monochloramine removal with different commercially available granular activated carbons (GACs) have been determined in fixed-bed column studies over a long term period. Experiments showed that, depending on the type of GAC used, the N_2 yield of the monochloramine reaction ranged between 0.5 % - 21.3 %. Chemical properties of the GACs, such as the concentration of acidic oxide surface groups and elemental compositions were analyzed and correlated with the observed N_2 yield of the reaction. Results indicate that the copper content of the carbons significantly correlates with the observed N_2 yield. This can be explained by direct catalysis of the disproportionation of monochloramine by Cu(II) forming dichloramine, which in turn is known to be completely degraded at the carbon surface to N_2.

Chloramines react further with dimethylamine in pool water forming highly cancerogenic N-nitrosodimethylamine (NDMA). Model calculations performed with a simplified numerical swimming pool model showed that the concentrations of inorganic chloramines and NDMA in the pool were lower for GACs that exhibit a high N_2 yield of the monochloramine-GAC reaction compared to those with a low N_2 yield. Model results further indicate that the reduction of chloramines and NDMA in pool water could be increased by a factor of 2 - 3 in case the tested commercially available GACs could be chemically modified to transform up to ~80 - 100 % of monochloramine to N_2.

6.1 Introduction

In water treatment processes, granular activated carbon (GAC) filtration is typically used for adsorptive removal of organic impurities [246]. However, previous studies showed that GAC filters additionally could serve as a chemical reducing agent for the reduction of inorganic chloramines (mono, di- and trichloramine) [265, 266, 350].

Inorganic chloramines are disinfection by-products (DBPs) primarily formed via the chlorination of ammonia (NH_3) [189-191] and urea (NH_2CONH_2) [136]. Among the variety of known DBPs, the occurrence and toxicological relevance of inorganic chloramines is one of the best known and most studied examples in the literature [61, 136, 189, 191]. Chloramines received particular attention because they were found to react with dimethylamine (DMA) forming highly carcinogenic N-nitrosodimethylamine (NDMA) [158, 159, 195, 196].

The removal of chloramines from the aqueous phase is relevant for a variety of different process in the water industry such as swimming pool water treatment, production of dialysate for kidney dialysis [310], production of drinking water from pre-chlorinated surface water, soft drink manufacturing or fish farming [340]. This study focuses on the treatment of swimming pool water exclusively.

At the neutral conditions and Cl:N ratios of swimming pool water, monochloramine is known to be the most dominant species among the inorganic chloramines [30]. Its concentrations in pool water are reported up to 1.88 mg L^{-1} (as Cl_2) [30]. Previous studies indicate that monochloramine is transformed at GAC filters either to ammonium (NH_4^+), by oxidation of free surface sites C^* (Equation (5.1)), or to N_2, by reduction of oxidized surface sites C^*O (Equation (5.2)). Until now, no direct evidence for the oxidative decomposition of monochloramine to N_2 according to Equation (5.2) has been presented.

The type of reaction product formed by degradation of monochloramine in GAC filters is of great interest for practical applications. Formed NH_4^+ for instance serves as substrate for microbiological processes leading to unintended microbiological contamination of GAC filters [245], which in turn was found to promote unwanted oxidation of ammonia to nitrite and nitrate [281]. Moreover, NH_4^+ would act as a precursor for the formation of chloramines in case the filter effluent is chlorinated [135]. This adverse repercussion is particularly interesting for the application of GAC filters in swimming pool water treatment, which by nature is not a single pass process but a closed water cycle between treatment section and pool. Thus, it is hypothesized that using GACs with a high N_2 yield (i.e. the molar ratio of N_2 formed

versus monochloramine removed) would sustainably reduce nitrogen available in the closed swimming pool system, which in turn mitigates the concentration of chloramines and NDMA in the basin.

To the best of our knowledge, data on modifying GACs to selectively foster monochloramine transformation to N_2 is very scarce. However, a few studies dealt with the importance of surface chemical carbon properties on the N_2 yield of unmodified carbons. Fairey at al. (2007) assumed that the N_2 yield of the monochloramine-GAC reaction does not significantly differ among a set of five commercial GACs [309]. These findings consider the chemical characteristics of the individual GACs as irrelevant with regard to the N_2 yield. However, the observed N_2 yields in the study ranged between 0 to 40 % and only the low accuracy of the detection method did not allow to significantly distinguish between the N_2 yields of the considered GACs [309]. Determination of the N_2 yield using a more precise detection method is still subject to investigation.

Previous findings indicate that the amount of formed N_2 correlates with the amount of oxide groups present at the GAC surface (see Equation (5.2)). In this context it is not known, whether additional surface oxides formed by the reaction of GACs with free chlorine (Equation (6.1)) [263, 264, 295, 351], which is typically present besides chloramines in pool water, affects monochloramine transformation to N_2.

$$C^* + HOCl \rightarrow C^*O + H^+ + Cl^- \quad (6.1)$$

Other evidence suggests that trace elemental constituents might favour monochloramine transformation to N_2. Various carbonaceous raw materials have been used to prepare activated carbons with different concentrations of hetero-atoms and trace elemental compositions [352-355]. Among those, iron, lead and copper were found to catalyse the process of monochloramine decay [356-360]. Copper appeared of particular interest because it favours disproportionation of monochloramine to form dichloramine [361], which in turn reacts at activated carbons forming N_2 [265].

Concluding from the current state of knowledge, the objectives of this Chapter were to (i) elucidate the importance of various chemical GAC properties on the N_2 yield of the GAC-monochloramine reaction and (ii) simulate the effect of the carbon type used on chloramine and NDMA concentrations in the basin of a simplified numerical pool model. The carbon reactivity and the N_2 yield were quantified in fixed-bed reactor (FBR) experiments for four different commercial GACs. Chemical carbon properties in means of oxygen containing surface groups, elemental composition and

traces of noble and transition metals were analysed and correlated with the observed N_2 yield. The expected results should give further indications for the modification of GACs with the aim to selectively foster monochloramine transformation to N_2. Simulations with a simplified numerical swimming pool model should help to judge whether GAC treatment with carbons that transform plenty of monochloramine to N_2 could be used to mitigate the concentration of chloramines and NDMA in swimming pool systems.

6.2 Materials and Methods

6.2.1 Experimental determination of the carbon reactivity, NH_4^+ yield and N_2 yield

Previous studies showed that the overall reactivity of a fixed-bed GAC filter for monochloramine removal follows first-order kinetics (see Section 5.2.1.1) and carbon reactivity could be expressed as the effective first-order reaction rate constant k_{eff} as given by Equation (5.3) [314, 315]. The procedure for determining k_{eff} in fixed-bed column experiments is described in detail in Section 5.2.1.

Fixed-bed column experiments were conducted over a long term period until stationary conditions in GAC reactivity were reached [266]. Table 6.1 summarizes operation conditions of the bench scale pilot plant. A more detailed description of the experimental method is given in Section 5.2.1.2.

Table 6.1: Operation conditions of the bench scale pilot plant.

Parameter	**Value**
Column diameter	34 mm
Bed depth, z_{bed}	94 mm
Flow velocity, v_{bed}	44.1 m h^{-1}
Temperature, T	30 °C
Monochloramine concentration, $c_{bed,in}$	4.5 (mg L^{-1} (as Cl_2))
pH	7

The NH_4^+ yield and the N_2 yield of the reaction were calculated from the slope of the linear regression between time dependent amount of substance of monochloramine removed ($F_{MCA}(t)$) and the time dependent amount of substance of ammonium formed ($F_{NH4+}(t)$) or N_2 formed ($F_{N2}(t)$). While $F_{MCA}(t)$ and $F_{NH4+}(t)$ were quantified analytically, $F_{N2}(t)$ was indirectly determined from the difference between $F_{MCA}(t)$ and $F_{NH4+}(t)$ assuming that ammonium and N_2 were the only nitrogenous reaction products present in the tank [265, 309].

To determine the impact of surface oxidation by HOCl on the N_2 yield of the monochloramine-GAC reaction, the carbons were pre-treated with HOCl. Therefore, the FBR system was operated as described before but instead of a solution of monochloramine, a constant concentration of 4.5 mg L^{-1} (as Cl_2) of HOCl was maintained in the tank by feedback-controlled dosing of a HOCl stock solution. Experiments with HOCl were run until ~2.2 mmol g_{GAC}^{-1} of HOCl (as Cl_2) reacted at the bench scale GAC filter. Immediately after HOCl treatment, the carbons were left in the filter column but the system was operated with a solution of monochloramine to determine the N_2 yield of the monochloramine-GAC reaction.

6.2.2 Used granular activated carbons and solutions

Four commercially available GACs, Hydraffin 30N from Donau Carbon GmbH (30N), Centaur from Chemviron Carbon GmbH (Centaur), Silcarbon K-835 from Silcarbon Aktivkohle GmbH (K835) and Saratec 100058 from Bluecher GmbH (100058) were used in this study. The raw materials of the carbons were anthracite coal (30N), coconut shells (K835), bituminous coal (Centaur) and non-porous polymer-based spheres (100058). According to specifications provided by the manufacturers, all carbons were produced by initial carbonisation of the different raw materials at low temperatures followed by physical activation with steam (30N, 100058) [362-364], steam and carbon dioxide (K835) [365] or impregnation with urea and subsequent heating (Centaur) [366, 367]. The fixed-bed column experiments were performed with the fresh carbons as they were provided by the producers.

Monochloramine stock solutions used in the fixed-bed column experiments were prepared as described in detail previously (see Section 5.2.2) by slowly purring a HOCl solution over an ammonia stock solution at final molar ratio of chlorine to ammonia ratio of 1.00:1.03 at pH 10. Monochlormaine and HOCl stock solutions were stored covered from light at 4 °C before use. Ultrapure water was produced by the Millipore direct Q UV3 water purification system from Merck Millipore (Germany).

6.2.3 Analytical methods

6.2.3.1 Quantification of monochloramine and free chlorine

Monochloramine and free chlorine concentrations in the tank of the FBR system were continuously analysed by a membrane-covered amperometric 2-electrode total chlorine sensor (CTE-1 DMT, Prominent, Germany), which was calibrated on a daily basis using the photometric DPD method [173].

The monochloramine stock solutions were standardized spectrophotometrically on a daily basis accounting the overlapping absorbance peaks of monochloramine and dichloramine ($NHCl_2$) at 245 nm and 295 nm ($\varepsilon_{NH2Cl,\ 245\ nm}$ = 445 mol^{-1} cm^{-1}, $\varepsilon_{NHCl2,\ 245\ nm}$ = 208 mol^{-1} cm^{-1}, $\varepsilon_{NH2Cl,\ 295\ nm}$ = 14 mol^{-1} cm^{-1}, $\varepsilon_{NHCl2,\ 295\ nm}$ = 267 mol^{-1} cm^{-1}) [325]. Spectroscopic measurements at 360 nm confirmed the absence of trichloramine εNCl_3) in the monochloramine stock solution ($\varepsilon_{NCl3,\ 360\ nm}$ = 126 mol^{-1} cm^{-1}) [326, 327]. T

The HOCl stock solutions were standardized spectrophotometrically at pH 10 as OCl^- ion using a molar absorption coefficient at 294 nm (ε_{294}) of 348 mol^{-1} cm^{-1} [324]. A Unicam UV2-200 UV/VIS spectrophotometer was used for spectroscopic and DPD measurements.

6.2.3.2 Quantification of ammonium

For quantification of ammonium (NH_4^+), samples were taken from the tank and analysed subsequently by size exclusion chromatography with organic carbon and organic nitrogen detection (LC-OCD-OND) as described elsewhere [63, 288]. It has to be noted here that the LC-OCD-OND was designed for organic nitrogen detection but was also capable to quantify ammonia (see Figure 8.5). Samples were stored in headspace free vials with screwcaps (25 mL) at ~4°C until analysis with LC-OCD-OND, which followed within 12 h after sampling. The limit of detection for ammonia is assumed to equal to that of urea previously found in deionized water using the LC-OCD-OND method (1 ppb [288]).

6.2.3.3 Concentration of oxygen containing surface groups

Quantification of oxygen groups present on the GAC surface was performed using the recently standardized method of Boehm [368-370]. This method allows distinguishing oxygen groups by their different acidity including phenols, lactonic groups and carboxyl groups.

For analysis, the fresh and aged GACs were dried at 70°C for 24 h. The drying temperature was kept low to avoid volatile surface oxides being removed by drying [295]. Then, 1.5 g of the carbon was suspended in 50 mL solutions (V_B) of either 0.05 mol L^{-1} $NaHCO_3$, Na_2CO_3 or NaOH (c_B). After shaking the suspension at 150 rpm for 24 h, the samples were filtrated by 0.45 µm polycarbonate track etch membrane filters. A 10 mL aliquot (V_a) of the filtrated $NaHCO_3$ and NaOH solution was acidified with 20 mL (V_{HCl}) 0.05 mol L^{-1} HCl (c_{HCl}) each, while a 10 mL aliquot of the filtrated $NaCO_3$ sample was acidified with 30 mL 0.05 mol L^{-1} HCl. CO_2 was

stripped from the acidified samples by subsequently degassing the sample with N_2 for 2 h. Finally 0.05 mol L^{-1} NaOH (c_{NaOH}) was carefully titrated to the acidified samples until pH 7 was reached. NaOH titration was performed under persisted degassing with N_2. The volume of 0.05 mol L^{-1} NaOH needed to reach pH 7 was denoted as V_{NaOH} and was determined in triplicate for each batch experiment. The amount of substance of carbon surface functionalities in terms of phenols, lactonic groups and carboxyl groups were calculated based on V_{NaOH} as described in the following [368]:

$$\eta_{CFS,B} = \frac{c_{HCl} V_{HCl}}{c_B V_a} c_B V_B - (c_{HCl} V_{HCl} - c_{NaOH} V_{NaOH}) \frac{V_B}{V_a} \quad (6.2)$$

$$\eta_{carboxyl} = \eta_{CFS,\ NaHCO_3} \quad (6.3)$$

$$\eta_{lactonic} = \eta_{CFS,Na_2CO_3} - \eta_{CFS,NaHCO_3} \quad (6.4)$$

$$\eta_{phenole} = \eta_{CFS,NaOH} - \eta_{CFS,Na_2CO_3} \quad (6.5)$$

6.2.3.4 Zeta potential and isoelectric point

To further elucidate the acidic character of the carbons, the zeta (ζ) potential of the fresh GACs was measured from their electrophoretic mobility [371] using a Zetasizer Nano ZS equipped with a MPT-2 autotitrator (Malvern Instruments, Worcestershire, UK). For zeta analysis, a suspension of grounded GACs was prepared in 0.01 mol L^{-1} KCl solution. After a settling time of ~24 h, the supernatant of the suspension was used for analysis.

Zeta potentials were analysed at different pH values as described previously [372]. Adjustment of the pH was performed by dosing solutions of either 0.1 mol L^{-1} HCl or 0.1 mol L^{-1} NaOH to the supernatant taken from the settled GAC suspensions. Zeta potentials are given as mean value of three repeated measurements. The isoelectric point of the GACs is taken to be the pH at which the surface exhibits a neutral net zeta potential.

6.2.3.5 Concentration of noble and transition metals

The concentration of two groups of elements widely used as catalysts (e.g. noble metals (Pd, Rh) and transition metals (Mn, Co, Cu, Fe and Ni) [373, 374]) were analysed in fresh GACs by inductively coupled plasma atomic emission mass spectroscopy (ICP-MS) using a PQexCell instrument (Thermo Fisher Scientific Inc., USA) according to the German standard DIN-EN-ISO-17294-2.

Prior to ICP-MS analysis, powdered samples of the dried fresh GACs were digested for 30 min in a closed PTFE vessel at 180°C by a microwave (MARS 5 CEM Corp., United States). For digestion, 0.5 g powdered carbon sample was suspended in a mixture of 5 mL concentrated nitric acid (HNO_3), 1 mL H_2O_2 (30 %) and 5 mL ultrapure water. Digested samples were filtered by a 0.45 µm polycarbonate track etch membrane filter (Satorius AG, Germany) and subsequently diluted with ultrapure water to 50 mL. Diluted samples were then analysed by ICP-MS. Concentrations of trace metals are reported as mean value of two repeated measurements. Limits of detection of the method were calculated as the threefold standard deviation of blank samples. Blank samples were prepared according to the above described routine but omitting the carbon sample.

6.2.3.6 Elemental micro analysis

Analysis of the carbon, hydrogen and nitrogen content of the GACs was performed using a CHN element analyzer (Vario EL, Elementar Analysesystem GmbH). The sulfur content of the carbons was analysed according to the German standard DIN 51724-3 using an Eltra CS 580 analyser. The following mass of powdered GAC samples were used: 5 - 7 mg (C, N, H) and 100 – 150 mg (S). The C, N, H and S content of the GACs is given as mean value of two repeated measurements. The limits of detection were 0.007 g g_{GAC}^{-1} (C), 0.017 g g_{GAC}^{-1} (N), 0.003 g g_{GAC}^{-1} (H) and <0.05 g g_{GAC}^{-1} (S).

6.2.4 Statistical analysis

Student's t-tests were used for hypothesis testing on the basis of a difference in NH_4^+ yields between the considered GACs. The null hypothesis, which stated that no differences were observed, was rejected for a probability of <0.05. If not mentioned otherwise, errors represent the 95 % confidence interval.

6.2.5 Simulating chloramine and NDMA concentrations in a simplified numerical swimming pool model with GAC filter

6.2.5.1 Model definition

The simplified numerical model of a swimming pool system (Figure 6.1) was used to determine the effect of carbon type used in the GAC filter (e.g. different N_2 yield and k_{eff}) on the concentration of chloramines and NDMA in the basin of a swimming pool. The model was established by combining the simplified hydraulic approach of a real scale horizontally flown swimming pool proposed by Cloteaux et al. (2013) [375] with the following widely accepted reaction models:

(i) Chloramination reaction model of Jafvert et al. (1992), which describes the formation of inorganic chloramines by chlorination of ammonia [135].
(ii) Urea chlorination model of Blatchley and Cheng (2010) as applied by Gérardin et al. (2015) [136, 376].
(iii) NDMA formation model proposed by Schreiber et al. (2006), which describes the formation of NDMA by the reaction of chloramines with DMA [157].

Chloramine removal over the bed depth of a GAC filter was calculated according to Equation (5.3) of this study.

Both, ammonia and DMA were considered to be introduced into the basin by the bathers and the filling water. A detailed description of the hydraulic approach, the reason for using two instead of one completely stirred batch reactor for simulating the swimming pool basin and the model reactions are given in Section 8.2.1 in the supporting information (SI).

Table 6.2 summarizes the relevant volumes, flow rates, bather load and process parameters of the simplified numerical pool model. According to usual practise in German pools, the temperature (T), pH and free chlorine concentration (c_{Cl2}) were assumed to be constant in the aqueous phase over the entire period of the simulations. Simulations were performed under continuous bather load and fresh water dosing until stationary concentrations of the respected reactants c_i were reached in the pool. Model calculations were performed using the software AQUASIM [131].

It should be noted here that the effect of outgassing of volatile substances (i.e. trichloramine) has only a little effect on the substance concentration in the swimming pool [61] and was therefore neglected in this study. Given that this work particularly aims at determining the impact of chloramine removal in GAC filters on pool water quality, the removal of substances in the GAC filter by adsorption was not expected.

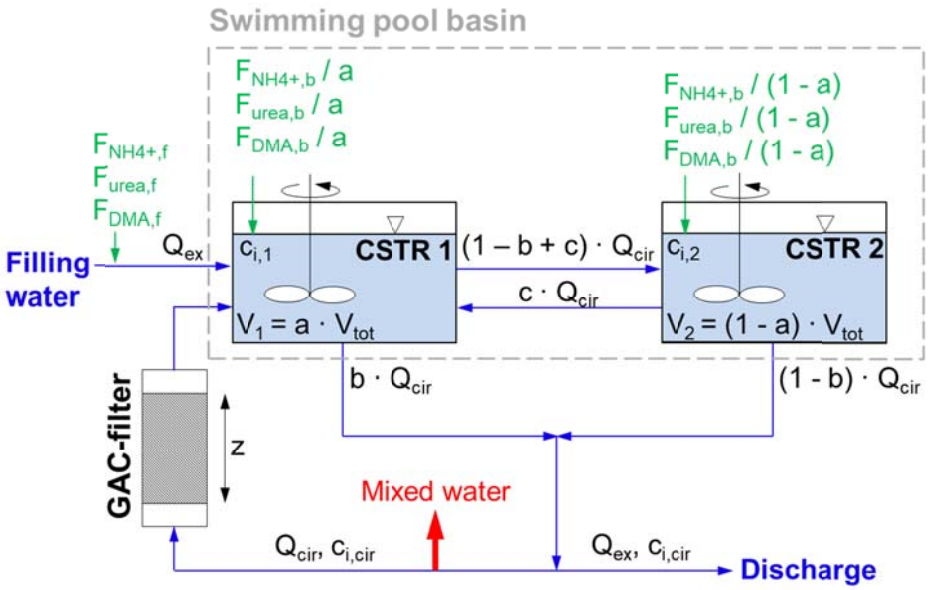

Figure 6.1: Scheme of the simplified numerical swimming pool model, CSTR1 and CSTR 2 stand for a system of two completely mixed reactors that represent the basin of the pool system [375], Q_{cir} stands for the circulated water flow, Q_{ex} for the external water flow (fresh water, urea and sweat), V_1 and V_2 for the water volume in CSTR 1 and CSTR 2 ($V_{tot} = V_1 + V_2$), $c_{i,1}$, $c_{i,2}$ and $c_{i,cir}$ for variable concentrations of substances i (see Table 8.2 (SI)) in CSTR 1, CSTR 2 and in the circulated water flow, $F_{NH4+,b}$, $F_{urea,b}$ and $F_{DMA,b}$ for the amount of ammonium, urea and DMA introduced into the pool by the bather and $F_{NH4+,f}$, $F_{urea,f}$ and $F_{DMA,f}$ for the amount of ammonium, urea and DMA introduced into the pool by fresh water. The water quality in the swimming pool basin is given after mixing water from CSTR 1 and CSTR 2 (see red arrow).

Table 6.2: Process parameters of the simplified numerical pool model.

Parameter	Value
Total volume, V_{tot} (25 m x 11 m x 1.95 m (L x W x D))[a]	536 m³
Circulated water flow, Q_{cir}[a]	180 m³ h^{-1}
Hydraulic parameters (a, b, c)[a]	0.46, 0.35, 1.22
Hydraulic retention times in the pool	2.98 h[b], 288 h[c]
Bather load[d]	62 bather h^{-1}
External water inflow, Q_{ex}[e]	1.86 m³ h^{-1}
Ammonium loading by bathers, $F_{NH4+,b}$[f]	35.79 g h^{-1}
Ammonium loading by fresh water, $F_{NH4+,f}$[f]	0.93 g h^{-1}
Urea loading by bathers, $F_{urea,b}$[g]	5.28 g h^{-1}
Urea loading by fresh water, $F_{urea,f}$[g]	0.0025 g h^{-1}
DMA loading by bathers, $F_{DMA,b}$[h]	0.335 g h^{-1}
DMA loading by fresh water, $F_{DMA,f}$[h]	0.004 g h^{-1}
pH	7
Free chlorine conc.	0.5 mg L^{-1} (as Cl_2)

[a] … Chosen according to Cloteaux et al. (2013) [375]. 1.95 m is the mean of the given range of pool depth (1.5 – 2.4 m)

[b] … Hydraulic retention time respecting the circulated water flow

[c] … Hydraulic retention time respecting the external water flow

[d] … Represents the maximum bather load calculated based on the surface area of the basin (275 m²) according to the German swimming pool standard DIN 19643 [56]

[e] … Includes (i) 30 L per bather of fresh water [56], (ii) 1.76 L per bather of sweat (maximum value given by [31]) and (iii) $1.17 \cdot 10^{-1}$ L per bather of urine (maximum value given by [31])

[f] … Fresh water contains 0.5 mg L^{-1} of ammonium (maximum value allowed according to DIN 19643 [56]), sweat contains 231.8 mg L^{-1} of ammonium [93] and urine contains 1447 mg L^{-1} of ammonium (mean value of the given concentration range in [38])

[g] … Fresh water is assumed to contain $8.1 \cdot 10^{-3}$ mg L^{-1} of urea (half of the maximum concentration for urea in German tap waters given by [288]), sweat contains $1.46 \cdot 10^{3}$ mg L^{-1} of urea [93] and urine contains $21.75 \cdot 10^{3}$ mg L^{-1} of urea (mean value of the given concentration range in [93])

[h] … Fresh water contains $2.2 \cdot 10^{-3}$ mg L^{-1} of DMA (mean value of the given concentration range in [50]), sweat contains 1.8 mg L^{-1} of DMA [377] and urine contains 19.2 mg L^{-1} of DMA [378]

6.2.5.2 Modelling chloramine removal in the GAC filters

The concentration of chloramines in dependence of the bed depth z of the theoretical GAC filter of the numerical pool model was derived from integration of the first-order approach given in Equation (5.3) as follows:

$$c(z)=c_{bed,in} \cdot e^{k_{eff} \cdot \frac{z_{bed}}{v_{bed}}} \tag{6.6}$$

According to the German swimming pool standard DIN 19643, z_{bed} and v_{bed} were chosen with 0.9 m and 30 m h^{-1}, respectively [56]. Assuming k_{eff} being constant

across the bed depth of the GAC filter, c(z) becomes a relative proportion of the inflow concentration ($c_{bed,in}$). Conclusively, chloramine degradation could be described as a relative loss across the total bed depth of a GAC filter (i.e. $c_{bed,out}/c_{bed,in}$).

It has to be considered here that the reaction rate constant k_{eff} for dichloramine is taken to be 20 fold higher compared to that found for monochloramine [266]. The same is assumed to be true for the removal of trichloramine by GAC filtration. Given a filter velocity of 30 m h^{-1} and a bed depth of 0.9 m, both di- and trichloramine are completely removed across the filter bed of a real scale GAC filter. This has been proven to be true for a wide range of k_{eff} (0 - 0.04 s^{-1}) (results not shown). Thus, for simplification, the complete amount of di- and trichloramine present in the filter inflow is considered to be removed across the GAC filter at any time or inflow concentration during the simulations. Contrary to monochloramine, di- and trichloramine were assumed to be completely transformed to N_2 in the GAC filter as they react with the carbon surface according to Equation (6.7) and (6.8) [265, 266, 313].

$$2\ NHCl_2 + H_2O + C^* \rightarrow N_2 + 4\ H^+ + 4\ Cl^- + C^*O \qquad (6.7)$$

$$2\ NCl_3 + 3\ H_2O + 3\ C^* \rightarrow N_2 + 6\ H^+ + 6\ Cl^- + 3C^*O \qquad (6.8)$$

6.3 Results and Discussion

6.3.1 Carbon reactivity and reaction products

Figure 6.2(A-D) shows the amount of substance of NH_4^+ produced and the observed reaction rate constant k_{eff} over the amount of substance of monochloramine degraded at the bench scale GAC filter (Figure 5.1) using filter beds of the 30N, K835, Centaur, and 100058 carbon. In agreement with previous findings, k_{eff} initially decreased until stationary conditions were reached [309], which was after 0.75 to 1.25 mmol g_{GAC}^{-1} of monochloramine reacted (equal to 75 - 125 h of filter run time). The reaction rate constants k_{eff} at steady state revealed in the following order: 0.015 s^{-1} (100058) < 0.016 s^{-1} (30N) < 0.018 s^{-1} (K835) < 0.024 s^{-1} (Centaur). The unusual course of k_{eff} for the 100058 carbon has been discussed previously (see Section 5.3.6) and was explained by a shift in the reaction controlling mechanism, which is caused by the inhomogeneous pore size distribution of the 100058 carbon.

The NH_4^+ yield of the considered carbons were derived from the slope of the correlation between the amount of substance of NH_4^+ produced versus the amount of monochloramine removed in the GAC filter column (see Figure 6.2(A-D)). The correlation was linear for all GACs indicating that the NH_4^+ yield did not change over the total course of the reaction. The coefficient of determination (r^2) for linear fitting ranged among 0.993 to 0.999, giving evidence that the linear regression provides an adequate fit to the experimental data. The NH_4^+ yields determined for the GACs varied within the range of 78.7±3.6 % to 99.5±4.2 %. To access the reliability of the measured NH_4^+ yields, experiments with the K835 carbon were repeated three times (data not shown). Hypothesis testing ($p<0.05$) showed no significant differences in NH_4^+ yield among the three repetitions, indicating a satisfying reproducibility of the detection method. It should be mentioned here that Fairey et al. (2007) reported a NH_4^+ yield of 69±11 % for the Centaur carbon in nutrient water [309] while a higher NH_4^+ yield of 95.8±2.2 % ($p < 0.001$) was determined in this study. This difference could be explained by the different batches of Centaur carbon used in both studies.

It is assumed that the amount of degraded monochloramine that has not been recovered as NH_4^+, is transformed to N_2 instead (Equation (5.1), (5.2)) [265]. LC-OCD-OND analysis confirmed that no other nitrogen containing precursors were present in the water samples taken from the tank. The N_2 yields were as follows: 21.3±4.1 % (K835) > 11.6±3.1 % (100058) > 4.2±3.0 % (Centaur)> 0.5±4.7 % (30N). Slightly higher values for the N_2 yield were reported in previous fixed-bed column studies (42 % [266], 23 to 40 % [309] and 27.3 % [313]). Contrary to the findings of

Fairey et al. (2007) [309], hypothesis testing ($p<0.05$) in this study showed that the differences in N_2 yield between the considered GACs were significant.

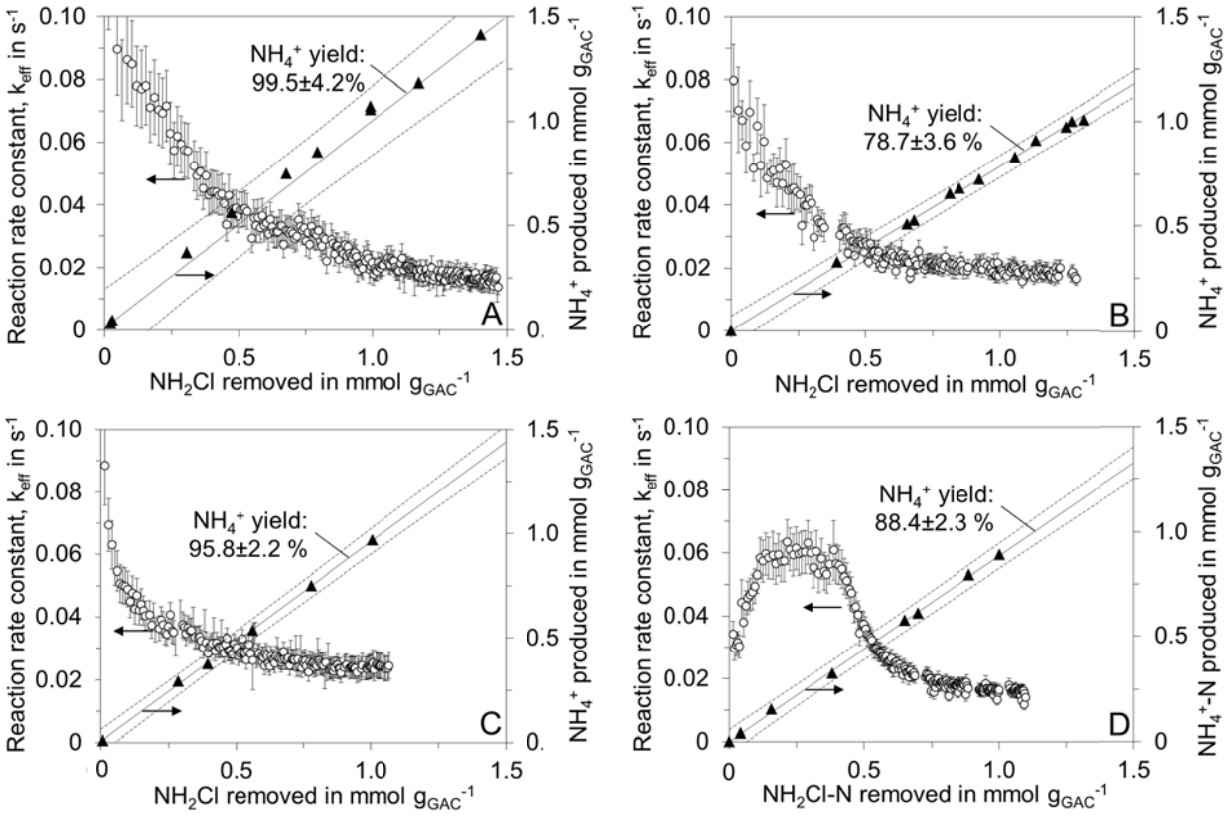

Figure 6.2: Reaction rate constant and amount of substance of NH_4^+ produced versus the amount of substance of monochloramine removed for the GACs 30N (A), K835 (B), Centaur (C) and 100058 (D). Error bars for k_{eff} represent the standard error as determined by Gaussian error reproduction. Solid lines represent linear least-squares best fit of the correlation between monochloramine removed and NH_4^+ produced. Dashed lines represent the corresponding 95% confidence bond of the fitted regression. The NH_4^+ yields for monochloramine removal were derived from the slope of the linear regressions. Errors of the NH_4^+ yield represent the error of the slope of the linear correlation.

6.3.2 Formation of surface oxygen groups

The amounts of acidic oxygen groups present on the surface of the GACs as determined by Boehm titration are shown in Table 6.3. The values are given for the fresh GACs and aged GACs as analysed at the end of the FBR experiments.

Table 6.3: Concentration of acidic oxygen containing groups on the surface of the fresh and aged GACs. The standard method deviations were as follows: 75 µmol g_{GAC}^{-1} (Total), 15 µmol g_{GAC}^{-1} (Phenolic), 76 µmol g_{GAC}^{-1} (Lactonic), 55 µmol g_{GAC}^{-1} (Carboxylic) (n = 8).

Carbon	**Concentration of acidic surface functionalities in µmol g_{GAC}^{-1}**							
	Total		**Phenolic**		**Lactonic**		**Carboxylic**	
	fresh	**aged**	**fresh**	**aged**	**fresh**	**aged**	**fresh**	**aged**
30N	1754	2036	0	76	62	155	1696	1805
K835	1795	2163	51	96	152	212	1592	1855
Centaur	1926	2166	43	110	105	208	1778	1849
100058	1728	2092	8	75	51	173	1670	1844

Characterization of fresh carbons

The fresh carbons comprised total acidic oxidized functionalities in a concentration range from 1728 to 1926 µmol g_{GAC}^{-1}. The majority of acidic oxygen containing groups is present as carboxylic groups, while only small amounts of lactonic and phenolic groups were present. This composition is typical for activated carbons [379-381].

The data in Figure 6.3 shows the ζ potential of the fresh GACs 100058, K835, and Centaur. It has to be envisaged that the effective effective chemical properties of the outer surface of the broken edges of the grinded carbon particles might be different from that of the native carbons used in the experiments. Conclusively, the ζ potential of the carbons analysed in this study carefully interpreted and critically discussed in the following. The data shown in Figure 6.3 indicates that the ζ potential of all carbons falls steeply with increasing pH until it remained constant at a pH of ~7 to 9. The net negative charge in this pH range could be explained by dissociation of the carboxylic groups, which occurs between pH 2 to 6 for activated carbons [372, 382]. The fresh 30N carbon has a higher isoelectric point (pH_{IEP}) of ~7.2 when compared to the other fresh GACs (pH_{IEP} = ~2). The fact that the ζ potential for the 30N carbon crosses the zero potential line indicates that a significant amount of groups with basic properties imparts the GAC surface. These

basic groups however, were not quantified by the Boehm titration method. The ζ potential at neutral pH, as it was used in the fixed-bed column experiments, was net negative for the fresh GACs 100058, K835, and Centaur (~-60 mV) while it was neutral for the fresh 30N carbon. It has to be noted, that the activated carbon particles had been ground prior to the determination of the zeta-potential. Grinding might have altered their surface´s chemical properties.

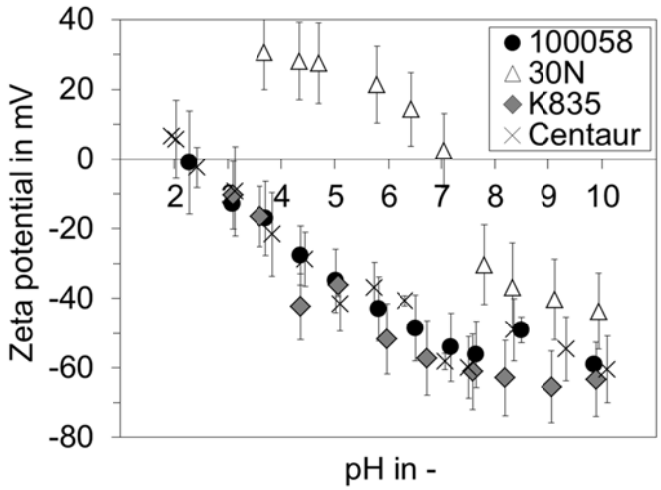

Figure 6.3: Zeta potentials of the fresh carbons 100058, 30N, K835 and Centaur over the pH. Error bars represent the standard derivation of three repeated experiments.

Characterization of aged carbons

The amounts of total acidic surface groups formed over the course of the FBR experiments were as follows: 369 µmol g_{GAC}^{-1} (K835) > 364 µmol g_{GAC}^{-1} (100058) > 278 µmol g_{GAC}^{-1} (30N) > 241 µmol g_{GAC}^{-1} (Centaur). Snoeyink et al. (1974) previously reported an increase in total acidic surface groups of ~1.000 µmol g_{GAC}^{-1} when oxidizing GACs with hypochlorous acid (HOCl) [295]. The high concentration of surface oxides found by Snoeyink et al. could be explained by the higher oxidation potential of HOCl (E_0 = 1.49 V) compared to that of monochloramine [28]. The proportion of phenolic groups increased by ~3 %, while the proportion of carboxylic groups decreased by ~7 % (mean value of all GACs). Hypothesis testing ($p<0.05$) showed that differences in the amount of lactonic groups were not significant.

A correlation analysis was conducted between the total amounts of oxygen containing surface groups present on the surface of the fresh and oxidized GACs and the corresponding N_2 yield. The p-value for the correlation was 0.79 for the fresh and 0.45 for the aged carbons and thus, was rated to be not significant.

In summary, it can be concluded that GAC surface oxidation by monochloramine leads to an increase in the amount of oxygen containing surface groups accompanied by a minor change in the composition of acidic oxygen functionalities. However, the N_2 yield of the monochloramine-GAC was unaffected by the type or amount of oxygen containing groups present at the carbon surface.

6.3.3 Impact of HOCl pre-treatment on the N_2 yield

In order to access the effect of HOCl oxidation, filter beds of the fresh K835 and Centaur carbon were pre-treated with HOCl prior to determination of the NH_4^+ yield of the monochloramine-GAC reaction. Figure 8.11 (SI) presents the reactivity of the K835 and Centaur carbon for HOCl removal with ongoing reaction time. As for monochloramine removal, the carbon reactivity for HOCl removal decreased until k_{eff} reached a constant value. The stationary first-order reaction rate constants for HOCl removal were higher by a factor of ~3 compared to those of monochloramine removal.

Figure 6.4(A,B) shows the reaction rate constant k_{eff} and amount of substance of NH_4^+ produced for the monochloramine-GAC reaction after HOCl pre-treatment. Following Equation (5.2), It is hypothesized that the formation of oxygen groups at the GAC surface caused by HOCl pre-treatment [295] enhances the transformation of monochloramine to N_2. However, as being compared to the NH_4^+ yield observed before the GACs were treated with HOCl (see Figure 6.2(B,C)), the differences were -0.5% (K835) and -5.8% (Centaur). With regards to the standard derivation of the observed N_2 yields, these differences were rated to be not significant.

Since no change in N_2 yield occurred after HOCl treatment, the impact of acidic oxygen functionalities present at the carbon surfaces on monochloramine transformation to N_2 was rated to be negligible. These findings contradict with the reaction mechanism reported previously (Equation (5.2)).

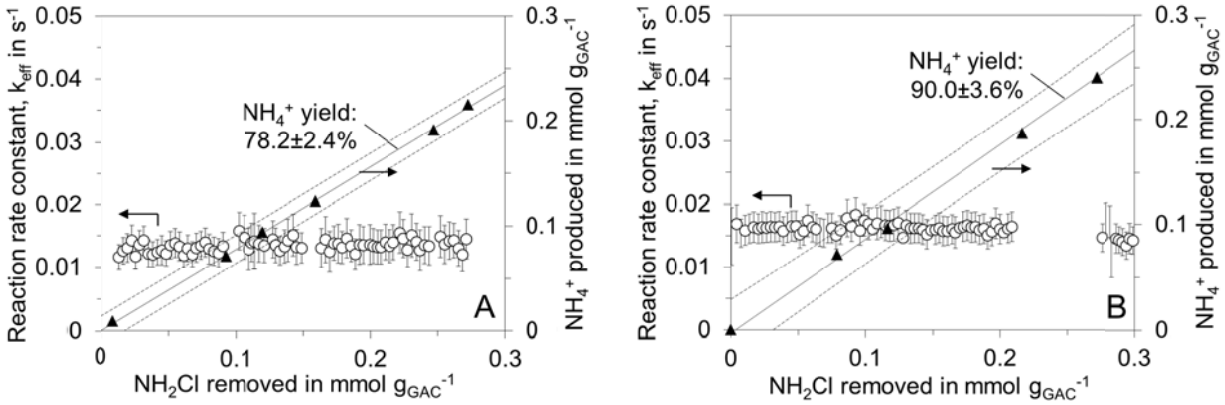

Figure 6.4: Reaction rate constant k_{eff} and amount of substance of NH_4^+ produced over the amount of substance of monochloramine degraded for the carbons K835 (A) and Centaur (B) after HOCl pre-treatment. Error bars for k_{eff} represent the standard error as determined by Gaussian error reproduction. Solid lines represent linear least-squares best fit of the correlation between monochloramine removed and NH_4^+ produced. Dashed lines represent the corresponding 95 % confidence bond of the fitted regression. Errors of the NH_4^+ yield represent the error of the slope of the linear correlation. Interruptions in the k_{eff} curve were caused by imperfect data acquisition.

6.3.4 Impact of trace elements on the N_2 yield

The elemental characteristics of the fresh carbons K835, Centaur, 30N and 100058 and results of the correlation analysis between N_2 yield and the elemental composition of the GACs are presented in Table 6.4. The elemental analysis showed that the Centaur carbon comprised the highest amount of nitrogen and second highest amount of sulphur among the tested carbons. The high nitrogen content could be explained by the manufacturing method of the Centaur carbon, which included impregnation of the carbonized raw material with urea prior to the activation step [366, 367]. Previous studies suggest an increased catalytic activity of carbons with high nitrogen content (e.g. for oxygen reduction reactions [383, 384]) and thiol groups (monochloramine removal [385]). However, hypothesis testing showed no significant correlation between the concentration of hetero-atoms in the carbons and the corresponding N_2 yield of the monochloramine-GAC reaction (Table 6.4).

The content of trace metals found in the considered carbons was typical for activated carbons prepared from natural raw products [352]. It has been shown in past studies that metals such as Fe, Pd or Cu can favour monochloramine conversion to either NH_4^+ or N_2 [356-359, 361]. However, p-values for the correlation of all trace metals with the N_2 yield were not significant and could be rated as random findings. The only exception was the correlation coefficient for Cu, which indicated a satisfying

significance ($p = 0.05$). The positive correlation coefficient indicated that copper promotes monochloramine conversion to N_2. Previous batch studies, that support our findings, showed that copper catalyses monochloramine decay by direct catalysis of Cu(II) and indirect catalysis by formed active radical intermediates. In case of direct catalysis, which was found to be the major reaction path [356], monochloramine is degraded to dichloramine (Equation (6.9) and (6.10)):

$$Cu^{2+} + NH_2Cl \rightarrow [Cu^{II}NH_2Cl]^{2+} \textit{ (complex)} \quad (6.9)$$

$$[Cu^{II}NH_2Cl]^{2+} + NH_2Cl \rightarrow NHCl_2 + NH_3 + Cu^{2+} \quad (6.10)$$

Assuming the same process occurring in GACs, dichloramine would be further transformed at active surface sites to N_2 according to Equation (6.7) [344]. This two-stage process provides a feasible explanation for the monochloramine transformation to N_2 found for GACs with a high Cu content. Table 8.3 in the supplementary material lists other processes that also could partially have an effect on the observed N_2 yield of the monochloramine-GAC reaction. Concluding from these findings, the influence of other process on the observed N_2 yields was rated as negligible.

Table 6.4: Elemental analysis of the tested GACs and correlation analysis of the dependency of N_2 yield from the elemental composition.

Carbon	**N_2 yield in % [a]**	**Elemental analysis in g g_{GAC}^{-1}**				**Trace metal concentration in µg g_{GAC}^{-1}**						
		C	**N**	**H**	**S**	**Fe**	**Mn**	**Co**	**Ni**	**Cu**	**Rh**	**Pd**
blank		n.d.	n.d.	n.d.	n.d.	8.3	0.05	n.d.	n.d.	0.4	n.d.	n.d.
K835	21.3±4.1	86.0±0.0	0.2±0.02	1.2±0.03	0.1±0.00	32±13	8.1±0.3	0.04±0.0	0.9±0.3	14.1±0.4	n.d.	0.004±0.001
Centaur	4.2±3.0	81.5±4.1	0.7±0.14	1.4±0.03	0.8±0.01	172±50	2.5±0.9	2.2±0.3	9.4±2.9	10.2±2.0	n.d.	0.050±0.005
30N	0.5±4.7	84.6±0.3	0.3±0.00	0.8±0.02	0.4±0.01	4306±216	90.5±11.2	9.2±1.0	16.0±0.1	6.8±0.3	n.d.	0.083±0.007
100058	11.6±3.0	96.9±0.0	0.1±0.01	0.5±0.00	1.4±0.03	2483±349	47.5±11.5	1.1±3.5	74.8±0.0	10.9±2.7	n.d.	0.004±0.01
r		0.32	0.55	0.03	0.26	-0.59	-0.55	-0.80	-0.02	0.95	-	-0.89
p-value		0.68	0.45	0.97	0.74	0.41	0.45	0.20	0.98	0.05	-	0.11

n.d. … None detected

[a] … Errors represent the standard deviation

6.3.5 Modelling concentrations of chloramines and NDMA in pool water depending on the carbon type used in the GAC filter

A brief description of the simplified numerical pool model including water treatment by GAC filtration is presented in Section 6.2.5 of this study. Simulations have been conducted using the k_{eff} values and N_2 yields of the four commercial GACs used in this study. Figure 6.5 shows simulated, relative monochloramine concentration profiles ($c(z)/c_{bed,in}$) over the bed depth of the theoretical real scale GAC filter. It should be noted here that the relative concentration profile of monochloramine over the bed depth of the GAC filter is independent of the inflow concentration (see Section 6.2.5.2). It revealed that monochloramine is only partially removed across the total bed depth of the GAC filter. The relative monochloramine removal in dependence of the used GAC type revealed in the following order: 92.6 % (Centaur) > 86.1% (K835) > 82.4% (30N) > 80.6 % (100058).

The relative amounts of transformation products (N_2 and NH_4^+) formed by monochloramine removal over the bed depth of the GAC filters is shown in Figure 8.12 (SI). Concluding from these results, the amount of monochloramine transformed to N_2 across the GAC filter rather depend on the N_2 yield than on the carbon reactivity k_{eff}, which highlights the particular importance of surface chemical properties of the used GACs.

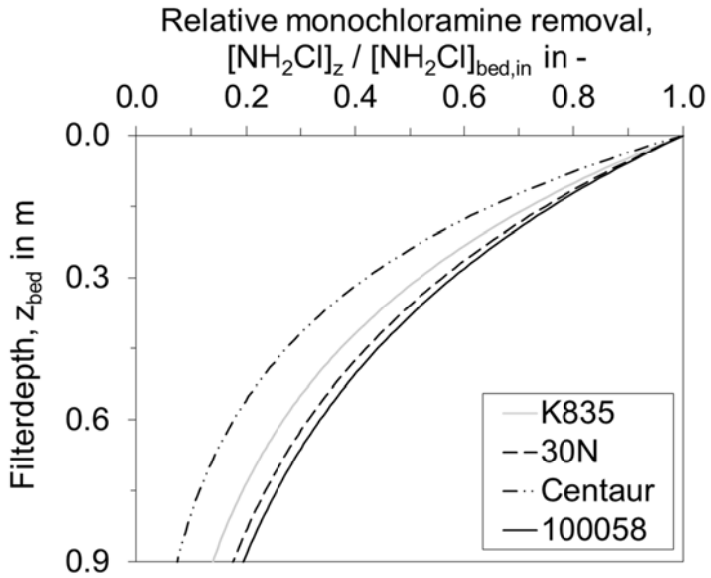

Figure 6.5: Simulated relative monochloramine concentrations over the bed depth of a theoretical GAC filter (z = 0.9 m) for the carbons K835, 30N, Centaur and 100058. Concentration profiles were calculated according to Equation (6.6) using v_{eff} of 30 m h^{-1}. The reaction rate constants and N_2 yields used for calculation were those observed when stationary conditions were reached (see Figure 6.2).

Figure 6.6 exemplarily shows simulated time dependent concentrations of inorganic chloramines and NDMA in the numerical pool model, in case the GAC filter comprises the K835 carbon. The time needed to reach stationary conditions in the pool was ~2 h for inorganic chloramines and up to ~1000 h for NDMA. This discrepancy could be explained by the higher rate constants for chloramine formation (reaction 1, 3 and 11, Table 8.2 (SI)) compared to the rate constant of the limiting NDMA formation step (reaction 27, Table 8.2 (SI)).

Modelled concentrations at steady-state were 0.17 mg L^{-1} (as Cl_2) combined chlorine (0.01 mg L^{-1} (as Cl_2) (monochloramine), 0.04 mg L^{-1} (as Cl_2) (dichloramine), 0.03 mg L^{-1} (as Cl_2) (trichloramine)) and 0.012 ng L^{-1} (NDMA). Concentrations of chloramines and NDMA found in real scale pools with almost equal concentrations of free chlorine were only slightly higher: 0.23 mg L^{-1} (as Cl_2) combined chlorine (monochloramine: 0.17 mg L^{-1} (as Cl_2), dichloramine: 0.05 mg L^{-1} (as Cl_2), trichloramine: 0.01 mg L^{-1} (as Cl_2)) [30] and 0.06 to 5.9 ng L^{-1} NDMA [159, 171, 386]. The reasonable comparability between modelled results and measurements in real pools confirm the capability of the applied reaction scheme and bather loading to simulate chloramine and NDMA formation in swimming pool water.

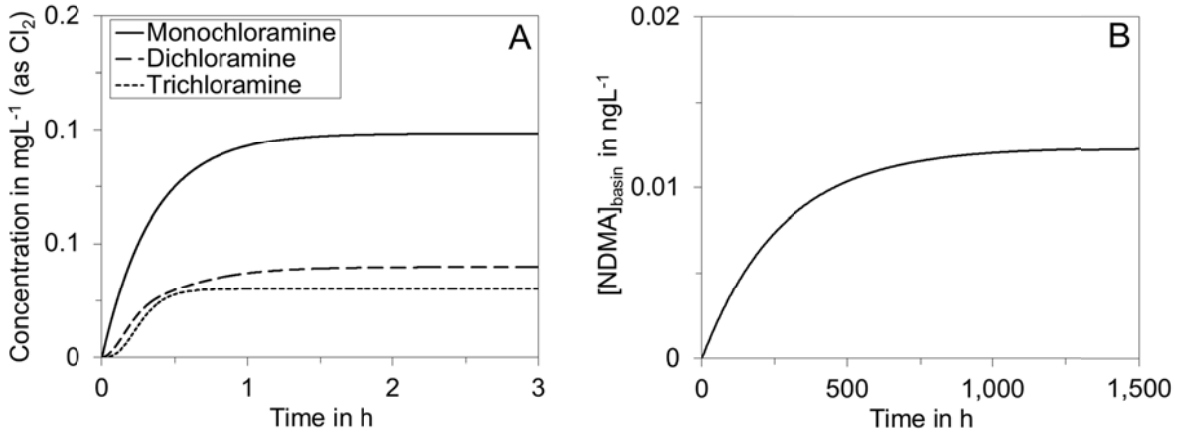

Figure 6.6: Evolution of simulated concentrations of mono-, di- and trichloramine (A) and NDMA (B) in the simplified numerical pool model. The carbon reactivity k_{eff} and N_2 yield of the carbon in the GAC filter were exemplarily chosen to be that of the K835 carbon (k_{eff} = 0.0183 s^{-1}, N_2 yield = 21.3 %).

Figure 6.7 shows the effect of GAC properties (k_{eff} and N_2 yield) on the stationary concentrations of inorganic chloramines (sum of mono-, di- and trichloramine) and NDMA in the basin of the simplified numerical pool model. Simulation results are displayed as relative reduction related to the scenario without GAC filter. For the purpose of comparison, the removal performance of the GACs used in this study (30N, K835, Centaur and 100058) and those considered in previous fixed-bed

column studies [266, 309, 313] are highlighted. Table 8.4 (SI) summarizes the used k_{eff} values and N_2 yields of the considered GACs, as taken form the literature. Among a variety of considered GACs, the relative reductions related to the scenario without GAC filter ranged between 0.5 to 2.7 % (inorganic chloramines) and 1.7 to 4.5 % (NDMA) depending on the GAC used. Thus, the model results confirm the initial hypothesis that increasing transformation of monochloramine to N_2 in GAC filters sustainably reduces the concentrations of inorganic chloramines and NDMA in the basin. Moreover, the results indicate that the reduction of chloramines and NDMA could be increased by a factor of ~2 if the considered GACs could be modified to comprise a N_2 yield of up to ~50 %.

Given a constant N_2 yield, concentrations of chloramines and NDMA in the basin did not significantly change for k_{eff} higher than ~0.025 s^{-1}. This could be explained by the fact that almost all monochloramine is removed across the GAC filter for reaction rate constants >~0.025 s^{-1}. Thus, increasing k_{eff} does not increase the overall transformation rate of monochloramine in the GAC filter.

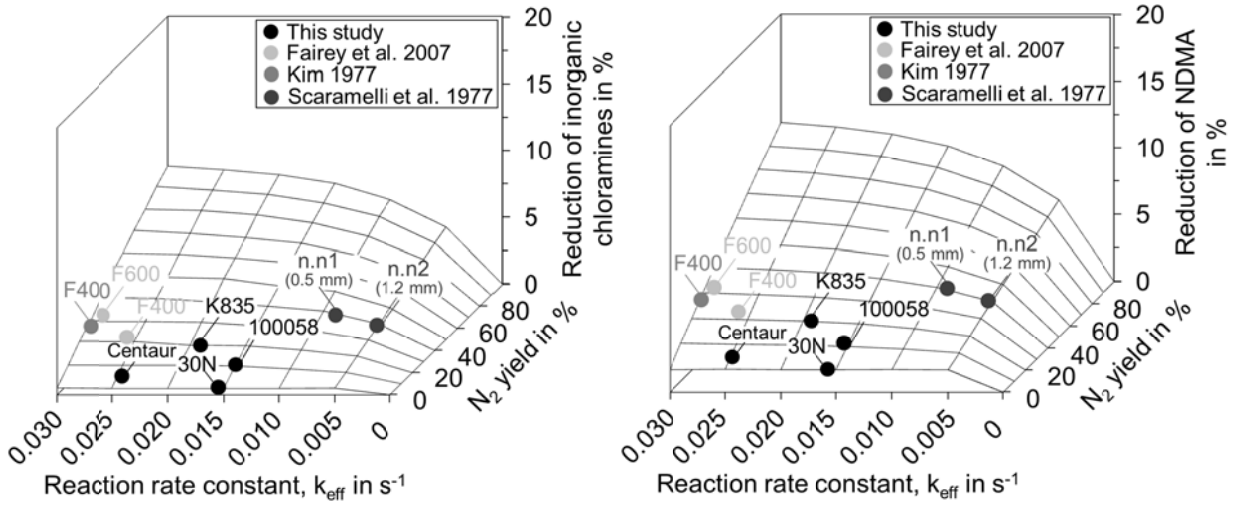

Figure 6.7: Impact of k_{eff} and N_2 yield on stationary concentrations of inorganic chloramines and NDMA in the simplified numerical swimming pool model (Figure 6.1). Results are displayed as relative reduction related to the scenario without GAC filter.

6.4 Summary and conclusions

To degrade hazardous inorganic chloramines (i.e. mono-, di- and trichloramine) in swimming pool water and thus, mitigate health risks for the bathers, water treatment by GAC filtration is typically applied. A detailed understanding of the reaction of GACs with monochloramine, the predominant chloramine species in swimming pools, is of particular interest because it is known to be either transformed to ammonium (NH_4^+), which remains in the aqueous phase and stays available for subsequent chlorination and thus, DBP formation, or to nitrogen gas (N_2), which leaves the aqueous phase.

In long term fixed-bed experiments, it is shown that the N_2 yield of the monochloramine-GAC reaction ranged among four commercially available GACs between 0.5±4.7 % and 21.3±4.1 %. Contrary to previous findings, it is assumed that monochloramine does not undergo a reaction with oxygen groups present at the carbon surface forming nitrogen gas. This hypothesis was derived from that fact that the amount of oxygen containing groups, especially carboxylic groups, formed by the monochloramine-GAC reaction increased with ongoing reaction time while the N_2 yield of the monochloramine-GAC reaction remained constant. Even after intense pre-oxidation of the GAC surface with hypochlorous acid (HOCl), the N_2 yield of the GAC did not significantly change.

The observed N_2 yield significantly correlated with the copper content of the carbons. This facilitates the interpretation that transformation of monochloramine to N_2 at GACs is a two-stage process, where monochloramine is transformed to dichloramine in a first step by direct catalysis at Cu(II). In a secondary step, dichloramine reacts further at free active sites at the carbon surface forming N_2. It has to be noted here that the number of used GAC in this study is very low (n=4) and further experiments using carbons with different amounts of Cu immobilized on the carbon surface are needed to validate the importance of the Cu content in GACs for the N_2 yield.

Simulations using a simplified numerical swimming pool model showed that monochloramine transformation to N_2 in GAC filters mitigates the concentration of inorganic chloramines and NDMA in the basin. Among the tested GACs, the relative reduction related to the scenario without GAC filter ranged between 0.5 to 2.7 % (inorganic chloramines) and 1.7 to 4.5 % (NDMA) depending on the type of GAC used. Model results indicate that the reduction of chloramine and NDMA in the pool could be increased by a factor of ~2 if the considered GACs could be modified to comprise a N_2 yield of ~50 %.

7 General conclusions and outlook

Swimming pool water is continuously circulated in a closed loop between the basin and a treatment section that consists of a combination of different treatment steps that pool water flows though subsequently. Among others, pool water treatment aims to reduce the concentration of harmful disinfection by-products (DBPs) formed by the reaction of free chlorine with organic DBP precursors introduced into the basin by bathers and filling water. This thesis provides profound knowledge about the potential of novel and conventional water treatment technologies to reduce hazardous impurities found in pool water. In particular, this thesis contributes to answer the following questions:

(i) To which extend do novel and conventional water treatment technologies contribute to the mitigation of DBPs and DBP precursors in swimming pool water?
(ii) Which mechanisms and processes determine the removal of inorganic chloramines in granular activated carbon filtration?
(iii) To which extend does granular activated carbon filtration contribute to the mitigation of inorganic chloramines and NDMA in pool water?

In this chapter the findings regarding every individual research question are summarized and final conclusions and recommendations are made at the end of each chapter.

(i) As outlined in Chapter 4, a pilot scale swimming pool model was developed that facilitated the comparison of various novel and conventional pool water treatment combinations under fully controlled and reproducible operation conditions. It has been found that concentrations of organic matter (measured as dissolved organic carbon (DOC)) increase with ongoing operation time of a pool followed by a stationary phase. It has been found that even a low removal of organic matter across the treatment train results in a significant reduction in the stationary concentration of organic matter in the basin. Surprisingly, conventional pool water treatment employing flocculation, sand filtration with subsequent granular activated carbon (GAC) filtration revealed the lowest concentrations of dissolved organic matter among the various tested treatment combinations. The good performance of this treatment concept was partially related to microbial degradation of organic matter in the deeper, chlorine free regions of the GAC filter. In spite of its good removal performance, biologically active carbon filters could potentially become contaminated by pathogens and even promote their growth in the swimming pool water cycle, thus, becoming a potential health issue for bathers. It will be subject to future research to

elucidate the applicability of biofilters for pool water treatment under the particular light of the microbiological safety.

Using powdered activated carbon (PAC) as a coating layer on the sand filter instead of a separate GAC filter revealed lower DOC removal over the treatment train and thus, leads to higher DOC concentrations in the basin. This effect could be explained by the low amounts of PAC typically used in pool water treatment. Using UV irradiation (low pressure (LP) or medium pressure (MP)) downstream to the filtration process (i.e. sand filter or ultrafiltration (UF) membrane) was not capable to significantly reduce the concentration of organic precursors in the basin compared to combinations using PAC addition instead.

Several of the treatment combinations examined in this study were capable to significantly reduce the concentration of volatile DBPs in pool water. As for the concentration of organic precursors, DPB concentrations were the lowest for conventional water treatment employing flocculation, sand filtration and subsequent GAC filtration. However, the results presented in this study demonstrate that an effective removal of DBPs across the treatment train does not necessarily result in low DBP concentrations in the pool. These findings raise the importance of the reactivity of organic matter towards chlorine and the DBP formation kinetics in the basin. The results presented in this study allow the conclusion that UV irradiation could, to some extent, induce structural changes of organic matter which result in a high reactivity with chlorine and thus, higher DBP concentrations in the basin. However, it could not clearly been excluded that UV induced formation of free chlorine from combined chlorine supported the additional DBP formation too. Further research should aim to validate this assumption.

Trichloramine is a DBP found in pool water known to cause severe adverse health effects. Trichloramine concentrations in the pool model varied only by a factor of 2 among the different treatment concepts tested (0.11 to 0.24 mg L^{-1} (as Cl_2)) while no correlation was observed with urea concentrations (p-value of 0.80). These results confirm previous finding by Soltermann et al. (2015), who found a strong correlation between the concentration of trichloramine and the level of free chlorine, which was held constant in the swimming pool model for all experiments (c_{Cl2} = 0.54 ± 0.13 mg L^{-1} (as Cl_2). It is intended that removing trichloramine in the treatment train does not compensate for the fast trichloramine formation occurring in the swimming pool basin and thus, is not a feasible mitigation strategy. To mitigate trichloramine in the pool water it is therefore recommended to reduce free chlorine concentrations in pool to the lowest levels permitted by local pool water standards.

In this thesis, water treatment technologies are basically compared based on their ability to reduce the concentration of chemical parameters such as dissolved organic precursors or DBPs. However, future research and on-site surveillance campaigns in swimming pools should aim to comprehensively assess pool water treatment using both, chemical and toxicological parameters. To this end, there is still the need for further evidence of direct links between DBPs found in pool water and health effects in human kind.

(ii) Among all treatment technologies tested in the pool model, activated carbon treatment and in particular granular activated carbon filtration (GAC filtration) showed the highest removal for inorganic chloramines, which are subject to continuous surveillance in German swimming pools. As known from literature, monochloramine is the predominant species of inorganic chloramines found in pool water and it is removed in GAC filters by a surface reaction rather than by adsorption. In Chapter 5 it is presented that monochloramine removal in a GAC filter could be described by a first order reaction. The activation energy of the heterogeneous reaction ranged between 20.4 - 29.8 kJ mol^{-1} depending on the carbon used and the Thiele Modulus was 3.0 – 42.1. These findings indicate that the overall process of monochloramine removal in GAC filters is strongly controlled by diffusional processes rather than by the intrinsic rate of the chemical reaction. Experiments performed using smaller grain size fractions and an increased filter velocity indicated that the overall reactivity is limited by diffusional processes in the pore system rather than by film diffusion. Pores <~1.3 nm are assumed to be hardly accessible for the monochloramine-GAC reaction while a large proportion of mesopores was important to achieve a high overall reactivity of the GAC filter for monochloramine removal. Further research is needed to find a well-balanced pore size distribution of carbons enabling fast diffusion processes for chloramines and thus, high overall reactivities of GAC filters.

It has been shown experimentally that the monochloramine-GAC reaction starts at the grains outer surface and then moves towards the center of the GAC grain leaving behind a low reactive carbon shell. This process is called the shrinking-core mechanism and explains the increasing diffusion paths of monochloramine in the pore system with increasing reaction time. This, in turn, is assumed to be the reason for the decreasing reactivity observed at the initial time of filter operation. Based on these findings, future research aiming to simulate GAC filtration for chloramine reduction in swimming pools could model the initial drop in reactivity of a GAC filter based on a mechanistical rather than on an empirical approach.

(iii) In long term fixed-bed experiments presented in Chapter 6, it is shown that monochloramine is transformed in GAC filters to N_2 and NH_4^+. The ratio of

monochloramine degraded and NH_4^+ formed in GAC filters is of particular interest since the latter is fed back into the pool where it reacts further with free chlorine forming hazardous inorganic chloramines again. Thus, monochloramine should be transformed to N_2 rather than NH_4^+ in pool water treatment. Among the different commercial GACs tested, the N_2 yield of the monochloramine-GAC reaction ranged between 0.5±4.7 % to 21.3±4.1 %. Correlations between the amount of oxygen containing groups on the surface of GAC particles and the observed N_2 yield of the monochloramine-GAC reaction were not significant. These findings indicate that reaction mechanisms for monochloramine with carbonaceous material proposed in previous works could not sufficiently describe the overall process.

A strong correlation between the copper content of the carbons and the N_2 yield was found in this work ($r = 0.95$). The following two-stage transformation pathway of monochloramine to N_2 at the used GACs has been derived from these findings: (i) conversion of monochloramine to dichloramine by direct catalysis via Cu(II) present on the carbon surface and (ii) reaction of dichloramine at free active surface sites forming N_2. Simulations using a simplified numerical swimming pool model showed that among the tested GACs, the relative reduction of inorganic chloramines related to the scenario without GAC filter ranged between 0.5 to 2.7 %.

Chloramines were found to react with dimethylamine (DMA) in swimming pool water forming highly carcinogenic N-nitrosodimethylamine (NDMA). Thus, reducing the level of chloramines in swimming pool water appears to be a suitable strategy to mitigate NDMA formation in pools. Simulations showed that among the tested GACs, the relative reduction of NDMA related to the scenario without GAC filter ranged between 1.7 to 4.5 %. Further, model results indicate that the reduction of chloramines and NDMA in the pool could be increased by a factor of ~2 if the considered GACs could be modified by Cu coatings to comprise a N_2 yield of ~50 %. Further studies using carbons with different amounts of Cu immobilized on the carbon surface are needed to validate this assumption. As a further step it appears meaningful to physically separate the processes of (i) Cu(II) catalysed monochloramine transformation to dichloramine and (ii) reduction of dichloramine at GACs to N_2. By separating these processes, highly specific copper-based catalysts with much higher efficiencies for monochloramine transformation compared to copper coated activated carbons could be used.

8 Supporting Information

8.1 Supporting Information for Chapter 4

8.1.1 Operation conditions of different treatment processes used in the swimming pool model

Table 8.1: Operation conditions of different water treatment processes used in the swimming pool model.

Treatment process	Operation conditions
Flocculation	- 0.07 g m^{-3} (as Al) polyaluminium chloride (sand filtration) or pre-hydrolysed aluminium chlorohydrate (UF) (Dr. Nüsken, Germany) - In-line dosing at a flow velocity of ~1 m s^{-1} - Dosed 10 s before entering the sand filter[a] - Dosed 40 s before reaching the UF-membrane[b]
PAC dosing	- In-line dosing of 1.5 g m^{-3} of a micro porous anthracite coal based PAC at a flow velocity of ~1 m s^{-1} - Zeta potential of the PAC at pH 7 = -30 mV - The PAC suspension was dosed shortly after adding the coagulant
Sand filtration	- Glass filter column (d_{column} = 150 mm) - 30 m h^{-1} superficial velocity (empty bed contact time = 1.87 min) - 1 m filter layer of quartz sand (0.71 - 1.25 mm), 0.2 m supporting layer of quartz sand (3.15 - 5.6 mm) - 1 m freeboard - Manually backwashed in case the pressure loss over the bed depth exceeds ~1.0 bar[c]
Ultrafiltration	- Dead-end inside-out driven capillary module with each capillary having a diameter of 1.5 mm (Dizzer S1.5 Multibore, Inge AG) - Molecular weight cut-off (MWCO) of the membrane is 100 kDa - Flux = 120 L m^{-2} h^{-1} - Automatically backwashed every 240 min[d]
GAC filtration	- Glass filter column (d_{column} = 150 mm) - 30 m h^{-1} superficial velocity (empty bed contact time = 1.87 min) - Coconut shell based GAC - 1 m filter layer of granular activated carbon (d_{60} = 1.57 mm) - 0.2 m supporting layer of quartz sand (3.15 - 5.6 mm) - 1 m freeboard - Manually backwashed at the same time as the sand filter[e]

(Continuation of Table 8.1)

Treatment process	Operation conditions
UV irradiation	- UV-lamp (LP): 65 mJ cm^{-2} [f,g] - UV-lamp (MP): 62 mJ cm^{-2} [f,g]
pH adjustment	- In-line dosing of either 0.1 mol L^{-1} H_2SO_4 or 0.1 mol L^{-1} NaOH (VWR, Germany) at the end of the treatment train - Feedback controlled dosing to maintain a constant pH at the uppermost sampling port of the basin
Chlorination	- In-line dosing of 0.16 mol L^{-1} NaOCl-solution (VWR, Germany) at the end of the treatment train - Feedback controlled dosing to maintain a constant concentration of free chlorine (0.5 mg L^{-1} (as Cl_2)) at the uppermost sampling port of the basin

[a] … As recommended by the German standard DIN 19643 [26]

[b] … As recommended by supplier of the UF-membrane

[c] … Backwashing procedure (according to German DIN 19643 [26]):
(i) Discharge of supernatant
(ii) Flushing with DOC-free drinking water at 60 m h^{-1} for t = 3 min
(iii) Air scour at 60 m h^{-1} for t = 5 min
(iv) flushing with DOC-free drinking water at 60 m h^{-1} for t = 5 min
(v) Filter to waste filtration at 0.57 m^3 h^{-1} for t = 3 min

[d] … Backwashing procedure (according to manufacturer):
(i) Normal backwash:
- Backwashing with DOC-free drinking water for t = 60 s at a flux of 230 L m^2 h^{-1}
(ii) Chemical enhanced backwash (according to manufacturer):
- After 3 filtration cycles with H_2SO_4
- After 6 filtration cycles with NaOH and H_2SO_4
- After 11 filtration cycles with NaOCl
- Backwashing with chemicals for t = 30 s at a flux of 120 L m^2 h^{-1} and a subsequent contact phase of t = 5 min

[e] … Backwashing procedure (according to German DIN 19643 [26]):
(i) Discharge of supernatant
(ii) Air scour at 60 mh^{-1} for t = 3 min
(iii) Settling phase of t = 3 min
(iv) Flushing with DOC-free drinking water at 60 mh^{-1} for t = 6 min
(v) Filter to waste filtration at 0.57 m^3 h^{-1} for t = 3 min

[f] … UV dose given for the transmission of the pool water which revealed under stationary conditions of Exp. 1 (92±1 % out of 10 mm)

[g] … Calibration performed by the supplier (biodosimetrically determined according to the method described in [387])

8.1.2 A simplified numerical model of the pilot scale swimming pool plant

A simplified numerical model of the pilot scale swimming pool was developed to determine the concentration of organic matter under the absence of water treatment (i.e. neglecting the removal of organic substances across the treatment-train and the transformation of organic substances by the reaction with chlorine). The complex hydraulics of the numerical model were described by a combination of simple compartments, such as completely stirred batch reactors (CSTR) and plug-flow reactors (PFR) [139, 388]. The compartment configuration was derived from the retention time distribution (RTD) of the pilot scale swimming pool plant.

The RTD was determined experimentally by performing a tracer experiment. Therefore, the basin was fed with DOC-free fresh water at a flow rate of 0.57 $m^3\ h^{-1}$ in single pass configuration (i.e. water was discharged instead of recirculating it into the splash water tank). At the experimental run time t = 0, dosing of a stock solution of the tracer sodium fluorescein (uranine) [389] was started upstream to the basin. During the tracer experiment, uranine was continuously monitored in the spill way of the basin (i.e. at the outlet). For quantification, the molar absorption coefficient at 490 nm was used ($\varepsilon_{uranine,\ 490\ nm}$ = 73,523 $mol^{-1}\ cm^{-1}$). Figure 8.1 shows the correlation between absorbance versus sodium fluorescein concentration in GAC-filtrated tap water (DOC-free).

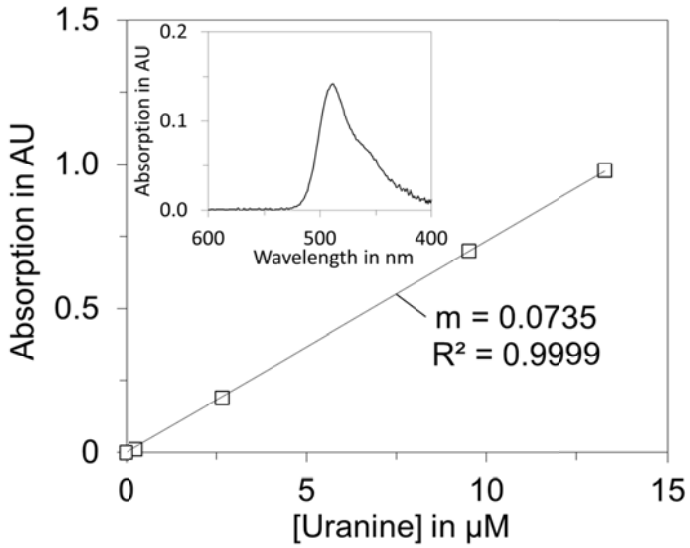

Figure 8.1: Absorbance plotted against the sodium fluorescein concentration (at 490 nm) and absorption spectrum of sodium fluorescein (2.7 µmol L^{-1}) in DOC-free tap water (inset). Spectroscopic measurements were performed using a Unicam UV2-200 UV/VIS spectrophotometer.

Figure 8.2 shows the relative uranine concentration ($c(t)/c_{in}$) over the run time of the tracer experiment. The dead time (t_d = ~0.35 h) at the start of the experiment could be represented by a small plug flow reactor (PFR) whose volume (V_{PFR}) is calculated with 0.20 m³ as follows:

$$V_{PFR} = \frac{t_d}{Q_{circ}} \tag{8.1}$$

Here, Q_{circ} is the circulation rate (0.57 m^3L^{-1}). At a run time of ~12 h, the uranine concentration reached its maximum concentration (c/c_{in} = 1). The residence time distribution between t_d and the end of the experiment is typical for a CSTR [139]. To respect the fact that the basin might consist of stagnant areas, a dead volume V_d was considered. Figure 8.2 shows that the modelled RTD turns out to be very close to the simulated RTD if V_d is chosen with 0.35 m³.

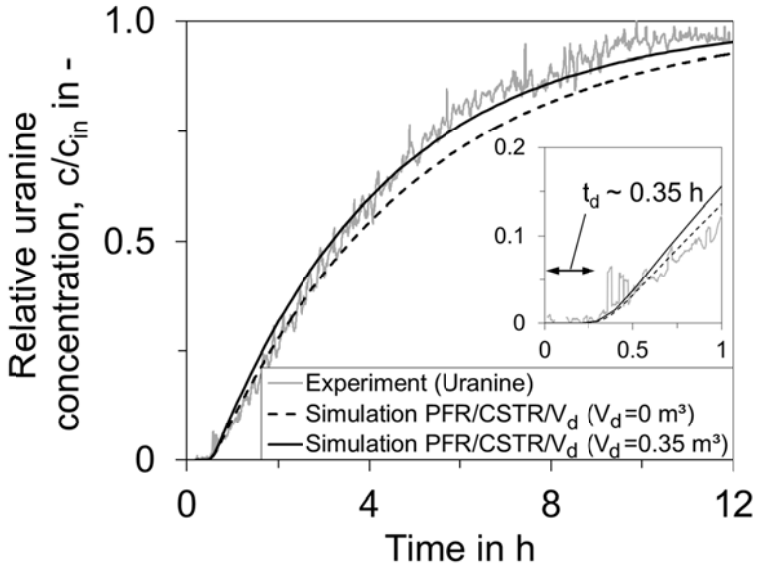

Figure 8.2: Measured and simulated residence time distribution in the basin of the pilot scale swimming pool model. The basin was operated in single pass configuration at a flow rate of 0.57 $m^3\ h^{-1}$ for both, experiment and simulations.

The final conceptual numerical model, as it was implemented in the model environment AQUASIM, is shown in Figure 8.3. It consists of the basin (PFR/CSTR/V_d), the stirred splash water tank (CSTR2), the recirculation flow of 0.57 $m^3\ h^{-1}$, the fresh water input, the release of pool water (8.5 L h^{-1}) and dosing of BFA and humic acids (HA). The amounts of BFA and HA added to into the water cycle are described in Section 4.2.1.2 of this study.

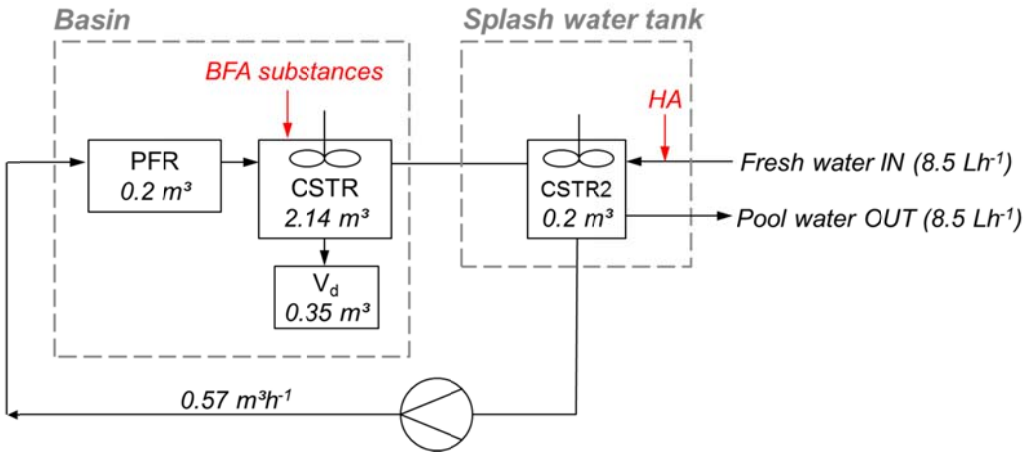

Figure 8.3: Dimensions and flow paths of the simplified numerical model of the pilot scale swimming pool.

8.1.3 Correlation between concentrations of DOC and NPOC

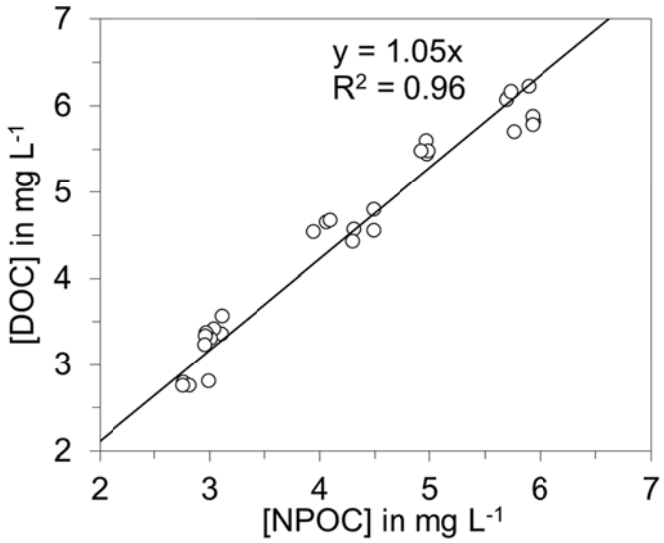

Figure 8.4: Correlation between DOC (measured with LC-OCD) and NPOC (measured with the catalytic combustion method) for several samples taken over the course of Exp. 1 – 7.

8.1.4 LC-OCD chromatograms of single substances

Figure 8.5(A) shows chromatograms of single BFA substances as acquired by the LC-OCD method operated with the normal eluent. It revealed that almost all BFA-compounds elute at approximately the same time of 63.8 - 73.6 min, which is primarily attributed to the fraction of low molecular neutrals. This is mainly caused by the equal molecular size of the BFA substances (1 - 9 C atoms). Different from other BFA substances, citric acid was detected at t_{max} = 45.5 min (primarily building blocks), less than 3 min after the humic acids (HA) peak. This was in accordance with previous findings for aliphatic di- and triprotic acids [288, 390].

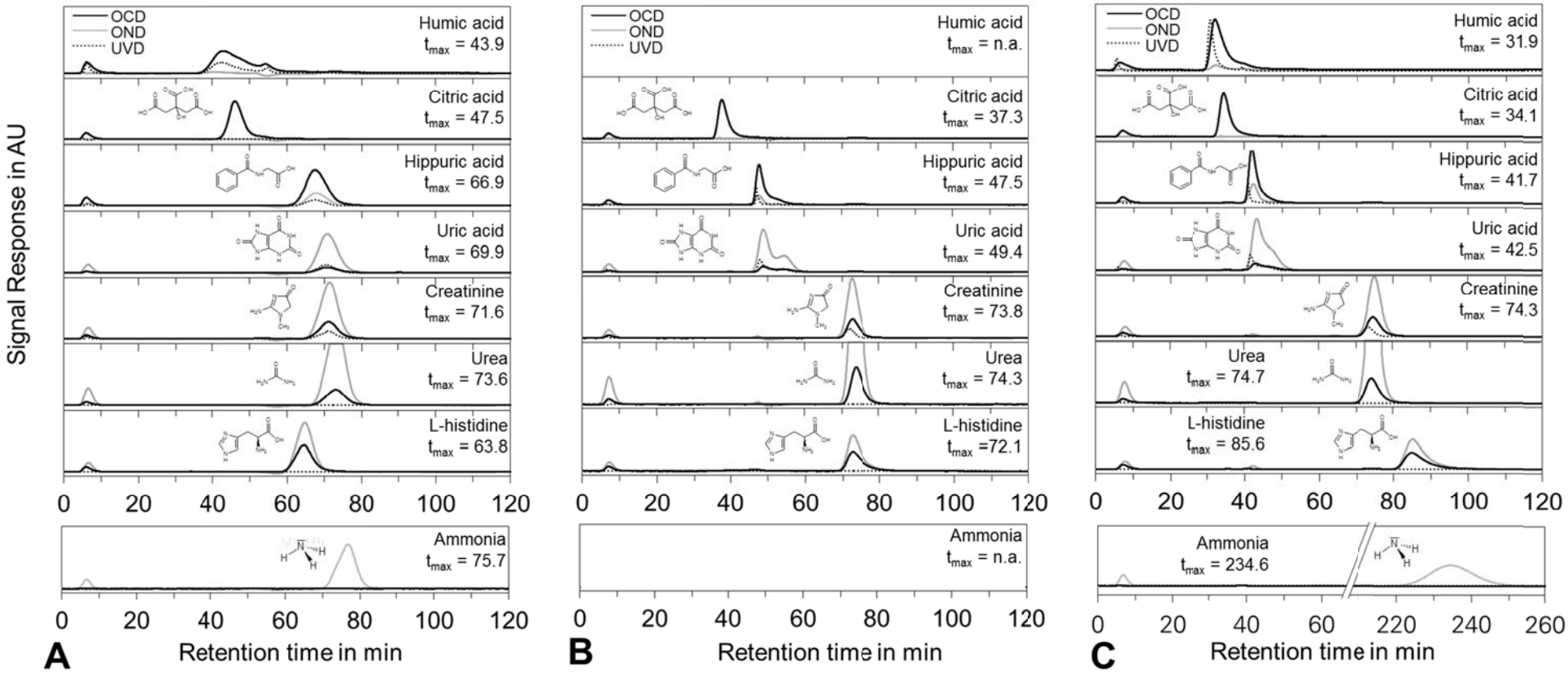

Figure 8.5: OCD, OND and UVD chromatograms of the BFA model substances using the LC-OCD method with (A) a normal eluent as described by Huber et al. 2011a [63], (B) a 5-fold diluted eluent as described by Huber et al. 2011b [288] and (C) a 10-fold diluted eluent. Substance concentrations were 2.5 mg L^{-1} except for humic acids with 1 mg L^{-1} (DOC). The retention time of the peak maxima t_{max} is given for the signal of the carbon detector (OCD) except for ammonia, where t_{max} is given for the signal of the nitrogen detector (OND).

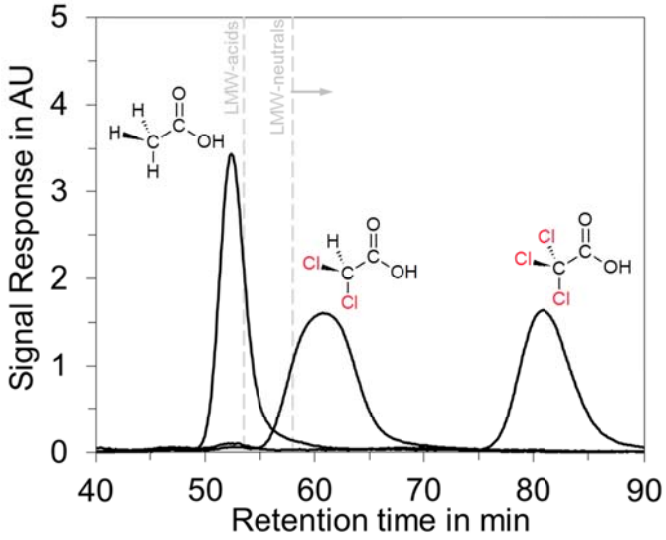

Figure 8.6: OCD chromatograms of acetic acid, dichloroacetic acid and trichloroacetic acid using the LC-OCD method with the normal eluent as described by Huber et al. 2011a [63]. Substance concentrations were 2 mg L^{-1} (as C).

8.1.5 Ammonia and Urea Analysis with the LC-OCD method

Huber et al. (2011) quantified urea down to the ppb concentration level using a 5-fold dilution of the normal eluent of the LC-OCD method [288]. The mild buffer concentration gave higher importance to cationic interactions between the resin and organic substances, which enhanced separation of urea and ammonia from the nitrate peak. Chromatograms of single BFA substances at normal, 5-fold and 10-fold diluted eluent are shown in Figure 8.5(A - C). Following our findings, using a 10-fold diluted eluent enhanced the separation of urea and ammonia even more compared to the 5-fold diluted eluent. Consequently, the 10-fold diluted eluent was used for quantification of ammonia and urea in this study. Ammonia was quantified by integrating the ON signal around its retention time at t_{max} = 234.6 min.

It should be noted here that the retention time of urea (t_{max} = 74.7 min) overlaps with that of creatinine (t_{max} = 74.3 min). However, due to its ring structure, creatinine has a UV signal (at λ = 254 nm) while urea has none. Thus, creatinine was directly quantified by its UV-signal and its OC-signal was than subtracted from the convoluted OC-chromatogram of the mixed sample. Urea was quantified after creatinine subtraction from the modified OC-chromatogram by integrating the OC signal around its retention time.

8.1.6 Simulated concentrations of organic substances in the reference state

Figure 8.7 shows simulated time dependent concentration profiles of single BFA substances and the humic acids in the basin of the swimming pool model in case water treatment as well as the reaction of free chlorine are neglected (i.e. reference state). Simulations were performed using the simplified AQUASIM model of the swimming pool pilot plant (Figure 8.3 (SI)).

Simulations were started assuming that the system was filled with DOC free water. All calculations were performed until stationary concentrations of the single BFA substances were reached. Concentrations of the simulated reference state were taken as mean value between 24.9 – 27 d, which was the time of sample taking in Exp. 1 to 6. The total DOC concentration in the simulated reference state was calculated as the sum of BFA substances and the HA.

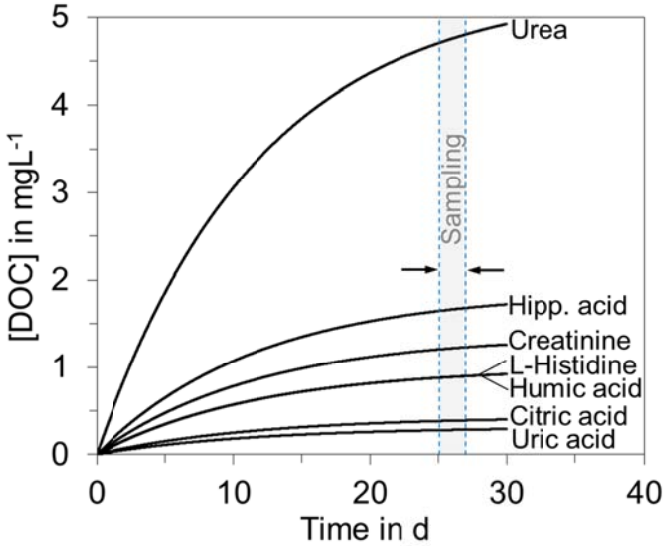

Figure 8.7: Simulated concentration of BFA substances in the CSTR of the simplified AQUASIM pool model (Figure 8.3 (SI)) over the experimental run time for the reference state (assuming no impact of the treatment section and chlorine reactions on the precursor concentration). Broken vertical lines (blue) represent the sampling period when stationary conditions were reached for Exp. 1 – 6.

Single BFA substances could not completely be allocated to one of the DOC fractions defined by the LC-OCD-OND method. Instead, their single substance peaks in the OCD signal could be allocated to two or more organic matter fractions. In order to transform simulated concentrations of single BFA substances to concentrations of organic matter fractions defined by the LC-OCD method, the following procedure was developed:

(i) Peak shape parameters of peaks in the OCD-chromatogram of standards of single BFA substances (see Figure 8.5) were determined using the peak fitting program Fityk (version 0.9.8) [391].

(ii) Based on the simulated concentration of single BFA substances (see Figure 8.7 (SI)), theoretical single substance chromatograms were calculated using the peak shape parameters of step (i) (Figure 8.8 (SI), blue lines).

(iii) A theoretical chromatogram of the mixture of simulated single BFA concentrations was calculated by superimposing the single substance chromatograms of step ii (Figure 8.8 (SI), red line).

(iv) The concentration of organic matter fractions was calculated from the superimposed OCD chromatogram using the ChromCALC software developed by DOC-LABOR Dr. Huber (Karlsruhe, Germany).

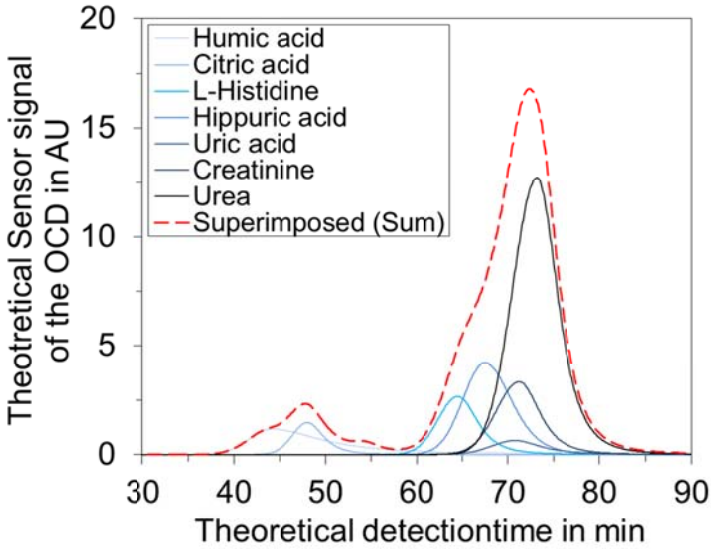

Figure 8.8: Calculated OCD-chromatograms of single BFA substance and Humic acids as well as the resulting superimposed OCD-chromatogram as it occurs in the reference state when stationary conditions are reached. Stationary concentrations of BFA substances and the humic acids were taken from Figure 8.7.

8.1.7 Calibration of the membrane inlet mass spectrometer for quantification of single DBPs

Standard preparation

Standards of each volatile DBP were prepared in a concentration range of ~1 - 150 µg L^{-1} prior to calibration. Except for trichloramine, standard were prepared

from stock solutions by dilution in methanol, followed by 2 dilution steps in ultrapure water.

Trichloramine standards were prepared by mixing solutions of ammonium chloride and hypochlorous acid (both pH 3.5) at a molar Cl:N ratio of 3:1. A slightly adapted version of the method of Soltermann et al. (2014), utilizing a T-mixing system with a dual channel peristaltic pump, was used for mixing both solutions [170]. Concentrations of the trichloramine solutions were standardized spectrophotometrically using a Unicam UV2 200 UV/VIS spectrophotometer ($\varepsilon_{336\ nm}$ = 190 mol cm^{-1}, $\varepsilon_{360\ nm}$ = 126 mol cm^{-1} [326]).

Calibration procedure

Plots of concentrations versus peak abundance for each of the considered DBPs were developed at their specific m/z values as they are needed for quantification. M/z values used for quantification are described in detail by Weaver et al. (2009) [30]. Each of the specific slopes revealed to be linear (data not shown). To consider changes in the response behaviour of the MIMS system, the MIMS was recalibrated periodically using chloroform standards as described previously by Weaver et al. (2009) [30]. The blank signal of each ion was determined previous to sample analysis by using deionized water.

Concentration determination

Since a mixture of volatile DBPs is ionized in the ionization chamber of the mass spectrometer, fragments of all volatile DBPs were measured in the mass spectrum at the same time. The concentration of single DBPs was evaluated from the mass spectrum according to the slightly modified method described previously by Weaver et al. (2011) based on linear algebra [30]. Gaussian error propagation was performed for each singe measurement respecting the following variables afflicted with errors: response factors, stability of the isotopic patterns, fluctuations of m/z signal used for calibration, fluctuations of the base signal.

8.1.8 *Composition of organic matter across the treatment trains of Exp. 1 to 7*

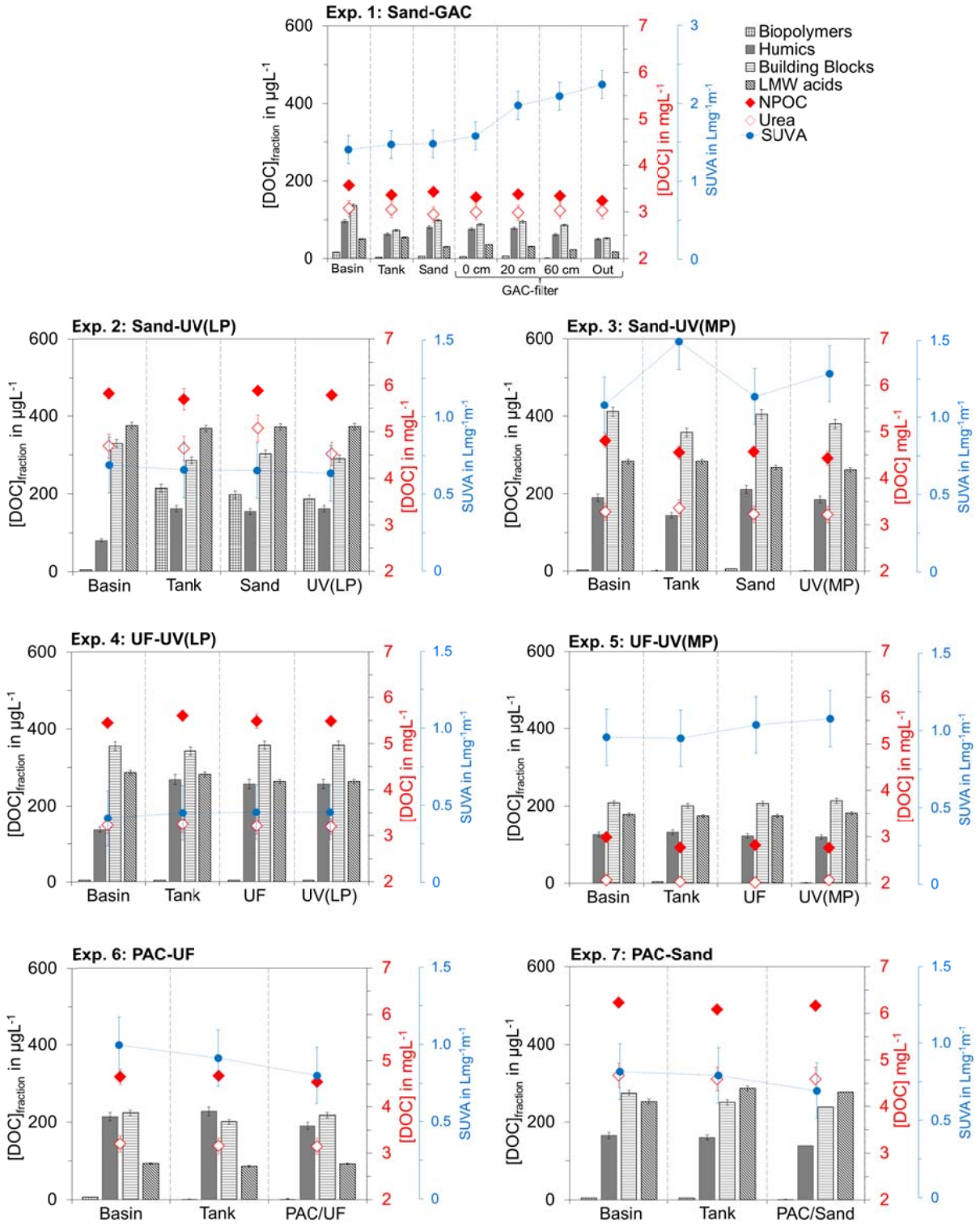

Figure 8.9: Mean concentrations of DOC and Urea as well as the DOC composition across the treatment trains of Exp. 1 – 7 under stationary conditions. Error bars represent the standard deviation for the total DOC and SUVA and the repeatability standard deviations for DOC fractions and Urea (red).

8.1.9 Volatile DBPs, free chlorine and combined chlorine across the treatment trains of Exp. 1 to 7

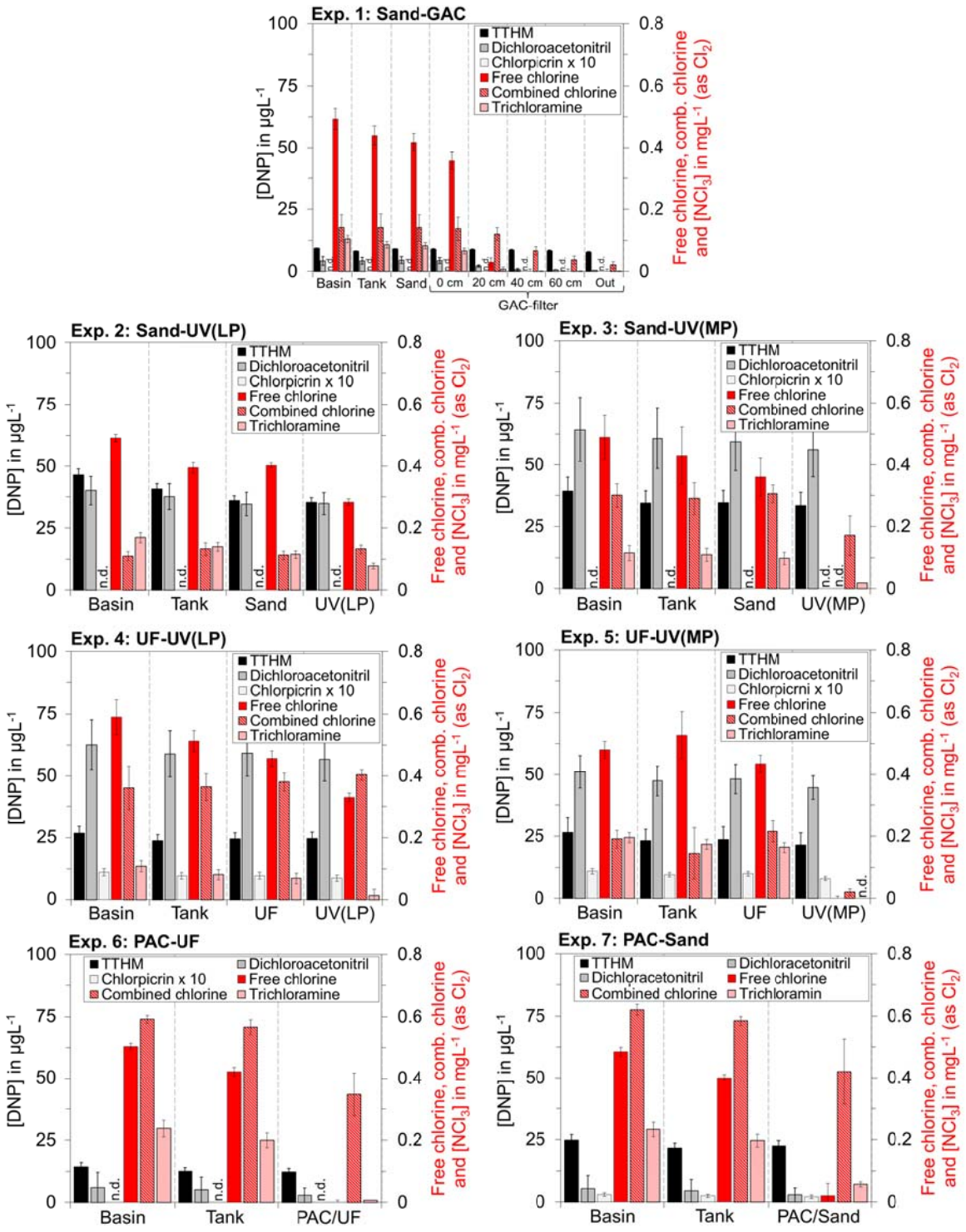

Figure 8.10: Mean concentrations of total trihalomethanes (TTHM), dichloroacetonitrile, chloropicrin, free chlorine, combined chlorine and trichloramine across the treatment trains of Exp. 1 -7 under stationary conditions. Error bars represent the 95% confidence level.

8.2 Supporting information for Chapter 6

8.2.1 Modelling swimming pool water quality

8.2.1.1 Hydraulic approach

A typical swimming pool system consists of a basin, a buffer tank and a treatment section [56]. The water flows gravity driven from the basin over a spillway into the buffer tank from where it is fed by circulation pumps over the treatment section back into the basin. In a recent survey by Cloteaux et al. (2013), the residence time characteristics of real swimming pools were found to be very close to that of continuous stirred tank reactors (CSTR) [139]. In particular, the authors identified two distinct areas in a numerical model of a common vertically flown pool (V_{tot} = 536 m³), one massive recirculation region which occupies half the pool and a second weakly agitated part. Both parts were in parallel position to one another. A simplified hydraulic model based on two completely stirred reactors (CSTR) with their own outlet and exchange flows between them was found to be an appropriate representation of the complicated hydraulics in the vertically flown pool [375]. A set of hydraulic parameters (a, b, c) defines these exchange flows (see Table 6.2). It must be noted here that the system of 2 CSTRs includes the water volume of the buffer tank.

8.2.1.2 Modelling chlorination of ammonia

Inorganic chloramines (i.e. mono-, di- and trichloramine) are known to be mainly formed by the reaction of ammonia with free chlorine, which is predominantly present as hypochlorite acid (HOCl) at neutral pool water pH. Ammonia is one of the main anthropogenic nitrogen containing precursors introduced into the swimming pool by bathers. The widely accepted kinetic model for the formation of inorganic chloramines from chlorination of ammonia as proposed by Jafvert et al. (1992) was applied in in this study [135]. The chloramination reaction scheme is presented in Table 8.2 below.

8.2.1.3 Modelling chlorination of urea

Chlorination of urea is known to lead to the formation of NCl_3 as end product. However, reactions schemes for chlorination of urea have been rarely described in the literature. The few studies known suggest that the overall reaction of urea with chlorine is very low compared to that of ammonia [136, 192]. The first reaction step of

urea chlorination leads to the formation of N-chlorourea and is assumed to be rate limiting for the overall reaction ($k = 2.35 \cdot 10^4$ mol^{-1} s^{-1}) [136]. The kinetic constants for the reactions of chlorourea and its intermediates with chlorine are assumed to be significantly faster [136, 376].

8.2.1.4 Modelling NDMA formation

Dimethylamine (DMA) has been found to be an important NDMA precursor in pool water, which is mainly introduced by humans. The initial process of NDMA formation from DMA has been explained primarily via reactions involving dichloramine [157]. The overall NDMA formation occurs slowly within days indicating that systems with high hydraulic retention times (i.e. swimming pool facilities) tend to have higher NDMA concentrations than those with short contact times [392]. A kinetic model of the proposed reaction mechanism has been proposed by Schreiber and Mitch (2006) [157] and was implemented in both CSTRs as well (Table 8.2).

Table 8.2: Model reactions used in the simplified numerical pool model.

No.	Stoichiometry	Rate constant	Rate expression
Chloramination [135, 393]			
1	$HOCl + NH_3 \rightarrow NH_2Cl + H_2O$	$4.17 \cdot 10^6$ $mol^{-1}\,s^{-1}$	$k[NH_3][HOCl]$
2	$H_2O + NH_2Cl \rightarrow HOCl + NH_3$	$2.11 \cdot 10^{-5}$ s^{-1}	$k[NH_2Cl]$
3[a]	$HOCl + NH_2Cl \rightarrow NHCl_2 + H_2O$	$1.50 \cdot 10^2$ $mol^{-1}\,s^{-1}$	$k[NH_2Cl][HOCl]$
4	$NHCl_2 + H_2O \rightarrow HOCl + NH_2Cl$	$6.39 \cdot 10^{-7}$ s^{-1}	$k[NHCl_2]$
5[b]	$2\,NH_2Cl + H^+ \rightarrow NH_4^+ + NHCl_2$	$6.94 \cdot 10^3$ $mol^{-1}\,s^{-1}$	$k[NH_2Cl]^2\,[H^+]$
6	$NHCl_2 + NH_3 \rightarrow NH_2Cl + NH_2Cl$	$6.00 \cdot 10^4$ $mol^{-2}\,s^{-1}$	$k[NHCl_2][NH_3][H^+]$
7	$NHCl_2 + H_2O \rightarrow I^c$	$1.11 \cdot 10^2$ $mol^{-1}\,s^{-1}$	$k[NHCl_2][OH^-]$
8	$I^c + NHCl_2 \rightarrow HOCl + products^d$	$2.78 \cdot 10^4$ $mol^{-1}\,s^{-1}$	$k[NHCl_2][I]$
9	$I^c + NH_2Cl \rightarrow products^d$	$8.33 \cdot 10^3$ $mol^{-1}\,s^{-1}$	$k[NH_2Cl][I]$
10	$NH_2Cl + NHCl_2 \rightarrow products^d$	$1.53 \cdot 10^{-2}$ $mol^{-1}\,s^{-1}$	$k[NH_2Cl][NHCl_2]$
11[e]	$HOCl + NHCl_2 \rightarrow NCl_3 + H_2O$	$3.18 \cdot 10^9$ $mol^{-1}\,s^{-1}$	$k[NHCl_2][HOCl][OH^-]$
12	$NHCl_2 + NCl_3 + 2\,H_2O \rightarrow 2\,HOCl + products^d$	$5.56 \cdot 10^{10}$ $mol^{-2}\,s^{-1}$	$k[NHCl_2][NCl_3][OH^-]$
13	$NH_2Cl + NCl_3 + H_2O \rightarrow HOCl + products^d$	$1.39 \cdot 10^9$ $mol^{-2}\,s^{-1}$	$k[NH_2Cl][NCl_3][OH^-]$
14[f]	$NCl_3 + H_2O \rightarrow HOCl + NHCl_2$	$3.20 \cdot 10^{-5}$ s^{-1}	$k[NCl_3]$
Urea chlorination [136, 376, 394]			
15	$Cl_2 + NH_2CONH_2 \rightarrow NH_2CONHCl + Cl^-$	$2.35 \cdot 10^4$ $mol^{-1}\,s^{-1}$	$k[Cl_2][NH_2CONH_2]$
16	$HOCl + NH_2CONHCl \rightarrow NHClCONHCl + H_2O$	0.75 $mol^{-1}\,s^{-1}$	$k[HOCl][NH_2CONHCl]$
17	$HOCl + NHClCONHCl \rightarrow NCl_2CONHCl + H_2O$	7.5 $mol^{-1}\,s^{-1}$	$k[HOCl][NHClCONHCl]$
18	$HOCl + NCl_2CONHCl \rightarrow NCl_2CONCl_2 + H_2O$	7.5 $mol^{-1}\,s^{-1}$	$k[HOCl][NCl_2CONHCl]$
19	$HOCl + NCl_2CONCl_2 \rightarrow CO_2 + NHCl_2 + NCl_3$	7.5 $mol^{-1}\,s^{-1}$	$k[HOCl][NCl_2CONCl_2]$
20	$NCl_3 + CO_3^{2-} + H_2O \rightarrow NHCl_2 + CO_3^{2-} + HOCl$	$6.5 \cdot 10^5$ $[HCO_3^-]\,[OH^-]\,s^{-1}$	$k[NCl_3]$
NDMA formation [157]			
21	$HOCl + (CH_3)_2NH \rightarrow (CH_3)_2NCl + H_2O$	$6.1 \cdot 10^7$ $mol^{-1}\,s^{-1}$	$k[HOCl][(CH_3)2NH]$
22	$(CH_3)_2NCl + NH_4^+ \rightarrow NH_2Cl + (CH_3)_2NH_2^+$	$5.8 \cdot 10^{-3}$ $mol^{-1}\,s^{-1}$	$k[(CH_3)_2NH_2][NH_2Cl]$
23	$NH_2Cl + (CH_3)_2NH \rightarrow (CH_3)_2NNH_2 + H^+ + Cl^-$	$8.1 \cdot 10^{-2}$ $mol^{-1}\,s^{-1}$	$k[NH_2Cl][(CH_3)_2NH]$
24	$NH_3 + (CH_3)_2NCl \rightarrow (CH_3)_2NNH_2 + H^+ + Cl^-$	$4.9 \cdot 10^{-3}$ $mol^{-1}\,s^{-1}$	$k[NH_3][(CH_3)_2NCl]$
25	$NHCl_2 + (CH_3)_2NH \rightarrow (CH_3)_2NNHCl + H^+ + Cl^-$	52 $mol^{-1}\,s^{-1}$	$k[NHCl_2][(CH_3)_2NH]$
26	$NHCl_2 + (CH_3)_2NNH_2 \rightarrow (CH_3)_2NH + products^c$	4.5 $mol^{-1}\,s^{-1}$	$k[NHCl_2][(CH_3)_2NNH_2]$
27	$NHCl_2 + (CH_3)_2NNHCl \rightarrow products^c$	$7.5 \cdot 10^{-1}$ $mol^{-1}\,s^{-1}$	$k[NHCl_2][(CH_3)_2NNHCl]$
28[g]	$O_2 + (CH_3)_2NNHCl \rightarrow (CH_3)_2NNO + HOCl$	1.4 $mol^{-1}\,s^{-1}$	$k[O_2][(CH_3)_2NNHCl]$

Continuation of Table 8.2

No.	Stoichiometry	Equilibrium constant
Acid-/Base Speciation [27, 130]		
E.1	$HOCl \leftrightarrow OCl^- + H^+$	$pK_a = 7.5\ mol^{-1}\ s^{-1}$
E.2	$NH_4^+ \leftrightarrow NH_3 + H^+$	$pK_a = 9.3\ mol^{-1}\ s^{-1}$
E.3	$CO_2 + H_2O \leftrightarrow HCO_3^- + H^+$	$pK_a = 6.4\ mol^{-1}\ s^{-1}$
E.4	$HCO_3^- \leftrightarrow CO_3^{2-} + H^+$	$pK_a = 10.3\ mol^{-1}\ s^{-1}$
E.5	$(CH_3)_2NH_2^+ \leftrightarrow (CH_3)_2NH + H^+$	$pK_a = 10.7\ mol^{-1}\ s^{-1}$
E.6	$(CH_3)_2NHNH_2^+ \leftrightarrow (CH_3)_2NNH_2 + H^+$	$pK_a = 7.2\ s^{-1}$

[a] … Rate constant taken from [393]

[b] … Acid catalysis by H_2CO_3 ($k = 0.75\ mol^{-2}\ s^{-1}$) and HCO_3^- ($k = 2.0 \cdot 10^{-3}\ mol^{-2}\ s^{-1}$) was also respected (It is assumed that the concentration of HCO_3^- in pool water equals the amount of acid capacity with sufficient accuracy. In this study, the pool waters' acid capacity is assumed to be constant at 0.35 mmol L^{-1}, which equals the maximum allowed value of the acid capacity to pH 4.3 according to DIN 19643 [56]. At pH 7, the concentration of CO_3^{2-} and H_2CO_3 is assumed to be zero.)

[c] … Unidentified intermediate

[d] … Products may include N_2, NO_3^-, H_2O, Cl^-, H^+ and other unidentified reaction products

[e] … Base catalysis by OCl^- ($k = 5.0 \cdot 10^4\ mol^{-2}\ s^{-1}$) was also respected (all rate constants of reaction 11 represent the low end of values given by [324])

[f] … Base catalysis by OH^- ($k = 18.8\ mol^{-1}\ s^{-1}$) was also respected

[g] … The concentration of dissolved oxygen was assumed to be constant at 8 mg L^{-1}

8.2.2 Assessing the role of other processes possibly affecting the observed N_2 yield

Table 8.3: Accession of other processes possibly affecting the observed N_2 yield of the monochloramine-GAC reaction in the FBR-system.

Process	Relevance	
Adsorptive removal of NH_4^+ in the GAC filter [311, 395, 396]	negligible	Due to the nonpolar surface chemistry of activated carbons, absorptivity for ammonium is reported to be very poor [248, 249]. At the end of the FBR experiments (see Figure 6.2), a theoretical ammonium loading q_e of the bench scale GAC filter of 0.001 to 0.053 mmol g_{GAC}^{-1} was roughly estimated. This loading equals ~0.02 to 3.5 % of the measured amount of ammonium formed from monochloramine transformation (~1.2 – 1.5 mmol g_{GAC}^{-1}), which is negligible considering the observed errors of the NH_4^+ yield reported (2.2 to 4.2 %). The adsorbed amount of ammonium was calculated using the Freundlich isotherm equation[a].

Continuation of Table 8.3

Process	Relevance	
Degradation of NH_4^+ by microbiological nitrification [397, 398]	negligible	Monochloramine, at concentrations used in this study (4.5 mg L^{-1} (as Cl_2)) is known to sufficiently inactivate microorganisms [399, 400] and thus, prevents microbiological contamination of the FBR-system. Analysis of nitrogenous reaction products showed that no nitrate was formed over the course of the experiment (data not shown), indicating that nitrification of ammonium did not occur.
Catalytic wet oxidation of NH_4^+ to N_2 [401-403]	negligible	Temperatures needed for catalytic wet oxidation of NH_4^+ were reported to be significantly higher (>200 °C) [404] as being compared to the mild conditions used in this study (30°C).

[a] … It is assumed that equilibrium conditions had been established between the concentration of NH_4^+ adsorbed in the GAC bed and the NH_4^+ concentration in the influent water [405]. The equilibrium was be described by the Freundlich isotherm equation $q_e=K_F \cdot c_e^{\frac{1}{n}}$. The carbon loading q_e was calculated by simultaneous solution of the Freundlich isotherm equation and the following mass balance: $q_e=\frac{(c_0-c_e)\cdot V_{sys}}{m_{GAC}}$. Here, c_e is the ammonium concentration in the tank of the FBR system at the end of the experiments, when ~1.5 mmol L^{-1} of monochloramine were transformed to ammonium (~44 mg_{NH4+} L^{-1}, see Figure 6.4), V_{sys} is the volume in the FBR-system (10.45 L) and m_{GAC} is the mass of carbon in the GAC filter used in the FBR-experiments (a mean value of 17 g was used). For calculation of q_e, ranges of Freundlich adsorption isotherm constants as reported in the literature for ammonium ion adsorption at various GACs were used (K_F = 0.001 – 0.218 (mg g_{GAC}^{-1})(mg $L^{-1})^n$, n = 0.79 – 3.23 [395, 406-409]).

8.2.3 Reactivity of filter beds of the considered GACs for HOCl removal

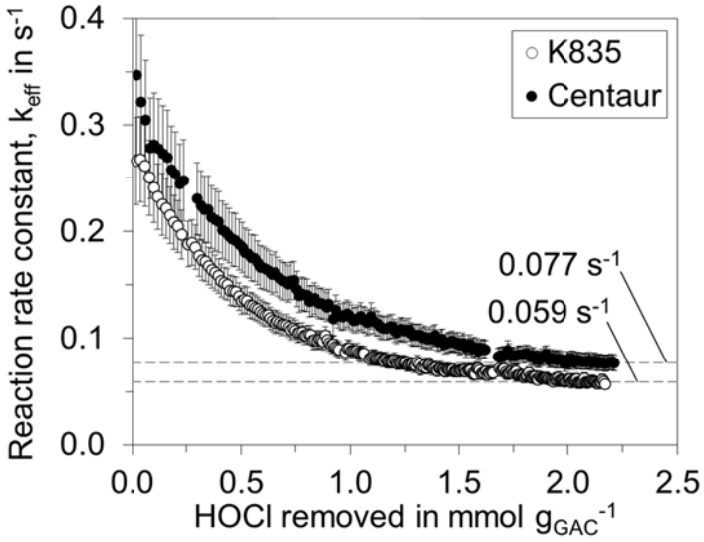

Figure 8.11: Effective reaction rate constant for HOCl removal versus the amount of HOCl removed for filter beds of the fresh unfractionated K835 and Centaur carbon. Error bars for k_{eff} represent the standard error as determined by Gaussian error reproduction. Dashed lines represent k_{eff} for both carbons as they occurred under stationary conditions.

8.2.4 *Simulated monochloramine removal and formation of transformation products over the bed depth of a real scale GAC filter*

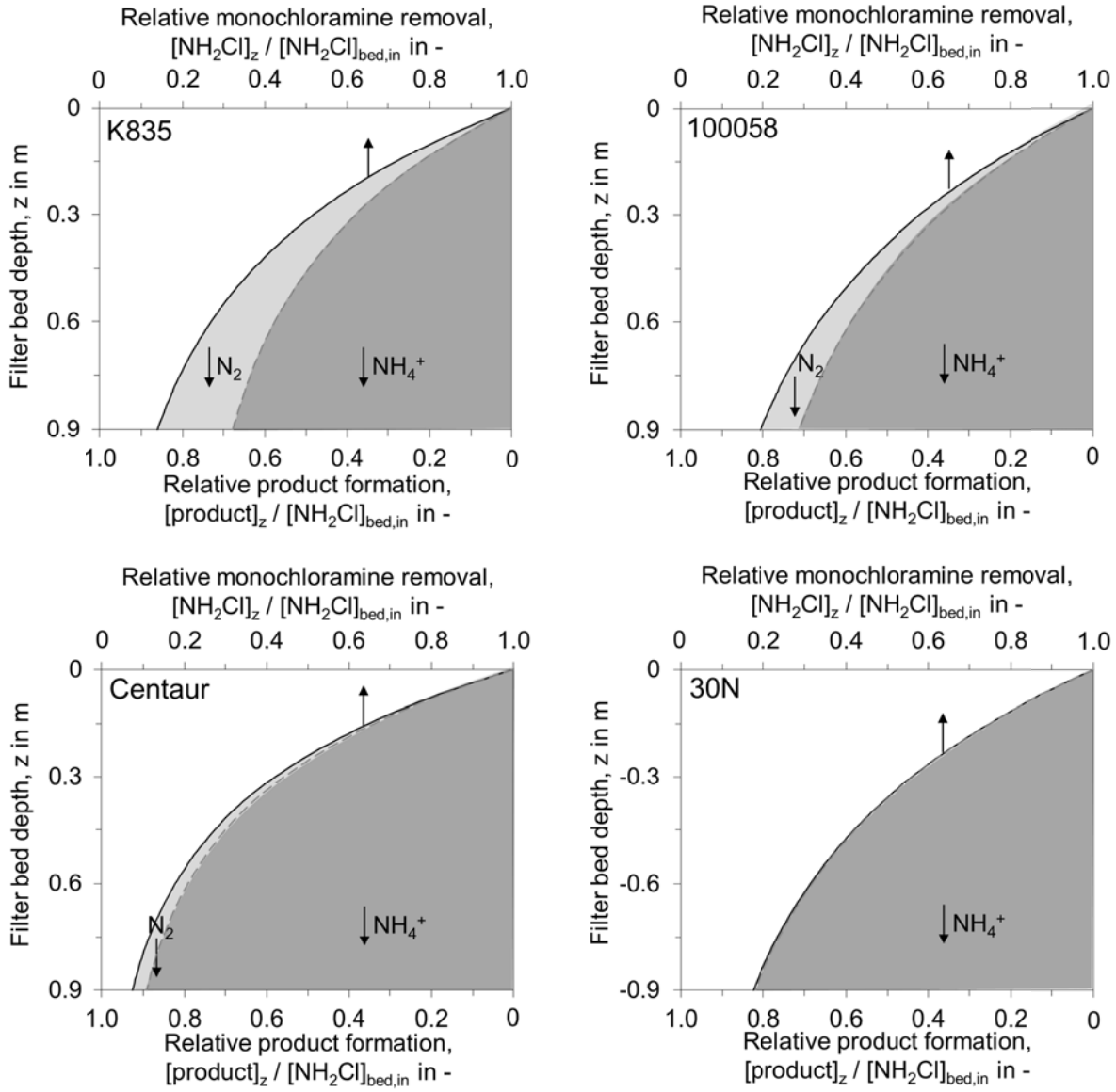

Figure 8.12: Simulated relative monochloramine removal and corresponding formation of transformation products over the bed depth of a theoretical GAC filter (z = 0.9 m) for the carbons K835, 30N, Centaur and 100058. Concentration profiles were calculated according to Equation (6.6) using a filter velocity (v_{eff}) of 30 m h^{-1}. The reaction rate constants and N_2 yields used for calculation were those when stationary conditions were reached (see Figure 6.4).

8.2.5 *Literature data sets of reaction rate constant and N_2 yield for various GACs*

Additionally to the experimental data from this study, five data sets of k_{eff} and N_2 yield for different GACs were extracted from fixed-bed column studies published by

Fairey et al. (2007) [309], Kim (1977) [313] and Scaramelli et al. (1977) [266] (Table 8.4).

Table 8.4: Literature data sets of reaction rate constants and N_2 yield for various GACs.

Name	Raw material	Operation conditions	Rate constant	N_2 yield	Ref.
F400	Coal-based	v_{bed} = 6.1 m h^{-1} z_{bed} = 15 cm T = 23 ± 3 °C $c_{bed,in}$ = 2 mg L^{-1} (as Cl_2)	0.026 s^{-1}	23 %	[309]
F600	Coal-based	see F400 (above)	0.028 s^{-1}	31 %	[309]
F400	Coal-based	v_{bed} = 7.6 m h^{-1} z_{bed} = 6.7 cm T = [b] $c_{bed,in}$ = 18 mg L^{-1} (as Cl_2)	0.030 s^{-1}	27.3 %	[313]
Sca_01[a]	Coal-based (d_p = 0.12 mm)	v_{bed} = 21 m h^{-1} z_{bed} = 140 cm T = 20 - 23 °C $c_{bed,in}$ = 63.8 mg L^{-1} (as Cl_2)	0.006 s^{-1}	42 %	[266]
Sca_02[a]	Coal-based (d_p = 0.05 mm)	*see Sca_01*	0.009 s^{-1}	42 %	[266]
30N	Anthracite coal	v_{bed} = 44.1 m h^{-1} z_{bed} = 3.53 cm T = 30 °C $c_{bed,in}$ = 4.5 mg L^{-1} (as Cl_2)	0.016 s^{-1}	0.5 %	[c]
K835	Coconut shell	see 30N	0.018 s^{-1}	21.3 %	[c]
Centaur	Bituminous coal	see 30N	0.024 s^{-1}	4.4 %	[c]
100058	Polymer-based spheres	see 30N	0.015 s^{-1}	11.6 %	[c]

[a] … Abbreviation chosen by the authors since no producer or name of the carbon has been provided in the corresponding reference

[b] … Not determined

[c] … This study

9 List of abbreviations, symbols and Greek symbols

Abbreviations

BB Building Blocks

BFA Body fluid analogue

CHN Carbon, hydrogen and nitrogen (analyser)

CSTR1, CSTR2
Completely mixed reactors 1 and 2

DBP Disinfection by-products

DMA Dimethylamine

DON Dissolved organic nitrogen

DOC Dissolved organic carbon

EBCT Empty bed contact time

FCM Flow cytometry

FBR Fixed bed reactor

GAC Granular activated carbon

HA Humic acid

HS Humic substances

ICP-MS Inductively coupled plasma mass spectrometry

LC-OCD-OND-UVD
Liquid chromatography with organic carbon, organic nitrogen und UV detection

LMW	Low molecular weight
MCA	Monochloramine
MF	Microfiltration
MIMS	Membrane inlet mass spectrometry
MWCO	Molecular weight cut-off
NDMA	N-Nitrosodimethylamine
NPOC	Non purgeable organic carbon
OM	Organic matter
PAC	Powdered activated carbon
PCM	Progressive Conversion Model
PSD	Pore size distribution
QSDFT	Quenched solid density functional theory
SCM	Shrinking-Core Model
SEM	Scanning Electron Microscopy
SUVA	Specific UV absorbance
TTHM	Total Trihalomethanes
UV(LP)	Low pressue UV irradiation
UV(MP)	Medium pressure UV irradiation
UF	Ultrafiltration

Symbols

a, b, c	Hydraulic parameters of the simplified pool model (dimensionless)
A_p	Total surface area of a pool basin (m²)
a_b	Specific surface area that a bather makes use of during his activities in the pool (m² bather^{-1})
a_o	bed volume specific outer surface area (m² m^{-3})
$c_{a,i}$	Aqueous concentration of substance i in the pool model (mg L^{-1})
$c_{bed,in}$	MCA in-flow concentrations of a GAC filter (mg L^{-1} as Cl_2)
$c_{bed,out}$	MCA out-flow concentrations of a GAC filter (mg L^{-1} as Cl_2)
$c_{i,1}$, $c_{i,2}$	Variable concentrations of substances i in CSTR 1 and CSTR 2 (mg L^{-1})
$c_{i,cir}$	Variable concentrations of substances i in the circulated water flow of the pool model (mg L^{-1})
c_{st}	Concentration of the monochloramine stock solution (mg L^{-1} as Cl_2)
$D_{bulk,MCA}$	Bulk diffusion coefficient of MCA in water (m² s^{-1})
$D_{E,MCA}$	Effective diffusion coefficient of MCA in the pore system of a GAC grain (m² s^{-1})
d_{hy}	Hydraulic diameter (m)
d_{MCA}	Minimal pore diameter of a GAC that is still accessible for a MCA molecule (nm)
$dm_{stock}\ dt^{-1}$	Time dependent mass loss of the MCA stock solution (g s^{-1})
$d_{p,i}$	Pore diameter of pore size i (nm)
$d_{grain,I}$	Grain size i (mm)

d_{hy} Hydraulic diameter (mm)

$d_{pore,i}$ Pore diameter of pore size i (nm)

E_0 Standard electrode potential (V)

E_A Activation energy (J mol^{-1})

$F_{NH4+,b}$, $F_{urea,b}$ and $F_{DMA,b}$
Amount of ammonium, urea and DMA introduced into the pool by the bather (mg h^{-1})

$F_{NH4+,f}$, $F_{urea,f}$ and $F_{DMA,f}$
Amount of ammonium, urea and DMA introduced into the pool by fresh water (mg h^{-1})

k_{eff} Observable pseudo first order reaction rate constant (s^{-1})

$k_{eff,a}$ Pseudo first order reaction rate constant normalized by the specific outer surface a_o of the GAC in the filter bed (m s^{-1})

k_0 Frequency factor (s^{-1})

k_f Mass transfer coefficient of MCA through the laminar film layer (m s^{-1})

K_{iH} Henry's law constant (mol m^{-3} Pa^{-1})

k_t Specific loading factor of a swimming pool (equals the maximum amount of bathers permitted to enter the pool per cubic meter of treated pool water) (m^{-3})

L Diffusion path length within the adsorbent (m)

N_b Maximum allowed attendance rate of bathers entering the pool (h^{-1})

n_b Frequency factor for bathers entering the pool (typically taken as 1 h^{-1})

p_i Vapour pressure of substance i (Pa)

Q Volumetric fluid flow rate (L s^{-1})

Q_{bed} Volumetric fluid flow through a GAC bed (L s^{-1})

Q_{ex} External water inlet (fresh water, urea and sweat) (L s^{-1})

q_i Mass fraction of the corresponding mean grain size i

Q_{st} Volumetric dosing rate of a MCA stock solution (L s^{-1})

Q_{circ} Circulation rate of a swimming pool (L s^{-1})

Re Reynolds number (dimensionless)

R_0 Universal gas constant (R = 8.314 J K^{-1} mol^{-1})

R_{sys} Time dependent loss of MCA in the system without GAC filter (mg s^{-1} as Cl_2)

Sc Schmidt number (dimensionless)

Sh Sherwood number (dimensionless)

Sh_E Sherwood number in the transient region between laminar and turbulent interfacial flow (dimensionless)

T Temperature (K)

t_d Dead time (s)

t_{EBCT} Empty bed contact time (EBCT) (s)

V_{bed} Bed volume (L)

v_{bed} Superficial filter velocity (m s^{-1})

V_{sys} Water volume in the FBR system (L)

z_{bed} Bed depth (m)

Greek symbols

ε	Molar absorption coefficient (mol^{-1} cm^{-1})
ζ	ζ-potential (mV)
η	Effectiveness factor of a heterogeneous reaction (dimensionless)
$\rho_{stock}(T)$	Temperature dependent density of a MCA stock solution ($g\ L^{-1}$)
ρ_{bed}	Bulk density (dry) ($g\ L^{-1}$)
ρ_{grain}	Density of the carbon grains (dry) ($g\ L^{-1}$)
$\rho_{st}(T)$	Temperature dependent density of a monochloramine stock solution ($g\ L^{-1}$)
τ	Tortuosity factor of a GAC (dimensionless)
Φ	Thiele modulus of a heterogeneous reaction (dimensionless)
ψ	Dimensionless correction factor accounting for the non-spherical form of GACs (dimensionless)

10 List of Figures

11 List of Tables

12 References

[1] L. Erdinger, K.P. Kuhn, F. Kirsch, R. Feldhues, T. Frobel, B. Nohynek, T. Gabrio, Pathways of trihalomethane uptake in swimming pools, Int. J. Hyg. Environ. Health, 207 (2004) 571-575.

[2] T. Grummt, H.G. Wunderlich, C. Zwiener, C. Schmalz, F.H. Frimmel, Pool Water Chemistry and Health (in German), Bundesgesundheitsblatt, 54 (2011) 136-141.

[3] C. Zwiener, S.D. Richardson, D.M. De Marini, T. Grummt, T. Glauner, F.H. Frimmel, Drowning in disinfection byproducts? Assessing swimming pool water, Environ. Sci. Technol., 41 (2007) 363-372.

[4] Brauerei VELTINS GmbH & Co. and the German Sports Federation, Veltins sport survey 2001 (in German), Meschede-Grevenstein, Germany, 2001.

[5] Fox, K., Leicha, R., Results from the sport and leisure module of the 2002 General Household Survey, London, 2002.

[6] T. Griffiths, The Complete Swimming Pool Reference, 2nd edition, Sagamore Publishing, 2003.

[7] German Federal Ministry of Economics and Technology (BMWi), The economic importance of sports facility construction (in German), Berlin, 2012.

[8] C. Ochsenbauer, The amount of public swimming pools in Germany is higher as expected (in German), A.B. Arch. Badew., 11 (2012) 723-725.

[9] German conference of sports ministers, German Sports Federation and German Association of Towns and Cities (DST), Sports facility statistic of German countries (in German), Berlin, 2002.

[10] F. Capoccia, Market Data 2009, Meeting of the European Union of Swimmingpool and Spa Associations (EUSA), Venice, 2010. http://www.eusaswim.eu (accessed 17/03/2016).

[11] World Health Organisation (WHO), Organization for Economic Cooperation and Development (OECD), Assessing microbial safety of drinking water - Improving Approaches and Method, IWA Publishing on behalf of the WHO and the OECD, London, 2003.

[12] R.G. Sinclair, E.L. Jones, C.P. Gerba, Viruses in recreational water-borne disease outbreaks: a review, J. Appl. Microbiol., 107 (2009) 1769-1780.

[13] M.C. Hlavsa, V.A. Roberts, A.M. Kahler, E.D. Hilborn, T.R. Mecher, M.J. Beach, T.J. Wade, J.S. Yoder, Outbreaks of Illness Associated with Recreational Water - United States, 2011–2012, Morb. Mortal. Wkly. Rep., 64 (2015) 663-668.

[14] F. Kee, G. Mcelroy, D. Stewart, P. Coyle, J. Watson, A Community Outbreak of Echovirus Infection Associated with an Outdoor Swimming Pool, J. Public Health Med., 16 (1994) 145-148.

[15] W.E. Keene, J.M. Mcanulty, F.C. Hoesly, L.P. Williams, K. Hedberg, G.L. Oxman, T.J. Barrett, M.A. Pfaller, D.W. Fleming, A Swimming-Associated Outbreak of Hemorrhagic Colitis Caused by Escherichia-Coli O157-H7 and Shigella-Sonnei, New Engl. J. Med., 331 (1994) 579-584.

[16] D.A. Hunt, S. Sebugwawo, S.G. Edmondson, D.P. Casemore, Cryptosporidiosis associated with a swimming pool complex, Communicable Disease Report Review, 4 (1994) R20-R22.

[17] T. Sundkvist, M. Dryden, R. Gabb, N. Soltanpoor, D. Casemoor, J. Stuart, Outbreak of cryptosporidiosis associated with a swimming pool in Andover, Communicable Disease Review, 7 (1997) R190-R192.

[18] M. Turner, G.R. Istre, H. Beauchamp, M. Baum, S. Arnold, Community Outbreak of Adenovirus Type-7a Infections Associated with a Swimming Pool, Southern Med. J., 80 (1987) 712-715.

[19] C. Papadopoulou, V. Economou, H. Sakkas, P. Gousia, X. Giannakopoulos, C. Dontorou, G. Filioussis, H. Gessouli, P. Karanis, S. Leveidiotou, Microbiological quality of indoor and outdoor swimming pools in Greece: investigation of the antibiotic resistance of the bacterial isolates, Int. J. Hyg. Environ. Health, 211 (2008) 385-397.

[20] G. Nichols, Infection risks from water in natural and man-made environments, Euro. Surveill., 11 (2006) 76-78.

[21] World Health Organisation (WHO), Guidelines for safe recreational water environments, Volume 2: Swimming Pools and Similar Environments, WHO, Geneva, 2006.

[22] M.G.A. Keuten, M.C.F.M. Peters, H.A.M. Daanen, M.K. de Kreuk, L.C. Rietveld, J.C. van Dijk, Quantification of continual anthropogenic pollutants released in swimming pools, Water Res., 53 (2014) 259-270.

[23] S.M. Elmir, M.E. Wright, A. Abdelzaher, H.M. Solo-Gabriele, L.E. Fleming, G. Miller, M. Rybolowik, M.T.P. Shih, S.P. Pillai, J.A. Cooper, E.A. Quaye, Quantitative evaluation of bacteria released by bathers in a marine water, Water Res., 41 (2007) 3-10.

[24] M.G.A. Keuten, F.M. Schets, J.F. Schijven, J.Q.J.C. Verberk, J.C. van Dijk, Definition and quantification of initial anthropogenic pollutant release in swimming pools, Water Res., 46 (2012) 3682-3692.

[25] Protection Against Infection Act (IfSG), Bundesgesetzesblatt Teil 1, Bundesanzeiger Verlag GmbH, Köln, 2000.

[26] DIN 19643-1, Treatment of water of swimming pools and baths, Part 1: General requirements (in German), Normenausschuss Wasserwesen (NAW) im DIN Deutsches Institut für Normung, Beuth Verlag, Berlin, 2012.

[27] M. Deborde, U. von Gunten, Reactions of chlorine with inorganic and organic compounds during water treatment - Kinetics and mechanisms: A critical review, Water Res., 42 (2008) 13-51.

[28] G.J. White, Handbook of chlorination and alternative disinfectants, 4th edition, John Wiley & Sons, New York, USA, 1999.

[29] J. Li, E.R. Blatchley, Volatile disinfection byproduct formation resulting from chlorination of organic-nitrogen precursors in swimming pools, Environ. Sci. Technol., 41 (2007) 6732-6739.

[30] W.A. Weaver, J. Li, Y.L. Wen, J. Johnston, M.R. Blatchley, E.R. Blatchley, Volatile disinfection by-product analysis from chlorinated indoor swimming pools, Water Res., 43 (2009) 3308-3318.

[31] S.C. Weng, E.R. Blatchley, Disinfection by-product dynamics in a chlorinated, indoor swimming pool under conditions of heavy use: National swimming competition, Water Res., 45 (2011) 5241-5248.

[32] A. Florentin, A. Hautemaniere, P. Hartemann, Health effects of disinfection by-products in chlorinated swimming pools, Int. J. Hyg. Environ. Health, 214 (2011) 461-469.

[33] S.D. Richardson, D.M. DeMarini, M. Kogevinas, P. Fernandez, E. Marco, C. Lourencetti, C. Balleste, D. Heederik, K. Meliefste, A.B. McKague, R. Marcos, L. Font-Ribera, J.O. Grimalt, C.M. Villanueva, What's in the pool? A comprehensive identification of disinfection by-products and assessment of mutagenicity of chlorinated and brominated swimming pool water, Environ. Health Perspect., 118 (2010) 1523-1530.

[34] K.M.S. Hansen, S. Willach, H. Mosbaek, H.R. Andersen, Particles in swimming pool filters - Does pH determine the DBP formation, Chemosphere, 87 (2012) 241-247.

[35] A. Kanan, T. Karanfil, Formation of disinfection by-products in indoor swimming pool water: The contribution from filling water natural organic matter and swimmer body fluids, Water Res., 45 (2011) 926-932.

[36] C. Lourencetti, J.O. Grimalt, E. Marco, P. Fernandez, L. Font-Ribera, C.M. Villanueva, M. Kogevinas, Trihalomethanes in chlorine and bromine disinfected swimming pools: Air-water distributions and human exposure, Environ. Int., 45 (2012) 59-67.

[37] B. Levesque, J.F. Duchesene, S. Gingras, R. Lavoie, D. Prud'Homme, E. Bernard, L.P. Boulet, P. Ernst, The determinants of prevalence of health complaints among young competitive swimmers, Int. Arch. Occup. Environ. Health, 80 (2006) 32-39.

[38] D. Eichelsdörfer, D. Slovak, D. Dirnagl, K. Schmidt, Studying irritating effects (conjunctivitis) of chlorine and chloramines in swimming pool water (in German), Vom Wasser, 45 (1975) 17-28.

[39] L. Erdinger, F. Kirsch, H.G. Sonntag, Irritating effects of disinfection by-products in swimming pools (in German), Zentralblatt für Hygiene und Umweltmedizin, 200 (1998) 491-503.

[40] A. Bernard, S. Carbonnelle, C. de Burbure, O. Michel, M. Nickmilder, Chlorinated pool attendance, atopy, and the risk of asthma during childhood, Environ. Health Perspect., 114 (2006) 1567-1573.

[41] A. Bernard, M. Nickmilder, C. Voisin, Outdoor swimming pools and the risks of asthma and allergies during adolescence, Eur. Respir. J., 32 (2008) 979-988.

[42] M. Nickmilder, A. Bernard, Ecological association between childhood asthma and availability of indoor chlorinated swimming pools in Europe, Occup. Environ. Med., 64 (2007) 37-46.

[43] K.M. Thickett, J.S. McCoach, J.M. Gerber, S. Sadhra, P.S. Burge, Occupational asthma caused by chloramines in indoor swimming-pool air, Eur. Respir. J., 19 (2002) 827-832.

[44] C.M. Villanueva, K.P. Cantor, J.O. Grimalt, N. Malats, D. Silverman, A. Tardon, R. Garcia-Closas, C. Serra, A. Carrato, G. Castano-Vinyals, R. Marcos, N. Rothman, F.X. Real, M. Dosemeci, M. Kogevinas, Bladder cancer and exposure to water disinfection by-products through ingestion, bathing, showering, and swimming in pools, Am. J. Epidemiol., 165 (2007) 148-156.

[45] S.D. Richardson, M.J. Plewa, E.D. Wagner, R. Schoeny, D.M. DeMarini, Occurrence, genotoxicity, and carcinogenicity of regulated and emerging disinfection by-products in drinking water: A review and roadmap for research, Mutat. Res. - Rev. Mut. Res., 636 (2007) 178-242.

[46] T. Glauner, P. Waldmann, F.H. Frimmel, C. Zwiener, Swimming pool water - fractionation and genotoxicological characterization of organic constituents, Water Res., 39 (2005) 4494-4502.

[47] R. Borgmann-Strahsen, Comparative assessment of different biocides in swimming pool water, Int. Biodeterior. Biodegrad., 51 (2003) 291-297.

[48] K.M.S. Hansen, R. Zortea, A. Piketty, S.R. Vega, H.R. Andersen, Photolytic removal of DBPs by Medium pressure UV in swimming pool water, Sci. Total Environ., 443 (2013) 850-856.

[49] D. Cassan, B. Mercier, F. Castex, A. Rambaud, Effects of medium-pressure UV lamps radiation on water quality in a chlorinated indoor swimming pool, Chemosphere, 62 (2006) 1507-1513.

[50] F. Soltermann, T. Widler, S. Canonica, U. von Gunten, Photolysis of inorganic chloramines and efficiency of trichloramine abatement by UV treatment of swimming pool water, Water Res., 56 (2014) 280-291.

[51] S.J. Judd, G. Bullock, The fate of chlorine and organic materials in swimming pools, Chemosphere, 51 (2003) 869-879.

[52] T. Glauner, F.H. Frimmel, C. Zwiener, Swimmung pool water. The required quality and what can be done technologically (in German), GWF, Wasser/Abwasser, 145 (2004) 706-713.

[53] S.J. Judd, S.H. Black, Disinfection by-product formation in swimming pool waters: A simple mass balance, Water Res., 34 (2000) 1611-1619.

[54] A.M. Klüpfel, T. Glauner, C. Zwiener, F.H. Frimmel, Nanofiltration for enhanced removal of disinfection by-product (DBP) precursors in swimming pool water-retention and water quality estimation, Water Sci. Technol., 63 (2011) 1716-1725.

[55] T. Glauner, F. Kunz, C. Zwiener, F.H. Frimmel, Elimination of swimming pool water disinfection by-products with advanced oxidation processes (AOPs), Acta Hydroch. Hydrob., 33 (2005) 585-594.

[56] DIN 19643-2, Treatment of water of swimming pools and baths, Part 2: Combinations of process with fixed bed filters and precoat filters (in German), Normenausschuss Wasserwesen (NAW) im DIN Deutsches Institut für Normung, Beuth Verlag, Berlin, 2012.

[57] S. Chowdhury, K. Alhooshani, T. Karanfil, Disinfection byproducts in swimming pool: Occurrences, implications and future needs, Water Res., 53 (2014) 68-109.

[58] S. Simard, R. Tardif, M.J. Rodriguez, Variability of chlorination by-product occurrence in water of indoor and outdoor swimming pools, Water Res., 47 (2013) 1763-1772.

[59] H. Kim, J. Shim, S. Lee, Formation of disinfection by-products in chlorinated swimming pool water, Chemosphere, 46 (2002) 123-130.

[60] B. Örmerci, K.G. Linden, Comparison of UV and chlorine inactivation of particle and non-particle associated coliform, Water Sci. Technol.: Water Sup., 2 (2002) 403-410.

[61] C. Schmalz, F.H. Frimmel, C. Zwiener, Trichloramine in swimming pools - Formation and mass transfer, Water Res., 45 (2011) 2681-2690.

[62] F. Soltermann, S. Canonica, U. von Gunten, Trichloramine reactions with nitrogenous and carbonaceous compounds: Kinetics, products and chloroform formation, Water Res., 71 (2015) 318-329.

[63] S.A. Huber, A. Balz, M. Abert, W. Pronk, Characterisation of aquatic humic and non-humic matter with size-exclusion chromatography - organic carbon detection - organic nitrogen detection (LC-OCD-OND), Water Res., 45 (2011) 879-885.

[64] J. van Smeden, M. Janssens, G.S. Gooris, J.A. Bouwstra, The important role of stratum corneum lipids for the cutaneous barrier function, Biochim. Biophys. Acta - Mol. Cell Biol. Lipids, 1841 (2014) 295-313.

[65] T. Poiger, H.R. Buser, M.E. Balmer, P.A. Bergqvist, M.D. Muller, Occurrence of UV filter compounds from sunscreens in surface waters: regional mass balance in two Swiss lakes, Chemosphere, 55 (2004) 951-963.

[66] S. González, M. Fernández-Lorente, Y. Gilaberte-Calzada, The latest on skin photoprotection, Clin. Dermatol., 26 (2008) 614-626.

[67] U.S. EPA, Nanomaterial Case Studies: Nanoscale Titanium Dioxide in Water Treatment and in Topical Sunscreen, Waashington, DC, 2010.

[68] G.M. Murphy, Sunblocks: Mechanisms of action, Photodermatol. Photo., 15 (1999) 34-36.

[69] P. Kullavanijaya, H.W. Lim, Photoprotection, J. Am. Acad. Dermatol., 52 (2005) 937-958.

[70] Scientific Committee on Consumer Safety (SCCS), Opinion on 2,2'-methylene-bis-(6(2H-benzotriazol-2-yl)-4-(1,1,3,3-tetramethylbutyl)phenol), 18 March 2013, revision of 23 July 2013, SCCS/1460/11.

[71] Ministry of Housing, Spatial Planning and the Environment (VROM), Research on filtration and pool water treatment in swimming pools (in Dutch), Publicatiereeks Milieubeheer (Series title Environment), Den Haag, 1985.

[72] J.E. Amburgey, K.J. Walsh, R.R. Fielding, M.J. Arrowood, Removal of Cryptosporidium and polystyrene microspheres from swimming pool water with sand, cartridge, and precoat filters, J. Water Health, 10 (2012) 31-42.

[73] J.B. Rose, G.S. Sun, C.P. Gerba, N.A. Sinclair, Microbial Quality and Persistence of Enteric Pathogens in Graywater from Various Household Sources, Water Res., 25 (1991) 37-42.

[74] C.P. Gerba, Assessment of Enteric Pathogen Shedding by Bathers during Recreational Activity and its Impact on Water Quality, Quant. Microbiol., 2 (2000) 55-68.

[75] N.B. Hanes, A.J. Fossa, A quantitative analysis of the effects of bathers on recreational water quality, in: Proceedings of the 5th International Water Pollution Research Conference, Pergamon Press, London, 1970.

[76] H. Althaus, C.A. Primavesi, Anthropogenic loading in Hot-Whirl-Pools (in German), A.B. Arch. Badew., 11 (1981) 417-420.

[77] B.G. Smith, A.P. Dufour, Effects of swimmers on the microbiological quality of recreational waters: A simulation study, in: Annual Meeting of the American Society for Microbiology American Society for Microbiology. Washington, DC, 1994, 406.

[78] J.H.G. Vreeburg, D. Schippers, J.Q.J.C. Verberk, J.C. van Dijk, Impact of particles on sediment accumulation in a drinking water distribution system, Water Res., 42 (2008) 4233-4242.

[79] J.Q.J.C. Verberk, J.H.G. Vreeburg, L.C. Rietveld, J.C. van Dijk, Particulate fingerprinting of water quality in the distribution system, Water Sa, 35 (2009) 192-199.

[80] J.Q.J.C. Verberk, L.A. Hamilton, K.J. O´Halloran, W. van der Horst, J. Vreeburg, Analysis of particle numbers, size and composition in drinking water transportation pipelines: results of online measurements, Water Sci. Technol.: Water Sup., 6 (2006) 35-43.

[81] P. van Thienen, J.H.G. Vreeburg, E.J.M. Blokker, Radial transport processes as a precursor to particle deposition in drinking water distribution systems, Water Res., 45 (2011) 1807-1817.

[82] G. Liu, F.Q. Ling, A. Magic-Knezev, W.T. Liu, J.Q.J.C. Verberk, J.C. Van Dijk, Quantification and identification of particle-associated bacteria in unchlorinated drinking water from three treatment plants by cultivation-independent methods, Water Res., 47 (2013) 3523-3533.

[83] Y. Matsui, T. Yamagishi, Y. Terada, T. Matsushita, T. Inoue, Suspended particles and their characteristics in water mains: developments of sampling methods, J. Water Sup. Res. Tech.-Aqua, 56 (2007) 13-24.

[84] F. Hammes, M. Berney, Y.Y. Wang, M. Vital, O. Koster, T. Egli, Flow-cytometric total bacterial cell counts as a descriptive microbiological parameter for drinking water treatment processes, Water Res., 42 (2008) 269-277.

[85] D. Hoefel, W.L. Grooby, P.T. Monis, S. Andrews, C.P. Saint, Enumeration of water-borne bacteria using viability assays and flow cytometry: a comparison to culture-based techniques, J. Microbiol. Methods, 55 (2003) 585-597.

[86] C.F. Consolazio, R.E. Johnson, L.J. Pecora, Physiological Measurements of Metabolic Functions in Man, McGraw-Hill, 1963.

[87] P.W.R. Lemon, D.T. Deutsch, W.R. Payne, Urea production during prolonged swimming, J. Sports Sci., 7 (1989) 241-246.

[88] F. Macaluso, V. Di Felice, G. Boscaino, G. Bonsignore, T. Stampone, F. Farina, G. Morici, Effects of three different water temperatures on dehydration in competitive swimmers, Sci. Sport, 26 (2011) 265-271.

[89] R.J. Maughan, L.A. Dargavel, R. Hares, S.M. Shirreffs, Water and Salt Balance of Well-Trained Swimmers in Training, Int. J. Sport Nutr. Exe., 19 (2009) 598-606.

[90] R.G. Mcmurray, S.M. Horvath, Thermoregulation in Swimmers and Runners, J. Appl. Physiol., 46 (1979) 1086-1092.

[91] B. Nielsen, G. Sjogaard, F. Bondepetersen, Cardiovascular, Hormonal and Body-Fluid Changes during Prolonged Exercise, Eur. J. Appl. Physiol. O., 53 (1984) 63-70.

[92] S. Robinson, A. Somers, Temperature Regulation in Swimming, J. Physiol.-Paris, 63 (1971) 406-409.

[93] K. Gunkel, H.-J. Jessen, Untersuchungen über den Harnstoffeintrag in das Badewasser (in German), Acta Hydrochim. Hydrobiol., 14 (1986) 451-461.

[94] L. Erdinger, F. Kirsch, H.G. Sonntag, Potassium as an indicator of anthropogenic contamination of swimming pool water (in German), Zentralblatt für Hygiene und Umweltmedizin, 200 (1997) 297-308.

[95] D. Eichelsdörfer, J. Jandik, W. Weil, Organic halogen compounds in swimming pool water II. Formation of volatile halogenated hydrocarbons in model experiments (in German), Zeitschrift für Wasser und Abwasserforschung, 13 (1980) 165-169.

[96] D.F. Putnam, Composition and concentrative properties of human urine, NASA Contractor Report CR-1802, McDonnell Douglas Astronautics Company, Washington, DC, 1971.

[97] E. Stottmeister, K. Voigt, Trichloramine in swimming pool air (in German), A.B. Arch. Badew., 3 (2006) 158-162.

[98] M. Tachikawa, T. Aburada, M. Tezuka, R. Sawamura, Occurrence and production of chloramines in the chlorination of creatinine in aqueous solution, Water Res., 39 (2005) 371-379.

[99] C. Carducci, M. Birarelli, V. Leuzzi, G. Santagata, P. Serafini, I. Antonozzi, Automated method for the measurement of amino acids in urine by high-performance liquid chromatography, J. Chromatogr. A, 729 (1996) 173-180.

[100] M.G.A. Keuten, J.Q.J.C. Verberk, J.C. van Dijk, Definition and quantification of anthropogenic initial and continual biochemical bathing load in swimming pools, in: Proceedings of the fourth International Conference Swimming Pool & Spa, Porto, 2011, 84-113.

[101] G. Potard, C. Laugel, A. Baillet, H. Schaefer, J.P. Marty, Quantitative HPLC analysis of sunscreens and caffeine during in vitro percutaneous penetration studies, Int. J. Pharm., 189 (1999) 249-260.

[102] T. Glauner, Swimming pool water treatment - Formation and detection of disinfection by-products and their mitigation with membrane and oxidation processes (in German), Doctoral thesis, Universität Karlsruhe, Karlsruhe, 2007.

[103] H. Chu, M.J. Nieuwenhuijsen, Distribution and determinants of trihalomethane concentrations in indoor swimming pools, Occup. Environ. Med., 59 (2002) 243-247.

[104] C.H. Xue, Q. Wang, W.H. Chu, M.R. Templeton, The impact of changes in source water quality on trihalomethane and haloacetonitrile formation in chlorinated drinking water, Chemosphere, 117 (2014) 251-255.

[105] A. Matilainen, E.T. Gjessing, T. Lahtinen, L. Hed, A. Bhatnagar, M. Sillanpaa, An overview of the methods used in the characterisation of natural organic matter (NOM) in relation to drinking water treatment, Chemosphere, 83 (2011) 1431-1442.

[106] D. Gang, T.E. Clevenger, S.K. Banerji, Relationship of chlorine decay and THMs formation to NOM size, J. Hazard. Mater., 96 (2003) 1-12.

[107] J. Peuravuori, A. Monteiro, L. Eglite, K. Pihlaja, Comparative study for separation of aquatic humic-type organic constituents by DAX-8, PVP and DEAE sorbing solids and tangential ultrafiltration: elemental composition, size-exclusion chromatography, UV-vis and FT-IR, Talanta, 65 (2005) 408-422.

[108] E. Vasyukova, R. Proft, J. Jousten, I. Slavik, W. Uhl, Removal of natural organic matter and trihalomethane formation potential in a full-scale drinking water treatment plant, Water Sci. Technol.: Water Sup., 13 (2013) 1099-1108.

[109] A. Matilainen, P. Iivari, J. Sallanko, E. Heiska, T. Tuhkanen, The role of ozonation and activated carbon filtration in the natural organic matter removal from drinking water, Environ. Technol., 27 (2006) 1171-1180.

[110] T.K. Nissinen, I.T. Miettinen, P. Martikainen, T. Vartiainen, Molecular size ditribution of natural organic matter in raw and drinking water, Chemosphere, 45 (2001) 865-873.

[111] M.Y. Chang, R.S. Juang, Adsorption of tannic acid, humic acid, and dyes from water using the composite of chitosan and activated clay, J. Colloid Interface Sci., 278 (2004) 18-25.

[112] R.G. Sinclair, J.B. Rose, S.A. Hashsham, C.P. Gerba, C.N. Haas, Criteria for Selection of Surrogates Used To Study the Fate and Control of Pathogens in the Environment, Appl. Environ. Microbiol., 78 (2012) 1969-1977.

[113] K.K. Philippe, C. Hans, J. MacAdam, B. Jefferson, J. Hart, S.A. Parsons, Photocatalytic oxidation of natural organic matter surrogates and the impact on trihalomethane formation potential, Chemosphere, 81 (2010) 1509-1516.

[114] W.L. Bradford, What bather put into a pool: A critical review of body fluids and a body fluid analog, Int. J. Aquat. Res. Educ., 8 (2014) 168-181.

[115] E.M. Thurman, R.L. Malcolm, Preparative Isolation of Aquatic Humic Substances, Environ. Sci. Technol., 15 (1981) 463-466.

[116] F.J. Rodriguez, P. Schlenger, M. Garcia-Valverde, A comprehensive structural evaluation of humic substances using several fluorescence techniques before and after ozonation. Part II: Evaluation of structural changes following ozonation, Sci. Total Environ., 476 (2014) 731-742.

[117] A. Matilainen, M. Sillanpaa, Removal of natural organic matter from drinking water by advanced oxidation processes, Chemosphere, 80 (2010) 351-365.

[118] R.L. Malcolm, P. Maccarthy, Limitations in the Use of Commercial Humic Acids in Water and Soil Research, Environ. Sci. Technol., 20 (1986) 904-911.

[119] F.J. Rodriguez, L.A. Nunez, Characterization of aquatic humic substances, Water Environ. J., 25 (2011) 163-170.

[120] A. Scheili, M.J. Rodriguez, R. Sadiq, Seasonal and spatial variations of source and drinking water quality in small municipal systems of two Canadian regions, Sci. Total Environ., 508 (2015) 514-524.

[121] M.B. Muller, D. Schmitt, F.H. Frimmel, Fractionation of natural organic matter by size exclusion chromatography - Properties and stability of fractions, Environ. Sci. Technol., 34 (2000) 4867-4872.

[122] D.M. Goeres, T. Palys, B.B. Sandel, J. Geiger, Evaluation of disinfectant efficacy against biofilm and suspended bacteria in a laboratory swimming pool model, Water Res., 38 (2004) 3103-3109.

[123] SIA 385/9, Water and water treatment in public pools (in German), Swiss society of engineers and architects (SIA), Zürich, 2011.

[124] ANSI/APSP-11, American National Standard for Water Quality in Public Pools and Spas, The Association of Pool and Spa Professionals, American National Standards Institute (ANSI), Alexandria, 2009.

[125] T.X. Wang, D.W. Margerum, Kinetics of Reversible Chlorine Hydrolysis - Temperature-Dependence and General Acid Base-Assisted Mechanisms, Inorg. Chem., 33 (1994) 1050-1055.

[126] J.C. Morris, Acid Ionization Constant of HOCl from 5 to 35 Degrees, J. Phys. Chem., 70 (1966) 3798-3805.

[127] J.D. Sivey, C.E. McCullough, A.L. Roberts, Chlorine monoxide (Cl2O) and molecular chlorine (Cl-2) as active chlorinating agents in reaction of dimethenamid with aqueous free chlorine, Abstracts of Papers of the American Chemical Society, 240 (2010).

[128] G. Zimmerman, F.C. Strong, Equilibria and Spectra of Aqueous Chlorine Solutions, J. Am. Chem. Soc., 79 (1957) 2062-2066.

[129] E.A. Voudrias, M. Reinhard, Reactivities of Hypochlorous and Hypobromous Acid, Chlorine Monoxide, Hypobromous Acidium Ion, Chlorine, Bromine, and Bromine Chloride in Electrophilic Aromatic-Substitution Reactions with P-Xylene in Water, Environ. Sci. Technol., 22 (1988) 1049-1056.

[130] V.L. Snoeyink, D. Jenkins, Water Chemistry, John Wiley & Sons, New York, 1998.

[131] P. Reichert, Aquasim - a tool for simulation and data-analysis of aquatic systems, Water Sci. Technol., 30 (1994) 21-30.

[132] Y.G. Feng, D.W. Smith, J.R. Bolton, Photolysis of aqueous free chlorine species (NOCl and OCl-) with 254 nm ultraviolet light, J. Environ. Eng. Sci., 6 (2007) 277-284.

[133] G.V. Buxton, M.S. Subhani, Radiation-Chemistry and Photochemistry of Oxychlorine Ions .2. Photodecomposition of Aqueous-Solutions of Hypochlorite Ions, J. Chem. Soc. Farad. T. 1, 68 (1972) 958-&.

[134] M.J. Watts, K.G. Linden, Chlorine photolysis and subsequent OH radical production during UV treatment of chlorinated water, Water Res., 41 (2007) 2871-2878.

[135] C.T. Jafvert, R.L. Valentine, Reaction Scheme for the Chlorination of Ammoniacal Water, Environ. Sci. Technol., 26 (1992) 577-586.

[136] E.R. Blatchley, M.M. Cheng, Reaction Mechanism for Chlorination of Urea, Environ. Sci. Technol., 44 (2010) 8529-8534.

[137] W. Lee, P. Westerhoff, Formation of organic chloramines during water disinfection - chlorination versus chloramination, Water Res., 43 (2009) 2233-2239.

[138] M. Soulard, F. Bloc, A. Hatterer, Diagrams of Existence of Chloramines and Bromamines in Aqueous-Solution, J. Chem. Soc. Dalton, (1981) 2300-2310.

[139] A. Cloteaux, F. Gérardin, N. Midoux, Influence of swimming pool design on hydraulic behavior: A numerical and experimental study, Eng. Min. J., (2013) 511-524.

[140] J.M. Shields, E.R. Gleim, M.J. Beach, Prevalence of Cryptosporidium spp. and Giardia intestinalis in swimming pools, Atlanta, Georgia, Emerg. Infect. Dis., 14 (2008) 948-950.

[141] R. Arnitz, M. Nagl, W. Gottardi, Microbicidal activity of monochloramine and chloramine T compared, J. Hosp. Infect., 73 (2009) 164-170.

[142] W. Gottardi, M. Nagl, Chlorine covers on living bacteria: the initial step in antimicrobial action of active chlorine compounds, J. Antimicrob. Chemother., 55 (2005) 475-482.

[143] W. Gottardi, R. Arnitz, M. Nagl, N-chlorotaurine and ammonium chloride: An antiseptic preparation with strong bactericidal activity, Int. J. Pharm., 335 (2007) 32-40.

[144] H. Chick, An investigation of the laws of disinfection, J. Hyg. Cambridge, 8 (1908) 92-158.

[145] H.E. Watson, A note on the variation of the rate of disinfection with change in the concentration of the disinfectant, J. Hyg. Cambridge, 8 (1908) 536-542.

[146] J.C. Hoff, Strength and weaknesses of using CT values to evaluate disinfection practice, in: Proceedings of the American Water Works Association Water Quality Technology Conference XIV, Portland, 2011.

[147] L. Wojcicka, R. Hofmann, C. Baxter, R.C. Andrews, I. Auvray, J. Liere, T. Miller, C. Chauret, H. Baribeau, Inactivation of environmental and reference strains of heterotrophic bacteria and Escherichia coli O157 : H7 by free chlorine and monochloramine, J. Water Sup. Res. Tech.-Aqua, 56 (2007) 137-150.

[148] M.M. Donnermair, E.R. Blatchley, Disinfection efficacy of organic chloramines, Water Res., 37 (2003) 1557-1570.

[149] J.N. Jensen, J.D. Johnson, Interferences by Monochloramine and Organic Chloramines in Free Available Chlorine Methods .1. Amperometric-Titration, Environ. Sci. Technol., 24 (1990) 981-985.

[150] W. Lee, P. Westerhoff, X. Yang, C. Shang, Comparison of colorimetric and membrane introduction mass spectrometry techniques for chloramine analysis, Water Res., 41 (2007) 3097-3102.

[151] E. Stottmeister, Occurrence of disinfection by-products in swimming pool waters (in German), Umweltmedizinischer Informationsdienst, 2 (1999) 21-29.

[152] L. Lian, E. Yue, J. Li, E.R. Blatchley, Volatile Disinfection Byproducts Resulting from Chlorination of Uric Acid: Implications for Swimming Pools, Environ. Sci. Technol., 48 (2014) 3210-3217.

[153] S.C. Weng, W.A. Weaver, M.Z. Afifi, T.N. Blatchley, J.S. Cramer, J. Chen, E.R. Blatchley, Dynamics of gas-phase trichloramine (NCl3) in chlorinated, indoor swimming pool facilities, Indoor Air, 21 (2011) 391-399.

[154] S.C. Weng, J. Li, K.V. Wood, H.I. Kenttamaa, P.E. Williams, L.M. Amundson, E.R. Blatchley, UV-induced effects on chlorination of creatinine, Water Res., 47 (2013) 4948-4956.

[155] W. Wang, Y.C. Qian, J.M. Boyd, M.H. Wu, S.E. Hrudey, X.F. Li, Halobenzoquinones in Swimming Pool Waters and Their Formation from Personal Care Products, Environ. Sci. Technol., 47 (2013) 3275-3282.

[156] F. Xiao, X.R. Zhang, H.Y. Zhai, I.M.C. Lo, G.L. Tipoe, M.T. Yang, Y. Pan, G.H. Chen, New Halogenated Disinfection Byproducts in Swimming Pool Water and Their Permeability across Skin, Environ. Sci. Technol., 46 (2012) 7112-7119.

[157] I.M. Schreiber, W.A. Mitch, Nitrosamine formation pathway revisited: The importance of chloramine speciation and dissolved oxygen, Environ. Sci. Technol., 40 (2006) 6007-6014.

[158] S.S. Walse, W.A. Mitch, Nitrosamine carcinogens also swim in chlorinated pools, Environ. Sci. Technol., 42 (2008) 1032-1037.

[159] F. Soltermann, M. Lee, S. Canonica, U. von Gunten, Enhanced N-nitrosamine formation in pool water by UV irradiation of chlorinated secondary amines in the presence of monochloramine, Water Res., 47 (2012) 79-90.

[160] S.W. Krasner, H.S. Weinberg, S.D. Richardson, S.J. Pastor, R. Chinn, M.J. Sclimenti, G.D. Onstad, A.D. Thruston, Occurrence of a new generation of disinfection byproducts, Environ. Sci. Technol., 40 (2006) 7175-7185.

[161] S.W. Krasner, The formation and control of emerging disinfection by-products of health concern, Philos Trans A Math Phys Eng Sci, 367 (2009) 4077-4095.

[162] N. Cimetiere, J. De Laat, Effects of UV-dechloramination of swimming pool water on the formation of disinfection by-products: A lab-scale study, Microchem. J., 112 (2014) 34-41.

[163] S.C. Weng, J. Li, E.R. Blatchley, Effects of UV254 irradiation on residual chlorine and DBPs in chlorination of model organic-N precursors in swimming pools, Water Res., 46 (2012) 2674-2682.

[164] A. Spiliotopoulou, K.M. Hansen, H.R. Andersen, Secondary formation of disinfection by-products by UV treatment of swimming pool water, Sci. Total Environ., 520 (2015) 96-105.

[165] F. Soltermann, Trichloramine in swimming pool water: analysis methods, factors influencing its fate and effects of UV treatment, Doctoral thesis, ETH Zurich, Zurich, 2015.

[166] A. Kanan, Occurrence and formation of disinfection by-products in indoor swimming pools water, Doctoral thesis, Clemson University, South Carolina, 2010.

[167] X.M. Wang, M.I.G. Leal, X.L. Zhang, H.W. Yang, Y.F. Xie, Haloacetic acids in swimming pool and spa water in the United States and China, Front. Env. Sci. Eng., 8 (2014) 820-824.

[168] M.G. Muellner, E.D. Wagner, K. McCalla, S.D. Richardson, Y.T. Woo, M.J. Plewa, Haloacetonitriles vs. regulated haloacetic acids: Are nitrogen-containing DBPs more toxic?, Environ. Sci. Technol., 41 (2007) 645-651.

[169] N. Massin, A.B. Bohadana, P. Wild, M. Hery, J. Toamain, G. Hubert, Respiratory symptoms and bronchial responsiveness in lifeguards exposed to nitrogen trichloride in indoor swimming pools, Occup. Environ. Med., 55 (1998) 258-263.

[170] F. Soltermann, T. Wider, S. Canonica, U. von Gunten, Comparison of a novel extraction-based colorimetric (ABTS) method with membrane introduction mass spectrometry (MIMS): Trichloramine dynamics in pool water, Water Res., 58 (2014) 258-268.

[171] M.J. Lee, Y.H. Lee, F. Soltermann, U. von Gunten, Analysis of N-nitrosamines and other nitro(so) compounds in water by high-performance liquid chromatography with post-column UV photolysis/Griess reaction, Water Res., 47 (2013) 4893-4903.

[172] M. Clemens, H.F. Schöler, Halogenated Organic Compounds in Swimming Pool Waters (in German), Zentralblatt für Hygiene, 193 (1992) 91-98.

[173] DIN EN ISO 7393-2, Water quality - Determination of free chlorine and total chlorine, Part 2: Colorimetric method using N,N-diethyl-1,4-phenylenediamine, for routine control purposes (in German), Normenausschuss Wasserwesen (NAW) im DIN Deutsches Institut für Normung, Beuth Verlag, Berlin, 2000.

[174] G. McKay, B. Sjelin, M. Chagnon, K.P. Ishida, S.P. Mezyk, Kinetic study of the reactions between chloramine disinfectants and hydrogen peroxide: Temperature dependence and reaction mechanism, Chemosphere, 92 (2013) 1417-1422.

[175] K. Doederer, W. Gernjak, H.S. Weinberg, M.J. Farre, Factors affecting the formation of disinfection by-products during chlorination and chloramination of secondary effluent for the production of high quality recycled water, Water Res., 48 (2014) 218-228.

[176] P.C. Singer, Control of Disinfection by-Products in Drinking-Water, J. Environ. Eng. ASCE, 120 (1994) 727-744.

[177] K.M.S. Hansen, S. Willach, M.G. Antoniou, H. Mosbæk, H.-J. Albrechtsen, H.R. Andersen, Effect of selection of pH in swimming pools on formation of chlorination by-products, in: Proceedings of the fourth International Conference Swimming Pool & Spa, Porto, 2011, 19-24.

[178] L. Liang, P.C. Singer, Factors influencing the formation and relative distribution of haloacetic acids and trihalomethanes in drinking water, Environ. Sci. Technol., 37 (2003) 2920-2928.

[179] M.Z. Afifi, E.R. Blatchley, Seasonal dynamics of water and air chemistry in an indoor chlorinated swimming pool, Water Res., 68 (2015) 771-783.

[180] M.J. Chen, J.M. Dugh, R.H. Shie, J.H. Weng, H.T. Hsu, Dynamic real-time monitoring of chloroform in an indoor swimming pool air using open-path Fourier transform infrared spectroscopy, Indoor Air 2015, (2015) 1-11.

[181] J. Caro, M. Gallego, Assessment of exposure of workers and swimmers to trihalomethanes in an indoor swimming pool, Environ. Sci. Technol., 41 (2007) 4793-4798.

[182] B. Schmoll, R. Kellner, D. Breuer, M. Buxtrup, C. Engel, G. Fliedner, U. Franke, C. Friedrich, A. Geilenkirchen, R. van Gelder, H.-D. Neumann, R. Radtke, D. Richter, U. Salvadori, F. Speckelsen, S. Stöcker, I. Thullner, B. Weber, W. Wegscheider, B. Wimmer, R. Zirbs, Trichloramine in indoor swimming pool air (in German), A.B. Arch. Badew., 10 (2009) 591-611.

[183] C. Schmalz, Formation, Phasetransfer and toxicity of halogenated disinfection by-products in the water cycle of swimming pools - focus on nitrogen containing substances (in German), Doctoral thesis, Karlsruher Instituts für Technologie (KIT), Karlsruhe, 2012.

[184] S.D. Boyce, J.F. Hornig, Reaction Pathways of Trihalomethane Formation from the Halogenation of Dihydroxyaromatic Model Compounds for Humic-Acid, Environ. Sci. Technol., 17 (1983) 202-211.

[185] P. Hua, Variable reaction rate models for chlorine decay and trihalomethanes formation in drinking water distribution systems, Doctoral thesis, Technische Universität Dresden, Dresden, 2016.

[186] H. Gallard, G.U. von, Chlorination of phenols: kinetics and formation of chloroform, Environ Sci Technol, 36 (2002) 884-890.

[187] P. Hua, X. Chen, E. Vasyukova, W. Uhl, Reaction kinetics of chlorine with human body fluids present in swimming pool water, in: C. Thompson, S. Gillespie, E. Goslan (Eds.) Disinfection By-products in Drinking Water, The Royal Society of Chemistry, Cambridge, UK, 2016.

[188] R.A. Larson, A.L. Rockwell, Citric-Acid - Potential Precursor of Chloroform in Water Chlorination, Naturwissenschaften, 65 (1978) 490-490.

[189] I. Weil, C. Morris, Kinetic Studies on the Chloramines. I. The Rates of Formation of Monochloramine, N-Chlormethylamine and N-Chlordimethylamine, J. Am. Chem. Soc., 71 (1949) 1664-1671.

[190] Z.M. Qiang, C.D. Adams, Determination of monochloramine formation rate constants with stopped-flow spectrophotometry, Environ. Sci. Technol., 38 (2004) 1435-1444.

[191] R.A. Isaac, J.C. Morris, Transfer of Active Chlorine from Chloramine to Nitrogenous Organic-Compounds. 1. Kinetics, Environ. Sci. Technol., 17 (1983) 738-742.

[192] J. De Laat, W.T. Feng, D.A. Freyfer, F. Dossier-Berne, Concentration levels of urea in swimming pool water and reactivity of chlorine with urea, Water Res., 45 (2011) 1139-1146.

[193] J.A. Wojtowicz, Chemistry of nitrogen compounds in swimming pool water, Journal of the swimming pool and spa industry, 4 (2001) 30-40.

[194] S.H. Zeisel, K.A. Dacosta, J.T. Lamont, Monomethylamine, Dimethylamine and Trimethylamine in Human Gastric Fluid - Potential Substrates for Nitrosodimethylamine Formation, Carcinogenesis, 9 (1988) 179-181.

[195] W.A. Mitch, D.L. Sedlak, Formation of N-nitrosodimethylamine (NDMA) from dimethylamine during chlorination, Environ. Sci. Technol., 36 (2002) 588-595.

[196] J.H. Choi, R.L. Valentine, Formation of N-nitrosodimethylamine (NDMA) from reaction of monochloramine: A new disinfection by-product, Water Res., 36 (2002) 817-824.

[197] G.H. Hua, D.A. Reckhow, DBP formation during chlorination and chloramination: Effect of reaction time, pH, dosage, and temperature, J. AWWA, 100 (2008) 82-95.

[198] J.S. Lakind, S.D. Richardson, B.C. Blount, The Good, the Bad, and the Volatile: Can We Have Both Healthy Pools and Healthy People?, Environ. Sci. Technol., 44 (2010) 3205-3210.

[199] H.J. Whitaker, M.J. Nieuwenhuijsen, N.G. Best, The relationship between water concentrations and individual uptake of chloroform: A simulation study, Environ. Health Perspect., 111 (2003) 688-694.

[200] J. Caro, M. Gallego, Alveolar air and urine analyses as biomarkers of exposure to trihalomethanes in an indoor swimming pool, Environ. Sci. Technol., 42 (2008) 5002-5007.

[201] B. Levesque, P. Ayotte, A. Leblanc, E. Dewailly, D. Prudhomme, R. Lavoie, S. Allaire, P. Levallois, Evaluation of Dermal and Respiratory Chloroform Exposure in Humans, Environ. Health Perspect., 102 (1994) 1082-1087.

[202] S. Landi, A. Naccarati, M.K. Ross, N.M. Hanley, L. Dailey, R.B. Devlin, M. Vasquez, R.A. Pegram, D.M. DeMarini, Induction of DNA strand breaks by trihalomethanes in primary human lung epithelial cells, Mutat. Res.-Genet. Toxicol. Environ. Mutag., 538 (2003) 41-50.

[203] C. Schmalz, H.G. Wunderlich, R. Heinze, F.H. Frimmel, C. Zwiener, T. Grummt, Application of an optimized system for the well-defined exposure of human lung cells to trichloramine and indoor pool air, J. Water Health, 9 (2011) 586-596.

[204] C.S.A. Sa, R.A.R. Boaventura, I.B. Pereira, Analysis of haloacetic acids in water and air (aerosols) from indoor swimming pools using HS-SPME/GC/ECD, J. Environ. Sci. Heal. A, 47 (2012) 176-183.

[205] M.J. Cardador, M. Gallego, Haloacetic Acids in Swimming Pools: Swimmer and Worker Exposure, Environ. Sci. Technol., 45 (2011) 5783-5790.

[206] C.M. Villanueva, K.P. Cantor, S. Cordier, J.J.K. Jaakkola, W.D. King, C.F. Lynch, S. Porru, M. Kogevinas, Disinfection byproducts and bladder cancer - A pooled analysis, Epidemiology, 15 (2004) 357-367.

[207] R.G. Tardiff, M.L. Carson, M.E. Ginevan, Updated weight of evidence for an association between adverse reproductive and developmental effects and exposure to disinfection by-products, Regul. Toxicol. Pharm., 45 (2006) 185-205.

[208] DIN 19643-4, Treatment of water of swimming pools and baths, Part 4: Combinations of process with ultrafiltration (in German), Normenausschuss Wasserwesen (NAW) im DIN Deutsches Institut für Normung, Beuth Verlag, Berlin, 2012.

[209] M.T. Martins, M.I.Z. Sato, M.N. Alves, N.C. Stoppe, V.M. Prado, P.S. Sanchez, Assessment of Microbiological Quality for Swimming Pools in South-America, Water Res., 29 (1995) 2417-2420.

[210] M. Singer, The Role of Antimicrobial Agents in Swimming Pools, Int. Biodeterior., 26 (1990) 159-168.

[211] K. Botzenhardt, K.K. Pfeilsticker, Comparison of European regulations for swimming pool hygiene (in German), Gesundheitsw., 61 (1999) 424-429.

[212] F. Brummel, Surveillance of swimming pool water quality according to §11 of the Federal Law on Infectious Disease (in German), A.B. Arch. Badew., 42 (1989) 291-296.

[213] M. Fehrle, Additional water treatment techniques for swimming pool water (in German), A.B. Arch. Badew., 42 (1989) 3-7.

[214] E. Stottmeister, The revised DIN 19643 " treatment of swimming pool water" (in German), A.B. Arch. Badew., (2013) 152-162.

[215] DIN 19643-3, Treatment of water of swimming pools and baths, Part 3: Combinations of process with ozonization (in German), Normenausschuss Wasserwesen (NAW) im DIN Deutsches Institut für Normung, Beuth Verlag, Berlin, 2012.

[216] DVGW W 213-1, Particle removal by filtration, Part 1: Fundamental terms and principles (in German), DVGW Deutsche Vereinigung des Gas- und Wasserfaches, DVGW e.V., Bonn, 2005.

[217] H. Maierski, D. Eichelsdörfer, K.-E. Quentin, Organic halogen compounds in swimming pool water III. Differentiated determination of the sum of chlorine in volatile and non-volatile chloroorganic compounds (in German), Zeitschrift für Wasser und Abwasserforschung, 15 (1982) 292-295.

[218] T. Gabrio, C. Sacré, Assessing the state of the art in swimming pool water treatment (in German), in: T. Glauner, A. Klüpfel (Eds.) Safety of swimming pool water from a health and water treatment related perspecive (in German), Federal Ministry of Education and Research (BMBF), Dresden, 2006, 9-37.

[219] F.H. Frimmel, T. Glauner, C. Zwiener, Pool water chemistry and health (in German), A.B. Arch. Badew., 57 (2004) 586-594.

[220] G.J. Medema, F.M. Schets, P.F.M. Teunis, A.H. Havelaar, Sedimentation of free and attached Cryptosporidium oocysts and Giardia cysts in water, Appl. Environ. Microbiol., 64 (1998) 4460-4466.

[221] J.E. Amburgey, Removal of Cryptosporidium-Sized Polystyrene Microspheres from Swimming Pool Water with a Sand Filter with and without Added Perlite Filter Media, J. Environ. Eng., 137 (2011) 1205-1208.

[222] B.T. Croll, C.R. Hayes, S. Moss, Simulated Cryptosporidium removal under swimming pool filtration conditions, Water Environ. J., 21 (2007) 149-156.

[223] T. Peters, Membrane treatment - Possibilities and limitations for swimming pool water treatment (in German), A.B. Arch. Badew., 57 (2004) 144-153.

[224] R. Hobby, G. Hagmeyer, B. Lange, R. Gimbel, Application of an ultrafiltration pilot plant for the treatment of swimming pool water. (in German), GWF, Wasser/Abwasser, 145 (2004) 700-704.

[225] F.W. Pontius, G.L. Amy, M.T. Hernandez, Fluorescent microspheres as virion surrogates in low-pressure membrane studies, J. Membr. Sci., 335 (2009) 43-50.

[226] H. Guo, Y. Wyart, J. Perot, F. Nauleau, P. Moulin, Low-pressure membrane integrity tests for drinking water treatment: A review, Water Res., 44 (2010) 41-57.

[227] I. Ivancev-Tumbas, R. Hobby, B. Kuchle, S. Panglisch, R. Gimbel, p-Nitrophenol removal by combination of powdered activated carbon adsorption and ultrafiltration - comparison of different operational modes, Water Res., 42 (2008) 4117-4124.

[228] O. Hofmann, D. Eichelsdörfer, Specific aspects of powdered activated carbon application for the treatment of swimming pool water (in German), bbr, 46 (1995) 33-40.

[229] S.E. Dunn, Effect of Powdered Activated Carbon Base Material and Size on Disinfection By-Product Precursor and Trace Organic Pollutant Removal, Master thesis, North Carolina State University, North Carolina, 2011.

[230] C.F. Lin, Y.J. Huang, I.J. Hao, Ultrafiltration processes for removing humic substances: Effect of molecular weight fractions and PAC treatment, Water Res., 33 (1999) 1252-1264.

[231] F.G. Reißmann, E. Schulze, V. Albrecht, Application of a combined UF/RO system for the reuse of filter backwash water from treated swimming pool water, Desalination, 178 (2005) 41-49.

[232] T. Glauner, P. Waldmann, F.H. Frimmel, C. Zwiener, Swimming pool water—fractionation and genotoxicological characterization of organic constituents, Water Res., 39 (2005) 4494-4502.

[233] C. Shang, W.L. Gong, E.R. Blatchley, Breakpoint chemistry and volatile byproduct formation resulting from chlorination of model organic-N compounds, Environ. Sci. Technol., 34 (2000) 1721-1728.

[234] T.V. Luong, C.J. Peters, R. Perry, Influence of bromide and ammonia upon the formation of trihalomethanes under water-treatment conditions, Environ. Sci. Technol., 16 (1982) 473-479.

[235] H.A. Duong, M. Berg, M.H. Hoang, H.V. Pham, H. Gallard, W. Giger, U. von Gunten, Trihalomethane formation by chlorination of ammonium- and bromide-containing groundwater in water supplies of Hanoi, Vietnam, Water Res., 37 (2003) 3242-3252.

[236] J. Hoigné, H. Bader, Rate constants of reactions of ozone with organic and inorganic compounds in water—I: Non-dissociating organic compounds, Water Res., 17 (1983) 173-183.

[237] D. Eichelsdörfer, J. Jandik, Long contact time ozonation for swimming pool water treatment, Ozone Sci. Eng., 7 (1985) 93-106.

[238] G. Kleiser, F.H. Frimmel, Removal of precursors for disinfection by-products (DBPs) — differences between ozone- and OH-radical-induced oxidation, Sci. Total Environ., 256 (2000) 1-9.

[239] T. Chaiket, P.C. Singer, A. Miles, M. Moran, C. Pallotta, Effectiveness of coagulation, ozonation, and biofiltration in controlling DBPs, J. AWWA, 94 (2002) 81-95.

[240] C.N. Chang, Y.S. Ma, F.F. Zing, Reducing the formation of disinfection by-products by pre-ozonation, Chemosphere, 46 (2002) 21-30.

[241] H.D. Johnson, W.J. Cooper, S.P. Mezyk, D.M. Bartels, Free radical reactions of monochloramine and hydroxylamine in aqueous solution, Radiat. Phys. Chem., 65 (2002) 317-326.

[242] K.M.S. Hansen, A. Spiliotopoulou, W.A. Cheema, H.R. Andersen, Effect of ozonation of swimming pool water on formation of volatile disinfection by-products – A laboratory study, Chem. Eng. J., 289 (2016) 277-285.

[243] W.R. Haag, J. Hoigne, Ozonation of Water Containing Chlorine or Chloramines. Reaction-Products and Kinetics, Water Res., 17 (1983) 1397-1402.

[244] W.R. Haag, J. Hoigné, Ozonation of water containing chlorine or chloramines. Reaction products and kinetics, Water Res., 17 (1983) 1397-1402.

[245] W. Uhl, C. Hartmann, Disinfection by-products and microbial contamination in the treatment of pool water with granular activated carbon, Water Sci. Technol., 52 (2005) 71-76.

[246] E. Worch, Adsorption Technology in Water Treatment: Fundamentals, Processes, and Modeling, Walter de Gruyter GmbH & Co. KG, Berlin/Boston, 2012.

[247] G. Newcombe, Charge vs. porosity — Some influences on the adsorption of natural organic matter (NOM) by activated carbon, Water Sci. Technol., 40 (1999) 191-198.

[248] S.J. Park, B.J. Kim, Ammonia removal of activated carbon fibers produced by oxyfluorination, J. Colloid Interface Sci., 291 (2005) 597-599.

[249] D. Kucic, I. Cosic, M. Vukovic, F. Briski, Sorption Kinetic Studies of Ammonium from Aqueous Solution on Different Inorganic and Organic Media, Acta. Chim. Slov., 60 (2013) 109-119.

[250] C. Moreno-Castilla, Adsorption of organic molecules from aqueous solutions on carbon materials, Carbon, 42 (2004) 83-94.

[251] T. Karanfil, J.E. Kilduff, Role of granular activated carbon surface chemistry on the adsorption of organic compounds. 1. Priority pollutants, Environ. Sci. Technol., 33 (1999) 3217-3224.

[252] T. Karanfil, M. Kitis, J.E. Kilduff, A. Wigton, Role of granular activated carbon surface chemistry on the adsorption of organic compounds. 2. Natural organic matter, Environ. Sci. Technol., 33 (1999) 3225-3233.

[253] L. Li, P.A. Quinlivan, D.R.U. Knappe, Effects of activated carbon surface chemistry and pore structure on the adsorption of organic contaminants from aqueous solution, Carbon, 40 (2002) 2085-2100.

[254] J.L. Fairey, G.E. Speitel, L.E. Katz, Impact of natural organic matter on monochloramine reduction by granular activated carbon: The role of porosity and electrostatic surface properties, Environ. Sci. Technol., 40 (2006) 4268-4273.

[255] K. Ebie, F.S. Li, Y. Azuma, A. Yuasa, T. Hagishita, Pore distribution effect of activated carbon in adsorbing organic micropollutants from natural water, Water Res., 35 (2001) 167-179.

[256] W. Cheng, S.A. Dastgheib, T. Karanfil, Adsorption of dissolved natural organic matter by modified activated carbons, Water Res., 39 (2005) 2281-2290.

[257] P.A. Quinlivan, L. Li, D.R.U. Knappe, Effects of activated carbon characteristics on the simultaneous adsorption of aqueous organic micropollutants and natural organic matter, Water Res., 39 (2005) 1663-1673.

[258] S. Velten, D.R.U. Knappe, J. Traber, H.P. Kaiser, U. von Gunten, M. Boller, S. Meylan, Characterization of natural organic matter adsorption in granular activated carbon adsorbers, Water Res., 45 (2011) 3951-3959.

[259] K.G. Babi, K.M. Koumenides, A.D. Nikolaou, C.A. Makri, F.K. Tzoumerkas, T.D. Lekkas, Pilot study of the removal of THMs, HAAs and DOC from drinking water by GAC adsorption, Desalination, 210 (2007) 215-224.

[260] J. Kim, B. Kang, DBPs removal in GAC filter-adsorber, Water Res., 42 (2008) 145-152.

[261] H.L. Tang, Y.F.F. Xie, Biologically active carbon filtration for haloacetic acid removal from swimming pool water, Sci. Total Environ., 541 (2016) 58-64.

[262] G. Ertl, H. Knözinger, J. Weitkamp, Handbook of heterogeneous catalysis, VCH Verlagsgesellschaft mbH, Weinheim, Germany, 1997.

[263] M.T. Suidan, V.L. Snoeyink, R.A. Schmitz, Reduction of Aqueous Free Chlorine with Granular Activated Carbon, pH and Temperature Effects, Environ. Sci. Technol., 11 (1977) 785-789.

[264] M.T. Suidan, V.L. Snoeyink, R.A. Schmitz, Reduction of Aqueous HOCl with Activated Carbon, J. Environ. Eng. Div. ASCE, 103 (1977) 677-691.

[265] R.C. Bauer, V.L. Snoeyink, Reactions of Chloramines with Active Carbon, J. Water Pollut. Con. F., 45 (1973) 2290-2301.

[266] A.B. Scaramelli, F.A. Digiano, Effect of sorbed organics on efficiency of ammonia removal by chloramine-carbon surface-reactions, J. Water Pollut. Con. F., 49 (1977) 693-705.

[267] A. Grohmann, Zur Frage der technischen unvermeidbaren Restkonzentrationen von Trihalomethanen und Chloraminen im Schwimm- und Badebeckenwasser., Bundesgesundheitsblatt, 10 (1995) 380-385.

[268] P.J. Vikesland, K. Ozekin, R.L. Valentine, Monochloramine decay in model and distribution system waters, Water Res., 35 (2001) 1766-1776.

[269] A. Dumetre, C. Le Bras, M. Baffet, P. Meneceur, J.P. Dubey, F. Derouin, J.P. Duguet, M. Joyeux, L. Moulin, Effects of ozone and ultraviolet radiation treatments on the infectivity of Toxoplasma gondii oocysts, Vet. Parasitol., 153 (2008) 209-213.

[270] J. De Laat, F. Berne, Theoretical and practical aspects of the dechloramination of swimming pool water by UV irradiation, Eur. J. Water Qual., 40 (2009) 129-149.

[271] D. Cassan, C. Drakidès, UV and applications in water treatment of commercial swimming pools, in: Proceedings of the fourth International Conference Swimming Pool & Spa, Porto, 2011, 78-83.

[272] W. Buchanan, F. Roddick, N. Porter, Formation of hazardous by-products resulting from the irradiation of natural organic matter: Comparison between UV and VUV irradiation, Chemosphere, 63 (2006) 1130-1141.

[273] E.H. Goslan, F. Gurses, J. Banks, S.A. Parsons, An investigation into reservoir NOM reduction by UV photolysis and advanced oxidation processes, Chemosphere, 65 (2006) 1113-1119.

[274] A. Parkinson, M.J. Barry, F.A. Roddick, M.D. Hobday, Preliminary toxicity assessment of water after treatment with UV-irradiation and UVC/H2O2, Water Res., 35 (2001) 3656-3664.

[275] J. Thomson, A. Parkinson, F.A. Roddick, Depolymerization of chromophoric natural organic matter, Environ. Sci. Technol., 38 (2004) 3360-3369.

[276] W. Liu, L.-M. Cheung, X. Yang, C. Shang, THM, HAA and CNCl formation from UV irradiation and chlor(am)ination of selected organic waters, Water Res., 40 (2006) 2033-2043.

[277] J. Li, E.R. Blatchley, UV photodegradation of inorganic chloramines, Environ. Sci. Technol., 43 (2009) 60-65.

[278] L.H. Nowell, J. Hoigne, Photolysis of aqueous chlorine at sunlight and ultraviolet wavelengths. 2. Hydroxyl radical production, Water Res., 26 (1992) 599-605.

[279] M.L. Magnuson, C.A. Kelty, C.M. Sharpless, K.G. Linden, W. Fromme, D.H. Metz, R. Kashinkunti, Effect of UV irradiation on organic matter extracted from treated Ohio River water studied through the use of electrospray mass spectrometry, Environ. Sci. Technol., 36 (2002) 5252-5260.

[280] J. De Laat, N. Boudiaf, F. Dossier-Berne, Effect of dissolved oxygen on the photodecomposition of monochloramine and dichloramine in aqueous solution by UV irradiation at 253.7 nm, Water Res., 44 (2010) 3261-3269.

[281] F. Becker, D. Stetter, U. Janowsky, H. Overath, Abbau von Monochloraminen durch Aktivkohlefilter (in German), Gwf Wasser - Abwasser, 131 (1990) 1-8.

[282] E. Barbot, P. Moulin, Swimming pool water treatment by ultrafiltration-adsorption process, J. Membr. Sci., 314 (2008) 50-57.

[283] G.H. Kristensen, M.M. Klausen, V.A. Hansen, F.R. Lauritsen, On-line monitoring of the dynamics of trihalomethane concentrations in a warm public swimming pool using an unsupervised membrane inlet mass spectrometry system with off-site real-time surveillance, Rapid Commun. Mass Spectrom., 24 (2010) 30-34.

[284] G.L. Kristensen, M.M. Klausen, H.R. Andersen, L. Erdinger, F. Lauritzen, E. Arvin, H.J. Albrechtsen, Full scale test of UV-based water treatment technologies at Gladsaxe Sport Centre - with and without advanced oxidation mechanisms, in: Proceedings of the third International Conference Swimming Pool & Spa, London, 2009, 1-15.

[285] G. Bullock, Disinfection of Swimming Pool Water (doctoral thesis), Doctoral thesis, Cranfield University, Cranfield, 2003.

[286] E.L. Sharp, S.A. Parsons, B. Jefferson, Seasonal variations in natural organic matter and its impact on coagulation in water treatment, Sci. Total Environ., 363 (2006) 183-194.

[287] A. Grefte, Removal of natural organic matter fractions by anion exchange, Doctoral thesis, Technische Universiteit Delft, Delft, 2013.

[288] S.A. Huber, A. Balz, M. Abert, New method for urea analysis in surface and tap waters with LC-OCD-OND (liquid chromatography-organic carbon detection-organic nitrogen detection), J. Water Sup. Res. Tech.-Aqua, 60 (2011) 159-166.

[289] F. Hammes, T. Broger, H.U. Weilenmann, M. Vital, J. Helbing, U. Bosshart, P. Huber, R.P. Odermatt, B. Sonnleitner, Development and laboratory-scale testing of a fully automated online flow cytometer for drinking water analysis, Cytom. Part A, 81A (2012) 508-516.

[290] DIN EN ISO 10304-1, Water quality - Determination of dissolved anions by liquid chromatography of ions, Part 1: Determination of bromide, chloride, fluoride, nitrate, nitrite, phosphate and sulfate (in German), Normenausschuss Wasserwesen (NAW) im DIN Deutsches Institut für Normung, Beuth Verlag, Berlin, 2009.

[291] D. Peng, F. Saravia, G. Abbt-Braun, H. Horn, Occurrence and simulation of trihalomethanes in swimming pool water: A simple prediction method based on DOC and mass balance, Water Res., 88 (2016) 634-642.

[292] J. Wang, J. Guan, S.R. Santiwong, T.D. Waite, Characterization of floc size and structure under different monomer and polymer coagulants on microfiltration membrane fouling, J. Membr. Sci., 321 (2008) 132-138.

[293] Q. Zhao, C. Shang, X.R. Zhang, G.Y. Ding, X. Yang, Formation of halogenated organic byproducts during medium-pressure UV and chlorine coexposure of model compounds, NOM and bromide, Water Res., 45 (2011) 6545-6554.

[294] J.L. Weishaar, G.R. Aiken, B.A. Bergamaschi, M.S. Fram, R. Fujii, K. Mopper, Evaluation of specific ultraviolet absorbance as an indicator of the chemical composition and reactivity of dissolved organic carbon, Environ. Sci. Technol., 37 (2003) 4702-4708.

[295] V.L. Snoeyink, H.T. Lai, J.H. Johnson, J.F. Young, Active carbon: Dechlorination and the adsorption of organic compounds, in: A. Rubin (Ed.) Chemistry of Water Supply, Treatment and Distribution, Ann Arbor Science Publishers, Ann Arbor, Michigan, 1974.

[296] H.S. Shin, K.H. Lim, Spectroscopic and elemental investigation of microbial decomposition of aquatic fulvic acid in biological process of drinking water treatment, Biodegradation, 7 (1996) 287-295.

[297] G. Holzwarth, R.G. Balmer, L. Soni, The fate of chlorine and chloramines in cooling towers - Henrys law constants for flashoff, Water Res., 18 (1984) 1421-1427.

[298] T. Bond, E.H. Goslan, S.A. Parsons, B. Jefferson, A critical review of trihalomethane and haloacetic acid formation from natural organic matter surrogates, Environ. Technol. Rev., 1 (2012) 93-113.

[299] I. Nicole, J. De Laat, M. Dore, J.P. Duguet, H. Suty, Etude de la degradation des trihalomethanes en milieu aqueux dilue par irradiation UV - determination du rendement quantique de photolyse a 253,7 nm., Environ. Technol., 12 (1991) 21-31.

[300] Z. Tebeje, Competitive adsorption of chloroform and bromoform using commercial bituminous and coconut based granular activated carbons, E. Afr. J. Sci., 4 (2010) 59-64.

[301] Z. Tebeje, GAC adsorption processes for chloroform removal from drinking water, Tanzania J. Nat. Appl. Sci., 2 (2011) 352-358.

[302] M.J. McGuire, K.D. Marshall, H.T. Carol, E.M. Aieta, E.W. Howe, J.C. Crittenden, Evaluating GAC for trihalomethane control, J. AWWA, 83 (1991) 38-48.

[303] C.P. Weisel, S.D. Richardson, B. Nemery, G. Aggazzotti, E. Baraldi, E.R. Blatchley, B.C. Blount, K.H. Carlsen, P.A. Eggleston, F.H. Frimmel, M. Goodman, G. Gordon, S.A. Grinshpun, D. Heederik, M. Kogevinas, J.S. LaKind, M.J. Nieuwenhuijsen, F.C. Piper, S.A. Sattar, Childhood Asthma and Environmental Exposures at Swimming Pools: State of the Science and Research Recommendations, Environ. Health Perspect., 117 (2009) 500-507.

[304] A. Bernard, S. Carbonnelle, O. Michel, S. Higuet, C. de Burbure, J.P. Buchet, C. Hermans, X. Dumont, I. Doyle, Lung hyperpermeability and asthma prevalence in schoolchildren: Unexpected associations with the attendance at indoor chlorinated swimming pools, Occup. Environ. Med., 60 (2003) 385-394.

[305] B. Schreiber, T. Brinkmann, V. Schmalz, E. Worch, Adsorption of dissolved organic matter onto activated carbon - the influence of temperature, absorption wavelength, and molecular size, Water Res., 39 (2005) 3449-3456.

[306] T. Asada, A. Okazaki, K. Kawata, K. Oikawa, Influence of Pore Properties and Solution pH on Removal of Free Chlorine and Combined Chlorine by Porous Carbon, J. Health Sci., 55 (2009) 649-656.

[307] E.F. Jaguaribe, L.L. Medeiros, M.C.S. Barreto, L.P. Araujo, The performance of activated carbons from sugarcane bagasse, babassu, and coconut shells in removing residual chlorine, Braz. J. Chem. Eng., 22 (2005) 41-47.

[308] T.L. Champlin, R.A. Velasco, J.L. Karlskint, L.P. Furland, M.N. Kaden, A.G. Greer, D.W. Yowell, B.E. Kennedy, Removal of Chloramines by Granular Activated Carbon, Florida Water Res. J., July (2002) 18-21.

[309] J.L. Fairey, G.E. Speitel, L.E. Katz, Monochloramine destruction by GAC - Effect of activated carbon type and source water characteristics, J. Am. Water Works Ass., 99 (2007) 110-120.

[310] J.D. Komorita, V.L. Snoeyink, Monochloramine Removal from Water by Activated Carbon, J. Am. Water Works Ass., 77 (1985) 62-65.

[311] C.L. Mangun, R.D. Braatz, J. Economy, A.J. Hall, Fixed bed adsorption of acetone and ammonia onto oxidized activated carbon fibers, Ind. Eng. Chem. Res., 38 (1999) 3499-3504.

[312] F. Maia, R. Silva, B. Jarrais, A.R. Silva, C. Freire, M.F.R. Pereira, J.L. Figueiredo, Pore tuned activated carbons as supports for an enantioselective molecular catalyst, J. Colloid Interface Sci., 328 (2008) 314-323.

[313] B.R. Kim, Analysis of batch and packed bed reactor models for the carbon-chloramine reactions, Doctoral thesis, University of Illinois at Urbana-Champaign, Illinois, 1977.

[314] H. Sontheimer, J.C. Crittenden, R.S. Summers, Activated carbon for water treatment (in German), DVGW-Forschungsstelle, Engler-Bunte-Institut, Universität Karlsruhe, Karlsruhe, Germany, 1988.

[315] O. Levenspiel, Chemical reaction engineering, Third Edition, John Wiley & Sons, New York, USA, 1999.

[316] T. Aoki, Continuous-Flow Method for Simultaneous Determination of Monochloramine, Dichloramine, and Free Chlorine - Application to a Water-Purification Plant, Environ. Sci. Technol., 23 (1989) 46-50.

[317] E.U. Schlünder, Einführung in die Wärme- und Stoffübertragung (in German), Friedrich Vieweg & Sohn GmbH, Braunschweig, Germany, 1975.

[318] J.E. Williamson, C.J. Geankoplis, K.E. Bazaire, Liquid-Phase Mass Transfer at Low Reynolds Numbers, Industrial & Engineering Chemistry Fundamentals, 2 (1963) 126-129.

[319] C.R. Wilke, P. Chang, Correlation of Diffusion Coefficients in Dilute Solutions, AIChE J., 1 (1955) 264-270.

[320] P. Harriott, Chemical reactor design, Marcel Dekker, New York, 2003.

[321] M. Luthardt, E. Than, H. Heckendorff, Limit of Decision, Limit of Detection and Limit of Determination of Analytical Methods, Fresenius Zeitschrift für Analytische Chemie, 326 (1987) 331-339.

[322] J.M. Smith, Chemical Engineering Kinetics, Second Edition, McGraw-Hill Book Co., New York, 1970.

[323] S. Yagi, D. Kunii, Studies on combustion of carbon particles in flames and fluidized beds, in: Symposium (International) on Combustion, New York, 1955, 231–244.

[324] V.C. Hand, D.W. Margerum, Kinetics and Mechanisms of the Decomposition of Dichloramine in Aqueous-Solution, Inorg. Chem., 22 (1983) 1449-1456.

[325] I.M. Schreiber, W.A. Mitch, Influence of the order of reagent addition on NDMA formation during chloramination, Environ. Sci. Technol., 39 (2005) 3811-3818.

[326] L.M. Schurter, P.P. Bachelor, D.W. Margerum, Nonmetal Redox Kinetics - Monochloramine, Dichloramine, and Trichloramine Reactions with Cyanide Ion, Environ. Sci. Technol., 29 (1995) 1127-1134.

[327] R.L. Valentine, K.I. Brandt, C.T. Jafvert, A Spectrophotometric Study of the Formation of an Unidentified Monochloramine Decomposition Product, Water Res., 20 (1986) 1067-1074.

[328] P.G.W. Hawkslei, The physics of particle size measerment: Part I. Fluid dynamics and the Stokes diameter, British Coal Utilisation Research Association, UK, 1951.

[329] DIN 66165-1, Particle size analysis; sieve analysis; general principles (in German), Normenausschuß Siebböden und Kornmessung (NASK) im DIN Deutsche Institut für Normung, Beuth Verlag, Berlin, 1987.

[330] A. Hazen, The filtration of public water-supplies, J. Wiley & Sons, New York, 1886.

[331] S. Brunauer, P.H. Emmett, E. Teller, Adsorption of gases in multimolecular layers, J. Am. Chem. Soc., 60 (1938) 309-319.

[332] A.V. Neimark, Y.Z. Lin, P.I. Ravikovitch, M. Thommes, Quenched solid density functional theory and pore size analysis of micro-mesoporous carbons, Carbon, 47 (2009) 1617-1628.

[333] C.E. Salmas, G.P. Androutsopoulos, A novel pore structure tortuosity concept based on nitrogen sorption hysteresis data, Ind. Eng. Chem. Res., 40 (2001) 721-730.

[334] B. Skibinski, P. Muller, W. Uhl, Rejection of submicron sized particles from swimming pool water by a monolithic SiC microfiltration membrane: Relevance of steric and electrostatic interactions, J. Membr. Sci., 499 (2016) 92-104.

[335] S. Brunauer, L.S. Deming, W.E. Deming, E. Teller, On a theory of the van der Waals adsorption of gases, J. Am. Chem. Soc., 62 (1940) 1723-1732.

[336] Z.H. Hu, M.P. Srinivasan, Y.M. Ni, Novel activation process for preparing highly microporous and mesoporous activated carbons, Carbon, 39 (2001) 877-886.

[337] S. Bashkova, F.S. Baker, X.X. Wu, T.R. Armstrong, V. Schwartz, Activated carbon catalyst for selective oxidation of hydrogen sulphide: On the influence of pore structure, surface characteristics, and catalytically-active nitrogen, Carbon, 45 (2007) 1354-1363.

[338] R.H. Crabtree, Resolving Heterogeneity Problems and Impurity Artifacts in Operationally Homogeneous Transition Metal Catalysts, Chem. Rev., 112 (2012) 1536-1554.

[339] E. Worch, Fixed-bed adsorption in drinking water treatment: a critical review on models and parameter estimation, J. Water Sup. Res. Tech.-Aqua, 57 (2008) 171-183.

[340] B.R. Kim, V.L. Snoeyink, The Monochloramine-GAC Reaction in Adsorption Systems, J. Am. Water Works Ass., 72 (1980) 488-490.

[341] B.R. Kim, V.L. Snoeyink, The Monochloramine-Activated Carbon Reaction: A Mathematical Model Solved Using the Orthogonal Collocation Method on Finite Elements, in: I.H. Suffet, M.J. McGuire (Eds.) Activated Carbon Adsorption of Organics from the Aqueaous Phase Ann Arbor Science, Michigan, USA, 1980, 463.

[342] H. Konno, R. Ohnaka, J.-I. Nishimura, T. Tago, Y. Nakasaka, T. Masuda, Kinetics of the catalytic cracking of naphtha over ZSM-5 zeolite: effect of reduced crystal size on the reaction of naphthenes, Catal. Sci. Tech., 4 (2014) 4265-4273.

[343] D.L. Sparks, Kinetics of Soil Chemical Processes, Academic Press, New York, 1989.

[344] B.R. Kim, V.L. Snoeyink, R.A. Schmitz, Removal of dichloramine and ammonia by granular carbon, J. Water Pollut. Con. F., 50 (1978) 122-133.

[345] O. Levenspiel, The Chemical Reactor Omnibook, OSU Book Stores Inc., Corvallis, Oregon, USA, 1996.

[346] R.A. Sayle, E.J. Milnerwhite, Rasmol - Biomolecular Graphics for All, Trends Biochem. Sci, 20 (1995) 374-376.

[347] C.L. McCallum, T.J. Bandosz, S.C. McGrother, E.A. Muller, K.E. Gubbins, A molecular model for adsorption of water on activated carbon: Comparison of simulation and experiment, Langmuir, 15 (1999) 533-544.

[348] M. Franz, H.A. Arafat, N.G. Pinto, Effect of chemical surface heterogeneity on the adsorption mechanism of dissolved aromatics on activated carbon, Carbon, 38 (2000) 1807-1819.

[349] O.P. Mahajan, C. Morenocastilla, P.L. Walker, Surface-Treated Activated Carbon for Removal of Phenol from Water, Sep. Sci. Technol., 15 (1980) 1733-1752.

[350] M. Sakuma, T. Matsushita, Y. Matsui, T. Aki, M. Isaka, N. Shirasaki, Mechanisms of trichloramine removal with activated carbon: Stoichiometric analysis with isotopically labeled trichloramine and theoretical analysis with a diffusion-reaction model, Water Res., 68 (2015) 839-848.

[351] M.T. Suidan, V.L. Snoeyink, W.E. Thacker, D.W. Dreher, Influence of Pore-Size Distribution on Hocl-Activated Carbon Reaction, Abstracts of Papers of the American Chemical Society, 173 (1977) 66-66.

[352] W.T. Tsai, C.Y. Chang, Surface-Chemistry of Activated Carbons and Its Relevance for Effects of Relative-Humidity on Adsorption of Chlorinated Organic Vapors, Chemosphere, 29 (1994) 2507-2515.

[353] Y. Sun, P.A. Webley, Preparation of activated carbons from corncob with large specific surface area by a variety of chemical activators and their application in gas storage, Chem. Eng. J., 162 (2010) 883-892.

[354] M. Sevilla, A.B. Fuertes, R. Mokaya, High density hydrogen storage in superactivated carbons from hydrothermally carbonized renewable organic materials, Energ. Environ. Sci., 4 (2011) 1400-1410.

[355] J.C. Wang, I. Senkovska, S. Kaskel, Q. Liu, Chemically activated fungi-based porous carbons for hydrogen storage, Carbon, 75 (2014) 372-380.

[356] J. Fu, J.H. Qu, R.P. Liu, X. Zhao, Z.M. Qiang, The influence of Cu(II) on the decay of monochloramine, Chemosphere, 74 (2009) 181-186.

[357] P.J. Vikesland, R.L. Valentine, Iron oxide surface-catalyzed oxidation of ferrous iron by monochloramine: Implications of oxide type and carbonate on reactivity, Environ. Sci. Technol., 36 (2002) 512-519.

[358] J.A. Switzer, V.V. Rajasekharan, S. Boonsalee, E.A. Kulp, E.W. Bohannan, Evidence that monochloramine disinfectant could lead to elevated Pb levels in drinking water, Environ. Sci. Technol., 40 (2006) 3384-3387.

[359] M. Edwards, A. Dudi, Role of chlorine and chloramine in corrosion of lead-bearing plumbing materials, J. AWWA, 96 (2004) 69-81.

[360] X.H. Zhang, S.O. Pehkonen, N. Kocherginsky, G.A. Ellis, Copper corrosion in mildly alkaline water with the disinfectant monochloramine, Corros. Sci., 44 (2002) 2507-2528.

[361] J. Fu, J.H. Qu, R.P. Liu, Z.M. Qiang, X. Zhao, H.J. Liu, Mechanism of Cu(II)-catalyzed monochloramine decomposition in aqueous solution, Sci. Total Environ., 407 (2009) 4105-4109.

[362] P.J. Branton, K.G. McAdam, M.G. Duke, C.A. Liu, M. Curle, M. Mola, C.J. Proctor, R.H. Bradley, Use of Classical Adsorption Theory to Understand the Dynamic Filtration of Volatile Toxicants in Cigarette Smoke by Active Carbons, Adsorpt. Sci. Technol., 29 (2011) 117-138.

[363] B. Böhringer, O.G. Gonzalez, I. Eckle, M. Müller, J.-M. Giebelhausen, C. Schrage, S. Fichtner, Polymer-based Spherical Activated Carbons – From Adsorptive Properties to Filter Performance, Chem. Ing. Tech., 83 (2011) 53-60.

[364] S. Fichtner, Adsorbents for various applications, F & S International Edition, 10 (2010) 67-70.

[365] H. Raave, I. Keres, K. Kauer, M. Noges, J. Rebane, M. Tampere, E. Loit, The impact of activated carbon on NO3--N, NH4+-N, P and K leaching in relation to fertilizer use, Eur. J. Soil Sci., 65 (2014) 120-127.

[366] R.A. Hayden, Method for reactivating nitrogen-treated carbon catalysts, US patent 5.466.645, 1995.

[367] T.M. Matviya, R.A. Hayden, Catalytic carbon, US patent 5.356.849, 1994.

[368] S.L. Goertzen, K.D. Theriault, A.M. Oickle, A.C. Tarasuk, H.A. Andreas, Standardization of the Boehm titration. Part I. CO(2) expulsion and endpoint determination, Carbon, 48 (2010) 1252-1261.

[369] A.M. Oickle, S.L. Goertzen, K.R. Hopper, Y.O. Abdalla, H.A. Andreas, Standardization of the Boehm titration: Part II. Method of agitation, effect of filtering and dilute titrant, Carbon, 48 (2010) 3313-3322.

[370] H.P. Boehm, Chemical identification of surface groups, in: D.D. Eley, H. Pines, P. Weisz (Eds.) Advances in catalysis, Academic Press, 1966.

[371] A. Sze, D. Erickson, L.Q. Ren, D.Q. Li, Zeta-potential measurement using the Smoluchowski equation and the slope of the current-time relationship in electroosmotic flow, J. Colloid Interface Sci., 261 (2003) 402-410.

[372] V. Strelko, D.J. Malik, M. Streat, Characterisation of the surface of oxidised carbon adsorbents, Carbon, 40 (2002) 95-104.

[373] Z.S. Liu, J.Y. Chen, Y.H. Peng, Activated carbon fibers impregnated with Pd and Pt catalysts for toluene removal, J. Hazard. Mater., 256 (2013) 49-55.

[374] A. Goifman, J. Gun, F. Gelman, I. Ekeltchik, O. Lev, J. Donner, H. Bornick, E. Worch, Catalytic oxidation of hydrogen sulfide by dioxygen on CoN4 type catalyst, Appl. Catal. B.-Environ., 63 (2006) 296-304.

[375] A. Cloteaux, F. Geradin, N. Midoux, Numerical simulation and modelling of a typical swimming pool for disinfection by-products assessment, in: Fifth International Conference Swimming Pool & Spa, Istituto Superiore di Sanità, Rome, Italy, 2013, 117-127.

[376] F. Gérardin, A. Cloteaux, N. Midoux, Modeling of variations in nitrogen trichloride concentration over time in swimming pool water, Process Saf. Environ. Prot., 94 (2015) 452-462.

[377] G. Stüttgen, S. Richter, D. Wildberger, Zur Erfassung biogener Amine in tierischer sowie menschlicher Haut und deren Tumoren mit dünnschicht chromatographischer Methodik (in German), Archiv für klinische und experimentelle Dermatologie, 230 (1967) 349-360.

[378] K.A. Dacosta, J.J. Vrbanac, S.H. Zeisel, The Measurement of Dimethylamine, Trimethylamine, and Trimethylamine N-Oxide Using Capillary Gas-Chromatography Mass-Spectrometry, Anal. Biochem., 187 (1990) 234-239.

[379] A.M. Kalijadis, M.M. Vukcevic, Z.M. Jovanovic, Z.V. Lausevic, M.D. Lausevic, Characterisation of surface oxygen groups on different carbon materials by the Boehm method and temperature-programmed desorption, J. Serb. Chem. Soc., 76 (2011) 757-768.

[380] A. Allwar, Characteristics of Pore Structures and Surface Chemistry of Activated Carbons by Physisorption, FTIR and Boehm Methods, J. Appl. Chem., 2 (2012) 9-15.

[381] B. Cagnon, X. Py, A. Guillot, J.P. Joly, R. Berjoan, Pore structure modification of pitch-based activated carbon by NaOCl and air oxidation/pyrolysis cycles, Microporous Mesoporous Mat., 80 (2005) 183-193.

[382] P. Chingombe, B. Saha, R.J. Wakeman, Surface modification and characterisation of a coal-based activated carbon, Carbon, 43 (2005) 3132-3143.

[383] B. Zhang, Z.H. Wen, S.Q. Ci, J.H. Chen, Z. He, Nitrogen-doped activated carbon as a metal free catalyst for hydrogen production in microbial electrolysis cells, RSC Adv., 4 (2014) 49161-49164.

[384] B. Zhang, Z.H. Wen, S.Q. Ci, S. Mao, J.H. Chen, Z. He, Synthesizing Nitrogen-Doped Activated Carbon and Probing its Active Sites for Oxygen Reduction Reaction in Microbial Fuel Cells, Acs Appl. Mater. Inter., 6 (2014) 7464-7470.

[385] J.G. Jacangelo, V.P. Olivieri, K. Kawata, Oxidation of Sulfhydryl-Groups by Monochloramine, Water Res., 21 (1987) 1339-1344.

[386] B. Jurado-Sanchez, E. Ballesteros, M. Gallego, Screening of N-nitrosamines in tap and swimming pool waters using fast gas chromatography, J. Sep. Sci., 33 (2010) 610-616.

[387] OENORM M 5873-1, Plants for the disinfection of water using ultraviolet radiation - Requirements and testing - Low pressure mercury lamp plants (in German), Beuth Verlag, Berlin, 2001.

[388] E. Müller-Erlwein, Chemical reaction engineering (in German), B.G. Teubner Verlag/GWV Fachverlage GmbH, Wiesbaden, Germany, 2007.

[389] T. Aley, M. Fletcher, The water tracer`s cookbook, Missouri Speleology, 16 (1976) 1-32.

[390] A.S. Ruhl, M. Jekel, Elution behaviour of low molecular weight compounds in size exclusion chromatography, J. Water Sup. Res. Tech.-Aqua, 61 (2012) 32-40.

[391] M. Wojdyr, Fityk: a general-purpose peak fitting program, J. Appl. Crystallogr., 43 (2010) 1126-1128.

[392] W.A. Mitch, J.O. Sharp, R.R. Trussell, R.L. Valentine, L. Alvarez-Cohen, D.L. Sedlak, N-nitrosodimethylamine (NDMA) as a drinking water contaminant: A review, Environ. Eng. Sci., 20 (2003) 389-404.

[393] B.S. Yiin, D.W. Margerum, Nonmetal Redox Kinetics - Reactions of Trichloramine with Ammonia and with Dichloramine, Inorg. Chem., 29 (1990) 2135-2141.

[394] K. Kumar, R.W. Shinness, D.W. Margerum, Kinetics and Mechanisms of the Base Decomposition of Nitrogen Trichloride in Aqueous-Solution, Inorg. Chem., 26 (1987) 3430-3434.

[395] M. Shi, Z.F. Wang, Z. Zheng, Effect of Na+ impregnated activated carbon on the adsorption of NH4+-N from aqueous solution, J. Environ. Sci.-China, 25 (2013) 1501-1510.

[396] G. Soto-Garrido, C. Aguilar, R. García, R. Arriagada, A peach stone activated carbon chemically modified to adsorb aqueous ammonia, J. Chil. Chem. Soc., 48 (2003).

[397] B. Halling-Sørensen, H. Hjuler, Simultaneous nitrification and denitrification with an upflow fixed bed reactor applying clinoptilolite as media, Water Treatment, 7 (1992) 77-88.

[398] B. HallingSorensen, S.N. Nielsen, A model of nitrogen removal from waste water in a fixed bed reactor using simultaneous nitrification and denitrification (SND), Ecol. Model., 87 (1996) 131-141.

[399] D. Berman, E.W. Rice, J.C. Hoff, Inactivation of Particle-Associated Coliforms by Chlorine and Monochloramine, Appl. Environ. Microbiol., 54 (1988) 507-512.

[400] M.W. Lechevallier, C.D. Cawthon, R.G. Lee, Inactivation of Biofilm Bacteria, Appl. Environ. Microbiol., 54 (1988) 2492-2499.

[401] K. Inazu, M. Kitahara, K. Aika, Decomposition of ammonium nitrate in aqueous solution using supported platinum catalysts, Catal. Today, 93-5 (2004) 263-271.

[402] C.M. Hung, Removal of ammonia from aqueous solutions by catalytic oxidation with copper-based rare earth composite metal materials: catalytic performance, characterization, and cytotoxicity evaluation, J. Rare Earth, 29 (2011) 632-637.

[403] C.-M. Hung, W.-B. Lin, Catalytic wet air oxidation of aqueous solution of ammonia in a continuous-flow trickle-bed reactor over metal supported in carbon materials, Sustain. Environ. Res., 20 (2010) 251-255.

[404] Lippits M. J., Gluhoi A. C., N.B. E., A comparative study of the selective oxidation of NH3 to N-2 over gold, silver and copper catalysts and the effect of addition of Li2O and CeOx, Catal. Today, 137 (2008) 446-452.

[405] K.G. Babi, K.M. Koumenidis, C.A. Makri, A.D. Nikolaou, T.D. Lekkas, Adsorption Capacity of GAC Pilot Filter-Adsorber and Postfilter-Adsorber for Individual THMs from Drinking Water, Athens, Global Nest J., 13 (2011) 50-58.

[406] A.A. Halim, H.A. Aziz, M.A.M. Johari, K.S. Ariffin, Comparison study of ammonia and COD adsorption on zeolite, activated carbon and composite materials in landfill leachate treatment, Desalination, 262 (2010) 31-35.

[407] A.A. Halim, M.T. Latif, A. Ithnin, Ammonia Removal from Aqueous Solution Using Organic Acid Modified Activated Carbon, World Appl. Sci. J., 24 (2013) 1-06.

[408] R. Zhijun, G. Di, G. Linlin, W. Yunchang, Adsorption Ammonia From Polluted Water On Fe Modified Activated Carbon (Ac-Fe), in: G. Lee (Ed.) Biomedical Engineering and Environmental Engineering, WIT Press, Southampton, UK, 2014, 427-433.

[409] M.H. Khamidun, M.A. Fulazzaky, M.F.M. Din, A.R.M. Yusoff, Resistance of mass transfer, kinetic and isotherm study of ammonium removal by using a Hybrid Plug-Flow Column Reactor (HPFCR), in: W.-P. ASung, J.C.M. Kao, R. Chen (Eds.) Environment, Energy and Sustainable Development, Taylor & Francis Group, Florida, USA, 2014.

13 Acknowledgements

First and foremost, I gratefully acknowledge my doctoral supervisors Prof. Wolfgang Uhl and Prof. Eckhard Worch. Both assisted me in important steps of my doctoral thesis with invaluable suggestions, support and encouragement.

The great work of my colleague Stephan Uhlig with regard to all aspects of the work presented in Chapter 4 is gratefully acknowledged. I thank Dr. Fabian Soltermann for his advices and fruitful discussions regarding the results obtained with the swimming pool model. Prof. Frants Lauritsen, Dr. Christina Schmalz and Pascal Müller are acknowledged for their great input in setting up the membrane inlet mass spectrometer. The help of Prof. Gunther Gansloser and Prof. Klaus Hagen in dimensioning the swimming pool model is highly appreciated. I thank Dr. Heike Brückner, Heiko Herrlich, Andreas Kimmig, Christoph Götze and Gerit Orzechowski for their assistance in the laboratory work presented in Chapter 4. Parts of the work presented in Chapter 4 were funded by the German Federal Ministry of Education and Research (BMBF) under grant 02WT1092 as part of the POOL project. I like to thank all co-workers of the project for our fruitful discussions during project meetings.

Further, I thank Dr. Viktor Schmalz for his valuable input in discussing the results presented in Chapter 5. Moreover, Dr. Constantinos Salmas is thanked for simulations with the CSTM model. Dr. Irena Senkovska and Dr. Stephan Böttcher are appreciated for performing the N_2 physisorption and mercury intrusion measurement and giving advice for QSDFT analysis.

Prof. Wladimir Reschetilowski and Dr. Irena Senkovska are thanked for their valuable discussions regarding the work presented in Chapter 6 of this thesis. Moreover, I thank Dr. Kathrin Gebauer and Dr. Arndt Weiske for performing the CNH and ICP-MS analysis.

I also sincerely thank Christian Gerhardts, Sven Kreigenfeld and Claudia Siegel at TUD’s European Project Center. Without your support and flexibility it would never have been possible for me combining my job and PhD work.

My greatest gratitude goes to my beloved parents, Martina and Gerth. Thank you for bringing me up as who I am!